2003

Group IV phosphinimide complexes in catalysis.

Emily Hollink
University of Windsor

Group IV Phosphinimide Complexes in Catalysis

by

Emily Hollink

A Dissertation
Submitted to the Faculty of Graduate Studies and Research
Through the Department of Chemistry and Biochemistry
In Partial Fulfillment of the Requirements for
The Degree of Doctor of Philosophy at the
University of Windsor

Windsor, Ontario, Canada
September, 2003

Your file Votre référence
ISBN: 0-494-04988-X
Our file Notre référence
ISBN: 0-494-04988-X

1021736

Abstract

Significant progress has been made in various aspects of the chemistry of Group IV phosphinimide complexes, particularly in their use as highly active catalysts for olefin polymerization upon activation by an appropriate Lewis acid. Advances in synthetic methods have provided routes for the preparation of phosphinimide amide inorganic and organometallic products via metathesis or protonation methods. Testing of $TiCp(NP^tBu_3)X_2$ (X = Cl, Me, NMe_2) as hydroamination catalysts has shown that these complexes are inactive for this purpose under the conditions employed. In addition, numerous synthetic endeavours have revealed that the titanium phosphinimide complexes are reluctant to form isolable imide derivatives. However, through efforts to prepare ligand transfer reagents, magnesium phosphinimide complexes have been developed that initiate the polymerization of methyl methacrylate at ambient temperatures, probably via a radical process.

Reliable approaches have been developed to obtain a series of polymerization catalyst precursors of general formulae $M[m\text{-}(CH_2PR_2N)_2C_6H_4]X_2$ (M = Ti, Zr; R = ^{t}Bu, Cy; X = Cl, NR_2) and $Zr(NP^tBu_3)_2X_2$ that possess *bis*(phosphinimide) ligands. Polymerization testing to determine the effect of increasing steric bulk of the ancillary ligands on polymerization activity was performed, although catalysts derived from $M(NPR_3)_2X_2$ (M = Ti, Zr; NPR_3 = chelated or non-chelated phosphinimide ligand; X = Cl, Me) were not active enough under the conditions employed to provide this information. Reactivity studies of the titanium *bis*(phosphinimide) derivatives have resulted in the isolation of $Ti(NP^tBu_3)_2(SiPh_3)_2$ and the generation of an insertion product (**3.22**) from thermolysis of $Ti(NP^tBu_3)_2Ph_2$ with *bis*(trimethylsilyl)acetylene.

Examination of the highly active phosphinimide polymerization catalysts inferred that the presence of a cyclopentadienide ligand, in addition to bulky alkyl groups on the phosphorus atom, was beneficial to prolong catalytic activity. In an effort to use catalysts that encompass this apparent advantage while preparing polymers of different composition that remain of industrial value, a series of bimetallic titanium complexes of the general formula $p\text{-}(CH_2PR_2NTiCp'X_2)_2C_6H_4$ (Cp' = Cp, Cp*; R = ^{t}Bu, Cy; X = Cl,

Me) were prepared. For comparison, their monometallic analogues, $TiCp(NPR_2Bn)X_2$, were also synthesized and tested using the same polymerization protocol. Several important features about these catalysts were ascertained upon examination of the polymer properties. Typically, high catalytic activities were observed, and low polydispersity polymers were generated when the discrete activator $[Ph_3C][B(C_6F_5)_4]$ was used. However, use of MAO as the activator in the presence of precatalysts that have a phosphinimide ligand with a benzyl substituent resulted in polymers with a broad molecular weight distribution. Another observation that transpired from this series of polymerization experiments was that the activity increased as the steric bulk of the ligands increased.

Finally, a systematic investigation into the synthesis and utility of zirconium phosphinimide complexes as olefin polymerization catalysts was performed. The polymerization activity was appreciably influenced by the mode of catalyst activation; when MAO was used, only moderate activities were attained, but when $B(C_6F_5)_3$ or $[Ph_3C][B(C_6F_5)_4]$ were used in the presence of low concentrations of T^iBAl as a solvent scrubber, activities that rivalled the industrial standard $ZrCp_2Me_2$ were observed. Isolation and characterization of several cationic derivatives were also performed, the products of which were found to be more susceptible to decomposition than those produced from $ZrCp_2Me_2$.

In summary, the syntheses of Group IV phosphinimide complexes that possess known or novel phosphinimide ligands have been surveyed. Of importance are the trends in polymerization activity that were established. Of particular significance is the determination that both the choice of co-catalyst and the ligand environment of the catalyst serve to influence the polymer products that are generated in a predictable manner in the series of precursors investigated.

This work is dedicated to my parents and my husband. Thanks for everything, yo!

Nach dem Spiel is vor dem Spiel.

S. Herberger

When a thing has been said, and said well, have no scruple. Take it and copy it.

A. France

Acknowledgements

I am extremely appreciative of the seemingly endless supply of assistance that originated from a multitude of people. Mr. Mike Fuerth has diligently performed numerous 2D NMR spectroscopy experiments, in addition to suffering a battery of technical questions. Dr. Pingrong Wei has painstakingly aided in mounting crystals when required, solved the majority of crystal structures, and provided me with any related information upon request. I am indebted to Mr. Steve Clemens and Mr. Dennis Hoffart for performing GPC and DSC analyses in the final hours. Ms. Sarah Hawkeswood and Mr. Chad Beddie are thanked especially for contributing to frequent (and fruitful) scientific discussions, and for performing the arduous and lackluster task of editing several versions of this manuscript along with Dr. James Gauld. Any errors that remain are solely due to my own incompetence. Finally, Dr. Douglas Stephan is particularly thanked for performing most of those roles, in addition to being the ever-constant provider.

Table of Contents

Abstract iv

Acknowledgements viii

List of Figures xiv

List of Tables xviii

Chapter 2 Compound Numbering Scheme xx

Chapter 3 Compound Numbering Scheme xxi

Chapter 4 Compound Numbering Scheme xxii

Chapter 5 Compound Numbering Scheme xxiii

List of Abbreviations xxiv

1 Introduction 1

1.1 Overture 1

1.2 Group IV Imide Complexes as Synthetic Targets 2

1.2.1 Common Synthetic Approaches 2

1.2.2 Group IV Imide Complexes as Catalysts 4

1.3 Olefin Polymerization Catalysis Employing Group IV Precursors 7

1.3.1 Overview 7

Activators 8

Polymer Analysis 9

1.3.2 Successful Group IV Polymerization Catalysts 10

Metallocenes 11

Constrained Geometry Catalyst (CGC) 12

Phosphinimide-Based Catalysts and Their Related Analogues 13

Fenokishi-Imin Haiishi (FI) Catalysts 14
Bimetallic Catalysts 15
1.3.3 Catalyst Considerations: From the Active Species to Cation Decomposition Pathways 16
Influence of the Counterion 16
Catalyst Decomposition Pathways 18
1.4 Relevance and Perspective 22
2 Group IV Phosphinimide Amide Complexes 23
2.1 Introduction 23
2.2 Experimental 24
2.2.1 General Considerations 24
2.2.2 Solvents 25
2.2.3 Materials 25
2.2.4 Reagents 25
2.2.5 Inorganic and Organometallic Syntheses 26
2.2.6 X-Ray Experimental 31
2.2.7 Polymerization Protocol 36
2.2.8 Attempted Hydroamination Protocol 36
2.3 Results and Discussion 36
Attempts to Generate Group IV Phosphinimide Imide Complexes 43
Testing for Hydroamination Catalysis 47
Magnesium Phosphinimide Complexes 47
Methyl Methacrylate (MMA) Polymerization by Magnesium Phosphinimide Complexes 50
2.4 Summary 52

3 Group IV Complexes with *Bis*(Phosphinimide) Ligands 54

3.1 Introduction 54

3.2 Experimental 56

3.2.1 General Considerations 56

3.2.2 Solvents 56

3.2.3 Reagents 57

3.2.4 Phosphines 57

3.2.5 Phosphinimines 59

3.2.6 Inorganic and Organometallic Syntheses 61

3.2.7 Reactivity of *Bis*(phosphinimide) Titanium Complexes 67

3.2.8 X-Ray Experimental 68

3.2.9 Polymerization Protocol 72

3.3 Results and Discussion 73

Utility as Ethylene Polymerization Catalysts 81

3.4 Summary 87

4 Bimetallic Titanium Phosphinimide Complexes 88

4.1 Introduction 88

4.2 Experimental 89

4.2.1 General Considerations 89

4.2.2 Solvents 89

4.2.3 Reagents 89

4.2.4 Organic Syntheses 90

4.2.5 Phosphine Syntheses 92

4.2.6 Phosphinimine Syntheses 94

4.2.7 Organometallic Syntheses 96

4.2.8 Reactions with Borane Reagents 102

4.2.9 X-Ray Experimental 103

4.2.10 Polymerization Protocol 109

4.3 Results and Discussion 110
Utility as Ethylene Polymerization Catalysts 118
A Conceptual Extension of Bimetallic Titanium Phosphinimide Complexes 132
4.4 Summary 133
5 Zirconium Half-Sandwich Phosphinimide Complexes 135
5.1 Introduction 135
5.2 Experimental 137
5.2.1 General Considerations 137
5.2.2 Solvents 137
5.2.3 Reagents 137
5.2.4 Inorganic and Organometallic Syntheses 138
5.2.5 Reactions with Borane Reagents 144
5.2.6 Reactions with Aluminum Reagents 147
5.2.7 X-Ray Experimental 148
5.2.8 Polymerization Protocol 152
5.3 Results and Discussion 152
Utility as Ethylene Polymerization Catalysts 163
5.4 Summary 169
6 Summary 171
References 174
Appendices 194
Appendix A – Supplementary Data for Chapter 2 194
Method for Obtaining Thermodynamic Data 194
Appendix B – Supplementary Data for Chapter 3 197
Aluminum *Bis*(Phosphinimide) Complex 197
Reactivity of Titanium *Bis*(Phosphinimide) Complexes 198
Appendix C – Supplementary X-ray Data for Chapters 2-5 201

Appendix D – Supplementary GPC and Polymer Yield Data for Chapters 3-5 201

Vita Auctoris 202

List of Figures

Figure 1.1: The first isolated titanium (**I**) and zirconium (**II**, **III**) imide complexes..... 3
Figure 1.2: Reversible C-H activation by a titanium imide complex. 5
Figure 1.3: Possible mechanism of imine metathesis as catalyzed by a zirconium imide complex..... 6
Figure 1.4: Proposed mechanism of hydroamination by Group IV imide complexes (M = Ti, Zr)..... 7
Figure 1.5: Insertion polymerization of ethylene performed by a generic Group IV cationic complex (M = Ti, Zr, L = ancillary ligand, R = alkyl substituent, X = ligand that may be abstracted, S = solvent or anion). 8
Figure 1.6: Use of borane or borate activators with $ZrCp_2Me_2$ to generate a single "cationic" site..... 9
Figure 1.7: Difference between a metallocene and an *ansa*-metallocene..... 11
Figure 1.8: The constrained geometry catalyst precursor..... 12
Figure 1.9: Active polymerization catalysts that possess the phosphinimide (NPR_3, **I**), ketimide (NCR_2, **II**) or guanidinide ($NC(NR)_2$, **III**) ligands..... 14
Figure 1.10: Highly active polymerization catalyst precursors derived from Group IV salicylaldiminide complexes..... 15
Figure 1.11: Bimetallic complexes based on a metallocene- (**I**) and CGC-type (**II**) ancillary ligand..... 16
Figure 1.12: Solvent-separated ion pair (**I**), contact ion pair (**II**) and resonance stabilized ion pair (**III**)..... 17
Figure 1.13: Different forms of stabilization of Group IV cations..... 18
Figure 1.14: Ligand redistribution affords $Zr[1,3\text{-}(SiMe_3)_2C_5H_3]_2Me(C_6F_5)$ (trimethylsilyl groups on the Cp ligands omitted for clarity)..... 19
Figure 1.15: Attack by the Group IV cationic metal centre on its "spectator" ligand..... 20
Figure 1.16: Methylene-methyl-bridged dimers isolated by the research groups of Sita and Piers..... 21
Figure 1.17: Dicationic titanium complexes..... 22

Figure 2.1: Generic routes to a Group IV imido species (L = spectator ligand; R, R' = alkyl or aryl). 23
Figure 2.2: Influence of R groups on the phosphorus atom to afford different products. 37
Figure 2.3: ORTEP drawings of $Ti(NP^tBu_3)(NMe_2)_3$ (**2.4**) (30% thermal ellipsoids due to disorder) and $TiCp^*(NMe_2)_3$ (additional methyl groups present due to disorder). 38
Figure 2.4: ORTEP drawings of $TiCp(NP^tBu_3)(NH(2,6\text{-}^iPr_2)C_6H_3)Cl$ (**2.8**) (molecule of benzene omitted for clarity), $Ti(NP^tBu_3)(NH(2,6\text{-}^iPr_2)C_6H_3)_3$ (**2.9**) and $ZrCp(NP^tBu_3)(NH(2,6\text{-}^iPr_2)C_6H_3)_2$ (**2.11**) (50% thermal ellipsoids). 39
Figure 2.5: Synthesis of $TiCp(NP^tBu_3)(NH(2,6\text{-}^iPr_2)C_6H_3)Cl$ (**2.8**), $Ti(NP^tBu_3)(NH(2,6\text{-}^iPr_2)C_6H_3)_3$ (**2.9**) and $ZrCp(NP^tBu_3)(NH(2,6\text{-}^iPr_2)C_6H_3)_2$ (**2.11**). 40
Figure 2.6: Synthesis of $ZrCp(NP^tBu_3)(NH(2,6\text{-}^iPr_2)C_6H_3)Me$ (**2.10**). 41
Figure 2.7: Variable-temperature ^1H NMR spectra of $TiCp(NP^tBu_3)(NH(2,6\text{-}^iPr_2)C_6H_3)Cl$ (**2.8**) in toluene-d_8. 42
Figure 2.8: Attempts to generate a Group IV phosphinimide imide complex from Mountford's precursor. 44
Figure 2.9: Power's magnesium imide transfer reagent. 45
Figure 2.10: The utility of TMA to generate a Sm imide complex. 45
Figure 2.11: Diversity in the reaction of $TiCp(NP^tBu_3)(NH(2,6\text{-}^iPr_2)C_6H_3)Cl$ (**2.8**) with TMA. 46
Figure 2.12: Synthesis of $Mg_2(\mu\text{-}NP^tBu_3)_2(NP^tBu_3)_2$ (**2.14**) and $Mg_3(\mu\text{-}NP^iPr_3)_4(NP^iPr_3)_2$ (**2.15**). 48
Figure 2.13: ORTEP diagrams of the core fragments of $Mg_2(\mu\text{-}NP^tBu_3)_2(NP^tBu_3)_2$ (**2.14**) and $Mg_3(\mu\text{-}NP^iPr_3)_4(NP^iPr_3)_2$ (**2.15**) (*t*-butyl and *i*-propyl groups omitted for clarity; 50% thermal ellipsoids). 49
Figure 2.14: ORTEP diagram of the core fragment of $Mg_2(\mu\text{-}NP^tBu_3)_2(NP^tBu_3)_2$ (**2.14**), highlighting the agnostic interaction. 49
Figure 2.15: Syndiotactic PMMA. 51
Figure 2.16: ^1H NMR spectrum (in $CDCl_3$, partial spectrum illustrated) of ~70% syndiotactic PMMA generated by $Mg_2(\mu\text{-}NP^tBu_3)_2(NP^tBu_3)_2$ (**2.14**). 51
Figure 3.1 Illustrations of the CGC (**I**) and FI (**II**) precatalysts. 55
Figure 3.2 56

Figure 3.3: Synthesis of the aryl phosphines **3.2** and **3.3**. 74
Figure 3.4: Synthesis of *bis*(phosphinimines) **3.4-3.8**. 75
Figure 3.5: ORTEP drawing of *m*-$(CH_2P^tBu_2NH)_2C_6H_4$ (**3.6**) (50% thermal ellipsoids). 76
Figure 3.6: Product of C-H activation of a phosphinimine ligand by $TiCl_4$. 77
Figure 3.7: Synthesis of *bis*(phosphinimide) titanium complexes. 78
Figure 3.8: Loss of four equivalents of toluene to give the presumed monomeric product $Zr[m\text{-}(CH_2P^tBu_2N)_2C_6H_4]_2$ (**3.20**). 80
Figure 4.1: Synthesis of R_2BnP and *p*-$(CH_2PR_2)_2C_6H_4$, and their trimethylsilyl-phosphinimine derivatives. 111
Figure 4.2: ORTEP drawings of *p*-$(CH_2P^tBu_2)_2C_6H_4$ (**4.5**), $Cy_2BnPNSiMe_3$ (**4.8**) and *p*-$(CH_2PCy_2NSiMe_3)_2C_6H_4$ (**4.10**) (50% thermal ellipsoids). 112
Figure 4.3: Synthesis of bimetallic titanium complexes, *p*-$(CH_2PR_2NTiCp'Cl_2)_2C_6H_4$. 113
Figure 4.4: Related bimetallic phosphinimide complexes. 113
Figure 4.5: ORTEP illustrations of $TiCp(NPCy_2Bn)Cl_2$ (**4.16**) and *p*-$(CH_2PCy_2NTiCpCl_2)_2C_6H_4$ (**4.20**) (CH_2Cl_2 molecule omitted for clarity), representative of a bimetallic complex and its related monometallic analogue (50% thermal ellipsoids). 114
Figure 4.6: Syntheses of *p*-$(CH_2PR_2NTiCp'Me_2)_2C_6H_4$ and $TiCp'(NPR_2Bn)Me_2$ 116
Figure 4.7: Differential molecular weight distribution of a monodisperse polymer sample. 123
Figure 4.8: Bimodal distribution of polymer generated from MAO activation of *p*-$(CH_2P^tBu_2NTiCpMe_2)_2C_6H_4$ (**4.27**). 125
Figure 4.9: A comparison of the polymer that was produced from catalysts derived from *p*-$(CH_2P^tBu_2NTiCp^*Cl_2)_2C_6H_4$ (**4.17**) and its monometallic derivative $TiCp^*(NP^tBu_2Bn)Cl_2$ (**4.13**). 127
Figure 4.10: Possible scenario of the polymer functioning as a large ancillary ligand of an active titanium polymerization catalyst. 127
Figure 4.11: Monitoring the molecular weight distribution over time of the polymer produced by $TiCp^*(NP^tBu_2Bn)Cl_2$ (**4.13**) upon activation with MAO. 128
Figure 4.12: The proposed extension of bimetallic titanium phosphinimide complexes. 132

Figure 5.1: Group IV olefin polymerization precatalysts that show different catalytic activities upon activation, depending on the metal centre. 136
Figure 5.2: An ORTEP depiction of $Zr(NP^tBu_3)_3(NMe_2)$ (**5.2**) (50% thermal ellipsoids). 153
Figure 5.3: Different routes for the synthesis of $Zr(NP^tBu_3)_3(NMe_2)$ (**5.2**). 153
Figure 5.4: Cleavage of the phosphinimide bond from zirconium by TMA. 155
Figure 5.5: Synthesis of assorted zirconium phosphinimide chloride derivatives..... 156
Figure 5.6: ORTEP drawings of $ZrCp(NP^tBu_3)Bn_2$ (**5.13**) and $ZrCp(NP^tBu_3)_2Bn$ (**5.15**) (50% thermal ellipsoids). 158
Figure 5.7: Formation of $ZrCp(NP^tBu_3)(C_6F_5)_2$ (**5.18**). 160
Figure 5.8: Synthesis of isolable cationic zirconium phosphinimide complexes. 161
Figure 5.9: ORTEP depictions of the heavy atom cores (50% thermal ellipsoids) of Zr (IV) cluster derivatives derived from the reaction of $ZrCp^*(NP^tBu_3)Cl_2$ (**5.4**) with TMA (a, b) compared with the proposed product $[ZrCpCl_2]_3CH$ (**5.25**)..... 162
Figure 5.10: Diversity of the anion-cation interaction upon modification of alkyl groups that are σ-bound to the zirconium centre. 167
Figure B.1: Two possible structures of the product of the reaction of *m*-$(CH_2P^tBu_2NH)_2C_6H_4$ (**3.6**) with TMA. 198
Figure B.2: Thermolytically induced loss of benzene, followed by trapping with BTMSA to provide an insertion product, **3.22**. 200

List of Tables

Table 2.1: Crystallographic parameters for **2.4**, **2.8**, **2.9**, **2.11**, **2.12**, **2.13**, **2.14** and **2.15**.. 33

Table 2.2: Select bond distances and angles for $TiCp(NP^tBu_3)(NH(2,6\text{-}^iPr_2)C_6H_3)Cl$ (**2.8**), $Ti(NP^tBu_3)(NH(2,6\text{-}^iPr_2)C_6H_3)_3$ (**2.9**) and $ZrCp(NP^tBu_3)(NH(2,6\text{-}^iPr_2)C_6H_3)_2$ (**2.11**). 41

Table 2.3: Select bond distances and angles for $[Mg(NP^tBu_3)_2]_2$ (**2.14**) and $[Mg(NP^iPr_3)_2]_3$ (**2.15**) 50

Table 3.1: Crystallographic parameters for **3.2**, **3.4**, **3.5**, **3.6**, **3.7**, **3.10**, **3.11**, **3.13**, and **3.14**. 69

Table 3.2: Nitrogen-phosphorus bond distances and $^{31}P\{^1H\}$NMR data (ppm) for the *bis*(phosphinimine) ligands. 76

Table 3.3: Key bond distances and angles for available data of X-ray analyses of chelate complexes of the form $TiLX_2$. 79

Table 3.4: Optimization of ethylene polymerization conditions using $Ti(NP^tBu_3)_2Me_2$ as a standard. 82

Table 3.5: Comparison of the polymerization activities using $Ti[m\text{-}(CH_2PR_2N)_2C_6H_4]X_2$ (R = ^{t}Bu, X = NMe_2 (**3.9**), Br (**3.13**), Me (**3.16**); R = Cy, X = NMe_2 (**3.11**), Cl (**3.14**)) or $Ti(NP^tBu_3)_2X_2$ (X = Cl, Me) as a precursor with activation by MAO 85

Table 3.6: Comparison of the polymerization activities using $Ti[m\text{-}(CH_2P^tBu_2N)_2C_6H_4]Me_2$ (**3.16**) or $Ti(NP^tBu_3)_2Me_2$ as a precursor while activated by $B(C_6F_5)_3$ or $[Ph_3C][B(C_6F_5)_4]$ (TB). 86

Table 4.1: Crystallographic parameters for **4.5**, **4.8**, **4.10**, **4.13**, **4.14**, **4.16**, **4.18**, **4.20**, **4.21**, **4.22**, **4.24**, **4.26**, **4.27** and **4.28**. 104

Table 4.2: Key bond distances and angles for available data from X-ray analysis of $p\text{-}(CH_2PR_2NTiCp'X_2)_2C_6H_4$ and $TiCp'(NPR_2Bn)X_2$ 115

Table 4.3: Comparison of NMR shifts (ppm) for $p\text{-}(CH_2PR_2NTiCp'X_2)_2C_6H_4$ and $TiCp'(NPR_2Bn)X_2$. 117

Table 4.4: Gibson's rating for catalytic performance of ethylene polymerization catalysts. 119

Table 4.5: Schlenk-line polymerization results. 121
Table 4.6: Büchi reactor polymerization results. 122
Table 4.7: Monitoring polymerization activity over time of the catalysts produced from activation of $TiCp^*(NP^tBu_2Bn)X_2$ (X = Cl (**4.13**), Me (**4.21**)) by MAO. 130
Table 4.8: Büchi reactor polymerization results using $[Ph_3C][B(C_6F_5)_4]$ as a discrete activator 131
Table 5.1: Crystallographic parameters for **5.1**, **5.2**, **5.3**, **5.4**, **5.5**, **5.6**, **5.13** and **5.15**. .. 149
Table 5.2: Key bond distances and angles from X-ray analyses of $Zr(NP^tBu_3)_2(NEt_2)_2$ (**5.1**) and $Zr(NP^tBu_3)_3(NMe_2)$ (**5.2**) 154
Table 5.3: Key bond distances and angles from X-ray analyses of various zirconium phosphinimide chloride complexes 157
Table 5.4: Comparison of the polymerization activities using $MCp'(NP^tBu_3)X_2$ (M = Ti, Zr; Cp' = Cp, Cp*; X = Cl, Me) as a precursor and activated by MAO. 164
Table 5.5: Comparison of the polymerization activities using $M(NP^tBu_3)_2X_2$ (M = Ti, Zr; X = Cl, Me) as a precursor when activated by MAO. 166
Table 5.6: Comparison of the polymerization activities using $MCp'(NP^tBu_3)Me_2$ (M = Ti, Zr; Cp' = Cp, Cp*) as a precursor when activated by with equivalents of $B(C_6F_5)_3$ or $[Ph_3C][B(C_6F_5)_4]$ 168
Table A.1: Raw data obtained from the VT NMR experiment 194

Chapter 2 Compound Numbering Scheme

2.1 $LiNH(2,6\text{-}^{i}Pr_2)C_6H_3$

2.2 $TiCp(NP^{t}Bu_3)(NMe_2)_2$

2.3 $TiCp(NPPh_3)(NMe_2)_2$

2.4 $Ti(NP^{t}Bu_3)(NMe_2)_3$

2.5 $TiCp_2(NMe_2)Cl$

2.6 $TiCp(NMe_2)_3$

2.7 $ZrCp(NP^{t}Bu_3)(NMe_2)_2$

2.8 $TiCp(NP^{t}Bu_3)(NH(2,6\text{-}^{i}Pr_2)C_6H_3)Cl$

2.9 $Ti(NP^{t}Bu_3)(NH(2,6\text{-}^{i}Pr_2)C_6H_3)_3$

2.10 $ZrCp(NP^{t}Bu_3)(NH(2,6\text{-}^{i}Pr_2)C_6H_3)Me$

2.11 $ZrCp(NP^{t}Bu_3)(NH(2,6\text{-}^{i}Pr_2)C_6H_3)_2$

2.12 $TiCp(NP^{t}Bu_3)MeCl$

2.13 $Al_2(\mu\text{-}NH(2,6\text{-}^{i}Pr_2)C_6H_3)_2Me_4$

2.14 $Mg_2(\mu\text{-}NP^{t}Bu_3)_2(NP^{t}Bu_3)_2$

2.15 $Mg_3(\mu\text{-}NP^{i}Pr_3)_4(NP^{i}Pr_3)_2$

Chapter 3 Compound Numbering Scheme

3.1 HP^tBu_2

3.2 *m*-$(CH_2P^tBu_2)_2C_6H_4$

3.3 *m*-$(CH_2PCy_2)_2C_6H_4$

3.4 *m*-$(CH_2P^tBu_2NSiMe_3)_2C_6H_4$

3.5 *m*-$(CH_2PCy_2NSiMe_3)_2C_6H_4$

3.6 *m*-$(CH_2P^tBu_2NH)_2C_6H_4$

3.7 *m*-$(CH_2P^tBu_2NH)_2C_6H_4 \cdot 2\ HBr$

3.8 *m*-$(CH_2PCy_2NH)_2C_6H_4$

3.9 Ti[*m*-$(CH_2P^tBu_2N)_2C_6H_4](NMe_2)_2$

3.10 Ti[*m*-$(CH_2P^tBu_2N)_2C_6H_4]Br(NMe_2)$

3.11 Ti[*m*-$(CH_2PCy_2N)_2C_6H_4](NMe_2)_2$

3.12 Zr[*m*-$(CH_2P^tBu_2N)_2C_6H_4](NEt_2)_2$

3.13 Ti[*m*-$(CH_2P^tBu_2N)_2C_6H_4]Br_2$

3.14 Ti[*m*-$(CH_2PCy_2N)_2C_6H_4]Cl_2$

3.15 Zr[*m*-$(CH_2P^tBu_2N)_2C_6H_4]Cl_2$

3.16 Ti[*m*-$(CH_2P^tBu_2N)_2C_6H_4]Me_2$

3.17 Ti[*m*-$(CH_2P^tBu_2N)_2C_6H_4]Bn_2$

3.18 $Ti(NP^tBu_3)_2(CH_2Si(CH_3)_3)_2$

3.19 $Ti(NP^tBu_3)_2(SiPh_3)_2$

3.20 Zr[*m*-$(CH_2P^tBu_2N)_2C_6H_4]_2$

3.21 Al[*m*-$(CH_2P^tBu_2N)(CH_2P^tBu_2NH)C_6H_4]Me_2$

3.22 $Ti(NP^tBu_3)_2Ph_2 + Me_3SiCCSiMe_3$

Chapter 4 Compound Numbering Scheme

4.1 *p*-$(CH_2C_9H_7)_2C_6H_4$

4.2 *p*-$(CH_2C_9H_6SiMe_3)_2C_6H_4$

4.3 $^tBu_2BnP$

4.4 Cy_2BnP

4.5 *p*-$(CH_2P^tBu_2)_2C_6H_4$

4.6 *p*-$(CH_2PCy_2)_2C_6H_4$

4.7 $^tBu_2BnPNSiMe_3$

4.8 $Cy_2BnPNSiMe_3$

4.9 *p*-$(CH_2P^tBu_2NSiMe_3)_2C_6H_4$

4.10 *p*-$(CH_2PCy_2NSiMe_3)_2C_6H_4$

4.11 *p*-$(CH_2P^tBu_2NH)_2C_6H_4$

4.12 *p*-$(CH_2PCy_2NH)_2C_6H_4$

4.13 $TiCp^*(NP^tBu_2Bn)Cl_2$

4.14 $TiCp^*(NPCy_2Bn)Cl_2$

4.15 $TiCp(NP^tBu_2Bn)Cl_2$

4.16 $TiCp(NPCy_2Bn)Cl_2$

4.17 *p*-$(CH_2P^tBu_2NTiCp^*Cl_2)_2C_6H_4$

4.18 *p*-$(CH_2PCy_2NTiCp^*Cl_2)_2C_6H_4$

4.19 *p*-$(CH_2P^tBu_2NTiCpCl_2)_2C_6H_4$

4.20 *p*-$(CH_2PCy_2NTiCpCl_2)_2C_6H_4$

4.21 $TiCp^*(NP^tBu_2Bn)Me_2$

4.22 $TiCp^*(NPCy_2Bn)Me_2$

4.23 $TiCp(NP^tBu_2Bn)Me_2$

4.24 $TiCp(NPCy_2Bn)Me_2$

4.25 *p*-$(CH_2P^tBu_2NTiCp^*Me_2)_2C_6H_4$

4.26 *p*-$(CH_2PCy_2NTiCp^*Me_2)_2C_6H_4$

4.27 *p*-$(CH_2P^tBu_2NTiCpMe_2)_2C_6H_4$

4.28 *p*-$(CH_2PCy_2NTiCpMe_2)_2C_6H_4$

4.29 $[TiCp^*(NP^tBu_2Bn)Me][MeB(C_6F_5)_3]$

Chapter 5 Compound Numbering Scheme

5.1 $Zr(NP^tBu_3)_2(NEt_2)_2$

5.2 $Zr(NP^tBu_3)_3(NMe_2)$

5.3 $ZrCp(NP^tBu_3)Cl_2$

5.4 $ZrCp^*(NP^tBu_3)Cl_2$

5.5 $ZrCp(NP^tBu_3)_2Cl$

5.6 $ZrCp_2(NP^tBu_3)Cl$

5.7 $Zr(NP^tBu_3)_2Cl_2$

5.8 $Zr(NP^tBu_3)_3Cl$

5.9 $ZrCp(NP^tBu_3)Me_2$

5.10 $ZrCp(NP^tBu_3)_2Me$

5.11 $ZrCp_2(NP^tBu_3)Me$

5.12 $Zr(NP^tBu_3)_2Me_2$

5.13 $ZrCp(NP^tBu_3)Bn_2$

5.14 $ZrCp^*(NP^tBu_3)Bn_2$

5.15 $ZrCp(NP^tBu_3)_2Bn$

5.16 $ZrCp(NP^tBu_3)[CH_2Si(CH_3)_3]_2$

5.17 $ZrCp(NP^tBu_3)Ph_2$

5.18 $ZrCp(NP^tBu_3)(C_6F_5)_2$

5.19 $[ZrCp(NP^tBu_3)_2][BnB(C_6F_5)_3]$

5.20 $[ZrCp(NP^tBu_3)(N^iPrC(CH_3)N^iPr)][MeB(C_6F_5)_3]$

5.21 $[ZrCp^*(NP^tBu_3)(N^iPrC(CH_3)N^iPr)][MeB(C_6F_5)_3]$

5.22 $[ZrCp(NP^tBu_3)Me(THF)][MeB(C_6F_5)_3]$

5.23 $[ZrCp(NP^tBu_3)Me(NMe_2Ph)][B(C_6F_5)_4]$

5.24 $[ZrCp^*(NP^tBu_3)Me][B(C_6F_5)_4]$

5.25 $[ZrCpCl_2]_3CH$

List of Abbreviations

Å	angstrom
ABq	AB quartet
Abs coeff	absorption coefficient
ACS	American Chemical Society
Anal. Calc'd	analysis calculated
Bn	benzyl
br	broad
BTMSA	*bis*(trimethylsilyl)acetylene
CCD	Charge Coupled Device
CD	compact disc
Cp	cyclopentadienyl
Cp*	pentamethylcyclopentadienyl
Cy	cyclohexyl
d	doublet
dd	doublet of doublets
ddd	doublet of doublet of doublets
D_{calc}	calculated density
DEPT	Distortion Enhancement by Polarization Transfer
d(m)	doublet of multiplets
DSC	differential scanning calorimetry
Et	ethyl
FI	*F*enokishi-*I*min Haiishi or *F*ujita group *I*nvented catalysts
g	gram(s)
GoF	goodness of fit
GPC	gel permeation chromatography
h	hour
H	proton(s)
HETCOR	HETeronuclear CORrelation spectroscopy
HMQC	Heteronuclear Multiple Quantum Coherence

HPLC	High Performance Liquid Chromatography
Hz	hertz
^{i}Pr	isopropyl
J	coupling constant
m	multiplet
m	meta
M	molar (mol L^{-1})
M_n	number molecular weight (g mol^{-1})
M_w	weight-averaged molecular weight (g mol^{-1})
M_z	z-molecular weight (weight^2 average, g mol^{-1})
MAO	methylaluminoxane
Me	methyl
MHz	megahertz
min	minute
mL	millilitre
μL	microlitre
MMAO	modified methylaluminoxane
mmol	millimole
mol	mole
^{n}Bu	normal butyl
NMR	nuclear magnetic resonance
o	ortho
ORTEP	Oak Ridge Thermal Ellipsoid Plot
p	para
Ph	phenyl
ppm	parts per million
pseudo t	pseudo triplet (i.e. overlapped dd)
q	quartet
R	residual
R_w	weighted residual
RT	room temperature

s	singlet
t	triplet
^{t}Bu	tertiary butyl
THF	tetrahydrofuran
T^{i}BAl	tri*iso*butylaluminum
δ	chemical shift

1 Introduction

1.1 Overture

The primary motivation of the work detailed in this thesis is to explore the synthesis and utility of Group IV phosphinimide complexes as possible catalytic precursors. In general, advances in the synthetic chemistry of Group IV complexes result from the search for catalytic precursors, particularly those for insertion olefin polymerization catalysis.[1-6] The desire to circumvent existing patents has encouraged numerous collaborative efforts between academic and industrial laboratories. However, despite the immense interest in generating new insertion polymerization catalysts, only a few have successfully made the transition to commercial application. In addition to producing a catalyst with a high turnover frequency and/or extended lifetime, it is often desirable to tailor the active site so that specific polymer products are manufactured. The most logical method to achieve this is to create different ligand environments or to tune the engineering of the polymerization to obtain the desired outcome. Ultimately, most targets do not function well as catalysts, therefore rationalization for the low activity or investigation into dominant deactivation processes is often performed to account for the observed results. Among the more profitable catalytic candidates, mechanistic information is obtained whenever possible.

In keeping with these objectives, the chemistry of Group IV complexes performed in the Stephan research laboratories has involved progress in olefin polymerization technology through the synthesis of new catalyst precursors or by determining the mode of catalyst activation or deactivation, where possible.[7-21] More specifically, the pioneering use of the phosphinimide ligand (NPR_3) as an ancillary ligand in highly active titanium polymerization catalysts has fostered an increased general interest, and other research groups have exploited this ligand system on a variety of metals for various catalytic purposes.[22-27] This thesis describes the manipulation of known and new organometallic complexes in an attempt to execute catalytic functions (Chapter 2), the design and synthesis of novel ligands applied to titanium complexes (Chapters 3 and 4),

and the extension of the use of phosphinimide ligands to prepare zirconium complexes and subsequently, examine their reactivity with strong Lewis acids (Chapter 5).

To assist the reader in appreciating the scope of this research, this chapter reviews Group IV inorganic and organometallic complexes and where possible, highlights their use as catalytic reagents. Emphasis of the synthetic achievements will be placed on those complexes pursued specifically for the purposes of improving olefin polymerization catalysis, either by attempting to create more active catalyst systems, or by preparing specific polymer products. It should be noted that this survey is not intended to be comprehensive, and olefin polymerization catalysis, including the synthesis of a variety of transition metal precatalysts, and pertinent theoretical and mechanistic investigations, has been extensively reviewed.[i, 28-40]

1.2 Group IV Imide Complexes as Synthetic Targets

1.2.1 Common Synthetic Approaches

The isolation or generation of Group IV imide complexes is a recent accomplishment.[41-43] Since the advent of this area, numerous research groups have developed new synthetic routes or used Group IV imide complexes as mediators for a variety of transformations.[44-48] The first isolated examples of zirconium imide complexes were reported by Bergman and co-workers,[41] while the first titanium imide derivative was reported by Roesky and co-workers[43] (Figure 1.1). Typically, an isolable monomeric structure is achieved in the presence of a Lewis base or with the use of bulky ancillary ligands. However, in the absence of Lewis bases or sufficiently bulky ligands, dimers normally result in which the imide ligand bridges two metal centres.[49-51] The latter dimeric type of structure has been exploited in the preparation of early-late heterobimetallic complexes,[52-54] although they will not be discussed in further detail.

[i] Thematic issues of *Chemical Reviews* and *Topics in Catalysis* have been published that provide an excellent synopsis of topics and papers related to insertion olefin polymerization, activators and theoretical and mechanistic insights. *Chem. Rev.* (**2000**), *100, 4*; *Topics in Catalysis* (**1999**), *7, 1*.

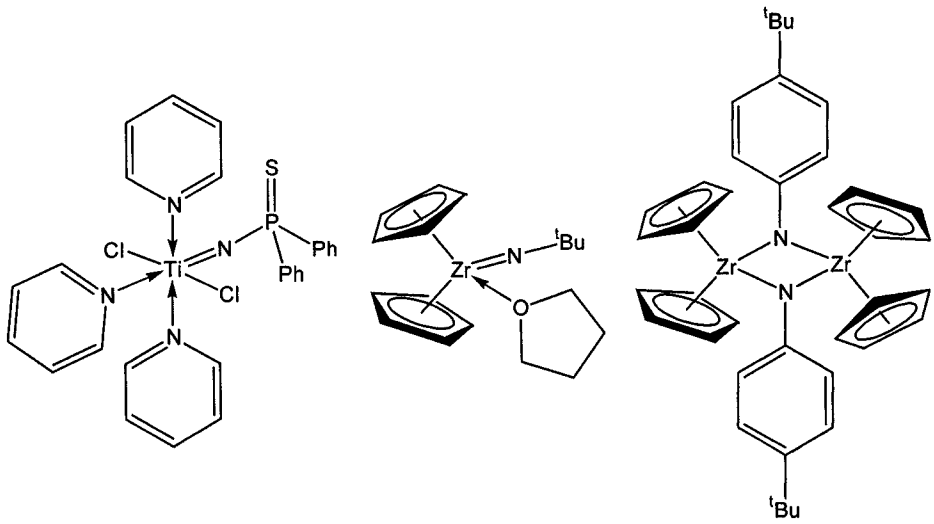

I **II** **III**

Figure 1.1: The first isolated titanium (**I**)[43] and zirconium (**II**, **III**)[41] imide complexes.

Several well-established routes to Group IV imide complexes exist. Thermolysis of $ML_2(NHR)R'$ (M = Ti, Zr; L = ancillary ligand; R = bulky group, R' = Ph, Me) or $ZrL_2(NHR)_2$ has resulted in the elimination of an alkane, arene or primary amine to provide the desired imide complex, even if only transiently.[41,42,50,55] Alternatively, Group IV imides have formed spontaneously at ambient temperatures. For example, addition of four equivalents of LiNHAr (Ar = 2,6-$^{i}Pr_2C_6H_3$) to $ZrCl_4 \cdot THF_2$ in the presence of THF and pyridine resulted in the formation of $Zr(NAr)(NHAr)_2Py_2$.[49] A related method reported by Mountford and co-workers described the reaction of an excess of $^{t}BuNH_2$ with $TiCl_4$, followed by addition of *t*-butyl pyridine (^{t}BuPy), to provide $Ti(N^{t}Bu)Cl_2(^{t}BuPy)_2$ in good isolated yield.[56] This imide product, and similar derivatives that have bulky aryl groups on the imide nitrogen atom, have served as synthetic precursors for conversion to a diverse number of inorganic[56-65] and organometallic[56,66,67] complexes.

1.2.2 Group IV Imide Complexes as Catalysts

Group IV imide complexes are of importance since they have demonstrated efficacy in a variety of catalytic processes. Although most frequently recognized for their role in reversible C-H activation,[68-70] imine metathesis[71-73] or hydroamination,[74-77] other applications have also been reported. For example, individual reports revealed that titanium imide complexes serve as initiators for the syndiospecific polymerization of methyl methacrylate,[78,79] perform kinetic resolution and stereoinversion of allenes,[80,81] or act as a mediator for the guanylation of amines and transamination of guanidines.[47] In order to demonstrate the value of Group IV imide complexes as catalysts, it is worthwhile to look at some specific illustrations.

Significant details of reversible C-H activation by imido complexes such as $Ti(NSi^tBu_3)(OSi^tBu_3)_2$ and $Zr(NSi^tBu_3)(NHSi^tBu_3)_2$ are known, primarily due to the mechanistic work performed by Wolczanski and co-workers.[42,68,69,82] Both imido species are transient in the absence of a Lewis base or some other stabilizing factor such as bulky ligands, attesting to their high reactivity. In an elegant demonstration, a series of precursors of the general formula $Ti(NHSi^tBu_3)(OSi^tBu_3)_2R$ were heated in the presence of different alkanes or arenes (R') to produce $Ti(NHSi^tBu_3)(OSi^tBu_3)_2R'$ (Figure 1.2). This equilibrium is proposed to be the result of a two-step process in which RH is extruded to form $Ti(NSi^tBu_3)(OSi^tBu_3)_2$ which then reacts with R'H to form the final product. Equilibrium constants were determined experimentally, and in combination with kinetic data, revealed that C-H bond addition is preferred in the order of Ph-H>CH_3-H>$PhCH_2$-H.[82] Supporting results from a recent theoretical investigation have suggested that alkane coordination to the titanium imide complex precedes the transition state.[83]

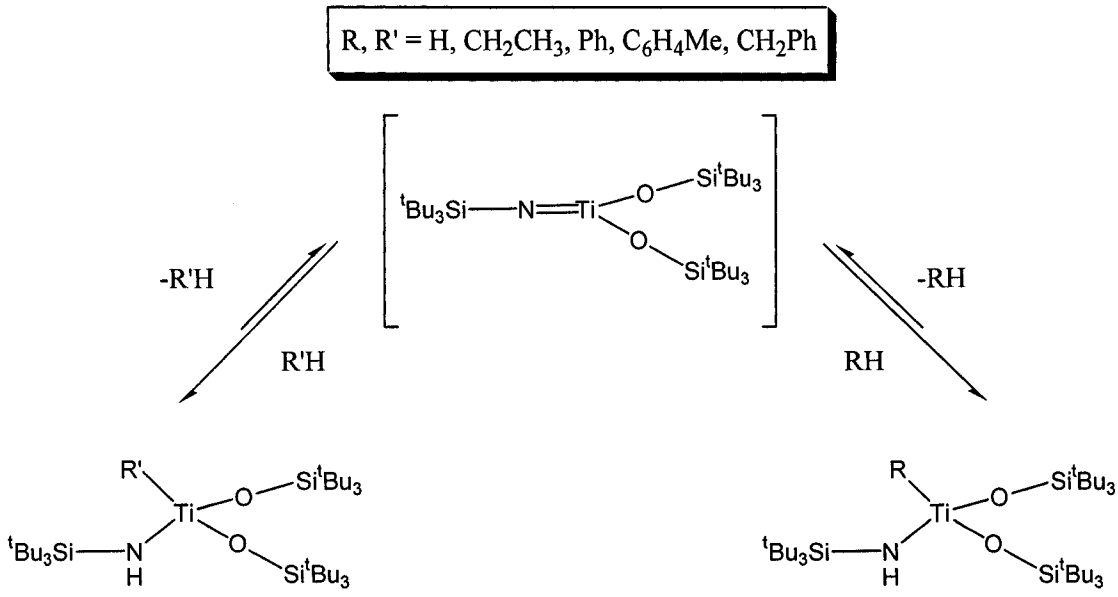

Figure 1.2: Reversible C-H activation by a titanium imide complex.[82]

Imine metathesis may be mediated by zirconium imide complexes.[71,72,84] Studies performed by Bergman and co-workers have indicated that the mechanism proceeds via a formal [2 + 2] cycloaddition reaction between the zirconium imide double bond and the imine fragment of the organic substrate (Figure 1.3).[73,84] The lifetimes of zirconium imide metathesis catalysts have been prolonged by increasing the steric bulk of the ancillary ligands. This effectively precludes dimerization of the active catalytic species, which was determined to be a deactivation pathway since its formation is irreversible under the catalytic conditions employed.[73]

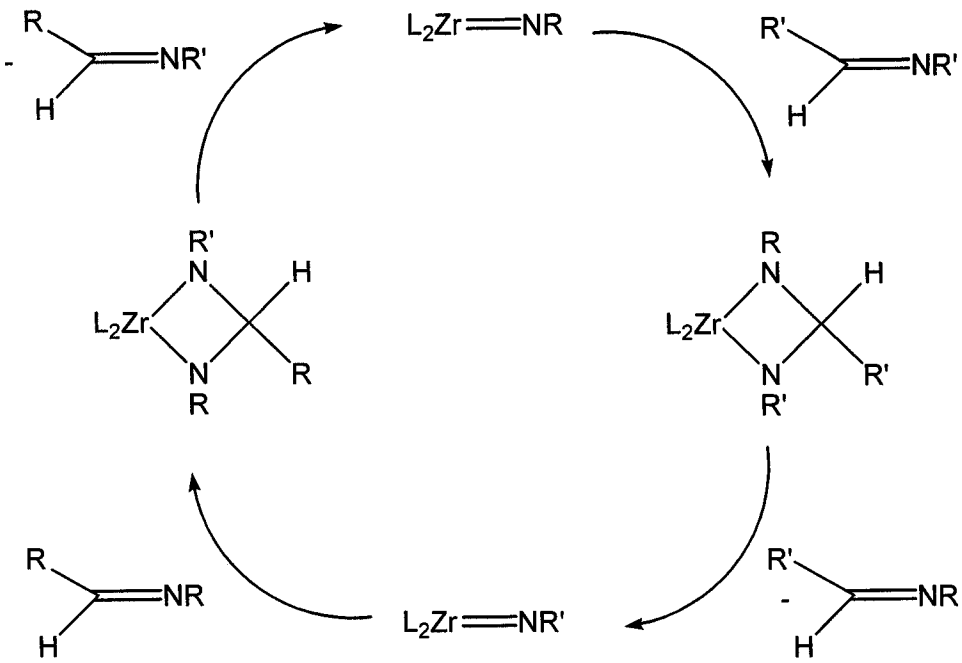

Figure 1.3: Possible mechanism of imine metathesis as catalyzed by a zirconium imide complex.[73]

Hydroamination is related to the imine metathesis reactions described above, since [2 + 2] coupling of an alkyne with the Group IV imide precursor is considered to be the first step of the catalytic cycle.[77,85,86] The proposed mechanism in the presence of an excess of primary amine involves cleavage of the metallaazacyclobutene intermediate by addition of the amine across the metal-carbon bond. Subsequent elimination of the enamine, which tautomerizes to the imine, regenerates the Group IV imide complex (Figure 1.4). Several reports describe hydroamination catalysis performed using a metal precursor that does not possess an imide ligand,[27,87] although in these cases, the metal-nitrogen double bond is presumed to be generated *in situ*.[86] Finally, a recent comparative study performed by Odom and co-workers has demonstrated that increasing the Lewis acidity of the titanium centre correlates to increased rates of hydroamination.[88]

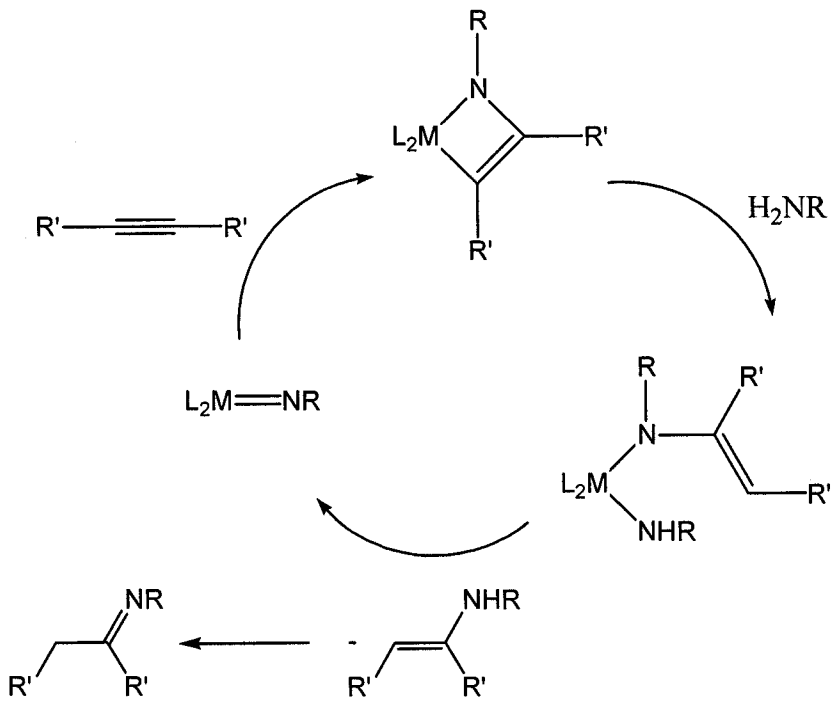

Figure 1.4: Proposed mechanism of hydroamination by Group IV imide complexes (M = Ti, Zr).[86]

1.3 Olefin Polymerization Catalysis Employing Group IV Precursors

1.3.1 Overview

Specific requirements exist for insertion polymerization catalysts derived from Group IV complexes. Typically, homogeneous polymerization catalysts are complexes that contain a titanium or zirconium metal in the +4 oxidation state, in addition to a metal-carbon σ-bond. A strongly Lewis acidic (cationic) site is generated by activation of the transition metal with a Group XIII-based co-catalyst such as methylaluminoxane (MAO).[1] Coordination of the monomer to generate a π-complex occurs, followed by insertion into the metal-carbon bond (Figure 1.5).[89] This necessitates rigorous exclusion of oxygen, water, and other impurities since Group IV cationic sites are by nature highly reactive and susceptible to deactivation by Lewis bases.[89]

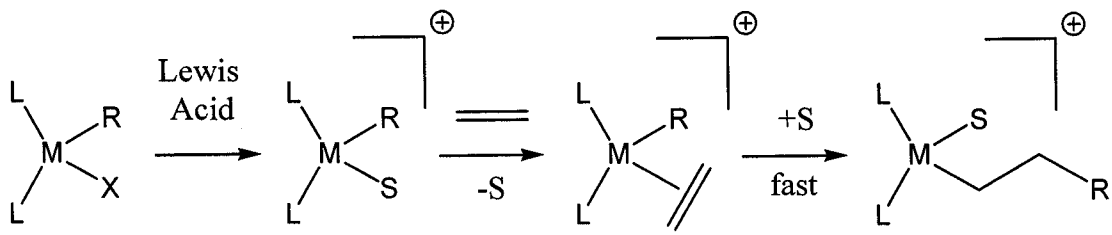

Figure 1.5: Insertion polymerization of ethylene performed by a generic Group IV cationic complex (M = Ti, Zr, L = ancillary ligand, R = alkyl substituent, X = ligand that may be abstracted, S = solvent or anion).[33,90,91]

Activators

The most commonly employed activator of Group IV olefin polymerization precatalysts is MAO, and it is often used in large excess (*ca.* 500-1000 equivalents). MAO has two purposes: it effectively eliminates impurities in the solvent or monomer feedstock that would ordinarily react with the catalyst, and it also provides the polymerization-active species by activating the Group IV metal centre.[92] This is performed by abstracting a ligand of a dialkyl precursor to generate a formally cationic centre, or by alkylating a dihalide precursor to generate ML_2MeX, which is subsequently converted to the active species upon abstraction of the second halide ligand. Since the initial synthesis of MAO from reaction of trimethylaluminum (TMA) with water,[93,94] a significant number of experimental[95,96] and theoretical[95,97] investigations were attempted to determine its exact composition.[92,98,99] MAO is presumed to be an oligomeric structure of general formula $[AlO(CH_3)]_n$, although modern ^1H NMR measurements suggest a methyl to aluminum ratio of 1.5 or higher, depending on the supplier. This NMR evidence indicates that TMA is present in MAO, which is significant because TMA can greatly influence the polymerization activity.[100]

Other co-catalysts that have received much attention include $B(C_6F_5)_3$[101,102] and $[Ph_3C][B(C_6F_5)_4]$.[103] These are efficient activators, since only one equivalent per metal centre is required to obtain an active catalyst (Figure 1.6). Boron-based co-catalysts are used extensively in academic studies since their well-defined molecular structures are better suited to mechanistic studies. Their use in commercial practice is limited to date

however, since they are expensive to manufacture relative to the aluminum-based alternatives (MAO).

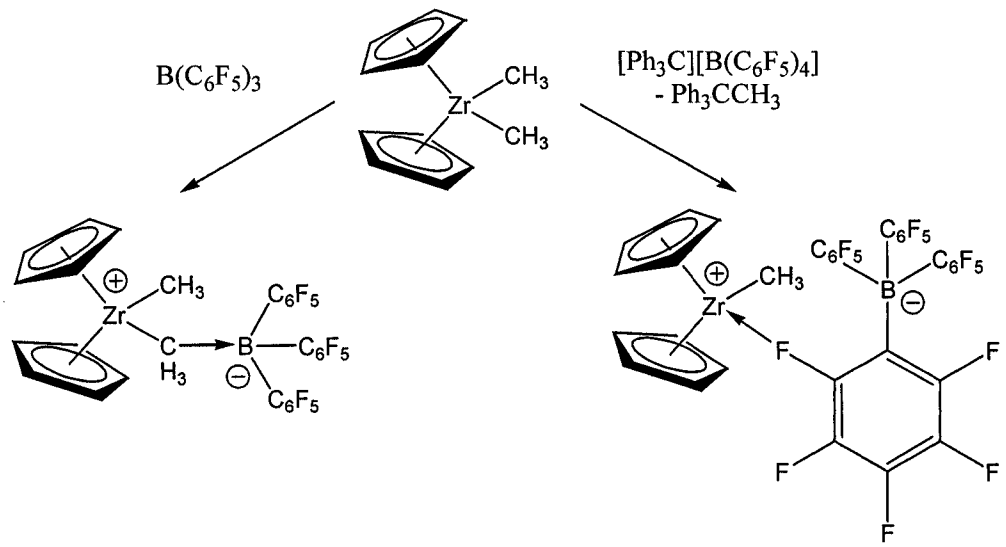

Figure 1.6: Use of borane or borate activators with $ZrCp_2Me_2$ to generate a single "cationic" site.[103,104]

Polymer Analysis

Characterization of the polymers that are produced by homogeneous polymerization Group IV catalysts is also a key component of polymer research. Although a variety of methods exist to characterize the polymer product,[89] gel permeation chromatography (GPC) is the technique most commonly used. Analysis by GPC serves to reveal the nature of the polymer molecular weight distribution. In particular, GPC analysis provides number averaged molecular weight (M_n in g mol^{-1}), weight averaged molecular weight (M_w in g mol^{-1}), and polydispersity index (PDI) (Equations 1.1.a-c) relative to standards that are used to calibrate the instrument. During the process of polymer analysis the solution is filtered, which effectively removes solids that could damage the column; however, any material that is filtered would be excluded from the

analysis, which is a significant source of error associated with GPC chromatography. Some of the physical polymer properties are dependent on the molecular weight distribution, and often specific values are desired to produce plastics for different types of applications.[105] When α-olefin monomer units are used as polymer precursors, it is advantageous to ascertain the tacticities of the product, since this influences the overall physical properties. However, this is not discussed in detail since it is not relevant for polyethylene products produced by Group IV catalysts.[ii]

$$M_n = \frac{\Sigma N_i M_i}{\Sigma N_i} \quad \textbf{a} \qquad M_w = \frac{\Sigma N_i M_i M_i}{\Sigma N_i M_i} \quad \textbf{b} \qquad PDI = \frac{M_w}{M_n} \quad \textbf{c}$$

N_i number of molecules of fraction i

M_i mass of molecules of fraction i

Equation 1.1.a-c: Statistical equations for M_n, M_w (g mol^{-1}) and PDI.

1.3.2 Successful Group IV Polymerization Catalysts

A considerable amount of synthetic effort has been expended in an attempt to produce novel Group IV complexes that function as catalysts for insertion olefin polymerization.[1-6] This continues to be an active field of research worldwide, and it is worthwhile to briefly describe some of the key successes in this domain, particularly when they are of commercial importance. Thus, several examples of efficient Group IV

[ii] Group IV catalysts that polymerize ethylene tend to produce linear polymers in the absence of an α-olefin co-monomer. The advent of late transition metal catalysts has transformed the focus of polymerization research, however: using ethylene as a single feedstock, highly branched polymers are produced due to the "chain-walking" phenomenon. Ittel, S. D.; Johnson, L. K.; Brookhart, M. *Chem. Rev.* **2000**, *100*, 1169-1203.

polymerization catalysts are highlighted to illustrate key advances in polymerization technology.

Metallocenes

The discovery that $ZrCp_2Cl_2$ polymerizes ethylene upon activation by MAO, originally reported by Sinn and Kaminsky,[106,107] initiated intense study into homogeneous polymerization catalysis by Group IV complexes that possess the metallocene framework.[33,108,109] This represents a significant advancement in polymerization technology for a number of reasons. First, the homogeneous nature of metallocene catalysts has been extremely helpful in mechanistic studies. In addition, metallocenes have provided access to different types of stereospecific polymers.[33,110] Zirconocene complexes function as single-site catalysts upon activation by MAO, producing polymers with narrow molecular weight distributions (PDI value of *ca.* 2). Modification of the cyclopentadienide ligands, and subsequently, the metallocene catalysts that are generated, can have a profound effect on the microstructure of the polymer when α-olefins are employed as the monomer. The polymerization activity is also greatly influenced by the cyclopentadienide ligands.[33,111,112] Modifications include the use of fluorenide or indenide substituents, tethering the two ligands by a bridging group to generate an *ansa*-metallocene complex (Figure 1.7), or addition of pendant bulky alkyl groups.[113] Heterogeneous catalysts have also been developed that incorporate zirconocenes, and these are of particular interest due to their applications in commercial processes.[114-116]

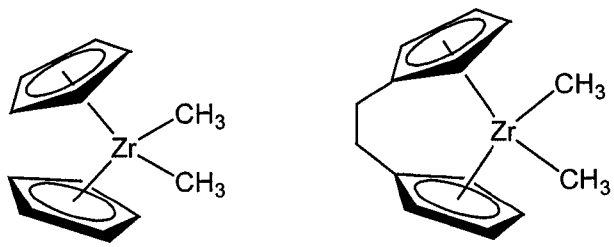

Figure 1.7: Difference between a metallocene and an *ansa*-metallocene.

Constrained Geometry Catalyst (CGC)

The half-sandwich ligand scaffold of the constrained geometry catalyst (CGC) was initially reported as part of a scandium complex by Bercaw and co-workers.[117] Soon after, use of the chelating ligand on titanium to afford a highly active catalyst for the polymerization of olefins upon activation by MAO was disclosed simultaneously by Dow and Exxon in the patent literature (Figure 1.8).[118,119] It was reported that the high polymerization activity is the result of a more open metal centre, hence the naming of "constrained geometry" to describe the ligand system. A direct consequence is better access of the cationic metal centre to the incoming monomer.[90] However, this feature appears to be part of a delicate balance, since similar catalysts that possess a bridging carbon atom rather than a silicon atom are not nearly as active. They are considered to be "too constrained", or readily subject to deactivation processes.[120,121] Efforts to produce an active constrained geometry type of polymerization catalyst with different heteroatoms have thus far been unsuccessful.[32,40,122-124]

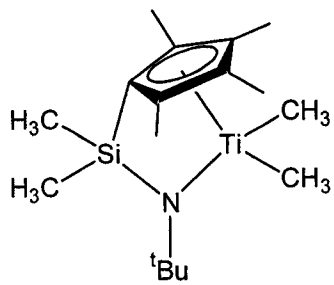

Figure 1.8: The constrained geometry catalyst precursor.

Constrained geometry catalysts readily incorporate α-olefin co-monomers, which permits the polymer properties to be modified by changing the type or concentration of co-monomer. The polyethylene polymers that are generated using the CGC have narrow polydispersities in addition to long-chain branches, which permits an ease of processing generally not observed with metallocene-based catalysts.[90] For these reasons, the

mechanism of polymerization performed by the CGC catalyst has been the subject of theoretical interest.[90,125-130]

Phosphinimide-Based Catalysts and Their Related Analogues

The complexes $TiCp(NPPh_3)Cl_2$ and $TiCp(NCBu^tBu)Cl_2$ were reported originally by Latham and workers in 1986,[131] however, it was only recently that modification of the phosphinimide[8,20,21,132,133] or ketimide[134,135] ligands has produced olefin polymerization catalyst precursors. For example, both $Ti(NP^tBu_3)_2Me_2$ and $TiCp(NP^tBu_3)X_2$ (X = Cl; X = Me, Figure 1.9) are extremely active polymerization catalysts upon activation with the appropriate Lewis acid, affording activities higher than those reported when $ZrCp_2Cl_2$ or the CGC catalyst are used as a precursor.[7,8,21] The explanation proffered for the high catalyst activity involved a steric and an electronic comparison of the $[NP^tBu_3]^-$ ligand to the $[Cp]^-$ ligand.

The steric argument involves examination of the similarities of the effective cone angles of the ancillary ligands.[136,137] The cyclopentadienide ligand has a cone angle of 83°, while the cone angle value reported for the tri-*t*-butyl phosphinimide ligand is 87°.[21] It is noteworthy that the steric bulk directly at the titanium centre is diminished relative to the *bis*-cyclopentadienide analogue, and an increase in polymerization activity may be rationalized in a similar manner as the CGC (*vide supra*), namely that a more "open" metal centre is more accessible to the monomer units. The electronic analogy of the $[NP^tBu_3]^-$ ligand to the $[Cp]^-$ ligand has been performed by Dehnicke and co-workers, and is based on the ability of the phosphinimide ligand to donate π-electron density to the metal centre.[138]

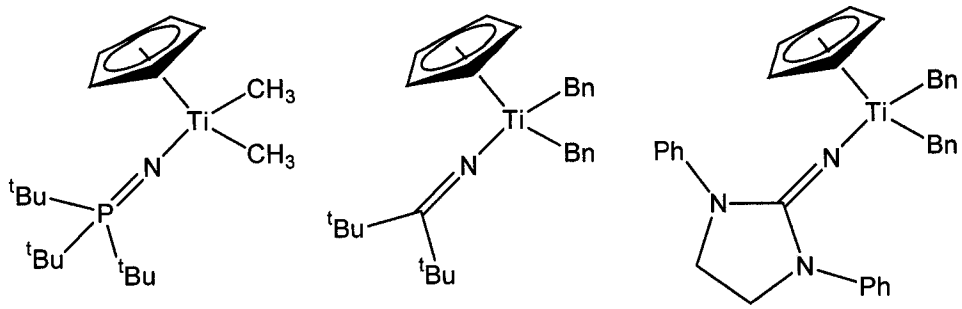

I **II** **III**

Figure 1.9: Active polymerization catalysts that possess the phosphinimide (NPR_3, **I**),[21] ketimide (NCR_2, **II**)[135] or guanidinide ($NC(NR)_2$, **III**)[139] ligands.

The related complexes $TiCp(NC^tBu_2)Bn_2$[134,135] and $TiCp\{NC[N(Ph)CH_2]_2\}Bn_2$[139] (Figure 1.9) are also highly efficient catalysts for olefin polymerization upon activation by $B(C_6F_5)_3$. Similar justification for high catalyst activity based on steric grounds and increased π-electron donation from the ancillary ligand to the metal centre was described.

Fenokishi-Imin Haiishi (FI) Catalysts

Recently, scientists from Mitsui Chemicals Inc. have disclosed a series of titanium- and zirconium-based polymerization catalysts of unprecedented activity (turnover frequency of 42,900 s^{-1})[140] based on the salicylaldiminide ligand to produce high molecular weight polyethylene (Figure 1.10).[140-147] The so-called FI catalysts are named for the Japanese nomenclature of phenoxy-imine (*Fenokishi-Imin*) ligands.[148] Similar titanium catalysts have been disclosed by Coates and co-workers,[149] and both research teams have independently reported that the catalysts could be used to prepare highly syndiospecific polymers using propylene as a feedstock.[147,149] This series of polymerization catalysts represents a significant achievement, both from industrial (high activity) and academic (mechanism,[150,151] living polymerization[145,149]) perspectives. The attainment of such high activity is attributed to an electron-rich, chelating ligand with sufficient steric bulk to stabilize the catalyst.[144]

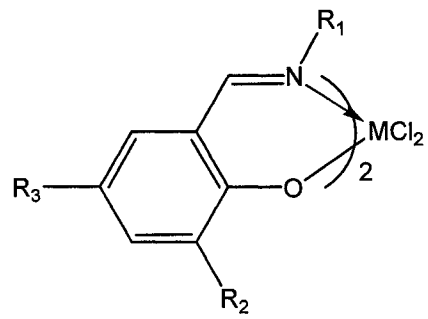

Figure 1.10: Highly active polymerization catalyst precursors derived from Group IV salicylaldiminide complexes.

Bimetallic Catalysts

Group IV bimetallic complexes have potential as catalytic precursors to synthesize polymers of atypical structure in a controlled and cooperative manner upon activation by an appropriate Lewis acid. Most bimetallic titanium or zirconium olefin polymerization catalysts that have been reported produce a polymer that possesses a broad molecular weight distribution.[152-157] From an industrial perspective, this is not undesirable, since polymers that have broad molecular weight distributions are more readily processed than those that have PDI values < 2.[158,159] However, the most sophisticated advances involve a demonstration of the cooperative nature of bimetallic polymerization catalysts.[160,161]

Active, bimetallic polymerization catalysts have been synthesized that incorporate a metallocene[162,163] or CGC-based[164] ligand system (Figure 1.11). In general, the bimetallic metallocene catalyst activity increased as the concentration of MAO increased, while the polymer molecular weight distribution remained narrow (PDI *ca.* 3). The authors note that this observation correlates with more active sites being produced upon addition of higher concentrations of activator.[162] In a separate example, $^{13}C\{^{1}H\}$ NMR analysis of the polymers generated by bimetallic constrained geometry catalysts revealed significant branching relative to the polymer produced by the monomeric analogues. Similarities in polymerization activities and polymer molecular weight distributions lead

Marks and co-workers to propose that the branching was a cooperative chain transfer effect between the two metal centres.

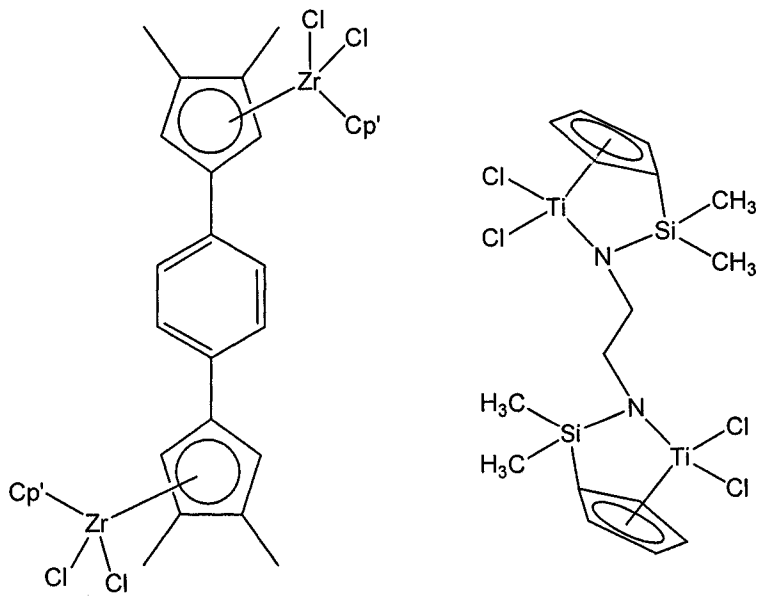

I **II**

Figure 1.11: Bimetallic complexes based on a metallocene- (**I**)[162] and CGC-type (**II**)[165] ancillary ligand.

1.3.3 Catalyst Considerations: From the Active Species to Cation Decomposition Pathways

Influence of the Counterion

Increasing evidence indicates that the active polymerization catalyst is strongly influenced by factors such as solvent or the anion.[99] Model systems, where a Group IV precursor is reacted with a Lewis acid such as $AlCl_3$ or $B(C_6F_5)_3$, have demonstrated the existence of solvent-separated (SSIP) or closed/contact (CIP) ion pairs and solvated cation-anion pairing (SCAP) or resonance-stabilized pairing of the catalyst with the anion (Figure 1.12).[166-169] In practice, the relative polymerization ability of the ion pairs is presumed to increase in the order of SCAP<CIP<<SSIP, however the validity of the

model of a SSIP, or a distinct Group IV cation, has been the subject of deliberation.[99] DFT experiments have proposed the "existence of a continuum" of bonding that varies between weak and strong ion-pair interactions.[170] Furthermore, an anion-exchange study of alkyl zirconocene borate ion pairs performed by Brintzinger and co-workers has suggested that it is likely zirconocene alkyl cations (SSIP) do not exist.[171] Direct endorsement for this was reported very recently by Landis and co-workers, who used NMR spectroscopy to observe *continuous* insertion polymerization *in situ* using *rac*-(C_2H_4(1-indenyl)$_2$)ZrMe(MeB(C_6F_5)$_3$). Continuous polymerization implies that the counterion re-coordinates to the cation subsequent to every monomer insertion; an intermittent polymerization mechanism would imply that that numerous insertions occur prior to the ion-pair reforming, and that the cation exists as a discrete entity.[172] It has even been proposed that the concept of the anion binding after every insertion may, in part, account for the tacticity of polymers generated when α-olefins are used as the monomer.[173]

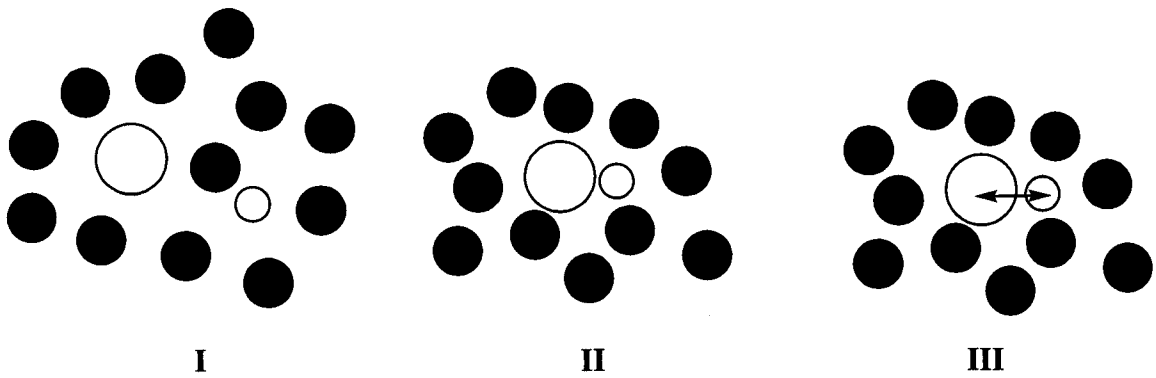

Figure 1.12: Solvent-separated ion pair (**I**), contact ion pair (**II**) and resonance stabilized ion pair (**III**). The dark circles represent solvent molecules, while the large and small white circles represent the anion and cation, respectively.[169]

In the absence of Lewis bases,[174-180] a variety of different types of stabilization of Group IV cationic complexes have been observed both in solution and in the solid state.[92,181,182] For example, in cases where dimethyl Group IV precursors are treated with $B(C_6F_5)_3$, select crystallographic analyses have identified that one of the methyl groups

bridges the zirconium metal and the boron centre (Figure 1.13).[8,104,183] Solution studies have demonstrated that the structure is dynamic, and the borane reagent switches from one methyl group to the other.[184,185] However, when dibenzyl Group IV complexes are used as metal precursors, several different modes of stabilization have been noted. Bochmann and co-workers have observed η^2-coordination of the zirconium centre to the *ipso* carbon of the tethered benzyl group (Figure 1.13) for a variety of metallocenes.[186,187] Alternatively, π-coordination of an aryl group originating from toluene solvent,[188-190] a tethered substituent with a phenyl ligand (Figure 1.13),[191-194] or the aryl group of a $PhCH_2B(C_6F_5)_3$ counterion[187,193,195] has been observed for zirconium complexes that are often more electron-deficient than the analogous metallocene derivatives.

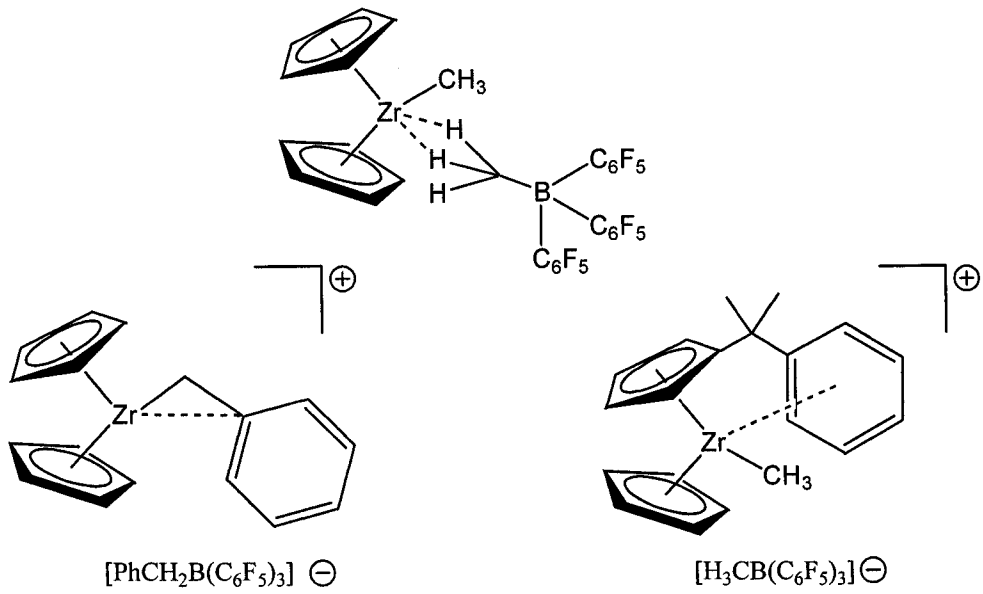

Figure 1.13: Different forms of stabilization of Group IV cations.[183,187,192]

Catalyst Decomposition Pathways

Many different routes of catalyst decomposition have been observed. Successful characterization of cationic decomposition products that are produced from different metal precursors and activators provides valuable insight for the design of robust next-

generation catalysts. For this reason, it is beneficial to consider different types of products that have been isolated, in addition to their influence on polymerization activity.

The tendency of Group IV polymerization catalysts to suffer from decomposition even in the absence of water or oxygen has been well documented. Specifically, when a zwitterionic complex is generated upon reaction of a metal precursor with the strong Lewis acid $B(C_6F_5)_3$, a diverse number of pathways exist that result in polymerization-inactive products. In this manner, Marks and co-workers noticed that ligand redistribution occurred over a period of several hours to produce $Zr[1,3\text{-}(SiMe_3)_2C_5H_3]_2Me(C_6F_5)$ (Figure 1.14).[167] Similar reactivity has been observed for metal complexes that possess a variety of ancillary ligands [196-200] or employing unusual boron-based activators.[201] Characterization of *bis*(C_6F_5) zirconium complexes that are prepared by this method is more rare, and is presumed to proceed via a stepwise process where the $ML_2Me(C_6F_5)$ (M = Ti, Zr) intermediate is activated by another equivalent of $B(C_6F_5)_3$ before it experiences the same ligand scrambling.[202-204]

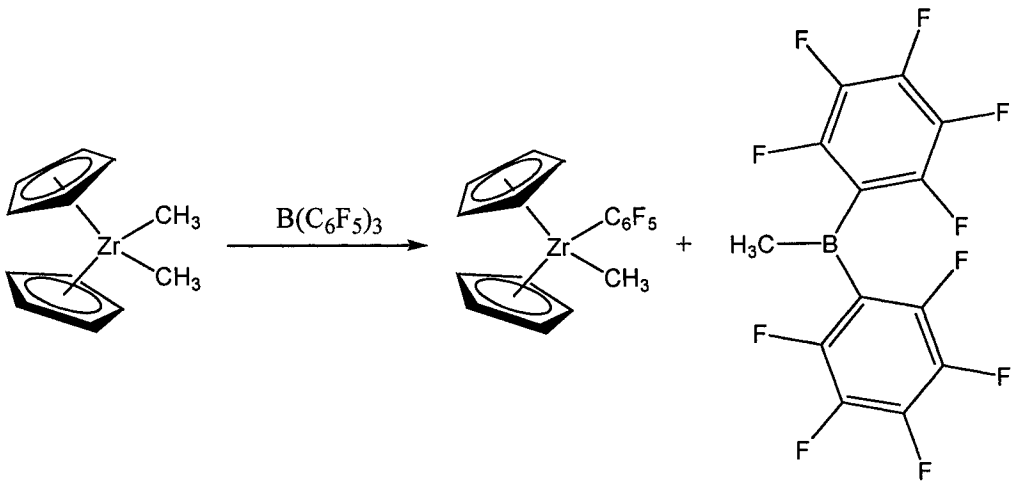

Figure 1.14: Ligand redistribution affords $Zr[1,3\text{-}(SiMe_3)_2C_5H_3]_2Me(C_6F_5)$ (trimethylsilyl groups on the Cp ligands omitted for clarity).[167]

Decomposition of the polymerization-active catalyst also occurs via C-H activation processes. The research groups of McConville[205,206] and Piers[134] have reported that loss of methane from their zwitterionic polymerization catalysts produced the neutral products $Ti[CH_2(CH_2NAr)_2](C_6F_5)[CH_2B(C_6F_5)_2]$ and

$TiCp(NC^tBu_2)(C_6F_5)[CH_2B(C_6F_5)_2]$, respectively. Attack by the Group IV cationic metal centre on its "spectator" ligands has also been documented. Cationic zirconium metallocenes that have bulky *t*-butyl[167] or trimethylsilyl[207] groups on the cyclopentadienide ligand cleanly undergo C-H activation to afford the corresponding ring-metallated products (Figure 1.15). Similar reactivity with one of the methyl groups on the cyclopentadienide ligand of the CGC[208] or on a mesityl portion of a diamide ligand[209] (Figure 1.15) has also been observed.

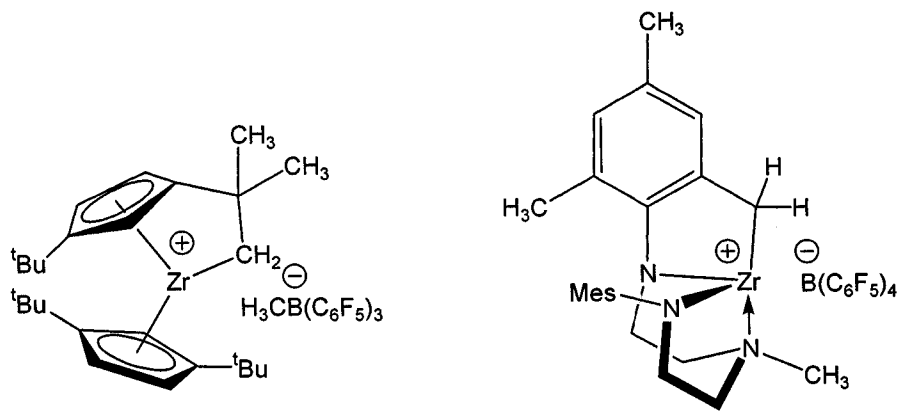

Figure 1.15: Attack by the Group IV cationic metal centre on its "spectator" ligand.[167,209]

The formation of dimeric cationic products has also been detected as a pathway to polymerization-inactive Group IV species. For example, reaction of $[ZrCp_2Me][B(C_6F_5)_4]$ with one equivalent of $ZrCp_2Me_2$ afforded the dimer $[Cp_2ZrMe(\mu\text{-}Me)MeZrCp_2][B(C_6F_5)_4]$.[210] Although traditionally the dimer is not considered to be an active catalyst,[iii] it is in equilibrium with its monomeric precursors, and its formation is thus not entirely detrimental.[210] Similar cationic dimers synthesized from a variety of metallocene precursors have been characterized by spectroscopic and crystallographic methods.[185,188,210,211] Interestingly, in two different examples, loss of one equivalent of

[iii] Recently, Sita and co-workers have suggested that their isolation of a dicationic dimer that is bridged by two methyl groups may suggest that these complexes participate in olefin polymerization, although there is no concrete evidence to support this as of yet. Keaton, R. J.; Jayaratne, K. C.; Fettinger, J. C.; Sita, L. R. *J. Am. Chem. Soc.* **2000**, *122*, 12909-12910.

methane was observed, providing a methylene-methyl-bridged dimer (Figure 1.16).[180,212] Halide-bridged dimers have also been isolated, and are presumed to be the result of reaction of the monomeric cationic complex with the solvent (CH_2Cl_2)[iv, 178] or the counterion (C_6F_5 groups).[167,213]

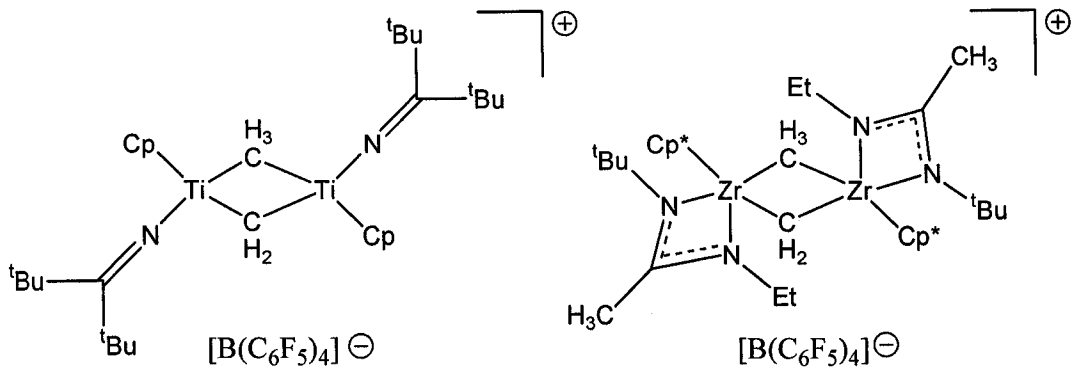

Figure 1.16: Methylene-methyl-bridged dimers isolated by the research groups of Sita[180] and Piers.[212]

Finally, two isolated cases have resulted in a dichotomy that has emerged for active titanium polymerization catalysts when they are subjected to an excess of a strong Lewis acid. Stephan and co-workers demonstrated that reaction of $Ti(NP^tBu_3)_2Me_2$ with an excess of $B(C_6F_5)_3$ afforded the di-zwitterionic product $Ti(NP^tBu_3)_2(\mu\text{-Me-}B(C_6F_5)_3)_2$ (Figure 1.17), which is inactive for the polymerization of ethylene.[214] Similarly, reaction of the CGC (Figure 1.17) or Zr[*rac*-$Me_2Si(Ind)_2$]Me_2 with an excess of $Al(C_6F_5)_3$ resulted in the isolation of the corresponding di-zwitterionic products.[215] This result was significant, since neither di-zwitterion may be produced using $B(C_6F_5)_3$ as the Lewis acid activator. Also noteworthy was the observed *increase* in polymerization activity upon double activation of the precatalyst with $Al(C_6F_5)_3$. The authors attributed this to be the result of the formation of $[ML_2(\mu\text{-Me-}Al(C_6F_5)_3)][(C_6F_5)_3Al\text{-}\mu^2\text{-Me-}Al(C_6F_5)_3]$ (M = Ti, L = CGC ligand; M = Zr, L = *rac*-$Me_2Si(Ind)_2$), which has a large, weakly-coordinating counterion.

[iv] N. L. S. Yue and L. Cabrera, unpublished results.

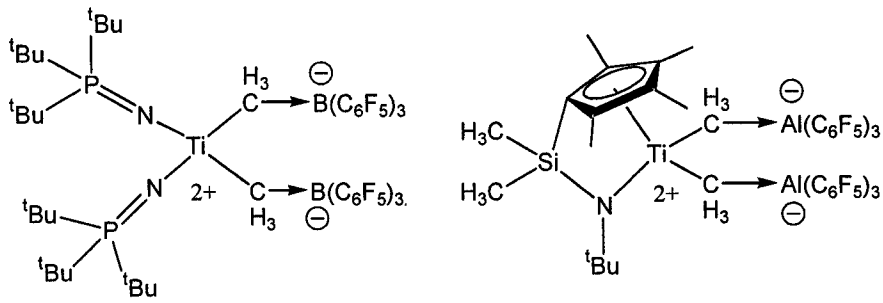

Figure 1.17: Dicationic titanium complexes.

1.4 Relevance and Perspective

It is evident that polymerization catalysis using Group IV complexes is a field of intensive investigation. Several revolutionary types of titanium and zirconium catalyst systems have been developed and fine-tuned over the past few decades, and polymerization engineering and processing has also advanced significantly. However, it is clear that this field continues to be a source of attraction from an academic standpoint since detailed mechanistic insights are not well-understood. In addition, the pursuit of innovative catalysts remains of commercial interest and continues to motivate a number of research groups.

Previous success in our lab involved contribution to the design and synthesis of a series of new and commercially relevant titanium olefin polymerization catalysts. It is valuable to explore the attributes of the titanium-phosphinimide system to understand what renders it such an active catalyst, and to discover information about the catalytic activity upon systematic modification of the catalyst structure, or adjustment of the catalytic conditions. In this manner, this thesis describes our attempts to apply the established catalyst $TiCp(NPR_3)X_2$ in hydroamination catalysis. Moreover, the use of the phosphinimide functional group on magnesium to evaluate its potential in ligand-transfer reactions will be described. Finally, the design and implementation of new and known ligands to titanium and zirconium to determine their effectiveness as olefin polymerization catalysts will be detailed.

2 Group IV Phosphinimide Amide Complexes

2.1 Introduction

Group IV amide complexes have received enormous attention due to their remarkable diversity. They have served as precursors for imido derivatives;[41,42,50,52,68] olefin polymerization catalysts upon activation by a Lewis acid;[206,216-220] precursors in chemical vapour deposition processes;[221-227] and as hydroamination (pre)catalysts.[77,88,228,229] Although in some circumstances the amide fragment remains a spectator ligand, in many instances, the metal-nitrogen bond participates in the reactivity of the metal complex to a considerable degree. For example, in the generation of either transient or isolable Group IV imido compounds, alkyl or amine groups are frequently eliminated upon thermolysis of the amide precursors (Figure 2.1). Often, these reactions are reversible. In particular, the propensity of titanium[55,83,230,231] or zirconium[42,50,73,232] imide reagents to effect C-H activation is the subject of theoretical and experimental interest. In addition, titanium and zirconium imide reagents are believed to be the active agents in hydroamination catalysis, generated *in situ* from the metal amide precursors,[77] or alternatively, from reaction of the Group IV dimethyl precursor with amines.[86]

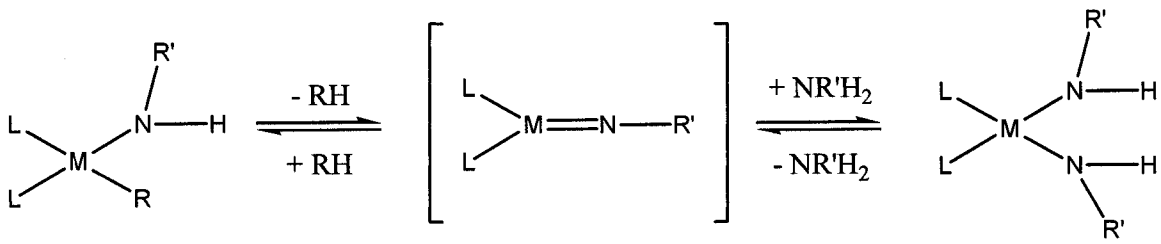

Figure 2.1: Generic routes to a Group IV imido species (L = spectator ligand; R, R' = alkyl or aryl).

Efforts within our own research group have demonstrated that when the phosphinimide ligand is used in place of the commonly employed cyclopentadienide

derivatives, it results in a titanium catalyst that exhibits a significant increase in olefin polymerization activity when compared to the titanium or zirconium metallocene analogues.[7,8] Further, it has been demonstrated that Group IV phosphinimide complexes can facilitate unusual C-H activation processes.[12,16,18,233,234] With this atypical reactivity in mind, we sought to investigate the reactivity of a series of Group IV amide complexes that possessed a phosphinimide ancillary ligand, with the aspiration of generating imide phosphinimide compounds.

2.2 Experimental

2.2.1 General Considerations

All syntheses were performed employing an atmosphere of dry, oxygen-free nitrogen in a Vacuum Atmospheres inert atmosphere glove box or standard Schlenk techniques using oven-dried (140°C) glassware unless otherwise stated. ^{1}H NMR data were acquired on a Bruker Avance 500 MHz spectrometer, while $^{13}C\{^{1}H\}$ and $^{31}P\{^{1}H\}$ NMR data were obtained from a Bruker Avance 300 MHz spectrometer. ^{1}H and $^{13}C\{^{1}H\}$ chemical shifts are listed relative to tetramethylsilane in parts per million, and were referenced to the residual proton or carbon peak of the solvent. $^{31}P\{^{1}H\}$ NMR data were referenced using 85% H_3PO_4 as an external standard. Galbraith Laboratories Inc. or University of Windsor Analytical Services (PerkinElmer 2400 Series II Instrument) performed the combustion analyses. GPC analysis of the poly(methyl methacrylate) (PMMA) sample was performed on a Waters 1500 series instrument using THF as the mobile phase at 35°C. The samples were prepared by dissolving the polymer in THF, and were filtered twice before injection. Molecular weights are expressed relative to polystyrene standards. The differential scanning calorimetry analysis of the PMMA sample was performed on a Mettler Toledo instrument.

2.2.2 *Solvents*

Reagent grade solvents were purchased from Aldrich Chemical Co., and were pre-dried using Grubbs' column systems, manufactured by Innovative Technologies, Inc.[235] Pentanes, PhH and PhMe were further dried over Na prior to distillation. Deuterated benzene, toluene and methylene chloride were purchased from Canadian Isotopes Laboratories and degassed by at least 4 freeze/pump/thaw cycles before storing over 4 Å molecular sieves.

2.2.3 *Materials*

Hyflo Super Cel ® (Celite) and 4 Å molecular sieves were purchased from Aldrich Chemical Co., and dried at 100°C *in vacuo* for 24 h prior to use. Alternatively, the Celite was dried in the oven at 140°C for 48 h prior to use.

2.2.4 *Reagents*

The compounds $Ti(NP^tBu_3)Cl_3$,[203] $TiCp(NPPh_3)Cl_2$[131] and $TiCp(NP^tBu_3)Cl_2$[8] were prepared according to literature methods, and $LiNH(2,6\text{-}^iPr_2)C_6H_3$ was prepared via a modification of a literature procedure.[236] The preparation and characterization of the new compounds $ZrCp(NP^tBu_3)Cl_2$ and $ZrCp(NP^tBu_3)Me_2$ are outlined in Section 5.2.4 of this thesis. The reagents ^{n}BuLi (2.0 M in hexanes), Al_2Me_6, $TiCp_2Cl_2$, $LiNMe_2$ and $NH_2(2,6\text{-}^iPr_2)C_6H_3$ were purchased from Aldrich Chemical Co.; $NH_2(2,6\text{-}^iPr_2)C_6H_3$ was vacuum-distilled from KOH, and all other reagents were used without further purification.

2.2.5 Inorganic and Organometallic Syntheses

$LiNH(2,6\text{-}^{i}Pr_2)C_6H_3$ (**2.1**):[236] A solution of 2.0 M $^{n}BuLi$ in hexanes (10.00 mL, 20 mmol) was added dropwise at RT to a solution of $NH_2(2,6\text{-}^{i}Pr_2)C_6H_3$ (2.60 mL, 20 mmol) in pentanes (80 mL). A white solid precipitated from solution immediately. After stirring for 1 additional h, the solid was filtered, washed with pentanes (3 x 15 mL), and dried *in vacuo*. Yield: 3.54 g, 97%. ^1H NMR (500 MHz, CD_2Cl_2) δ: 6.99 (d, 2H, $^3J_{H\text{-}H}$ = 8 Hz, $C_6\mathbf{H}_3$ (*m*-H)), 6.74 (t, 1H, $^3J_{H\text{-}H}$ = 8 Hz, $C_6\mathbf{H}_3$ (*p*-H)), 3.72 (br, 1H, N**H**), 2.92 (sep, 2H, $^3J_{H\text{-}H}$ = 7 Hz, $C(CH_3)_2\mathbf{H}$), 1.24 (d, 12H, $^3J_{H\text{-}H}$ = 7 Hz, $C(\mathbf{C}H_3)_2H$). $^{13}C\{^1H\}$ NMR (75.5 MHz, CD_2Cl_2) δ: 132.9 (s, $\mathbf{C}_6H_3$ (*ipso*-C)), 128.9 (s, $\mathbf{C}_6H_3$ (*o*-C)), 123.2 (s, $\mathbf{C}_6H_3$ (*m*-C)), 118.8 (s, $\mathbf{C}_6H_3$ (*p*-C)), 28.2 (s, $\mathbf{C}(CH_3)_2H$), 22.8 (s, $C(\mathbf{C}H_3)_2H$).

$TiCp(NP^{t}Bu_3)(NMe_2)_2$ (**2.2**): Solid $LiNMe_2$ (46 mg, 0.90 mmol) was added in several portions to a clear solution of $TiCp(NP^{t}Bu_3)Cl_2$ (179 mg, 0.45 mmol) in PhH (20 mL). The slurry was stirred for 20 h, after which time the mixture was filtered through Celite. The solvent was removed *in vacuo*, affording a bright orange solid. The residue was washed with pentanes (3 x 5 mL) and dried to afford a fine, orange powder (126 mg, 67%). Small quantities (typical yields *ca.* 10-15%) of $Ti(NP^{t}Bu_3)(NMe_2)_3$ were isolated from the pentanes washings; a preparative synthesis of this by-product is detailed below. ^1H NMR (500 MHz, C_6D_6) δ: 6.18 (s, 5H, $C_5\mathbf{H}_5$), 3.28 (s, 12H, $N(C\mathbf{H}_3)_2$), 1.24 (d, 27H, $^3J_{P\text{-}H}$ = 13 Hz, $C(C\mathbf{H}_3)_3$). $^{13}C\{^1H\}$ NMR (75.5 MHz, C_6D_6) δ: 109.7 (s, $\mathbf{C}_5H_5$), 50.5 (s, $N(\mathbf{C}H_3)_2$), 40.6 (d, $^1J_{P\text{-}C}$ = 28 Hz, $\mathbf{C}(CH_3)_3$), 29.7 (s, $C(\mathbf{C}H_3)_3$). $^{31}P\{^1H\}$ NMR (121.5 MHz, C_6D_6) δ: 28.9 (s). Anal. Calc'd for $C_{21}H_{44}N_3PTi$: C, 60.42; H, 10.62; N, 10.07. Found: C, 60.34; H, 10.52; N, 9.67.

$TiCp(NPPh_3)(NMe_2)_2$ (**2.3**): This was prepared in an analogous fashion to $TiCp(NP^{t}Bu_3)(NMe_2)_2$ (**2.2**) from $TiCp(NPPh_3)Cl_2$ to afford a yellow solid (312 mg, 77%). ^1H NMR (500 MHz, C_6D_6) δ: 7.75 (m, 6H, $C_6\mathbf{H}_5$), 7.06 (m, 9H, $C_6\mathbf{H}_5$), 5.99 (s, 5H, $C_5\mathbf{H}_5$), 3.34 (s, 12H, $N(C\mathbf{H}_3)_2$). $^{13}C\{^1H\}$ NMR (75.5 MHz, C_6D_6) δ: 135.9 (d, $^1J_{P\text{-}C}$ = 58 Hz, $\mathbf{C}_6H_5$ (*ipso*-C)), 132.4 (d, $^2J_{P\text{-}C}$ = 6 Hz, $\mathbf{C}_6H_5$ (*o*-C)), 128.3 (s, $\mathbf{C}_6H_5$ (*p*-C)), 128.6

(d, $^3J_{P-C}$ = 7 Hz, $\mathbf{C}_6H_5$ (*m*-C)), 109.8 (s, $\mathbf{C}_5H_5$), 50.1 (s, $N(\mathbf{C}H_3)_2$). $^{31}P\{^1H\}$ NMR (121.5 MHz, C_6D_6) δ: -9.3 (s).

$Ti(NP^tBu_3)(NMe_2)_3$ (**2.4**): A slurry of $LiNMe_2$ (44 mg, 0.87 mmol) in PhH (1 mL) was added to a suspension of $Ti(NP^tBu_3)Cl_3$ (105 mg, 0.28 mmol) in the same solvent (10 mL). After stirring for 12 h at RT, the mixture was filtered through Celite. Removal of the solvent *in vacuo* afforded an orange, crystalline solid (83 mg, 75%). ^1H NMR (500 MHz, C_6D_6) δ: 3.40 (s, 18H, $N(C\mathbf{H}_3)_2$), 1.27 (s, 27H, $^3J_{P-H}$ = 13 Hz, $C(C\mathbf{H}_3)_3$). $^{13}C\{^1H\}$ NMR (75.5 MHz, C_6D_6) δ: 46.3 (s, $N(\mathbf{C}H_3)_2$), 39.9 (d, $^1J_{P-C}$ = 48 Hz, $\mathbf{C}(CH_3)_3$), 29.5 (s, $C(\mathbf{C}H_3)_3$). $^{31}P\{^1H\}$ NMR (121.5 MHz, C_6D_6) δ: 29.8 (s). Anal. Calc'd for $C_{18}H_{45}N_4PTi$: C, 54.54; H, 11.44; N, 14.13. Found: C, 54.74; H, 11.63; N, 13.78. Deep orange-red crystals suitable for X-ray diffraction were grown by slow evaporation from hexanes/pentanes.

$TiCp_2(NMe_2)Cl$ (**2.5**): $TiCp_2Cl_2$ (75 mg, 0.30 mmol) was dissolved in PhH (10 mL), and a slurry of $LiNMe_2$ (16 mg, 0.30 mmol) in PhH (2 mL) was added at RT. The mixture was stirred for 16 h, after which time it was filtered through Celite. The solvent was removed *in vacuo* to afford **2.5** as a deep red-brown solid. (53 mg, 68%) ^1H NMR (500 MHz, C_6D_6) δ: 5.75 (s, 10H, $C_5\mathbf{H}_5$), 3.15 (s, 6H, $N(C\mathbf{H}_3)_2$). $^{13}C\{^1H\}$ NMR (75.5 MHz, C_6D_6) δ: 114.0 (s, $\mathbf{C}_5H_5$), 58.6 (s, $N(\mathbf{C}H_3)_2$).

$TiCp(NMe_2)_3$ (**2.6**): This red solid was isolated in various yields (< 100 mg, 40-60%) when the experiment above was repeated with 2 or 3 equivalents of the amide reagent. This compound has been previously reported,[237] although no spectroscopic data was detailed. ^1H NMR (500 MHz, C_6D_6) δ: 5.93 (s, 5H, $C_5\mathbf{H}_5$), 3.08 (s, 18H, $N(C\mathbf{H}_3)_2$). $^{13}C\{^1H\}$ NMR (75.5 MHz, C_6D_6) δ: 110.5 (s, $\mathbf{C}_5H_5$), 49.8 (s, $N(\mathbf{C}H_3)_2$).

$ZrCp(NP^tBu_3)(NMe_2)_2$ (**2.7**): Solid $LiNMe_2$ (193 mg, 3.6 mmol) was added in several portions at RT to a clear solution of $ZrCp(NP^tBu_3)Cl_2$ (**5.3**) (411 mg, 0.90 mmol) in PhH (50 mL). The slurry was stirred for 18 h, and was subsequently filtered through Celite. The solvent was removed *in vacuo*, affording **2.7** as a fine, white powder (340 mg, 82%).

^{1}H NMR (500 MHz, C_6D_6) δ: 6.32 (s, 5H, $C_5\mathbf{H}_5$), 3.14 (s, 12H, $N(C\mathbf{H}_3)_2$), 1.21 (s, 27H, $^3J_{P\text{-}H}$ = 12 Hz, $C(C\mathbf{H}_3)_3$). $^{13}C\{^1H\}$ NMR (75.5 MHz, C_6D_6) δ: 109.6 (s, $\mathbf{C}_5H_5$), 46.3 (s, $N(\mathbf{C}H_3)_2$), 39.9 (d, $^1J_{P\text{-}C}$ = 48 Hz, $\mathbf{C}(CH_3)_3$), 29.6 (s, $C(\mathbf{C}H_3)_3$). $^{31}P\{^1H\}$ NMR (121.5 MHz, C_6D_6) δ: 31.4 (s). Anal. Calc'd for $C_{21}H_{44}N_3PZr$: C, 54.74; H, 9.62; N, 9.12. Found: C, 53.73; H, 9.64; N, 8.49.

$TiCp(NP^tBu_3)(NH(2,6\text{-}^iPr_2)C_6H_3)Cl$ (**2.8**): Solid $LiNH(2,6\text{-}^iPr_2)C_6H_3$ (**2.1**) (1.51 g, 12.2 mmol) was added in small portions at RT over a 1 h period to a clear solution of $TiCp(NP^tBu_3)Cl_2$ (4.91 g, 12.2 mmol) in PhH (150 mL). The slurry was stirred for 20 h, after which time the mixture was filtered through Celite. The solution was concentrated *in vacuo* to *ca.* 20 mL, during which time a bright yellow solid precipitated. The solid was filtered, washed with pentanes (3 x 20 mL), and dried to afford a fine, yellow powder (5.94 g, 89%). ^{1}H NMR (500 MHz, C_6D_6) δ: 9.65 (br, 1H, N**H**), 7.23 (br, 2H, $C_6\mathbf{H}_3$ (*m*-H)), 7.05 (t, 1H, $^3J_{H\text{-}H}$ = 7 Hz, $C_6\mathbf{H}_3$ (*p*-H)), 6.21 (s, 5H, $C_5\mathbf{H}_5$), 3.26 (sep, *barely visible*, 2H, $^3J_{H\text{-}H}$ = 7 Hz, $C(CH_3)_2\mathbf{H}$), 1.39 (d, 12H, $^3J_{H\text{-}H}$ = 7 Hz, $C(C\mathbf{H}_3)_2H$), 1.19 (d, 27H, $^3J_{P\text{-}H}$ = 13 Hz, $C(C\mathbf{H}_3)_3$). $^{13}C\{^1H\}$ NMR (75.5 MHz, C_6D_6) δ: 153.9 (s, $\mathbf{C}_6H_3$ (*ipso*-C)), 128.3 (s, $\mathbf{C}_6H_3$ (*o*-C)), 123.3 (s, $\mathbf{C}_6H_3$ (*m*-C)), 123.1 (s, $\mathbf{C}_6H_3$ (*p*-C)), 112.8 (s, $\mathbf{C}_5H_5$), 41.5 (d, $^1J_{P\text{-}C}$ = 27 Hz, $\mathbf{C}(CH_3)_3$), 29.5 (s, $C(\mathbf{C}H_3)_3$), 28.1 (s, $\mathbf{C}(CH_3)_2H$), 22.6 (s, $C(\mathbf{C}H_3)_2H$). $^{31}P\{^1H\}$ NMR (121.5 MHz, C_6D_6) δ: 39.0 (s). Anal. Calc'd for $C_{29}H_{50}ClN_2PTi$: C, 64.38; H, 9.32; N, 5.18. Found: C, 63.95; H, 9.06; N, 4.74. Bright yellow crystals suitable for X-ray diffraction were grown by slow evaporation from PhH.

$Ti(NP^tBu_3)(NH(2,6\text{-}^iPr_2)C_6H_3)_3$ (**2.9**): A slurry of $LiNH(2,6\text{-}^iPr_2)C_6H_3$ (**2.1**) (591 mg, 4.8 mmol) in PhH (20 mL) was added over a 0.5 h period at RT to a clear solution of $TiCp(NP^tBu_3)Cl_2$ (380 mg, 0.96 mmol) in the same solvent (25 mL). The slurry was stirred for an additional 10 h, then filtered through Celite. The solvent was removed *in vacuo*, and the residue was washed with hexanes (3 x 10 mL) to afford a yellow solid (586 mg, 77%). ^{1}H NMR (500 MHz, C_6D_6) δ: 7.80 (br, 3H, N**H**), 7.11 (d, 6H, $^3J_{H\text{-}H}$ = 8 Hz, $C_6\mathbf{H}_3$ (*m*-H)), 6.96 (t, 3H, $^3J_{H\text{-}H}$ = 8 Hz, $C_6\mathbf{H}_3$ (*p*-H)), 3.70 (sep, 6H, $^3J_{H\text{-}H}$ = 7 Hz, $C(CH_3)_2\mathbf{H}$), 1.28 (d, 36H, $^3J_{H\text{-}H}$ = 7 Hz, $C(C\mathbf{H}_3)_2H$), 1.06 (d, 27H, $^3J_{P\text{-}H}$ = 13 Hz, $C(C\mathbf{H}_3)_3$). $^{13}C\{^1H\}$ NMR (75.5 MHz, C_6D_6) δ: 150.9 (s, $\mathbf{C}_6H_3$ (*ipso*-C)), 137.6 (s, $\mathbf{C}_6H_3$

(*o*-C)), 123.0 (s, $\mathbf{C}_6H_3$ (*m*-C)), 120.8 (s, $\mathbf{C}_6H_3$ (*p*-C)), 40.6 (d, $^1J_{P\text{-}C}$ = 46 Hz, $\mathbf{C}(CH_3)_3$), 29.4 (s, $C(\mathbf{C}H_3)_3$), 29.2 (s, $\mathbf{C}(CH_3)_2H$), 24.1 (s, $C(\mathbf{C}H_3)_2H$). $^{31}P\{^1H\}$ NMR (121.5 MHz, C_6D_6) δ: 37.4 (s). Anal. Calc'd for $C_{48}H_{81}N_4PTi$: C, 72.70; H, 10.30; N, 7.06. Found: C, 72.49; H, 10.60; N, 7.28. Deep red crystals suitable for X-ray diffraction were grown by slow evaporation from PhH.

$ZrCp(NP^tBu_3)(NH(2,6\text{-}^iPr_2)C_6H_3)Me$ (**2.10**): $NH_2(2,6\text{-}^iPr)C_6H_3$ (58 μL, 0.31 mmol) was added dropwise to a clear solution of $ZrCp(NP^tBu_3)Me_2$ (125 mg, 0.31 mmol) in PhH (20 mL) at RT. After stirring for 12 h, the volatile products were removed *in vacuo* to afford a beige solid (162 mg, 92%). ^1H NMR (500 MHz, C_6D_6) δ: 7.21 (d, 2H, $^3J_{H\text{-}H}$ = 8 Hz, $C_6\mathbf{H}_3$ (*m*-H)), 7.04 (t, 1H, $^3J_{H\text{-}H}$ = 8 Hz, $C_6\mathbf{H}_3$ (*p*-H)), 6.51 (br, 1H, N**H**), 6.20 (s, 5H, $C_5\mathbf{H}_5$), 3.45 (sep, 2H, $^3J_{H\text{-}H}$ = 7 Hz, $C(CH_3)_2\mathbf{H}$), 1.36 (d, 6H, $^3J_{H\text{-}H}$ = 7 Hz, $C(C\mathbf{H}_3)_2H$), 1.35 (d, 6H, $^3J_{H\text{-}H}$ = 7 Hz, $C(C\mathbf{H}_3)_2H$), 1.13 (d, 27H, $^3J_{P\text{-}H}$ = 13 Hz, $C(C\mathbf{H}_3)_3$), 0.47 (s, 3H, Zr-$C\mathbf{H}_3$). $^{13}C\{^1H\}$ NMR (75.5 MHz, C_6D_6) δ: 150.9 (s, $\mathbf{C}_6H_3$ (*ipso*-C)), 137.7 (s, $\mathbf{C}_6H_3$ (*o*-C)), 122.7 (s, $\mathbf{C}_6H_3$ (*m*-C)), 120.1 (s, $\mathbf{C}_6H_3$ (*p*-C)), 110.0 (s, $\mathbf{C}_5H_5$), 40.0 (d, $^1J_{P\text{-}C}$ = 47 Hz, $\mathbf{C}(CH_3)_3$), 29.0 (s, $C(\mathbf{C}H_3)_3$), 27.9 (s, Zr-$\mathbf{C}H_3$), 27.9 (s, $\mathbf{C}(CH_3)_2H$), 23.8 (s, $C(\mathbf{C}H_3)_2H$), 22.8 (s, $C(\mathbf{C}H_3)_2H$). $^{31}P\{^1H\}$ NMR (121.5 MHz, C_6D_6) δ: 34.3 (s). Anal. Calc'd for $C_{30}H_{53}N_2PZr$: C, 63.89; H, 9.47; N, 4.97. Found: C, 62.84; H, 9.43; N, 4.90.

$ZrCp(NP^tBu_3)(NH(2,6\text{-}^iPr_2)C_6H_3)_2$ (**2.11**): A slurry of $LiNH(2,6\text{-}^iPr_2)C_6H_3$ (**2.1**) (527 mg, 2.9 mmol) in PhH (20 mL) was added over a 15 min period at RT to a solution of $ZrCp(NP^tBu_3)Cl_2$ (**5.3**) (320 mg, 0.72 mmol) in the same solvent (25 mL). The slurry was stirred for an additional 10 h, after which time it was filtered through Celite. The solvent was removed *in vacuo*, and the residue was washed with hexanes (3 x 5 mL) to afford a beige solid (486 mg, 93%). ^1H NMR (500 MHz, C_6D_6) δ: 7.18 (d, 4H, $^3J_{H\text{-}H}$ = 8 Hz, $C_6\mathbf{H}_3$ (*m*-H)), 7.02 (t, 2H, $^3J_{H\text{-}H}$ = 8 Hz, $C_6\mathbf{H}_3$ (*p*-H)), 6.34 (s, 5H, $C_5\mathbf{H}_5$), 5.75 (s, 2H, N**H**), 3.73 (sep, 4H, $^3J_{H\text{-}H}$ = 7 Hz, $C(CH_3)_2\mathbf{H}$), 1.34 (d, 24H, $^3J_{H\text{-}H}$ = 7 Hz, $C(C\mathbf{H}_3)_2H$), 1.04 (d, 27H, $^3J_{P\text{-}H}$ = 13 Hz, $C(C\mathbf{H}_3)_3$). $^{13}C\{^1H\}$ NMR (75.5 MHz, C_6D_6) δ: 151.9 (s, $\mathbf{C}_6H_3$ (*ipso*-C)), 138.7 (s, $\mathbf{C}_6H_3$ (*o*-C)), 122.9 (s, $\mathbf{C}_6H_3$ (*m*-C)), 120.2 (s, $\mathbf{C}_6H_3$ (*p*-C)), 111.4 (s, $\mathbf{C}_5H_5$), 39.9 (d, $^1J_{P\text{-}C}$ = 47 Hz, $\mathbf{C}(CH_3)_3$), 29.5 (s, $C(\mathbf{C}H_3)_3$), 28.7 (s, $\mathbf{C}(CH_3)_2H$), 24.3 (s, $C(\mathbf{C}H_3)_2H$). $^{31}P\{^1H\}$ NMR (121.5 MHz, C_6D_6) δ: 35.8 (s). Anal. Calc'd for

$C_{41}H_{68}N_3PZr$: C, 67.90; H, 9.45; N, 5.79. Found: C, 66.62; H, 9.84; N, 5.86. Colourless crystals suitable for X-ray diffraction were grown by slow evaporation from PhH.

$TiCp(NP^tBu_3)(NH(2,6\text{-}^iPr_2)C_6H_3)Cl$ + 0.5 Al_2Me_6: Neat Al_2Me_6 (0.14 mL, 0.14 mmol) was added dropwise at RT to a clear orange solution of $TiCp(NP^tBu_3)(NH(2,6\text{-}^iPr_2)C_6H_3)Cl$ (153 mg, 0.28 mmol) in PhH (15 mL). The solution became deeper yellow in colour and was stirred for an additional 2 h, after which time the solvent was removed *in vacuo*. The residue was recrystallized from pentanes to afford yellow and colourless crystals. (combined yield: 162 mg, 94%) X-ray analysis of crystals isolated from the mixture confirmed the presence of $TiCp(NP^tBu_3)MeCl$ (**2.12**) and $Al_2(\mu\text{-}NH(2,6\text{-}^iPr_2)C_6H_3)_2Me_4$ (**2.13**), although due to their similar solubility properties, they could not be adequately separated. Thus, microanalysis was performed on the mixture, confirming a 1:1 ratio of the 2 products. Anal. Calc'd for $C_{32}H_{59}AlClN_2PTi$: C, 64.50; H, 9.83; N, 4.85. Found: C, 65.19; H, 10.25; N, 5.01. Both, however, were identified spectroscopically: $Al_2(\mu\text{-}NH(2,6\text{-}^iPr_2)C_6H_3)_2Me_4$: ^1H NMR (500 MHz, C_6D_6) δ: 7.06 (d, 2H, $^3J_{H\text{-}H}$ = 8 Hz, $C_6\mathbf{H}_3$ (*m*-H)), 6.98 (t, 1H, $^3J_{H\text{-}H}$ = 8 Hz, $C_6\mathbf{H}_3$ (*p*-H)), 4.58 (br, 1H, N**H**), 3.40 (sep, 2H, $^3J_{H\text{-}H}$ = 7 Hz, $C(CH_3)_2\mathbf{H}$), 1.26 (d, 12H, $^3J_{H\text{-}H}$ = 7 Hz, $C(C\mathbf{H}_3)_2H$), -0.32 (s, 6H, Al-$C\mathbf{H}_3$). $^{13}C\{^1H\}$ NMR (75.5 MHz, C_6D_6) δ: 139.2 (s, $\mathbf{C}_6H_3$ (*o*-C)), 137.7 (s, $\mathbf{C}_6H_3$ (*ipso*-C)), 124.6 (s, $\mathbf{C}_6H_3$ (*m*-C)), 123.8 (s, $\mathbf{C}_6H_3$ (*p*-C)), 29.0 (s, $\mathbf{C}(CH_3)_2H$), 25.0 (s, $C(\mathbf{C}H_3)_2H$), -7.2 (s, Al-$\mathbf{C}H_3$). The spectroscopic and crystallographic data for $Al_2(\mu\text{-}NH(2,6\text{-}^iPr_2)C_6H_3)_2Me_4$ were consistent with literature tabulations.[238,239] $TiCp(NP^tBu_3)MeCl$: ^1H NMR (500 MHz, C_6D_6) δ: 6.27 (s, 5H, $C_5\mathbf{H}_5$), 1.20 (s, 3H, Ti-$C\mathbf{H}_3$), 1.04 (d, 27H, $^3J_{P\text{-}H}$ = 20 Hz, $C(C\mathbf{H}_3)_3$). $^{13}C\{^1H\}$ NMR (75.5 MHz, C_6D_6) 113.3 (s, $\mathbf{C}_5H_5$), 41.4 (d, $^1J_{P\text{-}C}$ = 45 Hz, $\mathbf{C}(CH_3)_3$), 29.4 (s, $C(\mathbf{C}H_3)_3$), 25.2 (s, Ti-$\mathbf{C}H_3$). $^{31}P\{^1H\}$ NMR (121.5 MHz, C_6D_6) δ: 42.0 (s).

$Mg_2(\mu\text{-}NP^tBu_3)_2(NP^tBu_3)_2$ (**2.14**): To a solution of Mg^nBu_2 (2.40 mL, 2.4 mmol; 1.0 M in hexanes) in PhH (40 mL) was added a clear, colourless solution of HNP^tBu_3 (1.04 g, 4.8 mmol) in the same solvent (40 mL). After stirring at RT for 10 h, the volatile products were removed *in vacuo*, affording a white solid (980 mg, 89%). ^1H NMR (500 MHz, C_6D_6) δ: 1.49 (d, 54H, $^3J_{P\text{-}H}$ = 11 Hz, $C(C\mathbf{H}_3)_3$), 1.42 (d, 54H, $^3J_{P\text{-}H}$ = 12 Hz, $C(C\mathbf{H}_3)_3$).

$^{13}C\{^1H\}$ NMR (75.5 MHz, C_6D_6) δ: 40.8 (d, $^1J_{P-C}$ = 46 Hz, **C**$(CH_3)_3$), 40.1 (d, $^1J_{P-C}$ = 52 Hz, **C**$(CH_3)_3$), 31.1 (s, C(**C**$H_3)_3$), 30.9 (s, C(**C**$H_3)_3$). $^{31}P\{^1H\}$ NMR (121.5 MHz, C_6D_6) δ: 43.2 (s, 2P, μ-N**P**^{t}Bu$_3$), 25.2 (s, 2P, σ-N**P**^{t}Bu$_3$). Calc'd for $C_{24}H_{54}MgN_2P_2$: C, 63.08; H, 11.91; N, 6.13. Found: C, 63.12; H, 12.28; N, 6.16. Colourless crystals suitable for X-ray diffraction were grown from pentanes at -35°C.

$Mg_3(\mu\text{-}NP^iPr_3)_4(NP^iPr_3)_2$ (**2.15**): The synthetic methodology for the following compounds is analogous to the protocol described above for $Mg_2(\mu\text{-}NP^tBu_3)_2(NP^tBu_3)_2$ (**2.14**), using HP^iPr_3. White solid (1.23 g, 87%). ^1H NMR (500 MHz, C_6D_6) δ: 2.25 (m, 12H, C$(CH_3)_2$**H**), 1.85 (m, 6H, C$(CH_3)_2$**H**), 1.32 (dd, 72H, $^3J_{P-H}$ = 12 Hz, $^3J_{H-H}$ = 7 Hz, C(C**H**$_3)_2$H), 1.27 (dd, 36H, $^3J_{P-H}$ = 12 Hz, $^3J_{H-H}$ = 7 Hz, C(C**H**$_3)_2$H). $^{13}C\{^1H\}$ NMR (75.5 MHz, C_6D_6) δ: 28.8 (d, $^1J_{P-C}$ = 57 Hz, **C**$(CH_3)_2$H), 26.1 (d, $^1J_{P-C}$ = 64 Hz, **C**$(CH_3)_2$H), 18.8 (s, C(**C**$H_3)_2$H), 18.2 (s, C(**C**$H_3)_2$H). $^{31}P\{^1H\}$ NMR (121.5 MHz, C_6D_6) δ: 27.6 (s, 4P, μ-N**P**^{t}Bu$_3$), 7.9 (s, 2P, σ-N**P**^{t}Bu$_3$). Colourless crystals suitable for X-ray diffraction were grown from pentanes at -35°C.

2.2.6 X-Ray Experimental

X-ray Data Collection and Reduction: The crystals were manipulated and mounted in glass capillaries in a glove box, thus maintaining a dry, O_2-free environment. The diffraction experiments were performed on a Siemens SMART System CCD diffractometer at 20°C with Mo Kα radiation (λ = 0.71069 Å). The observed extinctions were consistent with the space groups determined for each sample. Measures of decay were obtained by re-collecting the first 50 frames of each data set. The intensities of reflections within these frames showed no statistically significant change over the duration of the respective data collections. Empirical absorption corrections based on redundant data were applied to each data set. Subsequent solution and refinement were performed using the SHELXTL solution package.

Structure Solutions and Refinements: Non-hydrogen atomic scattering factors were taken from literature tabulations.[240] The heavy atom positions were determined using direct methods or Patterson techniques. The remaining non-hydrogen atoms were located from successive difference Fourier map calculations. The refinements were carried out by using full-matrix least squares techniques on F, minimizing the function $\omega(|F_o|-|F_c|)^2$ where the weight ω is defined as $4F_o^2/2\sigma(F_o^2)$ and F_o and F_c are the observed and calculated structure factor amplitudes. In the final cycle of each refinement, all non-hydrogen atoms were assigned anisotropic temperature factors except where noted otherwise. Carbon-bound hydrogen atom positions were calculated and allowed to ride on the carbon to which they are bonded, assuming a C-H bond length of 0.95 Å. Hydrogen atom temperature factors were fixed at 1.2 times the isotropic temperature factor of the carbon atom to which they are bonded. The hydrogen atom parameters were calculated, but not refined.

X-ray structural solutions of $Ti(NP^tBu_3)(NMe_2)_3$ (**2.4**), $TiCp(NP^tBu_3)(NH(2,6\text{-}^iPr_2)C_6H_3)Cl$ (**2.8**), $Ti(NP^tBu_3)(NH(2,6\text{-}^iPr_2)C_6H_3)_3$ (**2.9**), $ZrCp(NP^tBu_3)(NH(2,6\text{-}^iPr_2)C_6H_3)_2$ (**2.11**), $Mg_2(\mu\text{-}NP^tBu_3)_2(NP^tBu_3)_2$ (**2.14**) and $Mg_3(\mu\text{-}NP^iPr_3)_4(NP^iPr_3)_2$ (**2.15**) were performed as described above. In addition, a preliminary solution was obtained for $TiCp(NP^tBu_3)MeCl$ (**2.12**), although a detailed discussion is precluded due to disorder of the methide and chloride ligands. A solution of $Al_2(\mu\text{-}NH(2,6\text{-}^iPr_2)C_6H_3)_2Me_4$ (**2.13**) was also obtained, although a search of the Cambridge structural database revealed that a similar crystallographic analysis had already been performed.[238,239] Cell parameters, R, R_w and GoF values are located in Table 2.1, while detailed structural parameters have been included as an appendix on CD (Appendix C). The solution for structure **2.15** is disordered, therefore 8 of the atoms were refined isotropically, while 63 of the 69 atoms were refined anisotropically (2 extra atoms due to disorder). The solution for structure **2.8** included one molecule of C_6H_6, and the 6 additional atoms were refined anisotropically. No residual electron density remained in any of the solutions that were of any chemical significance. ORTEP drawings of **2.4**, **2.8**, **2.9**, **2.11**, **2.14** and **2.15** are depicted in Figures 2.3, 2.4, 2.12 and 2.13, while select bond distances and angles are provided in the text.

Table 2.1: Crystallographic parameters for $Ti(NP^tBu_3)(NMe_2)_3$ (**2.4**), $TiCp(NP^tBu_3)(NH(2,6\text{-}^iPr_2)C_6H_3)Cl$ (**2.8**), $Ti(NP^tBu_3)(NH(2,6\text{-}^iPr_2)C_6H_3)_3$ (**2.9**).

	2.4	**2.8**	**2.9**
Molecular formula	$C_{18}H_{45}N_4PTi$	$C_{29}H_{49}ClN_2PTi$	$C_{48}H_{78}N_4PTi$
Formula weight	396.42	540.01	790.00
a(Å)	14.066(6)	11.334(6)	11.73(4)
b(Å)	14.066(6)	11.891(6)	41.9(2)
c(Å)	11.023(7)	13.769(7)	20.68(8)
α(°)	90.00	100.315(9)	90.00
β(°)	90.00	101.464(9)	91.97(8)
γ (°)	120.00	107.256(9)	90.00
Crystal system	Trigonal	Triclinic	Monoclinic
Space group	R3	P-1	$P2_1/c$
Volume ($Å^3$)	1888.9(7)	1680(1)	1015(7)
D_{calc} (gcm^{-3})	1.046	1.147	1.038
Z	3	2	4
Abs coeff, μ, mm^{-1}	0.410	0.403	0.233
θ range (°)	2.49-22.96	1.56-23.27	1.38-22.50
Reflections collected	2639	7162	39320
Data $F_o^2 > 3\sigma(F_o^2)$	965	4078	7952
Parameters	73	343	973
R(%)	0.1088	0.0365	0.0959
R_w(%)	0.3150	0.1018	0.1769
Goodness of Fit	1.490	1.028	1.043

The data was collected at 20°C with Mo Kα radiation (λ = 0.71069 Å)

$R = \Sigma \, | \, |F_o| - |F_c| \, | \, / \, \Sigma \, |F_o|$, $R_w = [\Sigma(|F_o| - |F_c|)^2 / \Sigma \, |F_o|^2]^{0.5}$

Table 2.1 (continued): Crystallographic parameters for $ZrCp(NP^tBu_3)(NH(2,6\text{-}^iPr_2)C_6H_3)_2$ (**2.11**), $TiCp(NP^tBu_3)MeCl$ (**2.12**)[v], $Al_2(\mu\text{-}NH(2,6\text{-}^iPr_2)C_6H_3)_2Me_4$ (**2.13**).

	2.11	**2.12**	**2.13**
Molecular formula	$C_{41}H_{68}N_3PZr$	$C_{18}H_{35}ClNPTi$	$C_{28}H_{46}Al_2N_2$
Formula weight	725.17	379.77	464.64
a(Å)	19.38(2)	10.294(5)	18.810(8)
b(Å)	19.77(2)	14.828(8)	10.160(4)
c(Å)	21.92(2)	28.49(1)	15.901(7)
α(°)	90.00	90.00	90.00
β(°)	90.00	90.00	90.00
γ (°)	90.00	90.00	90.00
Crystal system	Orthorhombic	Orthorhombic	Orthorhombic
Space group	Pbca	Pbca	$Pna2_1$
Volume ($Å^3$)	8400(2)	4348	3039(2)
D_{calc} (gcm^{-3})	1.147		1.016
Z	8		4
Abs coeff, μ, mm^{-1}	0.329		0.112
θ range (°)	1.74-23.46		2.28-23.21
Reflections collected	34645		12226
Data $F_o^2 > 3\sigma(F_o^2)$	3049		2965
Parameters	415		289
R(%)	0.0416		0.0442
R_w(%)	0.0629		0.1013
Goodness of Fit	1.022		1.056

The data was collected at 20°C with Mo Kα radiation (λ = 0.71069 Å)

$R = \Sigma \, | \, |F_o| - |F_c| \, | \, / \, \Sigma \, |F_o|$, $R_w = [\Sigma \, (|F_o| - |F_c|)^2 / \Sigma \, |F_o|^2]^{0.5}$

[v]Only preliminary X-ray data were obtained and the structure was not refined, thus only the cell parameters are listed.

Table 2.1(continued): Crystallographic parameters for $Mg_2(\mu\text{-}NP^tBu_3)_2(NP^tBu_3)_2$ (**2.14**) and $Mg_3(\mu\text{-}NP^iPr_3)_4(NP^iPr_3)_2$ (**2.15**).

	2.14	**2.15**
Molecular formula	$C_{48}H_{108}Mg_2N_4P_4$	$C_{54}H_{120}Mg_3N_6P_6$
Formula weight	913.90	1112.31
a(Å)	13.479(9)	21.19(1)
b(Å)	20.00(1)	12.574(7)
c(Å)	22.44(2)	28.14(2)
α(°)	101.73(1)	90.00
β(°)	93.18(1)	106.87(1)
γ (°)	94.80(1)	90.00
Crystal system	Triclinic	Monoclinic
Space group	P-1	$P2_1/c$
Volume ($Å^3$)	5886(7)	7174(7)
D_{calc} (gcm^{-3})	1.031	1.030
Z	2	4
Abs coeff, μ, mm^{-1}	0.181	0.210
θ range (°)	0.93-23.30	2.04-22.50
Reflections collected	24378	28021
Data $F_o^2 > 3\sigma(F_o^2)$	5325	3610
Parameters	1045	600
R(%)	0.0913	0.0609
R_w(%)	0.1549	0.1133
Goodness of Fit	0.884	1.030

The data was collected at 20°C with Mo Kα radiation (λ = 0.71069 Å)

$R = \Sigma \, | \, |F_o| - |F_c| \, | \, / \, \Sigma \, |F_o|$, $R_w = [\Sigma \, (|F_o| - |F_c|)^2 / \Sigma \, |F_o|^2]^{0.5}$

2.2.7 Polymerization Protocol

Purification of Reagents: PhMe, ACS grade MeOH and methyl methacrylate (MMA) were purchased from Aldrich Chemical Co. The PhMe was purified as described in Section 2.2.2, MMA was vacuum-distilled from CaH_2, and MeOH was used without purification.

Representative Polymerization: $Mg_2(\mu\text{-}NP^tBu_3)_2(NP^tBu_3)_2$ (**2.14**) or $Mg_3(\mu\text{-}NP^iPr_3)_4(NP^iPr_3)_2$ (**2.15**) was dissolved in PhMe to afford a concentration of 5 mmol L^{-1}, and cooled, if desired, for 30 min to permit thermal equilibrium. The MMA was injected via syringe, and the polymerization was performed for the prescribed period of time. The reaction was quenched with a large excess of MeOH (50-100 mL), and the precipitated polymer was filtered, washed with MeOH (3 x 20 mL), and dried *in vacuo* to a constant weight.

2.2.8 Attempted Hydroamination Protocol

The general attempted procedure is as follows: the titanium precatalyst was dissolved in toluene and combined with ten equivalents of amine ($NH_2{}^tBu$, NH_2Et, $NH_2(2,6\text{-}{}^iPr_2)C_6H_3$) and acetylene (PhCCH, PhCCPh, 1-hexyne, 3-hexyne) reagents, then heated in a glass bomb for 24-48 hours at 80-100°C. The volatile products were removed *in vacuo*, and the residue was dissolved in C_6D_6 for NMR analysis; none of the attempts were successful.

2.3 Results and Discussion

Since Group IV metal complexes that possess dimethyl amide ligands are commonly employed as hydroamination catalysts,[27,228,229] complexes of formula $TiCp(NPR_3)(NMe_2)_2$ (R = ^tBu (**2.2**), Ph (**2.3**)) were prepared via salt metathesis of $TiCp(NPR_3)Cl_2$ with a slight excess of $LiNMe_2$. The reaction where R = Ph proceeded

cleanly, and afforded only the desired product, however, where R = ^{t}Bu, the by-product Ti(NP^{t}Bu$_3$)(NMe$_2$)$_3$ (**2.4**) was also generated in low yields (*ca.* 10-15%) (Figure 2.2). Examination of the chemical shift from the protons of the dimethyl amide ligands of TiCp(NPR$_3$)(NMe$_2$)$_2$ (R = ^{t}Bu (**2.2**), Ph (**2.3**)) indicated a downfield shift from 3.28 to 3.34 ppm as the phosphinimide substituent changed from *t*-butyl to the less basic phenyl group.

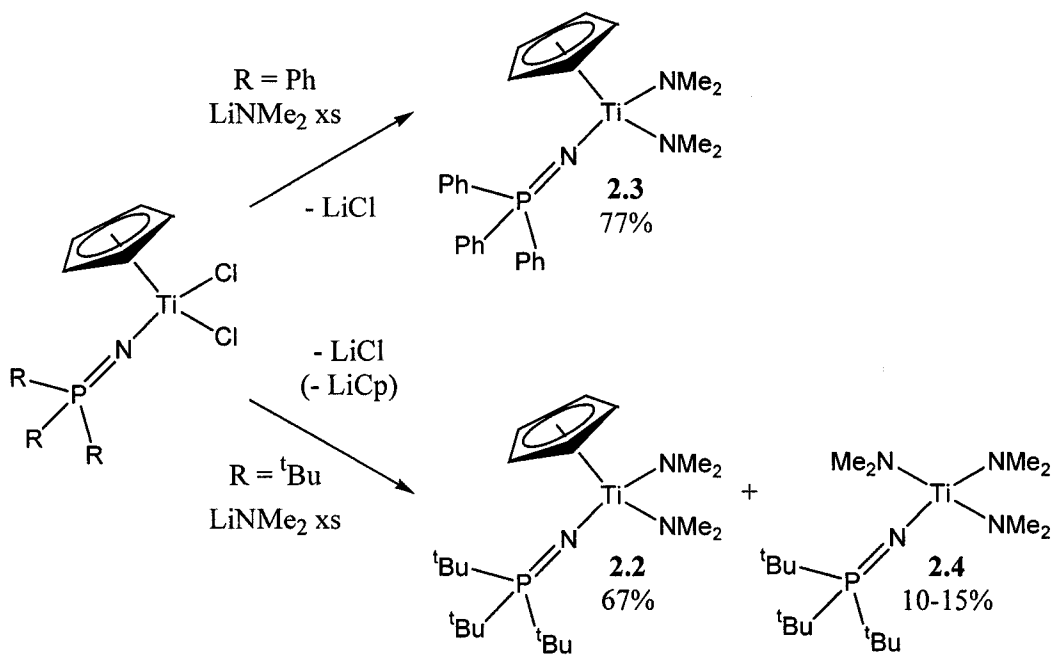

Figure 2.2: Influence of R groups on the phosphorus atom to afford different products.

The by-product Ti(NP^{t}Bu$_3$)(NMe$_2$)$_3$ (**2.4**) was prepared in a more conventional manner by a metathesis route from Ti(NP^{t}Bu$_3$)Cl$_3$ and an excess of the lithium amide reagent. Judicious syntheses of the related complexes TiCp(NMe$_2$)$_3$ (Cp = C$_5$H$_5$ (**2.6**), C$_5$Me$_5$, indenide) have been reported,[218,237] however, the formation of Ti(NP^{t}Bu$_3$)(NMe$_2$)$_3$ (**2.4**) from TiCp(NP^{t}Bu$_3$)Cl$_2$ was somewhat unexpected. Although cleavage of a cyclopentadienide ligand from titanium or zirconium is rare, it is not entirely without precedent. This has been observed in the reaction of MCp$_2$Cl$_2$ with an excess of lithium amide reagent (M = Ti),[241] dithiolate ligands (M = Ti),[242] in related hydroamination chemistry,[87] or by radical (M = Zr)[243] or thermal redistribution (M = Ti)[244,245] processes. In an attempt to confirm that cleavage of cyclopentadienide occurs in the absence of the phosphinimide ligand, different stoichiometries of LiNMe$_2$ were

reacted with $TiCp_2Cl_2$. The outcome was the clean isolation of $TiCp_2(NMe_2)Cl$ (**2.5**) when less than one equivalent of amide reagent was employed, or mixtures of $TiCp(NMe_2)_3$ (**2.6**) and $TiCp_2Cl_2$ if more than one equivalent of the lithium amide reagent was used. Reasons for the preferential formation of $TiCp(NMe_2)_3$ (**2.6**) rather than $TiCp_2(NMe_2)_2$ remain unclear, however these reactions are frustratingly reproducible.

X-ray quality crystals of $Ti(NP^tBu_3)(NMe_2)_3$ (**2.4**) were isolated, and the solid-state structure is comparable to the related titanium complex $TiCp^*(NMe_2)_3$ (Figure 2.3).[246] The titanium amide bond distances (symmetry related) of 1.72(2)Å for $Ti(NP^tBu_3)(NMe_2)_3$ (**2.4**) are significantly shorter than the values of 1.912(9) and 1.92(1)Å for the titanium amide bond distances that were obtained from X-ray analysis of $TiCp^*(NMe_2)_3$.[246] Given that the calculated Ti-N single bond distance is 1.981Å [247] and steric issues are not a factor, it is reasonable to suggest that the amide ligands in both compounds are functioning as σ,π donors. It is also worthwhile to compare the chemical shift from the methyl protons of the amide groups, which are 3.40 and 3.09 ppm in deuterated benzene, for $TiL(NMe_2)_3$ (L = NP^tBu_3 and Cp*, respectively). These features in solution and the solid state suggest that Cp* donates more electron density that NP^tBu_3 in the complexes $TiL(NMe_2)_3$.

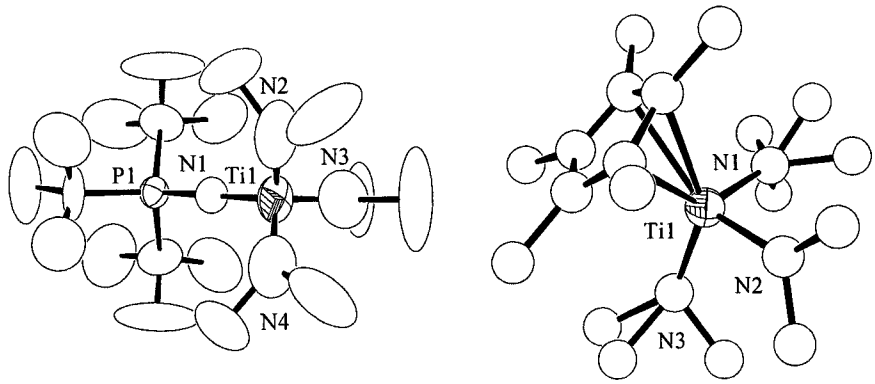

2.4

Figure 2.3: ORTEP drawings of $Ti(NP^tBu_3)(NMe_2)_3$ (**2.4**) (30% thermal ellipsoids due to disorder) and $TiCp^*(NMe_2)_3$ (additional methyl groups present due to disorder).[246]

The related zirconium derivative $ZrCp(NP^tBu_3)(NMe_2)_2$ (**2.7**) was prepared from the dichloride precursor with an excess of the lithium reagent. Unlike the titanium version, no evidence for cleavage of the Cp ligand was observed.

Similar efforts to investigate the products from reaction of $MCp(NP^tBu_3)Cl_2$ with $LiNH(2,6\text{-}^iPr_2)C_6H_3$ (**2.1**) were also undertaken. In this manner, $TiCp(NP^tBu_3)(NH(2,6\text{-}^iPr_2)C_6H_3)Cl$ (**2.8**), $Ti(NP^tBu_3)(NH(2,6\text{-}^iPr_2)C_6H_3)_3$ (**2.9**) and $ZrCp(NP^tBu_3)(NH(2,6\text{-}^iPr_2)C_6H_3)_2$ (**2.11**) were successfully isolated (Figure 2.5). Unlike the dialkyl amide reaction, preparation of $TiCp(NP^tBu_3)(NH(2,6\text{-}^iPr_2)C_6H_3)_2$ could not be achieved cleanly. All three compounds were characterized crystallographically (Figure 2.4, Table 2.2). In all three complexes, the metal-nitrogen bond of the phosphinimide ligand was shorter than the metal-nitrogen bond of the amide ligand(s). In addition, the zirconium-nitrogen bond distances for **2.11** were slightly longer than in the titanium complexes, reflecting the difference in the size of the transition metal. Accompanying the increased Zr-N phosphinimide bond length was a decrease in the nitrogen-phosphorus bond distance (Table 2.2). Also of interest was the Ti-N-P bond angle, which approached linearity (**2.8** 173.18(11)° and **2.11** 176.4(2)°) for the two complexes that were not as sterically crowded at the metal centre.

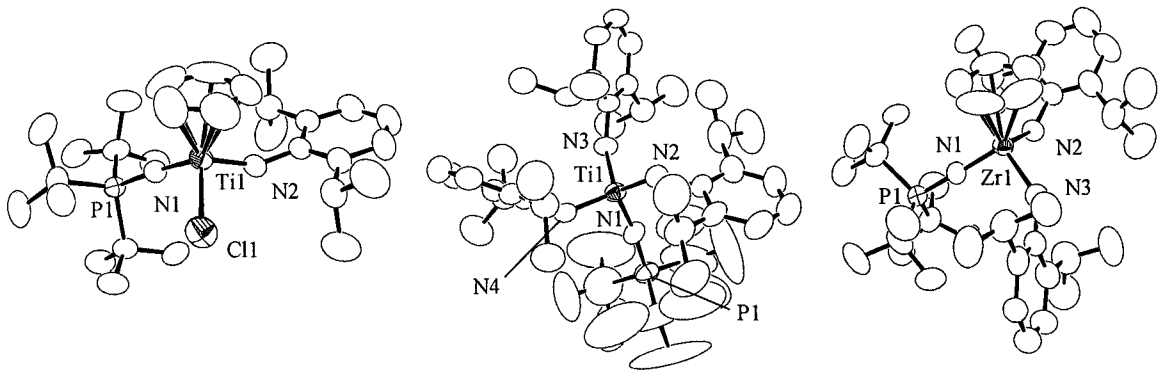

2.8 **2.9** **2.11**

Figure 2.4: ORTEP drawings of $TiCp(NP^tBu_3)(NH(2,6\text{-}^iPr_2)C_6H_3)Cl$ (**2.8**) (molecule of benzene omitted for clarity), $Ti(NP^tBu_3)(NH(2,6\text{-}^iPr_2)C_6H_3)_3$ (**2.9**) and $ZrCp(NP^tBu_3)(NH(2,6\text{-}^iPr_2)C_6H_3)_2$ (**2.11**) (50% thermal ellipsoids).

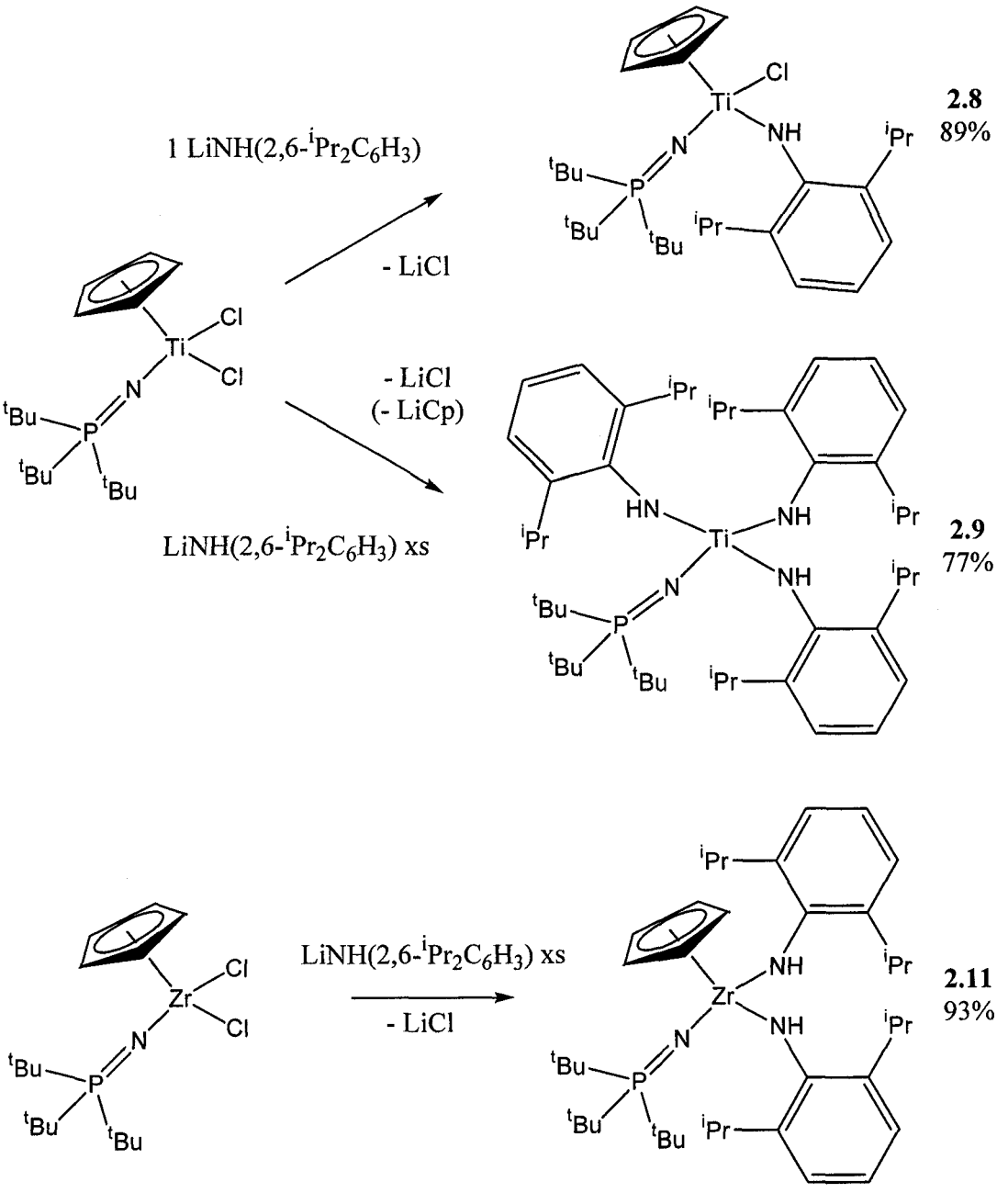

Figure 2.5: Synthesis of $TiCp(NP^tBu_3)(NH(2,6\text{-}^iPr_2)C_6H_3)Cl$ (**2.8**), $Ti(NP^tBu_3)(NH(2,6\text{-}^iPr_2)C_6H_3)_3$ (**2.9**) and $ZrCp(NP^tBu_3)(NH(2,6\text{-}^iPr_2)C_6H_3)_2$ (**2.11**)

Table 2.2: Select bond distances and angles for $TiCp(NP^tBu_3)(NH(2,6\text{-}^iPr_2)C_6H_3)Cl$ (**2.8**), $Ti(NP^tBu_3)(NH(2,6\text{-}^iPr_2)C_6H_3)_3$ (**2.9**) and $ZrCp(NP^tBu_3)(NH(2,6\text{-}^iPr_2)C_6H_3)_2$ (**2.11**).

Compound	M-N Å (amide)	M-N Å (phosphinimide)	N-P Å	M-N-P ° (terminal)
2.8	1.946(2)	1.790(2)	1.601(2)	173.2(1)
2.9	1.915(8) 1.950(6) 1.971(7)	1.774(7)	1.604(7)	167.1(3)
2.11	2.107(4) 2.111(3)	1.939(3)	1.591(3)	176.4(2)

Attempts to prepare the titanium *bis*(amide) derivative $TiCp(NP^tBu_3)(NH(2,6\text{-}^iPr_2)C_6H_3)_2$ via reaction of the neutral amine with $TiCp(NP^tBu_3)X_2$ (X = Cl, Me), by *in situ* generation of the lithium amide reagent, or by conducting the amide metathesis reaction in a polar solvent (THF) were all ineffective. It is possible that steric factors preclude formation of the desired product. Synthesis of $ZrCp(NP^tBu_3)(NH(2,6\text{-}^iPr_2)C_6H_3)Me$ (**2.10**), however, was accomplished by reaction of the appropriate dimethyl metal precursor with the neutral amine at ambient temperature (Figure 2.6). Attempts to generate the *bis*(amide) derivative by this method were not successful; rather, extrusion of free $NH_2(2,6\text{-}^iPr_2)C_6H_3$ and HNP^tBu_3 occurred in varying amounts upon thermolysis, suggesting the possible formation of an imido species.

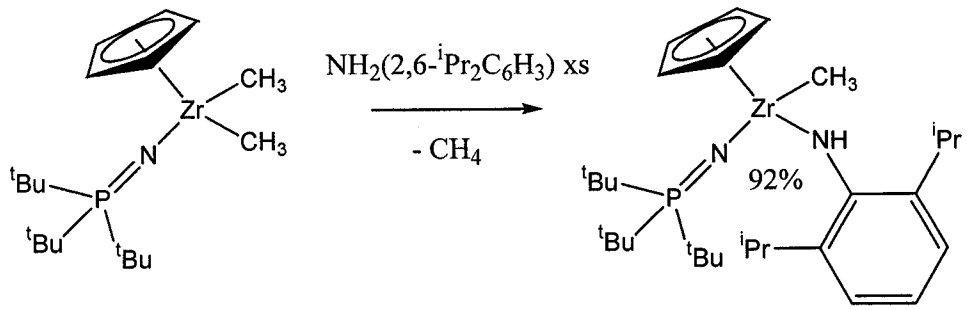

Figure 2.6: Synthesis of $ZrCp(NP^tBu_3)(NH(2,6\text{-}^iPr_2)C_6H_3)Me$ (**2.10**).

The room temperature proton NMR spectrum of $TiCp(NP^tBu_3)(NH(2,6\text{-}^iPr_2)C_6H_3)Cl$ (**2.8**) did not exhibit the expected features. The methine protons on the *i*-propyl groups were not visible, while the doublet signal originating from the methyl groups did not integrate well relative to the other ligands. Variable temperature NMR analysis confirmed the restricted rotation about the titanium-nitrogen amide bond (Figure 2.7). Coalescence of the methine protons of the *i*-propyl groups formally occurs at 308 K, which accounts for the near-absence of an NMR signal using the standard conditions for an NMR experiment (i.e. ambient temperature). Analysis of the data (Appendix A) indicated a free energy of activation ($\Delta G^{\ddagger}$) for rotation of the N-C_{ipso} bond of the amide ligand to be 58.1 $\pm$ 0.5 kJ mol^{-1} at 298 K. This value is greater than those reported for $Ti(NR_2)_3Cl$ (R = Me, Et) (< 42 kJ mol^{-1}), but compares well with an estimation of 55.6 kJ mol^{-1} obtained for rotation of the N-C_{ipso} bond in the related complex $Zr\{[(N(2,6\text{-}^iPr_2)C_6H_3)CH_2]_2CH_2\}Me_2$.[248] The higher values are simply reflective of the crowded steric environment around the metal centres.[249,250]

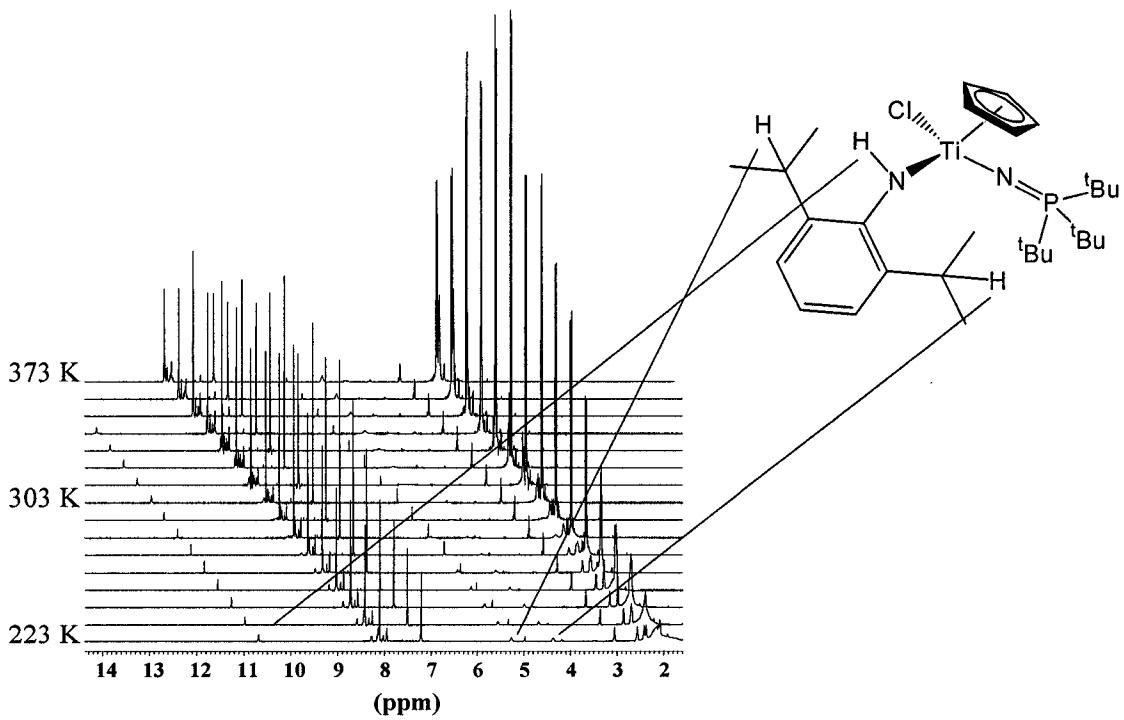

Figure 2.7: Variable-temperature ^1H NMR spectra of $TiCp(NP^tBu_3)(NH(2,6\text{-}^iPr_2)C_6H_3)Cl$ (**2.8**) in toluene-d_8.

The chemical shift of the amide proton in the ^{1}H NMR spectra varied greatly among this series of compounds. Values of 9.65, 7.80, 6.51 and 5.75 ppm were obtained for $TiCp(NP^tBu_3)(NH(2,6\text{-}^iPr_2)C_6H_3)Cl$ (**2.8**), $Ti(NP^tBu_3)(NH(2,6\text{-}^iPr_2)C_6H_3)_3$ (**2.9**), $ZrCp(NP^tBu_3)(NH(2,6\text{-}^iPr_2)C_6H_3)Me$ (**2.10**) and $ZrCp(NP^tBu_3)(NH(2,6\text{-}^iPr_2)C_6H_3)_2$ (**2.11**), respectively, in deuterated benzene. Despite the chemical shift of 9.65 ppm obtained for **2.8**, solid state characterization provided no evidence for hydrogen bonding that could account for this anomalously downfield resonance.

Attempts to Generate Group IV Phosphinimide Imide Complexes

A number of diverse methods to obtain Group IV imide phosphinimide complexes were attempted. Two commonly employed routes to imido derivatives involve thermolysis of precursors that possess *bis*(amide)[41,50,85,251] or mixed alkyl/aryl amide groups[41,42,50,68,80,252] adjacent to one another (Figure 2.1). Attempts to exploit this approach did not yield imide products. Rather, elimination of both free amine and HNP^tBu_3 was observed from a variety of titanium or zirconium phosphinimide-containing precursors, in the presence or absence of donors such as THF or pyridines. A different tactic involved reaction of Mountford's precursor $Ti(N^tBu)Cl_2(^tBuPy)_2$[56] with a variety of phosphinimide reagents (Figure 2.8), including HNP^tBu_3, $LiNP^tBu_3$ and $Mg_2(\mu\text{-}NP^tBu_3)_2(NP^tBu_3)_2$ (**2.14**) (*vide infra*). Although this is successful for an enormous variety of ancillary ligands,[56-67] it did not prove to be a useful synthetic approach for preparing complexes that include the phosphinimide ligand system.

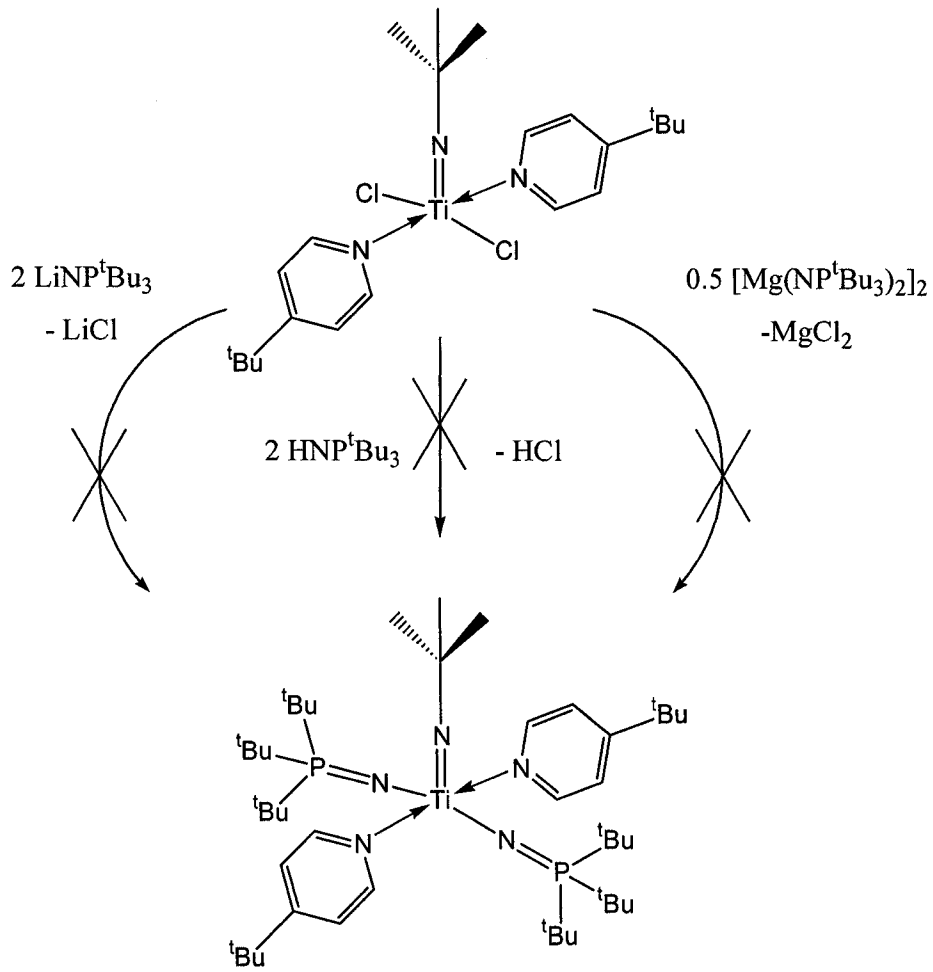

Figure 2.8: Attempts to generate a Group IV phosphinimide imide complex from Mountford's precursor.[56]

Other less common methods were also attempted to generate titanium imide phosphinimide complexes. Power and co-workers have used the magnesium imide $(THFMgNPh)_6$ as an imide transfer reagent to prepare Group IV metallocene imide complexes (Figure 2.9).[51,253] When the analogous reagent $(THFMgN(2,6\text{-}^iPr_2)C_6H_3)_x$ was treated with $TiCp(NP^tBu_3)Cl_2$, $TiCp(NP^tBu_3)(NH(2,6\text{-}^iPr_2)C_6H_3)Cl$ (**2.8**) was isolated exclusively, even when meticulously dry conditions were used. The same outcome resulted whether the magnesium imide was prepared *in situ*, or isolated, then used. This result was disappointing, and the origin of the proton source remains unexplained.

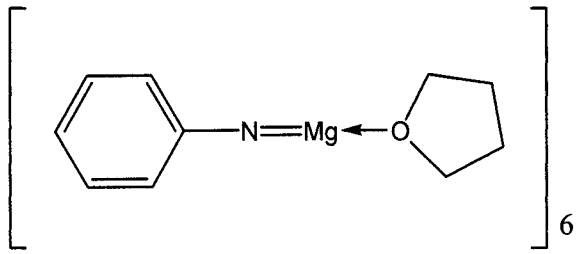

Figure 2.9: Power's magnesium imide transfer reagent.[253]

Yet another approach involved the use of trimethylaluminum (TMA). Recently, a samarium *tris*(amide) precursor was treated with an excess of TMA to give an imide product upon elimination of methane (Figure 2.10).[254] Thus, $TiCp(NP^tBu_3)(NH(2,6\text{-}^iPr_2)C_6H_3)Cl$ (**2.8**) was reacted with 1-4 equivalents of TMA. When an excess of aluminum reagent was used, $TiCp(NP^tBu_3)Me_2$ was isolated cleanly in near-quantitative yield. However, when 1 equivalent of TMA was used, $TiCp(NP^tBu_3)MeCl$ (**2.12**) and the dimer $Al_2(\mu\text{-}NH(2,6\text{-}^iPr_2)C_6H_3)_2Me_4$ (**2.13**) were obtained (Figure 2.11). This is not entirely unusual, since TMA has been used as a methylating reagent to remove alkoxide[255] or amide[256] functional groups.

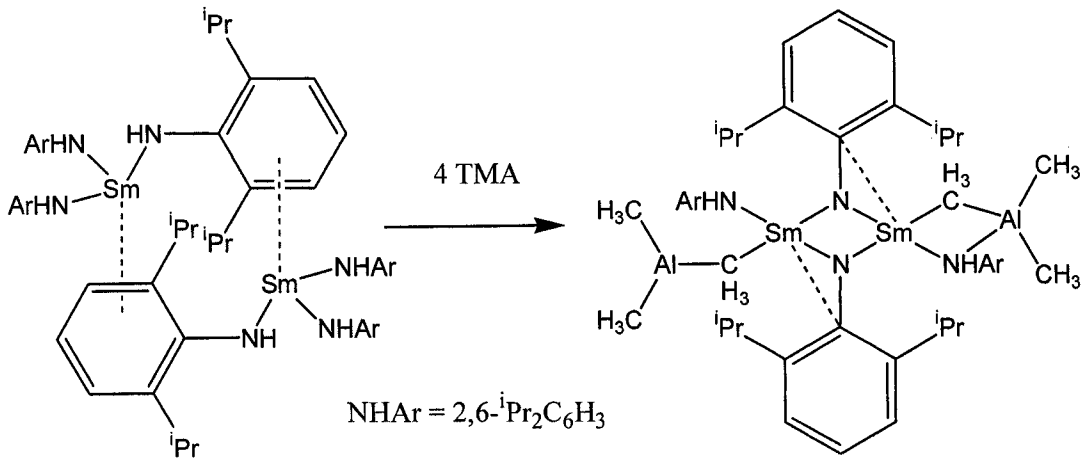

Figure 2.10: The utility of TMA to generate a Sm imide complex.

NMR spectroscopy indicated that the desired product TiCp(NP^{t}Bu$_3$)(N(2,6-^{i}Pr$_2$)C$_6$H$_3$)μ–ClAlMe$_2$ was not generated but that two distinct compounds were actually obtained. Additional characterization techniques served to confirm this unambiguously. X-ray analysis of both compounds isolated from the mixture, in addition to a satisfactory microanalysis, confirmed a 1:1 ratio of TiCp(NP^{t}Bu$_3$)MeCl (**2.12**) and Al$_2$(μ-NH(2,6-^{i}Pr$_2$)C$_6$H$_3$)$_2$Me$_4$ (**2.13**). The aluminum dimer has previously been characterized by X-ray crystallography, and the bond distances and angles derived from our analysis were comparable.[vi, 238,239] In addition, TiCp(NP^{t}Bu$_3$)MeCl (**2.12**) features a ^{31}P{^{1}H} chemical shift of 42.0 ppm, which is between the chemical shift region for where the comparable dichloride (31.3 ppm) and dimethyl (45.2 ppm) derivatives are observed.[21]

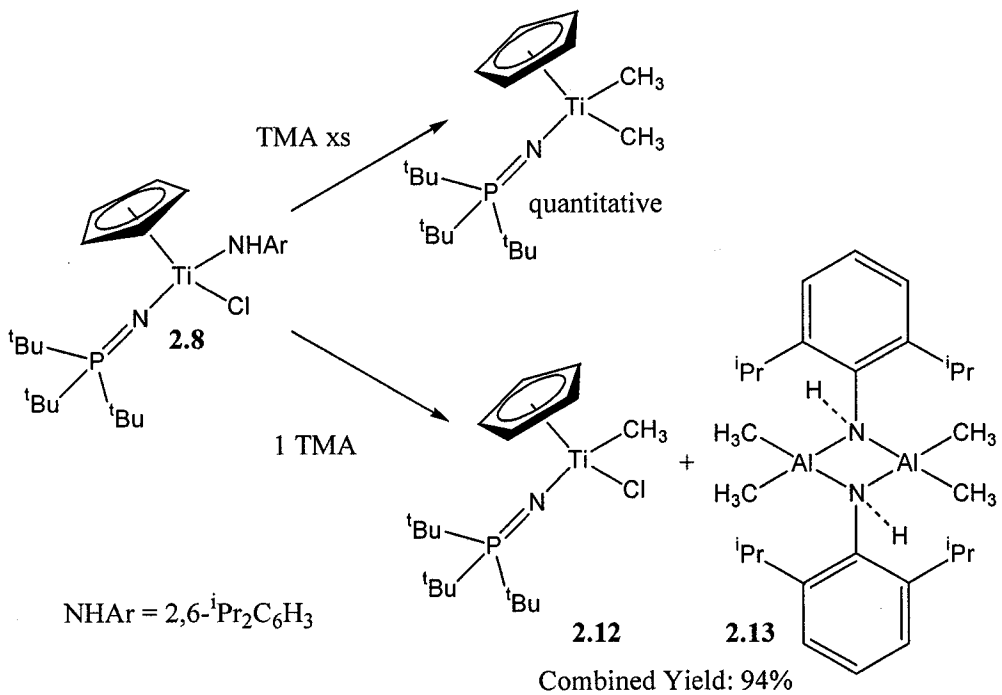

Figure 2.11: Diversity in the reaction of TiCp(NP^{t}Bu$_3$)(NH(2,6-^{i}Pr$_2$)C$_6$H$_3$)Cl (**2.8**) with TMA.

[vi] Both crystals were solved in the orthorhombic crystal system (Power Pbn2$_1$; Stephan Pna2$_1$). Selected bond distances from literature data, representative of the dimeric structure obtained include: Al(1)-N(1) 1.970 Å, Al(2)-N(1) 1.991 Å, Al(1)-N(2) 1.954 Å, Al(2)-N(2) 1.982 Å, Al(1)-C(1) 1.951 Å, Al(1)-C(2) 1.926 Å, Al(2)-C(3) 1.951 Å, Al(2)-C(4) 1.969 Å. Waggoner, K. M.; Hope, H.; Power, P. P. *Angew. Chem.* **1988**, *100*, 1765-1766. Waggoner, K. M.; Power, P. P. *J. Am. Chem. Soc.* **1991**, *113*, 3385-3393.

Testing for Hydroamination Catalysis

Doye and co-workers report moderate conversion of 3-hexyne and 4-methylaniline to the secondary amine (upon workup with zinc-modified $NaBH_3CN$ in methanol) using $TiCp(NPPh_3)Me_2$ as a catalyst.[27] However, similar transformations were not observed for any of the catalyst precursors tested in our laboratories. When $Ti(NP^tBu_3)(NHAr)_3$ (**2.9**), $MCp(NPR_3)(NMe_2)_2$ (M = Ti, R = Ph (**2.3**); M = Ti (**2.2**), Zr (**2.7**), R = ^{t}Bu) or $ZrCp(NP^tBu_3)(NH(2,6\text{-}^iPr_2)C_6H_3)_xMe_y$ (x = y = 1 (**2.10**); x = 2, y = 0 (**2.11**)) were used as a catalyst, free amine or $HNPR_3$ were the only products that were soluble in aromatic solvents, whereas when $TiCp(NP^tBu_3)(NHAr)Cl$ (**2.8**) was employed, $[H_2NP^tBu_3][Cl]$ was the only observable product. These results indicate that the phosphinimide ligand is not a useful ancillary ligand for Group IV complexes to provide active hydroamination catalysts while employing the attempted conditions.

Magnesium Phosphinimide Complexes

A tangential result that originated from the exploration of Group IV amide-phosphinimide chemistry was the preparation of the *magnesium* compounds $Mg_2(\mu\text{-}NP^tBu_3)_2(NP^tBu_3)_2$ (**2.14**) and $Mg_3(\mu\text{-}NP^iPr_3)_4(NP^iPr_3)_2$ (**2.15**) as "soft" phosphinimide transfer reagents. They were synthesized from Mg^nBu_2 and two equivalents of the appropriate parent phosphinimine in good yields (87-89%, Figure 2.12). Both products are extremely soluble in pentanes (*ca.* 1 g in 2 mL), and may be isolated from saturated solutions as colourless crystals at -35°C. NMR spectroscopy for $Mg_2(\mu\text{-}NP^tBu_3)_2(NP^tBu_3)_2$ (**2.14**) indicated a dimeric structure in deuterated benzene, since 2 sets of signals were observed for the *t*-butyl groups in the ^1H and $^{13}C\{^1H\}$ NMR spectra, in addition to 2 equal-intensity signals in the $^{31}P\{^1H\}$ NMR spectrum (43.2, 25.2 ppm). Similar NMR evidence for $Mg_3(\mu\text{-}NP^iPr_3)_4(NP^iPr_3)_2$ (**2.15**) indicated a trimeric structure in the same solvent: a 2:1 ratio of downfield to upfield ^1H and ^{13}C chemical shifts for the *i*-propyl groups was observed, and a similar ratio of intensities were also observed in the $^{31}P\{^1H\}$ NMR spectrum (27.6, 7.9 ppm). All of the resonances that occur downfield are

attributed to be a result of the bridging phosphinimide ligands, while the resonances that occur upfield are due to the terminal ligands.

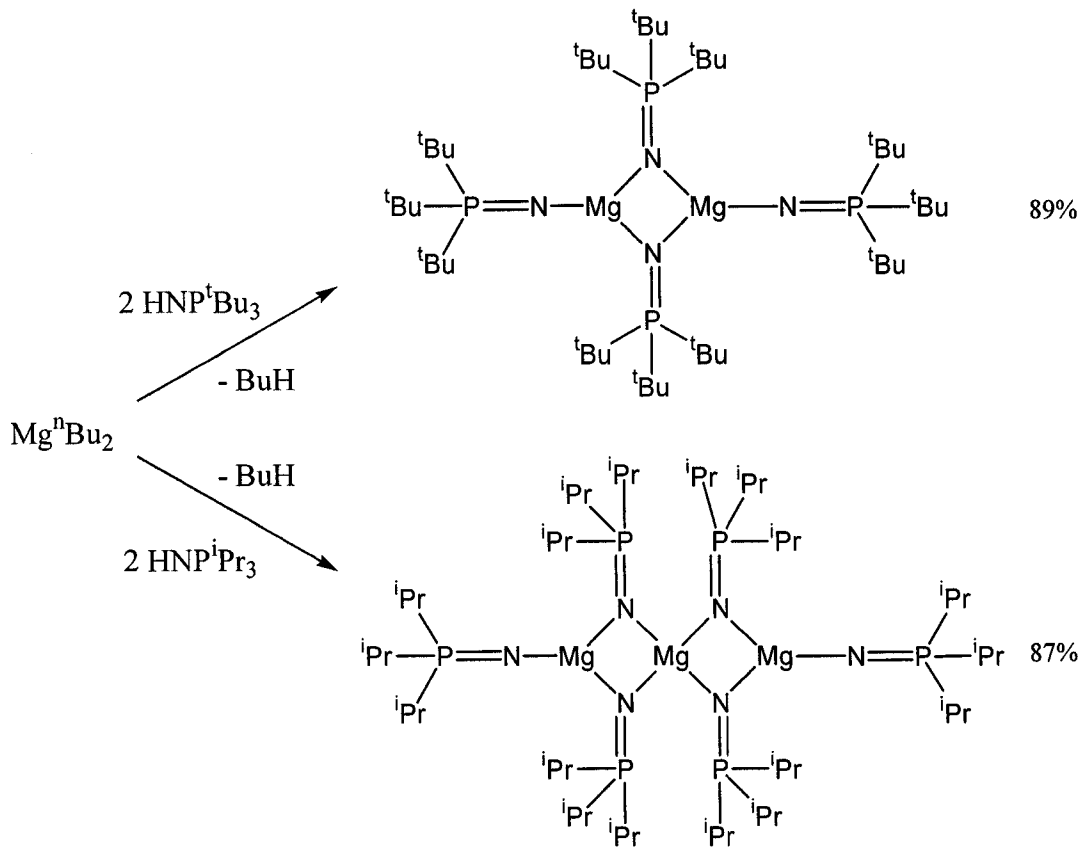

Figure 2.12: Synthesis of $Mg_2(\mu\text{-}NP^tBu_3)_2(NP^tBu_3)_2$ (**2.14**) and $Mg_3(\mu\text{-}NP^iPr_3)_4(NP^iPr_3)_2$ (**2.15**).

X-ray analysis of single crystals of **2.14** and **2.15** confirmed that the proposed solution structures of a dimer and a trimer also existed in the solid state (Figure 2.13, Table 2.3). The bridging and terminal phosphinimide ligands have similar bond lengths in both compounds. However, the two terminal Mg-N-P bond angles in $Mg_3(\mu\text{-}NP^iPr_3)_4(NP^iPr_3)_2$ (**2.15**) are closer to linearity. Of interest is that in $Mg_2(\mu\text{-}NP^tBu_3)_2(NP^tBu_3)_2$ (**2.14**), an agostic interaction between one of the hydrogen atoms on a *t*-butyl group was observed (2.298 and 2.374 Å; 2 independent molecules in the asymmetric unit, Figure 2.14).

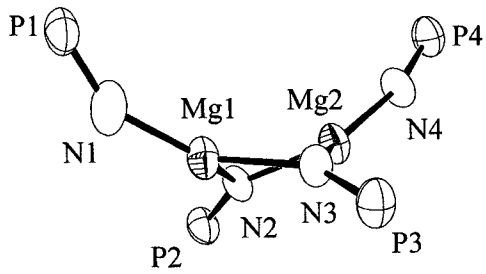

2.14

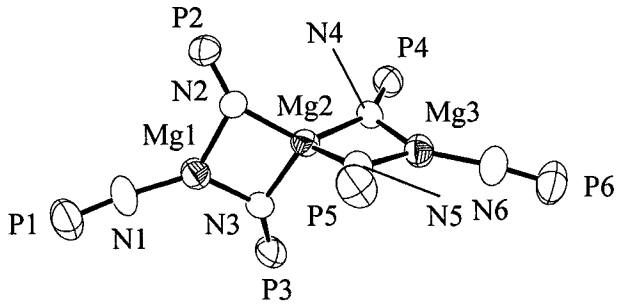

2.15

Figure 2.13: ORTEP diagrams of the core fragments of $Mg_2(\mu\text{-}NP^tBu_3)_2(NP^tBu_3)_2$ (**2.14**) and $Mg_3(\mu\text{-}NP^iPr_3)_4(NP^iPr_3)_2$ (**2.15**) (*t*-butyl and *i*-propyl groups omitted for clarity; 50% thermal ellipsoids).

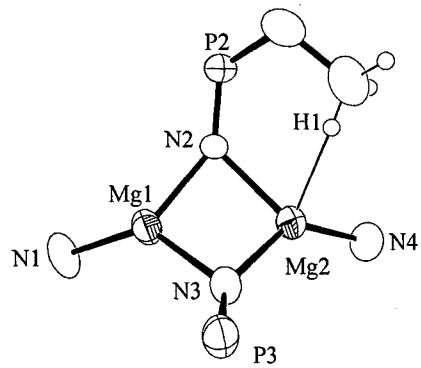

Figure 2.14: ORTEP diagram of the core fragment of $Mg_2(\mu\text{-}NP^tBu_3)_2(NP^tBu_3)_2$ (**2.14**), highlighting the agnostic interaction (additional groups omitted for clarity; 50% thermal ellipsoids; Mg-H distance 2.298 or 2.374 Å since there are 2 independent molecules in the asymmetric unit).

Although $Mg_2(\mu\text{-}NP^tBu_3)_2(NP^tBu_3)_2$ (**2.14**) did not prove useful as a transfer reagent when $Ti(N^tBu)Cl_2(^tBuPy)_2$ was used as a metal precursor, it reacted with $ZrCp(NP^tBu_3)Cl_2$ (**5.1**) to afford $ZrCp(NP^tBu_3)_2Cl$ (**5.2**) cleanly in good yield (*ca.* 85%).

Table 2.3: Select bond distances and angles for $[Mg(NP^tBu_3)_2]_2$ (**2.14**) and $[Mg(NP^iPr_3)_2]_3$ (**2.15**).[a]

Compound	Mg-N Å (bridging)	Mg-N Å (terminal)	N-P Å (bridging)	N-P Å (terminal)	Mg-N-P ° (terminal)
$[Mg(NP^tBu_3)_2]_3$ (**2.14**)	Mg(1) 2.043(5)	1.922(6)	1.541(5)	1.541(6)	150.3(4)
	Mg(1) 2.101(6)	1.902(6)	1.545(5)	1.543(5)	164.5(4)
	Mg(2) 2.050(5)				
	Mg(2) 2.089(6)				
	Mg(3) 2.046(6)	1.920(6)	1.554(6)	1.545(6)	151.2(4)
	Mg(3) 2.069(6)	1.913(6)	1.556(5)	1.545(6)	165.8(4)
	Mg(4) 2.049(6)				
	Mg(4) 2.071(6)				
$[Mg(NP^iPr_3)_2]_3$ (**2.15**)	2.0793(35)	1.9039(38)	1.5555(33)	1.5300(35)	174.96(28)
	2.0905(35)	1.8958(41)	1.5597(35)	1.5274(37)	174.53(27)
	2.0982(40)		1.5566(31)		
	2.1082(37)		1.5655(34)		

a) **2.14** has 2 independent molecules in the unit cell; Mg(1) and Mg(2) are the labels for one molecule, while Mg(3) and Mg(4) are the labels for the other molecule. Unlike the bond distances obtained for **2.15**, the distances between the bridging nitrogen atoms and the two magnesium centres are different within each dimer, therefore all values are given. The two asymmetric molecules are separated by a row division.

Methyl Methacrylate (MMA) Polymerization by Magnesium Phosphinimide Complexes

One interesting application of $Mg_2(\mu\text{-}NP^tBu_3)_2(NP^tBu_3)_2$ (**2.14**) is its ability to function as a single-component catalyst for the polymerization of MMA to produce *ca.* 70% syndiotactic poly(methyl methacrylate) (PMMA) at room temperature (Figure 2.15). Evidence from characterization of the polymer product, in addition to preliminary reactivity experiments, infers that the MMA polymerization occurs via a radical process.

The polymer physical properties include M_n = 45,427 g mol^{-1}, M_w = 87,512 g mol^{-1} and a polydispersity index (PDI) = 1.9. ^{1}H NMR spectroscopy (Figure 2.16) clearly demonstrated the primarily (*ca.* 70%) syndiotactic nature of the polymer (signature peaks due to syndiotactic PMMA: 1.82 and 0.86 ppm).[257] Surprisingly, $Mg_3(\mu\text{-}NP^iPr_3)_4(NP^iPr_3)_2$ (**2.15**) did not initiate polymerization of MMA at low,[258-263] or ambient temperatures.

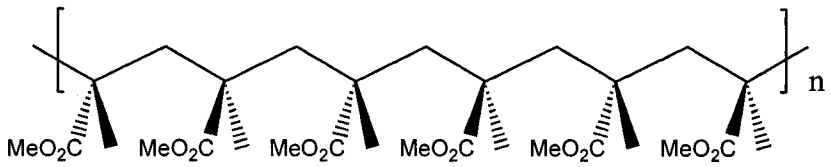

Figure 2.15: Syndiotactic PMMA.

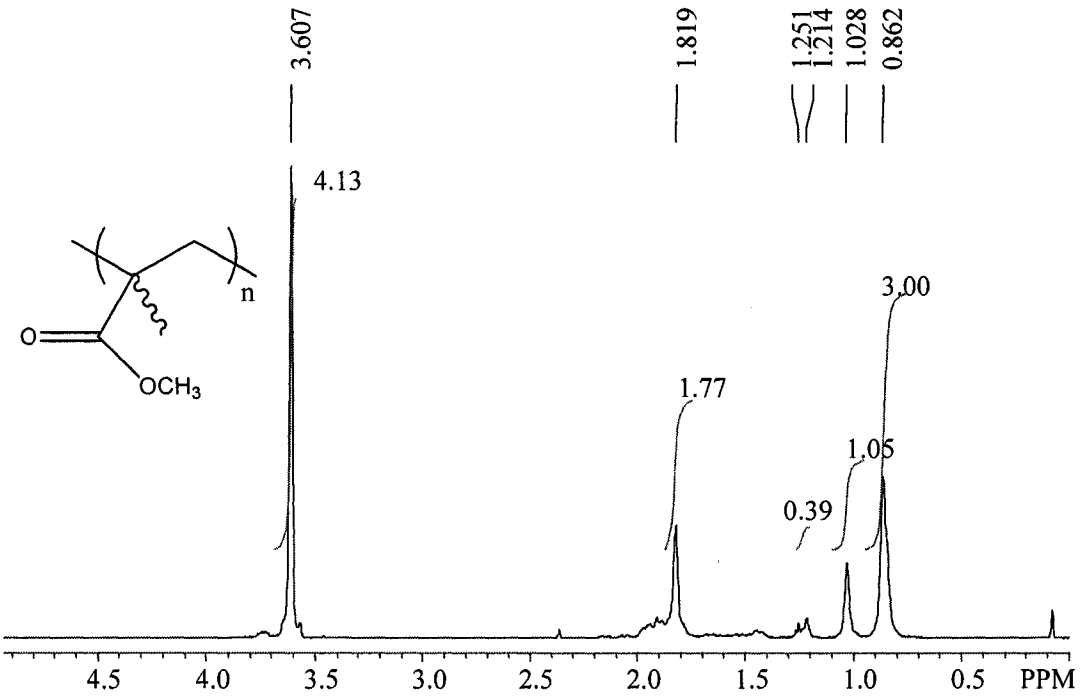

Figure 2.16: ^{1}H NMR spectrum (in $CDCl_3$, partial spectrum illustrated) of ~70% syndiotactic PMMA generated by $Mg_2(\mu\text{-}NP^tBu_3)_2(NP^tBu_3)_2$ (**2.14**).

In addition, differential scanning calorimetry (DSC) analysis of the polymer indicated a glass transition or softening temperature (T_g) of *ca.* 125°C, indicative of primarily syndiotactic PMMA. Since PMMA that is generated by free radical methods has ~67% syndiotactic polymer, this indicates that the PMMA may have been generated by a free radical process.[264] As a demonstration of its ability to give up a radical, $Mg_2(\mu\text{-}NP^tBu_3)_2(NP^tBu_3)_2$ (**2.14**) was treated with benzophenone. No immediate reaction ensued as evidenced by ^1H NMR spectroscopy, however, upon stirring in benzene for several hours, the solution changed from colourless to a deep blue, reminiscent of the presence of a ketyl radical.[265] Additional investigations would be required however, to unambiguously confirm that the polymerization occurs by a radical process.

2.4 Summary

A series of Group IV compounds that possess both phosphinimide and amide ligands have been prepared and characterized by spectroscopic and crystallographic methods. A variety of methods were attempted to generate the corresponding Group IV imido complexes that still possess phosphinimide ligands, although without profit. Perhaps of synthetic interest is the feasibility of producing $Ti(NP^tBu_3)(NRR')_3$ derivatives from reaction of half-sandwich dichloride precursors with an excess of lithium amide. It is noteworthy that this does not occur with the corresponding zirconium derivatives.

Attempts to induce hydroamination catalysis using any of the phosphinimide amide Group IV precursors was unsuccessful under the conditions employed. In general, it appears that the phosphinimide ligand will react readily with a proton source, resulting in its elimination from the metal centre.

The most interesting peripheral result is the synthesis of the magnesium phosphinimide complexes $Mg_2(\mu\text{-}NP^tBu_3)_2(NP^tBu_3)_2$ (**2.14**) and $Mg_3(\mu\text{-}NP^iPr_3)_4(NP^iPr_3)_2$ (**2.15**), which exhibit different reactivity in the presence of MMA, consistent with the differences in steric protection provided by the phosphinimide ligands. The dimer **2.14** appears to be a radical source, and probably for this reason, it successfully polymerizes methyl methacrylate at room temperature to generate low molecular weight polymers

(>750 insertions). It seems reasonable to suggest that future efforts should endeavour to rationalize how this process occurs, possibly using a combined synthetic and computational approach.

3 Group IV Complexes with *Bis*(Phosphinimide) Ligands

3.1 Introduction

Efforts to discover new, highly active olefin polymerization catalysts that are not covered by existing patents have stimulated a number of research groups[32,40] to produce commercially viable alternatives such as the constrained-geometry catalyst (CGC, **I**).[118] Recently, titanium FI catalysts (**II**, Figure 3.1) have been reported, and they also exhibit extremely high polymerization activities using mild conditions.[145] In an equally effective demonstration, Stephan and co-workers have described the enormous potential of titanium half-sandwich phosphinimide complexes as precursors for olefin polymerization.[8,21,132] The *bis*(phosphinimide) titanium complex $Ti(NP^tBu_3)Me_2$ acts as an extremely efficient catalyst upon activation with $[Ph_3C][B(C_6F_5)_4]$ when the polymerization is conducted employing industrially relevant conditions.[7] However, the *bis*(phosphinimide) catalyst precursors suffer from rapid decomposition to polymerization-inactive products upon exposure to aluminum reagents, especially trimethylaluminum (TMA).[18] In an attempt to combat this decomposition route, a chelating, di-anionic, *bis*(phosphinimide) supporting ligand was envisioned: additional bulk of the scaffold tethering the two phosphinimide fragments together might preclude certain decomposition pathways from occurring. Furthermore, it would create a more "open" metal centre, a concept that was exploited by the CGC to produce an extremely active polymerization catalyst.[118]

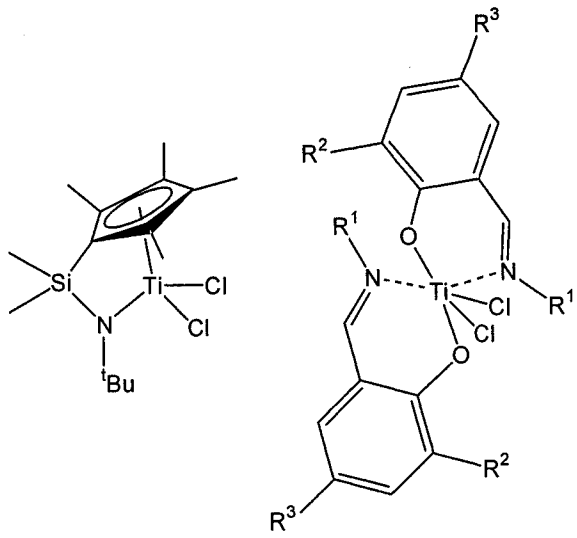

I **II**

Figure 3.1 Illustrations of the CGC (**I**) and FI (**II**) precatalysts.

This chapter details an extension of the work initiated by Dr. Jeffrey C. Stewart,[266] namely the preparation of titanium and zirconium complexes that possess a di-anionic, *bis*(phosphinimide) chelating ligand. It is worth mentioning that several chelating *bis*(phosphinimide) complexes of titanium have been reported, however, no investigation of their utility as olefin polymerization catalysts has been reported.[22,267-270] Polymerization testing of the new complexes described herein, in addition to the parent precatalyst $Ti(NP^tBu_3)_2Me_2$ will be detailed. Preliminary reactivity studies of *bis*(phosphinimide) titanium complexes will be described, both in this Chapter, and in Appendix B.

3.2 Experimental

3.2.1 General Considerations

The synthetic protocol and characterization by multinuclear NMR spectroscopy, X-ray crystallography and microanalysis were analogous to those described in Section 2.2.1 with additions noted below. $^{11}B\{^1H\}$ and ^{19}F NMR data were acquired on a Bruker Avance 300 MHz spectrometer, and were referenced using external standards: $BF_3{\cdot}Et_2O$, and 80% CCl_3F in $CDCl_3$, respectively. Thick-wall glass flasks equipped with Teflon stopcocks are referred to as "glass bombs". GPC analyses of the polymers were performed by NOVA Chemicals Corp., employing a Waters 150C GPC instrument using 1,2,4-trichlorobenzene as the mobile phase at 140°C. The samples were prepared by dissolving the polymer in the mobile phase solvent in an external oven at 0.1% (w/v) and were filtered before injection. Molecular weights are expressed as polyethylene equivalents with a relative standard deviation of 2.9% and 5.0% for the M_n and M_w, respectively. Figure 3.2 illustrates the convention used for labelling the proton and carbon NMR chemical shifts.

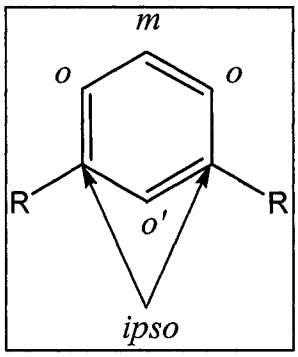

Figure 3.2

3.2.2 Solvents

Reagent grade pentanes, hexanes, PhH, PhMe, THF and Et_2O were purchased from Aldrich Chemical Co., and were pre-dried using Grubbs' column systems, manufactured by Innovative Technologies, Inc.[235] All solvents were further dried over Na prior to distillation. HPLC grade MeOH and ^{i}PrOH were purchased from Aldrich Chemical Co. and dried over Mg prior to distillation. Reagent grade NEt_3 was purchased from Fluka

Chemical Co. and was dried over KOH prior to distillation. Deuterated solvents were purified by the methods described in Section 2.2.2.

3.2.3 Reagents

The phosphines HP^tBu_2 (**3.1**) and *m*-$(CH_2PR_2)_2C_6H_4$ (R = ^{t}Bu (**3.2**), Cy (**3.3**)),[271] and the organometallic reagents $LiPCy_2$, $LiSiPh_3$,[272] $Ti(NP^tBu_3)_2Me_2$, $Ti(NP^tBu_3)_2Ph_2$[203] and $ZrBn_4$[273] were prepared via modifications of literature procedures. The reagents MeMgBr, Me_3SiCH_2MgCl, ClP^tBu_2, Me_3SiN_3, Me_3SiX (X = Cl, Br), $LiAlH_4$ and α,α'-dibromo-*m*-xylene were purchased from Aldrich Chemical Co., and $HPCy_2$, $Ti(NMe_2)_4$ and $Zr(NEt_2)_4$ were purchased from Strem Chemical Co.; all were used without further purification. The borane $B(C_6F_5)_3$ (prepared in-house) was generously donated by NOVA Chemicals Corp. and was used as received. It should be noted that the compounds *m*-$(CH_2P^tBu_2NSiMe_3)_2C_6H_4$ (**3.4**), Ti[*m*-$(CH_2P^tBu_2N)_2C_6H_4$]Me_2 (**3.16**) and Ti[*m*-$(CH_2P^tBu_2N)_2C_6H_4$]Bn_2 (**3.17**) were previously prepared by Dr. Jeffrey C. Stewart.[266]

3.2.4 Phosphines

Caution: This reaction is exothermic, and the products are volatile. Ensure that a vessel >10 times the reaction volume is employed.

Di-*tert*-butylphosphine (HP^tBu_2, **3.1**):[271] In a round-bottom flask, $LiAlH_4$ (980 mg, 25.8 mmol) was added in several portions over a 1 h period at RT to neat ClP^tBu_2 (11.72 g, 64.9 mmol). The slurry was transferred to a glass bomb, and was stirred at RT for 50 h, after which time Et_2O (5 mL) was added. The mixture was filtered twice through Celite, and the solvent was removed *in vacuo* affording a clear, colourless liquid (8.62 g, 91%). The ^{1}H NMR spectrum indicated no evidence of Et_2O, and was consistent with literature values. ^{1}H NMR (500 MHz, C_6D_6) δ: 3.18 (d, 1H, $^1J_{P\text{-}H}$ = 240 Hz, **H**P^tBu_2), 1.16 (d, 18H, $^3J_{P\text{-}H}$ = 19 Hz, C(C**H**$_3$)$_3$). $^{13}C\{^1H\}$ NMR (75.5 MHz, C_6D_6) δ: 31.9 (d, $^2J_{P\text{-}C}$ = 14

Hz, $C(\mathbf{C}H_3)_3$), 30.0 (d, $^1J_{P\text{-}C}$ = 27 Hz, $\mathbf{C}(CH_3)_3$). $^{31}P\{^1H\}$ NMR (121.5 MHz, C_6D_6) δ: 20.1 (s).

1,3-*bis*-[(di-*tert*-butylphosphinyl)methyl]benzene (*m*-$(CH_2P^tBu_2)_2C_6H_4$, **3.2**):[271] α,α'-dibromo-*m*-xylene (3.30 g, 12.50 mmol) was added to a Schlenk flask. MeOH was added via cannula to generate a slurry, and HP^tBu_2 (3.84 g, 26.26 mmol) was added via syringe at RT. The mixture was stirred for 16 h, during which time the solution grew homogeneous. NEt_3 was added via syringe (2.65 g, 26.26 mmol), and the phosphine precipitated as a fluffy white solid from solution. It was washed with MeOH (3 x 20 mL), and dried under vacuum for 5 h. A second crop was obtained by concentrating the mother liquor, and precipitating the product with degassed water; no degradation in purity was noted by ^1H NMR spectroscopy. The product was recrystallized from PhH to remove traces of $HBr{\cdot}NEt_3$. Yield: 4.40 g (89%). Spectroscopic data were consistent with literature values.[271] ^1H NMR (500 MHz, C_6D_6) δ: 7.61 (s, 1H, $C_6\mathbf{H}_4$ (*o'*-H)), 7.28 (d, 2H, $^3J_{H\text{-}H}$ = 4 Hz, $C_6\mathbf{H}_4$ (*o*-H)), 7.18 (t, 1H, $^3J_{H\text{-}H}$ = 4 Hz, $C_6\mathbf{H}_4$ (*m*-H)), 2.75 (s, 4H, $\mathbf{CH}_2P^tBu_2$), 1.08 (d, 36H, $^3J_{P\text{-}H}$ = 15 Hz, $C(C\mathbf{H}_3)_3$). $^{13}C\{^1H\}$ NMR (75.5 MHz, C_6D_6) δ: 141.8 (s, $\mathbf{C}_6H_4$ (*ipso*-C)), 131.5 (s, $\mathbf{C}_6H_4$ (*o*-C), 128.4 (s, $\mathbf{C}_6H_4$ (*o'*-C)), 127.2 (s, $\mathbf{C}_6H_4$ (*m*-C)), 31.7 (d, $^1J_{P\text{-}C}$ = 15 Hz, $\mathbf{C}(CH_3)_3$), 29.9 (s, $C(\mathbf{C}H_3)_3$), 29.1 (d, $^1J_{P\text{-}C}$ = 15 Hz, $\mathbf{C}H_2P^tBu_2$). $^{31}P\{^1H\}$ NMR (121.5 MHz, C_6D_6) δ: 33.2 (s). Colourless crystals suitable for X-ray diffraction were grown by slow evaporation from a mixture of benzene/pentanes.

1,3-*bis*-[(dicyclohexylphosphinyl)methyl]benzene (*m*-$(CH_2PCy_2)_2C_6H_4$, **3.3**):[271] *Method 1*: α,α'-dibromo-*m*-xylene (5.71 g, 21.6 mmol) was added to a Schlenk flask. MeOH was added via cannula to generate a slurry, and $HPCy_2$ (9.43 g, 47.5 mmol) was added via syringe at RT. The mixture was stirred for 16 h during which time the solution grew homogeneous. NEt_3 (4.80 g, 47.5 mmol) was added via syringe, and the solution was cooled to –30°C to afford the phosphine as fine, colourless needles (9.65g, 89%). *Method 2*: α,α'-dibromo-*m*-xylene (130 mg, 0.49 mmol) was dissolved in THF (20 mL), and the solution was cooled to -78°C. A clear solution of $LiPCy_2$ (210 mg, 1.03 mmol) in the same solvent (10 mL) was added dropwise, and the mixture was stirred for 4 h

before it was gradually warmed to RT. The solvent was removed *in vacuo*, and the product was extracted with hexanes. Following filtration through Celite, the solution was concentrated, and the product was recrystallized from pentanes to afford colourless needles (180 mg, 72%). ^{1}H NMR (500 MHz, C_6D_6) δ: 7.51 (s, 1H, $C_6\mathbf{H}_4$ (*o'*-H)), 7.18 (m, 2H, $C_6\mathbf{H}_4$ (*o*-H)), 7.17 (m, 1H, $C_6\mathbf{H}_4$ (*m*-H)), 2.77 (s, 4H, $C\mathbf{H}_2PCy_2$), 1.84-1.16 (m, 44H, $P(C_6\mathbf{H}_{11})_2$). $^{13}C\{^{1}H\}$ NMR (75.5 MHz, C_6D_6) δ: 140.8 (s, $\mathbf{C}_6H_4$ (*ipso*-C)), 130.9 (s, $\mathbf{C}_6H_4$ (*o*-C)), 128.5 (s, $\mathbf{C}_6H_4$ (*o'*-C)), 127.0 (s, $\mathbf{C}_6H_4$ (*m*-C)), 34.0 (d, $^{1}J_{P\text{-}C}$ = 24 Hz, $\mathbf{C}H_2PCy_2$), 30.3 (d, $^{1}J_{P\text{-}C}$ = 13 Hz, $P(\mathbf{C}_6H_{11})_2$ (*ipso*-C)), 29.8 (d, $^{2}J_{P\text{-}C}$ = 10 Hz, $P(\mathbf{C}_6H_{11})_2$ (*o*-C)), 27.7 (br s, $P(\mathbf{C}_6H_{11})_2$ (*m*-C)), 26.9 (s, $P(\mathbf{C}_6H_{11})_2$ (*p*-C)). $^{31}P\{^{1}H\}$ NMR (121.5 MHz, C_6D_6) δ: 1.9 (s).

3.2.5 Phosphinimines[274,275]

m-$(CH_2P^tBu_2NSiMe_3)_2C_6H_4$ (**3.4**): Solid *m*-$(CH_2P^tBu_2)_2C_6H_4$ (2.06 g, 5.22 mmol) and Me_3SiN_3 (3.01 g, 26.10 mmol) were combined in a Schlenk flask to generate a slurry. The mixture was heated at reflux for 15 h, after which time the excess Me_3SiN_3 was removed *in vacuo*. The resulting beige solid was crushed with a mortar and pestle into a fine powder and dried for an additional 5 h. Yield: 2.30 g (94%). This oxidation is also successful when PhMe is employed as a solvent. ^{1}H NMR (500 MHz, C_6D_6) δ: 7.53 (s, 1H, $C_6\mathbf{H}_4$ (*o'*-H)), 7.32 (d, 2H, $^{3}J_{H\text{-}H}$ = 5 Hz, $C_6\mathbf{H}_4$ (*o*-H)), 7.23 (t, 1H, $^{3}J_{H\text{-}H}$ = 5 Hz, $C_6\mathbf{H}_4$ (*m*-H)), 2.93 (d, 4H, $^{2}J_{P\text{-}H}$ = 10 Hz, $C\mathbf{H}_2P^tBu_2$), 1.09 (d, 36H, $^{3}J_{P\text{-}H}$ = 10 Hz, $C(C\mathbf{H}_3)_3$), 0.36 (s, 18H, $Si(C\mathbf{H}_3)_3$). $^{13}C\{^{1}H\}$ NMR (75.5 MHz, C_6D_6) δ: 135.3 (s, $\mathbf{C}_6H_4$ (*ipso*-C)), 132.7 (s, $\mathbf{C}_6H_4$ (*o*-C)), 128.8 (s, $\mathbf{C}_6H_4$ (*o'*-C)), 127.6 (s, $\mathbf{C}_6H_4$ (*m*-C)), 37.2 (d, $^{1}J_{P\text{-}C}$ = 60 Hz, $\mathbf{C}(CH_3)_3$), 31.0 (d, $^{1}J_{P\text{-}C}$ = 56 Hz, $\mathbf{C}H_2P^tBu_2$), 27.4 (s, $C(\mathbf{C}H_3)_3$), 4.9 (s, $Si(\mathbf{C}H_3)_3$). $^{31}P\{^{1}H\}$ NMR (121.5 MHz, C_6D_6) δ: 24.8 (s). Anal. Calc'd for $C_{30}H_{62}N_2P_2Si_2$: C, 63.33; H, 10.98; N, 4.92. Found: C, 63.38; H, 10.89; N, 4.90. Colourless crystals suitable for X-ray diffraction were grown by slow evaporation from benzene.

m-$(CH_2PCy_2NSiMe_3)_2C_6H_4$ (**3.5**): This was prepared by an analogous method as described for *m*-$(CH_2P^tBu_2NSiMe_3)_2C_6H_4$ (**3.4**) to afford a white solid (2.30 g, 94%). ^{1}H

NMR (500 MHz, C_6D_6) δ: 7.57 (s, 1H, $C_6\mathbf{H}_4$ (*o'*-H)), 7.22 (br, 2H, $C_6\mathbf{H}_4$ (*o*-H)), 7.16 (br, 1H, $C_6\mathbf{H}_4$ (*m*-H)), 2.82 (d, 4H, $^2J_{P-H}$ = 12 Hz, $C\mathbf{H}_2PCy_2$), 1.82-1.05 (m, 44H, $P(C_6\mathbf{H}_{11})_2$), 0.38 (s, 18H, $Si(C\mathbf{H}_3)_3$). $^{13}C\{^1H\}$ NMR (75.5 MHz, C_6D_6) δ: 134.9 (s, $\mathbf{C}_6H_4$ (*ipso*-C)), 132.3 (s, $\mathbf{C}_6H_4$ (*o*-C)), 128.3 (s, $\mathbf{C}_6H_4$ (*o'*-C)), 128.0 (s, $\mathbf{C}_6H_4$ (*m*-C)), 37.8 (d, $^1J_{P-C}$ = 65 Hz $P(\mathbf{C}_6H_{11})_2$ (*ipso*-C)), 34.0 (d, $^1J_{P-C}$ = 60 Hz, $\mathbf{C}H_2PCy_2$), 27.1 (br, $P(\mathbf{C}_6H_{11})_2$ (*o*-C)), 26.4 (s, $P(\mathbf{C}_6H_{11})_2$ (*m*-C)), 25.7 (s, $P(\mathbf{C}_6H_{11})_2$ (*p*-C)), 5.2 (s, $Si(\mathbf{C}H_3)_3$). $^{31}P\{^1H\}$ NMR (121.5 MHz, C_6D_6) δ:13.5 (s). Anal. Calc'd for $C_{38}H_{70}N_2P_2Si_2$: C, 67.81; H, 10.48; N, 4.16. Found: C, 67.66; H, 10.60; N, 4.03. Colourless crystals suitable for X-ray diffraction were grown by slow evaporation from pentanes.

m-$(CH_2P^tBu_2NH)_2C_6H_4$ (**3.6**): Solid *m*-$(CH_2P^tBu_2NSiMe_3)_2C_6H_4$ (570 mg, 1.2 mmol) and MeOH (30 mL) were heated at reflux for 16 h, after which time the volatile products were removed *in vacuo*. The residue was re-dissolved in PhH (10 mL) and filtered through Celite. Following removal of the solvent, the oily residue was washed with hexanes (3 x 10mL) and dried to ultimately afford a beige foam (320 mg, 81%). ^1H NMR (500 MHz, C_6D_6) δ: 7.75 (s, 1H, $C_6\mathbf{H}_4$ (*o'*-H)), 7.29 (d, 2H, $^3J_{H-H}$ = 4 Hz, $C_6\mathbf{H}_4$ (*o*-H)), 7.12 (br, 1H, $C_6\mathbf{H}_4$ (*m*-H)), 2.86 (d, 4H, $^2J_{P-H}$ = 18 Hz, $C\mathbf{H}_2P^tBu_2$), 1.11 (d, 36H, $^3J_{P-H}$ = 22 Hz, $C(C\mathbf{H}_3)_3$). $^{13}C\{^1H\}$ NMR (75.5 MHz, C_6D_6) δ: 135.8 (s, $\mathbf{C}_6H_4$ (*ipso*-C)), 132.6 (s, $\mathbf{C}_6H_4$ (*o*-C)), 128.3 (s, $\mathbf{C}_6H_4$ (*o'*-C)), 128.0 (s, $\mathbf{C}_6H_4$ (*m*-C)), 36.2 (d, $^1J_{P-C}$ = 56 Hz, $\mathbf{C}(CH_3)_3$), 30.1 (d, $^1J_{P-C}$ = 39 Hz, $\mathbf{C}H_2P^tBu_2$), 27.9 (s, $C(\mathbf{C}H_3)_3$). $^{31}P\{^1H\}$ NMR (121.5 MHz, C_6D_6) δ:48.2 (s). Anal. Calc'd for $C_{24}H_{46}N_2P_2$: C, 67.89; H, 10.92; N, 6.60. Found: C, 67.82; H, 10.93; N, 6.61. Colourless crystals suitable for X-ray diffraction were grown by slow evaporation from pentane.

m-$(CH_2P^tBu_2NH)_2C_6H_4$·2 HBr (**3.7**): The white solid was isolated as a by-product from the above reaction; its presence was due to HBr salts that originated from the phosphine synthesis. (PhH insol.; yield: *ca.* 20 mg, 5%) ^1H NMR (500 MHz, C_6D_6) δ: 8.60 (s, 1H, $C_6\mathbf{H}_4$ (*o'*-H)), 7.31 (t, 1H, $^3J_{H-H}$ = 8 Hz, $C_6\mathbf{H}_4$ (*m*-H)), 7.22 (d, 2H, $C_6\mathbf{H}_4$ (*o*-H)), 3.59 (d, 4H, $^2J_{P-H}$ = 11 Hz, $C\mathbf{H}_2P^tBu_2$), 1.44 (d, 36H, $^3J_{P-H}$ = 15 Hz, $C(C\mathbf{H}_3)_3$). $^{13}C\{^1H\}$ NMR (75.5 MHz, C_6D_6) δ: 134.3 (s, $\mathbf{C}_6H_4$ (*ipso*-C)), 132.2 (s, $\mathbf{C}_6H_4$ (*o*-C)), 130.7 (s, $\mathbf{C}_6H_4$ (*o'*-C)), 129.8 (s, $\mathbf{C}_6H_4$ (*m*-C)), 36.3 (d, $^1J_{P-C}$ = 50 Hz, $\mathbf{C}(CH_3)_3$), 27.7 (d, $^1J_{P-C}$ = 50 Hz,

$CH_2P^tBu_2$), 27.7 (s, $C(CH_3)_3$). $^{31}P\{^1H\}$ NMR (121.5 MHz, C_6D_6) δ: 64.3 (s). Anal. Calc'd for $C_{24}H_{48}Br_2N_2P_2$: C, 49.16; H, 8.25; N, 4.78. Found: C, 49.88; H, 8.40; N, 4.52. Colourless crystals suitable for X-ray diffraction were grown by slow evaporation from CD_2Cl_2.

m-$(CH_2PCy_2NH)_2C_6H_4$ (**3.8**): Solid *m*-$(CH_2PCy_2NSiMe_3)_2C_6H_4$ (1.08 g, 1.8 mmol) and ^iPrOH (25 mL) were heated at reflux for 16 h. Removal of the volatile products *in vacuo* afforded spectroscopically pure white solid (910 mg, 96%). ^1H NMR (500 MHz, CD_2Cl_2) δ: 10.67 (br, 2H, N-**H**), 8.30 (s, 1H, $C_6\mathbf{H}_4$ (*o'*-H)), 7.38 (t, 1H, $^3J_{H-H}$ = 8 Hz, $C_6\mathbf{H}_4$ (*m*-H)), 7.15 (d, 2H, $^3J_{H-H}$ = 8 Hz, $C_6\mathbf{H}_4$ (*o*-H)), 3.51 (d, 4H, $^2J_{P-H}$ = 12 Hz, $C\mathbf{H}_2PCy_2$), 2.34-1.23 (m, 44H, $P(C_6\mathbf{H}_{11})_2$). $^{13}C\{^1H\}$ NMR (75.5 MHz, CD_2Cl_2) δ: 140.8 (s, $\mathbf{C}_6H_4$ (*ipso*-C)), 130.9 (s, $\mathbf{C}_6H_4$ (*o*-C)), 128.5 (s, $\mathbf{C}_6H_4$ (*o'*-C)), 127.0 (s, $\mathbf{C}_6H_4$ (*m*-C)), 34.0 (d, $^1J_{P-C}$ = 24 Hz, $\mathbf{C}H_2PCy_2$), 30.3 (d, $^1J_{P-C}$ = 13 Hz, $P(\mathbf{C}_6H_{11})_2$ (*ipso*-C)), 29.8 (br, $P(\mathbf{C}_6H_{11})_2$ (*o*-C)), 27.7 (s, $P(\mathbf{C}_6H_{11})_2$ (*m*-C)), 26.9 (s, $P(\mathbf{C}_6H_{11})_2$ (*p*-C)). $^{31}P\{^1H\}$ NMR (121.5 MHz, CD_2Cl_2) δ: 36.2 (s).

3.2.6 Inorganic and Organometallic Syntheses

Ti[*m*-$(CH_2P^tBu_2N)_2C_6H_4$]$(NMe_2)_2$ (**3.9**): $Ti(NMe_2)_4$ (0.72 mL, 3.05 mmol) was dissolved in PhH (20 mL), and a solution of *m*-$(CH_2P^tBu_2NH)_2C_6H_4$ (**3.6**) (1.29 g, 3.05 mmol) in the same solvent (30 mL) was added dropwise at RT over a 15 min period. The clear yellow solution was stirred for 12 h, after which time the solvent was removed *in vacuo* to afford a sticky yellow residue. The product was washed with pentanes and dried to give a spectroscopically pure yellow solid. Yield: 1.22 g, 79%. ^1H NMR (500 MHz, C_6D_6) δ: 8.46 (s, 1H, $C_6\mathbf{H}_4$ (*o'*-H)), 7.09 (t, 1H, $^3J_{H-H}$ = 8 Hz, $C_6\mathbf{H}_4$ (*m*-H)), 6.89 (d, 2H, $^3J_{H-H}$ = 8 Hz, $C_6\mathbf{H}_4$ (*o*-H)), 3.45 (s, 12H, $N(C\mathbf{H}_3)_2$), 2.85 (d, 4H, $^2J_{P-H}$ = 9 Hz, $C\mathbf{H}_2P^tBu_2$), 1.19 (d, 36H, $^3J_{P-H}$ = 13 Hz, $C(C\mathbf{H}_3)_3$). $^{13}C\{^1H\}$ NMR (75.5 MHz, C_6D_6) δ: 134.9 (s, $\mathbf{C}_6H_4$ (*o*-C)), 134.5 (s, $\mathbf{C}_6H_4$ (*ipso*-C)), 127.4 (s, $\mathbf{C}_6H_4$ (*o'*-C)), 127.1 (s, $\mathbf{C}_6H_4$ (*m*-C)), 47.3 (s, $N(\mathbf{C}H_3)_2$), 37.1 (d, $^1J_{P-C}$ = 56 Hz, $\mathbf{C}(CH_3)_3$), 30.0 (d, $^1J_{P-C}$ = 44 Hz, $\mathbf{C}H_2P^tBu_2$), 27.7 (s, $C(\mathbf{C}H_3)_3$). $^{31}P\{^1H\}$ NMR (121.5 MHz, C_6D_6) δ: 12.7 (s).

Ti[*m*-($CH_2P^tBu_2N)_2C_6H_4$]Br(NMe_2) (**3.10**): Yellow crystals were isolated as a by-product from the above reaction; its presence was due to HBr salts that originated from the phosphine synthesis. Due to the relative insolubility of **3.10** in pentanes, it could be isolated from a crude mixture of **3.9** and **3.10** by dissolving the mixture in a minimum amount of pentanes and filtering the slurry; the solid fraction was mostly pure **3.10**, while the solution contained mostly pure **3.9**. (pentanes insol.; yield: *ca.* 125 mg, 8%) ^{1}H NMR (500 MHz, C_6D_6) δ: 8.67 (s, 1H, $C_6\mathbf{H}_4$ (*o'*-H)), 7.07 (t, 1H, $^3J_{H\text{-}H}$ = 8 Hz, $C_6\mathbf{H}_4$ (*m*-H)), 6.86 (d, 2H, $^3J_{H\text{-}H}$ = 8 Hz, $C_6\mathbf{H}_4$ (*o*-H)), 3.67 (s, 6H, $N(C\mathbf{H}_3)_2$), 2.89 (d, 2H, $^2J_{P\text{-}H}$ = 14 Hz, $C\mathbf{H}_2P^tBu_2$), 2.80 (d, 2H, $^2J_{P\text{-}H}$ = 14 Hz, $C\mathbf{H}_2P^tBu_2$), 1.24 (d, 18H, $^3J_{P\text{-}H}$ = 14 Hz, $C(C\mathbf{H}_3)_3$), 1.04 (d, 18H, $^3J_{P\text{-}H}$ = 14 Hz, $C(C\mathbf{H}_3)_3$). $^{13}C\{^1H\}$ NMR (75.5 MHz, C_6D_6) δ: 174.9 (s, $\mathbf{C}_6H_4$ (*ipso*-C)), 129.5 (s, $\mathbf{C}_6H_4$ (*o*-C)), 128.3 (s, $\mathbf{C}_6H_4$ (*o'*-C)), 127.7 (s, $\mathbf{C}_6H_4$ (*m*-C)), 48.6 (s, $N(\mathbf{C}H_3)_2$), 38.2 (d, $^1J_{P\text{-}C}$ = 56 Hz, $\mathbf{C}(CH_3)_3$), 36.2 (d, $^1J_{P\text{-}C}$ = 56 Hz, $\mathbf{C}(CH_3)_3$), 29.2 (d, $^1J_{P\text{-}C}$ = 44 Hz, $\mathbf{C}H_2P^tBu_2$), 27.3 (s, $C(\mathbf{C}H_3)_3$), 27.2 (s, $C(\mathbf{C}H_3)_3$). $^{31}P\{^1H\}$ NMR (121.5 MHz, C_6D_6) δ: 17.2 (s). Due to the presence of Ti[*m*-($CH_2P^tBu_2N)_2C_6H_4$]($NMe_2)_2$ impurity that could not be completely removed (*ca.* 5% as evidenced by ^{1}H NMR spectroscopy, the repeated microanalyses gave high carbon and hydrogen values. Anal. Calc'd for $C_{26}H_{50}BrN_3P_2Ti$: C, 52.54; H, 8.48; N, 7.07. Found: C, 55.04; H, 8.81; N, 7.11. Pale yellow crystals suitable for X-ray diffraction were grown by slow evaporation from benzene/pentanes.

Ti[*m*-($CH_2PCy_2N)_2C_6H_4$]($NMe_2)_2$ (**3.11**): This was prepared in an analogous method as described for Ti[*m*-($CH_2P^tBu_2N)_2C_6H_4$]($NMe_2)_2$ (**3.9**), thus only the analytical data is included. The product may be obtained as a yellow solid when washed with cold pentanes. Yield: 124 mg, 54%. Typical low yields are a direct result of the relative difficulty of obtaining pure *m*-($CH_2PCy_2NH)_2C_6H_4$ (**3.8**). ^{1}H NMR (500 MHz, C_6D_6) δ: 8.60 (s, 1H, $C_6\mathbf{H}_4$ (*o'*-H)), 7.11 (t, 1H, $^3J_{H\text{-}H}$ = 7.5 Hz, $C_6\mathbf{H}_4$ (*m*-H)), 7.86 (d, 2H, $^3J_{H\text{-}H}$ = 7.5 Hz, $C_6\mathbf{H}_4$ (*o*-H)), 3.57 (s, 12H, $N(C\mathbf{H}_3)_2$), 2.69 (d, 4H, $^2J_{P\text{-}H}$ = 11 Hz, $C\mathbf{H}_2PCy_2$), 1.95-1.32 (m, 44H, $P(C_6\mathbf{H}_{11})_2$). $^{13}C\{^1H\}$ NMR (75.5 MHz, C_6D_6) δ: 134.0 (s, $\mathbf{C}_6H_4$ (*ipso*-C)), 133.9 (s, $\mathbf{C}_6H_4$ (*o*-C)), 127.3 (s, $\mathbf{C}_6H_4$ (*o'*-C)), 127.1 (s, $\mathbf{C}_6H_4$ (*m*-C)), 48.1 (s, $N(\mathbf{C}H_3)_2$), 37.8 (d, $^1J_{P\text{-}C}$ = 62 Hz, $P(\mathbf{C}_6H_{11})_2$ (*ipso*-C)), 33.1 (d, $^1J_{P\text{-}C}$ = 48 Hz, $\mathbf{C}H_2PCy_2$), 27.4 (d, $^2J_{P\text{-}}$

$_C$ = 12 Hz, $P(\mathbf{C}_6H_{11})_2$ (*o*-C)), 26.6 (s, $P(\mathbf{C}_6H_{11})_2$ (*m*-C)), 26.5 (s, $P(\mathbf{C}_6H_{11})_2$ (*p*-C)). $^{31}P\{^1H\}$ NMR (121.5 MHz, C_6D_6) δ: 1.6 (s). Anal. Calc'd for $C_{36}H_{64}N_4P_2Ti$: C, 65.24; H, 9.73; N, 8.45. Found: C, 64.37; H, 9.58; N, 8.42.

Zr[*m*-$(CH_2P^tBu_2N)_2C_6H_4$]$(NEt_2)_2$ (**3.12**): $Zr(NEt_2)_4$ (199 mg, 0.53 mmol) was dissolved in PhH (15 mL), and a clear solution of *m*-$(CH_2P^tBu_2NH)_2C_6H_4$ (**3.6**) (223 mg, 0.53 mmol) in the same solvent (10 mL) was added dropwise at RT. The solution was stirred at RT for 24 h, after which time the volatile products were removed *in vacuo* to afford an oily residue. Pentanes were added to precipitate a pale yellow solid, which was subsequently filtered, washed with pentanes and dried. Yield: 302 mg, 87%. ^1H NMR (500 MHz, C_6D_6) δ: 8.20 (s, 1H, $C_6\mathbf{H}_4$ (*o'*-H)), 7.09 (t, 1H, $^3J_{H\text{-}H}$ = 8 Hz, $C_6\mathbf{H}_4$ (*m*-H)), 6.88 (d, 2H, $^3J_{H\text{-}H}$ = 8 Hz, $C_6\mathbf{H}_4$ (*o*-H)), 3.59 (q, 8H, $^3J_{H\text{-}H}$ = 7 Hz, $N(C\mathbf{H}_2CH_3)_2$), 2.83 (d, 4H, $^2J_{P\text{-}H}$ = 10 Hz, $C\mathbf{H}_2P^tBu_2$), 1.38 (t, 12H, $^3J_{H\text{-}H}$ = 7 Hz, $N(CH_2C\mathbf{H}_3)_2$), 1.17 (d, 36H, $^3J_{P\text{-}H}$ = 13 Hz, $C(C\mathbf{H}_3)_3$). $^{13}C\{^1H\}$ NMR (75.5 MHz, C_6D_6) δ: 134.9 (d, $^3J_{P\text{-}C}$ = 9 Hz, $\mathbf{C}_6H_4$ (*o*-C)), 133.7 (s, $\mathbf{C}_6H_4$ (*ipso*-C)), 127.5 (s, $\mathbf{C}_6H_4$ (*o'*-C)), 127.4 (s, $\mathbf{C}_6H_4$ (*m*-C)), 45.8 (s, $N(\mathbf{C}H_2CH_3)_2$), 37.1 (d, $^1J_{P\text{-}C}$ = 56 Hz, $\mathbf{C}(CH_3)_3$), 30.4 (d, $^1J_{P\text{-}C}$ = 44 Hz, $\mathbf{C}H_2P^tBu_2$), 27.9 (s, $C(\mathbf{C}H_3)_3$), 17.1 (s, $N(CH_2\mathbf{C}H_3)_2$). $^{31}P\{^1H\}$ NMR (121.5 MHz, C_6D_6) δ: 16.0 (s). Anal. Calc'd for $C_{32}H_{64}N_4P_2Zr$: C, 58.41; H, 9.80; N, 8.51. Found: C, 55.07; H, 9.13; N, 7.64.

Ti[*m*-$(CH_2P^tBu_2N)_2C_6H_4$]Br_2 (**3.13**): A 1:9 mixture of Ti[*m*-$(CH_2P^tBu_2N)_2C_6H_4$]$Br(NMe_2)$ (**3.10**) and Ti[*m*-$(CH_2P^tBu_2N)_2C_6H_4$]$(NMe_2)_2$ (**3.9**) (551 mg, *ca.* 1.1 mmol) was dissolved in PhH (40 mL) to give a clear yellow solution, and Me_3SiBr (0.30 mL, 2.2 mmol) was added dropwise at RT. The solution was stirred for 20 h, during which time a precipitate formed. The beige solid that precipitated was filtered, washed with pentanes (3 x 5 mL) and dried *in vacuo*. Yield: 522 mg (76%). ^1H NMR (500 MHz, CD_2Cl_2) δ: 8.70 (s, 1H, $C_6\mathbf{H}_4$ (*o'*-H)), 7.19 (t, 1H, $^3J_{H\text{-}H}$ = 7 Hz, $C_6\mathbf{H}_4$ (*m*-H)), 7.12 (d, 2H, $^3J_{H\text{-}H}$ = 7 Hz, $C_6\mathbf{H}_4$ (*o*-H)), 3.27 (d, 4H, $^2J_{P\text{-}H}$ = 10 Hz, $C\mathbf{H}_2P^tBu_2$), 1.34 (d, 36H, $^3J_{P\text{-}H}$ = 14 Hz, $C(C\mathbf{H}_3)_3$). ^1H NMR (500 MHz, C_6D_6) δ: 8.92 (s, 1H, $C_6\mathbf{H}_4$ (*o'*-H)), 7.04 (t, 1H, $^3J_{H\text{-}H}$ = 8 Hz, $C_6\mathbf{H}_4$ (*m*-H)), 6.80 (d, 2H, $^3J_{H\text{-}H}$ = 8 Hz, $C_6\mathbf{H}_4$ (*o*-H)), 2.78 (d, 4H, $^2J_{P\text{-}H}$ = 10 Hz, $C\mathbf{H}_2P^tBu_2$), 1.10 (d, 36H, $^3J_{P\text{-}H}$ = 14 Hz, $C(C\mathbf{H}_3)_3$). $^{13}C\{^1H\}$

NMR (75.5 MHz, CD_2Cl_2) δ: 135.4 (s, $\mathbf{C}_6H_4$ (*o'*-C)), 133.0 (d, $^2J_{P\text{-}C}$ = 8 Hz, $\mathbf{C}_6H_4$ (*ipso*-C)), 128.6 (s, $\mathbf{C}_6H_4$ (*o*-C)), 128.2 (s, $\mathbf{C}_6H_4$ (*m*-C)), 39.1 (d, $^1J_{P\text{-}C}$ = 54 Hz, $\mathbf{C}(CH_3)_3$), 29.4 (d, $^1J_{P\text{-}C}$ = 45 Hz, $\mathbf{C}H_2P^tBu_2$), 27.8 (s, $C(\mathbf{C}H_3)_3$). $^{31}P\{^1H\}$ NMR (121.5 MHz, CD_2Cl_2) δ: 24.7 (s). $^{31}P\{^1H\}$ NMR (121.5 MHz, C_6D_6) δ: 22.4. Anal. Calc'd for $C_{24}H_{44}Br_2N_2P_2Ti$: C, 45.74; H, 7.04; N, 4.44. Found: C, 45.31; H, 7.11; N, 4.25.

The following compounds were prepared in a similar fashion, with use of the silyl reagent Me_3SiCl, thus only the characterization is described.

Ti[*m*-$(CH_2PCy_2N)_2C_6H_4$]Cl_2 (**3.14**): White solid (342 mg, 73%). An alternative route afforded the desired product in low yields (ca. 10-20%) via Me_3SiCl elimination from the reaction of $TiCl_4$ with *m*-$(CH_2PCy_2NSiMe_3)_2C_6H_4$ (**3.5**) as described by Dr. Jeff Stewart.[266] ^1H NMR (500 MHz, C_6D_6) δ: 8.94 (s, 1H, $C_6\mathbf{H}_4$ (*o'*-H)), 7.09 (t, 1H, $^3J_{H\text{-}H}$ = 7.5 Hz, $C_6\mathbf{H}_4$ (*m*-H)), 6.83 (d, 2H, $^3J_{H\text{-}H}$ = 7.5 Hz, $C_6\mathbf{H}_4$ (*o*-H)), 2.64 (d, 4H, $^2J_{P\text{-}H}$ = 11 Hz, $C\mathbf{H}_2PCy_2$), 2.10-0.99 (m, 44H, $P(C_6\mathbf{H}_{11})_2$). $^{13}C\{^1H\}$ NMR (75.5 MHz, C_6D_6) δ: 135.1 (s, $\mathbf{C}_6H_4$ (*ipso*-C)), 132.4 (s, $\mathbf{C}_6H_4$ (*o*-C)), 128.1 (s, $\mathbf{C}_6H_4$ (*o'*-C)), 128.0 (s, $\mathbf{C}_6H_4$ (*m*-C)), 37.3 (d, $^1J_{P\text{-}C}$ = 62 Hz, $P(\mathbf{C}_6H_{11})_2$ (*ipso*-C)), 31.4 (d, $^1J_{P\text{-}C}$ = 49 Hz, $\mathbf{C}H_2PCy_2$), 26.9 (d, $^2J_{P\text{-}C}$ = 8 Hz, $P(\mathbf{C}_6H_{11})_2$ (*o*-C)), 26.7 (d, $^2J_{P\text{-}C}$ = 6 Hz, $P(\mathbf{C}_6H_{11})_2$ (*o*-C)), 26.2 (br s, $P(\mathbf{C}_6H_{11})_2$ (*m*-C)), 26.1 (br s, $P(\mathbf{C}_6H_{11})_2$ (*m*-C)), 25.9 (s, $P(\mathbf{C}_6H_{11})_2$ (*p*-C)). $^{31}P\{^1H\}$ NMR (121.5 MHz, C_6D_6) δ: 8.8 (s). Anal. Calc'd for $C_{32}H_{52}Cl_2N_2P_2Ti$: C, 59.54; H, 8.12; N, 4.34. Found: C, 59.92; H, 8.45; N, 4.43. Colourless crystals suitable for X-ray diffraction were grown by slow evaporation from benzene/pentanes.

Zr[*m*-$(CH_2P^tBu_2N)_2C_6H_4$]Cl_2 (**3.15**): White solid (120 mg, 75%). ^1H NMR (500 MHz, C_6D_6) δ: 7.56 (s, 1H, $C_6\mathbf{H}_4$ (*o'*-H)), 7.31 (d, 2H, $^3J_{H\text{-}H}$ = 7 Hz, $C_6\mathbf{H}_4$ (*o*-H)), 7.23 (t, 1H, $^3J_{H\text{-}H}$ = 7 Hz, $C_6\mathbf{H}_4$ (*m*-H)), 2.92 (d, 4H, $^2J_{P\text{-}H}$ = 11 Hz, $C\mathbf{H}_2P^tBu_2$), 1.05 (d, 36H, $^3J_{P\text{-}H}$ = 13 Hz, $C(C\mathbf{H}_3)_3$). $^{13}C\{^1H\}$ NMR (75.5 MHz, CD_2Cl_2) δ: 129.3 (s, $\mathbf{C}_6H_4$ (*o'*-C)), 135.0 (s, $\mathbf{C}_6H_4$ (*ipso*-C)), 127.1 (s, $\mathbf{C}_6H_4$ (*o*-C)), 125.6 (s, $\mathbf{C}_6H_4$ (*m*-C)), 37.2 (d, $^1J_{P\text{-}C}$ = 60 Hz, $\mathbf{C}(CH_3)_3$), 31.0 (d, $^1J_{P\text{-}C}$ = 56 Hz, $\mathbf{C}H_2P^tBu_2$), 27.6 (s, $C(\mathbf{C}H_3)_3$). $^{31}P\{^1H\}$ NMR (121.5 MHz, C_6D_6) δ: 24.5 (s).

Ti[*m*-$(CH_2P^tBu_2N)_2C_6H_4$]Me_2 (**3.16**): Ti[*m*-$(CH_2P^tBu_2N)_2C_6H_4$]Br_2 (250 mg, 0.40 mmol) was slurried in Et_2O (30 mL), and MeMgBr (0.29 mL, 0.88 mmol, 3M solution in Et_2O) was added dropwise at RT. The solution was stirred for 12 h, after which time the solvent was removed *in vacuo*. The product was extracted with pentanes (3 x 10 mL) and filtered through Celite. The solvent was removed *in vacuo*, affording a beige solid. Yield: 102 mg, 50%. ^{1}H NMR (500 MHz, C_6D_6) δ: 8.48 (s, 1H, $C_6\mathbf{H}_4$ (*o'*-H)), 7.05 (t, 1H, $^3J_{H\text{-}H}$ = 8 Hz, $C_6\mathbf{H}_4$ (*m*-H)), 6.84 (d, 2H, $^3J_{H\text{-}H}$ = 8 Hz, $C_6\mathbf{H}_4$ (*o*-H)), 2.84 (d, 4H, $^2J_{P\text{-}H}$ = 10 Hz, $C\mathbf{H}_2P^tBu_2$), 1.17 (d, 36H, $^3J_{P\text{-}H}$ = 14 Hz, $C(C\mathbf{H}_3)_3$), 0.88 (s, 6H, Ti-$C\mathbf{H}_3$). $^{13}C\{^1H\}$ NMR (75.5 MHz, C_6D_6) δ: 134.0 (s, $\mathbf{C}_6H_4$ (*ipso*-C)), 128.2 (s, $\mathbf{C}_6H_4$ (*o*-C)), 127.8 (s, $\mathbf{C}_6H_4$ (*o'*-C)), 127.2 (s, $\mathbf{C}_6H_4$ (*m*-C)), 37.9 (d, $^1J_{P\text{-}C}$ = 57 Hz, $\mathbf{C}(CH_3)_3$), 36.9 (s, Ti-$\mathbf{C}H_3$), 29.7 (d, $^1J_{P\text{-}C}$ = 44 Hz, $\mathbf{C}H_2P^tBu_2$), 27.6 (s, $C(\mathbf{C}H_3)_3$). $^{31}P\{^1H\}$ NMR (121.5 MHz, C_6D_6) δ: 12.4 (s). The spectroscopic data were similar to that reported by Dr. Jeffrey Stewart, who had previously obtained microanalytical data.[266] Anal. Calc'd for $C_{26}H_{50}N_2P_2Ti$: C, 62.39; H, 10.07; N, 5.60. Found: C, 63.59; H, 10.06; N, 5.22.

The synthetic methodology for the compounds **3.17** and **3.18** is analogous to the protocol described for **3.16** using the appropriate Grignard reagent (BnMgCl, Me_3SiCH_2MgCl) and titanium chloride precursor, thus only the analytical data is included.

Ti[*m*-$(CH_2P^tBu_2N)_2C_6H_4$]Bn_2 (**3.17**): Yellow-orange solid (62 mg, 74%). ^{1}H NMR (500 MHz, C_6D_6) δ: 8.21 (s, 1H, $C_6\mathbf{H}_4$ (*o'*-H)), 7.30 (d, 4H, $^3J_{H\text{-}H}$ = 8 Hz, $C_6\mathbf{H}_5$ (*o*-H)), 7.24 (pseudo t, 4H, $^3J_{H\text{-}H}$ = 8 Hz, $C_6\mathbf{H}_5$ (*m*-H)), 7.00 (t, 1H, $^3J_{H\text{-}H}$ = 8 Hz, $C_6\mathbf{H}_4$ (*m*-H)), 6.89 (t, 2H, $^3J_{H\text{-}H}$ = 8 Hz, $C_6\mathbf{H}_5$ (*p*-H)), 6.82 (d, 2H, $^3J_{H\text{-}H}$ = 8 Hz, $C_6\mathbf{H}_4$ (*o*-H)), 2.86 (s, 4H, $C\mathbf{H}_2Ph$), 2.75 (d, 4H, $^2J_{P\text{-}H}$ = 14 Hz, $C\mathbf{H}_2P^tBu_2$), 1.02 (d, 36H, $^3J_{P\text{-}H}$ = 16 Hz, $C(C\mathbf{H}_3)_3$). $^{13}C\{^1H\}$ NMR (75.5 MHz, C_6D_6) δ: 151.9 (s, $\mathbf{C}_6H_5$ (*ipso*-C)), 134.0 (s, $\mathbf{C}_6H_4$ (*ipso*-C)), 133.6 (s, $\mathbf{C}_6H_4$ (*o'*-C)), 128.5 (s, $\mathbf{C}_6H_5$ (*o*-C)), 128.2 (s, $\mathbf{C}_6H_4$ (*o*-C)), 127.5 (s, $\mathbf{C}_6H_4$ (*m*-C)), 127.0 (s, $\mathbf{C}_6H_5$ (*m*-C)), 120.1 (s, $\mathbf{C}_6H_5$ (*p*-C)), 67.5 (s, $\mathbf{C}H_2Ph$), 37.4 (d, $^1J_{P\text{-}C}$ = 56 Hz, $\mathbf{C}(CH_3)_3$), 29.8 (d, $^1J_{P\text{-}C}$ = 43 Hz, $\mathbf{C}H_2P^tBu_2$), 27.7 (s, $C(\mathbf{C}H_3)_3$). $^{31}P\{^1H\}$ NMR (121.5 MHz, C_6D_6) δ: 15.5 (s).

$Ti(NP^tBu_3)_2(CH_2SiMe_3)_2$ (**3.18**): White solid (77%). ^1H NMR (500 MHz, C_6D_6) δ: 1.38 (d, 54H, $^3J_{P-H}$ = 13 Hz, $C(CH_3)_3$), 1.21 (s, 4H, $CH_2Si(CH_3)_3$), 0.43 (s, 18H, $CH_2Si(CH_3)_3$). $^{13}C\{^1H\}$ NMR (75.5 MHz, C_6D_6) δ: 53.4 (s, $CH_2Si(CH_3)_3$), 41.0 (d, $^1J_{P-C}$ = 47 Hz, $C(CH_3)_3$), 30.1 (s, $C(CH_3)_3$), 3.9 (s, $CH_2Si(CH_3)_3$). $^{31}P\{^1H\}$ NMR (121.5 MHz, C_6D_6) δ: 26.1 (s).

$Ti(NP^tBu_3)_2(SiPh_3)_2$ (**3.19**):[272] Solid Ph_3SiLi (207 mg, 0.68 mmol) was added in several portions at RT to a clear solution of $Ti(NP^tBu_3)_2Cl_2$ (214 mg, 0.34 mmol) in PhH (20 mL). After stirring for 12 h, the dark green slurry was filtered through Celite. Removal of the solvent afforded a dark green solid; to obtain spectroscopically pure colourless product, the solid was recrystallized from PhMe at –30°C (242 mg, 71%). ^1H NMR (500 MHz, C_6D_6) δ: 7.66 (dd, 12H, $^3J_{H-H}$ = 8 Hz, $^4J_{H-H}$ = 2 Hz, C_6H_5 (*o*-H)), 7.60 (m, 6H, C_6H_5 (*p*-H)), 7.18 (m, 12H, C_6H_5 (*m*-H)), 1.49 (d, 54H, $^3J_{P-H}$ = 13 Hz, $C(CH_3)_3$). $^{13}C\{^1H\}$ NMR (75.5 MHz, C_6D_6) δ: 136.9 (s, C_6H_5 (*o*-C)), 136.4 (s, C_6H_5 (*p*-C)), 135.1 (s, C_6H_5 (*ipso*-C)), 129.8 (s, C_6H_5 (*m*-C)), 41.1 (d, $^1J_{P-C}$ = 48 Hz, $C(CH_3)_3$), 30.6 (s, $C(CH_3)_3$). $^{31}P\{^1H\}$ NMR (121.5 MHz, C_6D_6) δ: 25.8 (s).

$Zr[m\text{-}(CH_2P^tBu_2N)_2C_6H_4]_2$ (**3.20**): Solid $ZrBn_4$ (100 mg, 0.22 mmol) was added at RT to a clear solution of $m\text{-}(CH_2P^tBu_2NH)_2C_6H_4$ (**3.6**) (191 mg, 0.45 mmol) in PhH (20 mL). The slurry became dark brown and homogeneous upon stirring for 16 h. Following filtration through Celite, the solvent was removed *in vacuo*, affording a colourless solid. It was washed with pentanes (3 x 5 mL) and dried *in vacuo*. Yield: 96 mg, 47%. ^1H NMR (500 MHz, C_6D_6) δ: 8.34 (s, 1H, C_6H_4 (*o'*-H)), 7.12 (t, 1H, $^3J_{H-H}$ = 7 Hz, C_6H_4 (*m*-H)), 6.97 (d, 2H, $^3J_{H-H}$ = 7 Hz, C_6H_4 (*o*-H)), 3.00 (d, 4H, $^2J_{P-H}$ = 10 Hz, $CH_2P^tBu_2$), 1.28 (d, 36H, $^3J_{P-H}$ = 13 Hz, $C(CH_3)_3$). $^{13}C\{^1H\}$ NMR (75.5 MHz, C_6D_6) δ: 135.7 (s, C_6H_4 (*ipso*-C)), 133.4 (s, C_6H_4 (*o'*-C)), 127.3 (s, C_6H_4 (*o*-C)), 126.9 (s, C_6H_4 (*m*-C)), 37.4 (d, $^1J_{P-C}$ = 56 Hz, $C(CH_3)_3$), 31.9 (d, $^1J_{P-C}$ = 44 Hz, $CH_2P^tBu_2$), 28.7 (s, $C(CH_3)_3$). $^{31}P\{^1H\}$ NMR (121.5 MHz, C_6D_6) δ: 11.7 (s).

Generation of Al[*m*-($CH_2P^tBu_2N$)($CH_2P^tBu_2NH$)C_6H_4]Me_2 (**3.21**): Al_2Me_6 (110 μL, 1.20 mmol Al) was added dropwise to a clear solution of *m*-($CH_2P^tBu_2NH$)$_2C_6H_4$ (**3.6**) (52 mg, 0.12 mmol) in C_6D_6 (0.7 mL) at RT. The solution was stirred for 1 h, then transferred to an NMR tube for analysis; quantitative conversion to product was observed in addition to excess Al_2Me_6). ^1H NMR (500 MHz, C_6D_6) δ: 7.72 (br s, 1H, $C_6\mathbf{H}_4$ (*o'*-H)), 7.16 (br, 1H, $^3J_{H-H}$ = 8 Hz, $C_6\mathbf{H}_4$ (*m*-H)), 7.01 (br, 2H, $^3J_{H-H}$ = 8 Hz, $C_6\mathbf{H}_4$ (*o*-H)), 3.00 (br d, 4H, $^2J_{P-H}$ = 12 Hz, $C\mathbf{H}_2P^tBu_2$), 0.68 (d, 36H, $^3J_{P-H}$ = 14 Hz, $C(C\mathbf{H}_3)_3$), 0.14 (s, 6H, Al-$C\mathbf{H}_3$). $^{13}C\{^1H\}$ NMR (75.5 MHz, C_6D_6) δ: 133.0 (s, $\mathbf{C}_6H_4$ (*ipso*-C)), 132.9 (s, $\mathbf{C}_6H_4$ (*o*-C)), 130.2 (s, $\mathbf{C}_6H_4$ (*o'*-C)), 129.2 (s, $\mathbf{C}_6H_4$ (*m*-C)), 35.9 (d, $^1J_{P-C}$ = 30 Hz, $\mathbf{C}(CH_3)_3$), 27.8 (d, $^1J_{P-C}$ = 32 Hz, $\mathbf{C}(CH_3)_3$), 26.9 (s, $C(\mathbf{C}H_3)_3$), 1.4 (s, Al-$\mathbf{C}H_3$). $^{31}P\{^1H\}$ NMR (121.5 MHz, C_6D_6) δ: 62.6 (s).

3.2.7 Reactivity of Bis(phosphinimide) Titanium Complexes

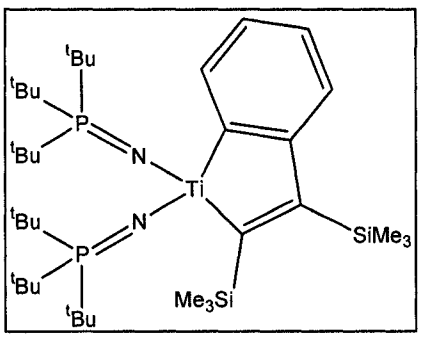

Ti(NP^tBu_3)$_2$[*o*-(Me_3SiC=$CSiMe_3$)C_6H_4] (**3.22**): Ti(NP^tBu_3)$_2Ph_2$ (46 mg, 0.07 mmol) was dissolved in PhMe-d_8 (0.75 mL), and $Me_3SiCCSiMe_3$ (17 μL, 0.07 mmol) was added via syringe. The clear solution was transferred to a glass bomb, and the solution was freeze/pump/thaw degassed (x 3). The solution was heated under static vacuum for 48 h at 90°C, resulting in a 50% conversion to the insertion product. PhH (50%) was also seen in the ^1H NMR spectrum, proffering evidence of the desired benzyne intermediate. ^1H NMR (500 MHz, C_6D_6) δ: 7.50 (d, 1H, $^3J_{H-H}$ = 8 Hz, $C_6\mathbf{H}_4$ (*o*-H)), 7.37 (dd, 1H, $^3J_{H-H}$ = 7 Hz, $^4J_{H-H}$ = 1 Hz, $C_6\mathbf{H}_4$ (*o'*-H)), 7.11 (td, 1H, $^3J_{H-H}$ = 8 Hz, $^4J_{H-H}$ = 1 Hz, $C_6\mathbf{H}_4$ (*m'*-H)), 6.89 (td, 1H, $^3J_{H-H}$ = 7 Hz, $^4J_{H-H}$ = 1 Hz, $C_6\mathbf{H}_4$ (*m*-H)), 1.32 (d, 36H, $^3J_{P-H}$ = 13 Hz, $C(C\mathbf{H}_3)_3$), 0.57 (s, 9H, $Si(C\mathbf{H}_3)_3$), 0.50 (s, 9H, $Si(C\mathbf{H}_3)_3$). $^{13}C\{^1H\}$ NMR (75.5 MHz, C_6D_6) δ: 192.7 (s, (*quaternary*-C)), 188.8 (s, (*quaternary*-C)), 167.9 (s, (*quaternary*-C)), 146.7 (s, (*quaternary*-C)), 134.2 (s, $\mathbf{C}_6H_4$ (*o'*-C)), 126.3 (s, $\mathbf{C}_6H_4$ (*o*-C)), 126.2 (s, $\mathbf{C}_6H_4$ (*m'*-C)), 122.9 (s, $\mathbf{C}_6H_4$ (*m*-C)), 41.0 (d, $^1J_{P-C}$ =

47 Hz, $C(CH_3)_3$), 30.0 (s, $C(CH_3)_3$), 4.24 (s, $Si(CH_3)_3$), 4.16 (s, $Si(CH_3)_3$). $^{31}P\{^1H\}$ NMR (121.5 MHz, C_6D_6) δ: 28.4 (s).

3.2.8 X-Ray Experimental

X-ray structural solutions of *m*-$(CH_2P^tBu_2)_2C_6H_4$ (**3.2**), *m*-$(CH_2P^tBu_2NSiMe_3)_2C_6H_4$ (**3.4**), *m*-$(CH_2PCy_2NSiMe_3)_2C_6H_4$ (**3.5**), *m*-$(CH_2P^tBu_2NH)_2C_6H_4$ (**3.6**), Ti[*m*-$(CH_2P^tBu_2N)_2C_6H_4]Br(NMe_2)$ (**3.10**), Ti[*m*-$(CH_2PCy_2N)_2C_6H_4](NMe_2)_2$ (**3.11**), and Ti[*m*-$(CH_2PCy_2N)_2C_6H_4]Cl_2$ (**3.14**) were obtained using direct methods or by a Patterson map. Preliminary solutions were obtained for *m*-$(CH_2P^tBu_2NH)_2C_6H_4$·2 HBr (**3.7**) and Ti[*m*-$(CH_2P^tBu_2N)_2C_6H_4]Br_2$ (**3.13**), although the data were too poor for a detailed discussion. Cell parameters, R, R_w and GoF values are located in Table 3.1, while additional structural parameters have been included as an appendix on CD. The solution for structure **3.11** is disordered, therefore 21 of the atoms were refined isotropically (two cyclohexyl groups), while 31 of the 43 atoms were refined anisotropically (9 extra atoms due to disorder). The solution for structure **3.10** included two molecules of C_6H_6, and the 12 additional atoms were refined anisotropically. No residual electron density remained in any of the solutions that was of any chemical significance. An ORTEP drawing of **3.6** is depicted in Figure 3.5, while select bond distances and angles are provided in Tables 3.2, 3.3 and in the text.

Table 3.1: Crystallographic parameters for *m*-$(CH_2P^tBu_2)_2C_6H_4$ (**3.2**), *m*-$(CH_2P^tBu_2NSiMe_3)_2C_6H_4$ (**3.4**) and *m*-$(CH_2PCy_2NSiMe_3)_2C_6H_4$ (**3.5**).

	3.2	**3.4**	**3.5**
Molecular formula	$C_{24}H_{44}P_2$	$C_{30}H_{62}N_2P_2Si_2$	$C_{38}H_{70}N_2P_2Si_2$
Formula weight	394.53	568.94	673.08
a(Å)	25.55(1)	9.860(9)	10.541(6)
b(Å)	8.449(5)	14.08(1)	15.118(8)
c(Å)	12.046(6)	14.83(1)	15.328(9)
α(°)	90.00	65.98(2)	67.282(9)
β(°)	93.01(1)	75.78(2)	71.043(9)
γ (°)	90.00	84.34(2)	75.16(1)
Crystal system	Monoclinic	Triclinic	Triclinic
Space group	Cc	P-1	P-1
Volume ($Å^3$)	2597(2)	1824(3)	2107(2)
D_{calc} (gcm^{-3})	1.009	1.036	1.061
Z	4	2	2
Abs coeff, μ, mm^{-1}	0.173	0.204	0.186
θ range (°)	3.03-23.24	1.58-23.66	2.71-23.37
Reflections collected	5318	7834	8928
Data $F_o^2 > 3\sigma(F_o^2)$	2266	3816	4583
Parameters	235	325	397
R(%)	0.0408	0.0438	0.0449
R_w(%)	0.1159	0.1177	0.1246
Goodness of Fit	1.047	0.959	1.036

The data was collected at 20°C with Mo Kα radiation (λ = 0.71069 Å)

$R = \Sigma \, | \, |F_o| - |F_c| \, | \, / \, \Sigma \, |F_o|$, $R_w = [\Sigma(|F_o| - |F_c|)^2 / \Sigma \, |F_o|^2]^{0.5}$

Table 3.1 (continued): Crystallographic parameters for *m*-$(CH_2P^tBu_2NH)_2C_6H_4$ (**3.6**), *m*-$(CH_2P^tBu_2NH)_2C_6H_4 \cdot 2$ HBr (**3.7**), Ti[*m*-$(CH_2P^tBu_2N)_2C_6H_4$]Br(NMe_2) (**3.10**).

	3.6	**3.7**	**3.10**
Molecular formula	$C_{24}H_{46}N_2P_2$	$C_{24}H_{48}Br_2N_2P_2$	$C_{38}H_{62}BrN_3P_2Ti$
Formula weight	424.57	586.41	750.66
a(Å)	13.457(8)	24.20(2)	14.413(8)
b(Å)	13.908(8)	15.02(1)	17.579(9)
c(Å)	14.713(8)	19.79(1)	17.190(9)
α(°)	90.00	90.00	90.00
β(°)	108.388(10)	94.89(1)	103.449(11)
γ (°)	90.00	90.00	90.00
Crystal system	Monoclinic	Monoclinic	Monoclinic
Space group	$P2_1/n$	C2/c	$P2_1/n$
Volume ($Å^3$)	2613(3)	7167(8)	4236(4)
D_{calc} (gcm^{-3})	1.079	1.385	1.177
Z	4	8	4
Abs coeff, μ, mm^{-1}	0.178	1.344	1.248
θ range (°)	1.79-23.17	1.86-23.33	1.68-23.26
Reflections collected	10896	5122	17553
Data $F_o^2 > 3\sigma(F_o^2)$	2709	1860	3638
Parameters	253	293	406
R(%)	0.0422	0.1083	0.0686
R_w(%)	0.1236	0.2272	0.2067
Goodness of Fit	1.011	1.195	1.002

The data was collected at 20°C with Mo Kα radiation (λ = 0.71069 Å)

$R = \Sigma \, | \, |F_o| - |F_c| \, | \, / \, \Sigma \, |F_o|$, $R_w = [\Sigma(|F_o| - |F_c|)^2 / \Sigma \, |F_o|^2]^{0.5}$

Table 3.1 (continued): Crystallographic parameters for Ti[*m*-$(CH_2PCy_2N)_2C_6H_4$]$(NMe_2)_2$ (**3.11**), Ti[*m*-$(CH_2P^tBu_2N)_2C_6H_4$]Br_2 (**3.13**)[vii], Ti[*m*-$(CH_2PCy_2N)_2C_6H_4$]Cl_2 (**3.14**).

	3.11	**3.13**	**3.14**
Molecular formula	$C_{36}H_{64}N_4P_2Ti$	$C_{24}H_{44}N_2P_2TiBr_2$	$C_{32}H_{52}Cl_2N_2P_2Ti$
Formula weight	662.75	630.24	645.50
a(Å)	8.726(5)	23.78(1)	11.47(1)
b(Å)	12.389(8)	14.930(8)	17.37(2)
c(Å)	18.38(1)	18.92(1)	17.70(2)
α(°)	102.84(1)	90.00	90.00
β(°)	93.06(1)	113.365(7)	101.95(2)
γ (°)	90.69(1)	90.00	90.00
Crystal system	Triclinic	Monoclinic	Monoclinic
Space group	P-1	$P2_1/c$	$P2_1/c$
Volume ($Å^3$)	1934(2)	6164.85	3452(8)
D_{calc} (gcm^{-3})	1.138		1.242
Z	2		4
Abs coeff, μ, mm^{-1}	0.332		0.519
θ range (°)	2.28-23.29		1.66-23.55
Reflections collected	8246		14456
Data $F_o^2 > 3\sigma(F_o^2)$	3079		2608
Parameters	364		352
R(%)	0.0680		0.1585
R_w(%)	0.1975		0.3607
Goodness of Fit	0.862		1.010

The data was collected at 20°C with Mo Kα radiation (λ = 0.71069 Å)

$R = \Sigma \, | \, |F_o| - |F_c| \, | \, / \, \Sigma \, |F_o|$, $R_w = [\Sigma(|F_o| - |F_c|)^2 / \Sigma \, |F_o|^2]^{0.5}$

[vii] Only preliminary X-ray data were obtained and the structure was not refined, thus only the cell parameters are listed.

3.2.9 Polymerization Protocol

Purification of Reagents: Reagent grade PhMe was purchased from Aldrich Chemical Co., and dried using Grubbs' column systems, manufactured by Innovative Technologies, Inc.[235] ACS grade MeOH was purchased from Aldrich Chemical Co., and HCl was purchased from EM Science; both were used as received. Ethylene was purchased from Matheson Gas Co., and was dried over alumina and 3Å molecular sieves. MAO, T^iBAl (Akzo Nobel), $B(C_6F_5)_3$ and $[Ph_3C][B(C_6F_5)_4]$ (prepared in-house) were generously donated by NOVA Chemicals Corp., and were used as received.

Description of the Büchi autoclave:[viii] The Büchi autoclave is a jacketed 1 L borosilicate vessel, and is enclosed by top and bottom stainless steel plates. The vessel is equipped on the top plate with inlets for addition of reagents via syringe, solvent, nitrogen/vacuum, monomer (ethylene), a thermocouple well, and a rupture valve. An external stirrer is powered by a 220 V motor, and the rate may be adjusted from 0-2400 rpm. The temperature is controlled using a water bath, and the tubing is only rated to 75°C therefore rendering this the maximum operating temperature. The autoclave is located in a fumehood (rather than in a specified "bomb room"), thus the maximum temperature above boiling point of the solvent is 20°C, while the maximum operating pressure is 87 psi.

(i-Procedure using MAO) A 1L Büchi autoclave was dried *in vacuo* (10^{-2} mmHg) for several hours. PhMe (500 mL) was transferred into the vessel under a positive pressure of N_2 and was heated to 30°C. The temperature was controlled (to *ca.* ±2°C) with an external heating/cooling bath and was monitored by a thermocouple that extended into the polymerization vessel. The vessel was vented of N_2 and then pressurized with C_2H_4 (1.82 atm) while the solvent stirred at a rate of 150 rpm. A solution of MAO (500 eq, 10% in PhMe) was injected and the mixture was stirred for 5 min. A solution of the precatalyst (in 2 mL PhMe, 25 μmol) was injected, and the rate of stirring was increased to 1000 rpm, while the solution stirred for 30 min. Any recorded exotherm was within

[viii] For a detailed description, including illustrations, refer to Chapter 2 of C. L. Beddie's Ph.D. Dissertation.

the allowed temperature differential of the heating/cooling system. The reaction was quenched with 1 M HCl in MeOH, and the precipitated polymer was subsequently washed with HCl, HCl/MeOH and PhMe before drying at 50°C for at least 48 h prior to weighing.

(ii-Procedure using $T^iBAl/B(C_6F_5)_3$ Activator) The polymerization protocol, in addition to the isolation of the polymer, was performed as described above with the following modifications: A solution of T^iBAl (20 eq, 25% in heptanes) was injected and the mixture was stirred for 5 min. A solution of the precatalyst (in 2 mL PhMe, 25 μmol), followed immediately by $B(C_6F_5)_3$ (PhMe, 2 eq) was injected. The solution was then stirred for the prescribed amount of time. Whenever an exception to this method was performed, it is noted appropriately in the polymerization tables.

The masses of reagents used for the polymerizaitons and polyethylene products, in addition to the raw GPC data, may be viewed in Appendix D (on CD).

3.3 Results and Discussion

The phosphines HP^tBu_2 (**3.1**) and *m*-$(CH_2PR_2)_2C_6H_4$ (R = ^{t}Bu (**3.2**), Cy (**3.3**)) were prepared via a modification of a literature procedure.[271] Addition of diethyl ether to extract the secondary phosphine **3.1** from the slurry, prepared from ClP^tBu_2 and $LiAlH_4$, afforded clean material, thus negating any requirement for further purification. Subsequent reaction of **3.1**, or commercially available $HPCy_2$ with *m*-$(CH_2Br)_2C_6H_4$ in methanol generated the corresponding *bis*(phosphonium) salt, which was deprotonated *in situ* with a slight excess of triethylamine to afford *m*-$(CH_2PR_2)_2C_6H_4$ (R = ^{t}Bu (**3.2**), Cy (**3.3**)) (Figure 3.3). Evidence suggested (crystallographic characterization of HBr salts; *vide infra*) that purification of the phosphines by washing with methanol was not sufficient to completely remove NEt_3·HBr. To avoid ammonium salt contamination, the phosphines were recrystallized from pentanes (R = ^{t}Bu) or methanol (R = Cy) at -35°C. In this manner, crystals suitable for X-ray diffraction were obtained for **3.2**. The NMR

chemical shifts for **3.2** were consistent with literature values.[271] The phosphine **3.3** has been reported in several organometallic complexes, however, the NMR data for this ligand have not been divulged. Spectroscopic characterization of **3.3** was consistent with the reported formulation.[276-278]

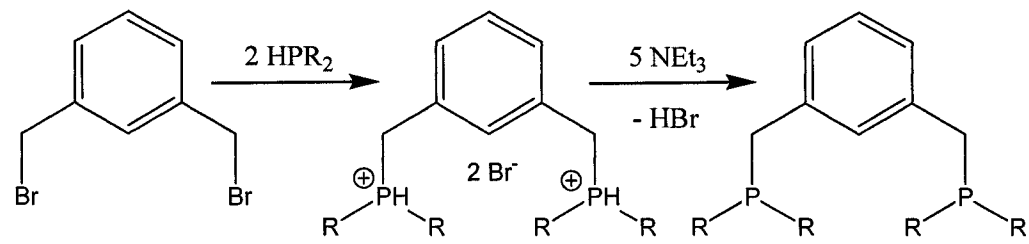

Figure 3.3: Synthesis of the aryl phosphines **3.2** and **3.3**.

Conversion of the aryl phosphines to the corresponding *bis*(phosphinimines), *m*-$(CH_2PR_2NSiMe_3)_2C_6H_4$ (R = ^{t}Bu (**3.4**), Cy (**3.5**)), was readily achieved by reaction with an excess of trimethylsilylazide (Figure 3.4). It is noteworthy that Dr. Jeffrey C. Stewart first performed this reaction to obtain **3.4**.[266] Characteristic downfield shifts in the $^{31}P\{^1H\}$ NMR spectra and X-ray characterization of both ligands corroborated formation of the oxidized products in near-quantitative yield (Table 3.2).[21,266,279] The trimethylsilyl phosphinimines reacted with methanol (R = ^{t}Bu) or isopropanol (R = Cy) to afford the parent phosphinimines *m*-$(CH_2PR_2NH)_2C_6H_4$ (R = ^{t}Bu (**3.6**), Cy (**3.8**)). The use of isopropanol with smaller alkyl groups on the phosphorus atom often permits formation of undesireable oxide by-products (Figure 3.4).[ix] Extraction of the crude oils with benzene provided spectroscopically pure product, although the cyclohexyl derivative proved especially susceptible to decomposition, probably since the smaller groups on the phosphorus atom provided access to these pathways. Signature downfield shifts in the

[ix] E. Hollink and S. B. Hawkeswood, unpublished results. When appropriate, MeOH may replace ^{i}PrOH, although this requires lower temperatures and shorter reaction times.

$^{31}P\{^{1}H\}$ NMR spectra were once again observed upon conversion to the parent phosphinimines (Table 3.2).[x, 266,279]

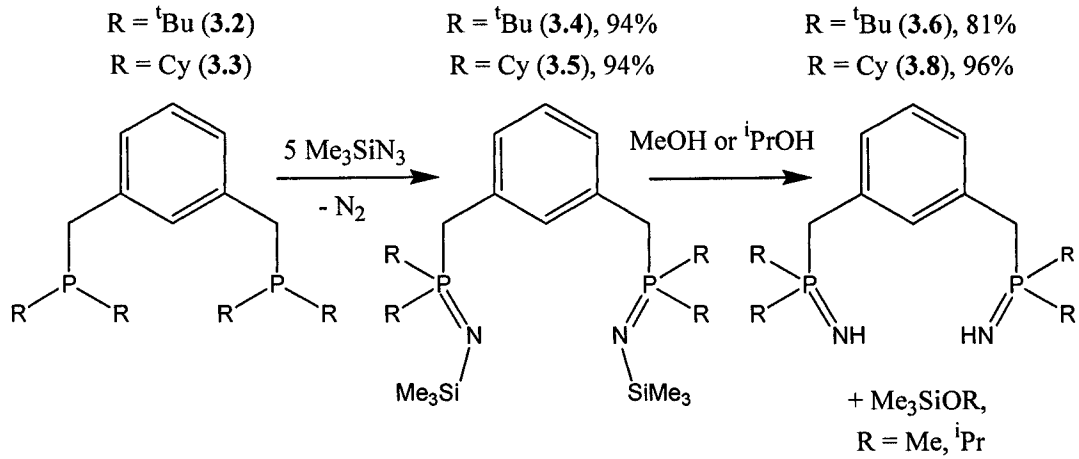

Figure 3.4: Synthesis of *bis*(phosphinimines) **3.4-3.8**.

[x] E. Hollink and S. B. Hawkeswood, unpublished results. Unfortunately, most of the reviews only cover differences in X-ray results or simply provide lists of phosphinimines that have been prepared. Dehnicke, K.; Krieger, M.; Massa, W. *Coord. Chem. Rev.* **1999**, *182*, 19-65. Gololobov, Y. G.; Zhmurova, I. N.; Kasukhin, L. F. *Tetrahedron* **1981**, *37*, 437-472. Gololobov, Y. G.; Kasukhin, L. F. *Tetrahedron* **1992**, *48*, 1353-1406. Dehnicke, K.; Weller, F. *Coord. Chem. Rev.* **1997**, *158*, 103-169.

Table 3.2: Nitrogen-phosphorus bond distances and $^{31}P\{^{1}H\}$NMR data (ppm)[a] for the *bis*(phosphinimine) ligands.

Compound	N-P Å	$^{31}P\{^{1}H\}$ (ppm)
m-$(CH_2P^tBu_2NSiMe_3)_2C_6H_4$ (**3.4**)	1.538(2) 1.531(2)	24.8
m-$(CH_2PCy_2NSiMe_3)_2C_6H_4$ (**3.5**)	1.533(2)	13.5
m-$(CH_2P^tBu_2NH)_2C_6H_4$ (**3.6**)	1.577(2) 1.581(2)	48.2
m-$(CH_2P^tBu_2NH)_2C_6H_4$·2 HBr (**3.7**)	b	64.3[c]
m-$(CH_2PCy_2NH)_2C_6H_4$ (**3.8**)	n/a	36.2

a) C_6D_6 solvent unless otherwise noted.

b) Only preliminary X-ray data were obtained.

c) CD_2Cl_2 solvent.

Crystals of **3.6** suitable for X-ray diffraction were grown from pentanes (Table 3.2, Figure 3.5) and similarly, crystals of the side product *m*-$(CH_2P^tBu_2NH)_2C_6H_4$·2 HBr (**3.7**) were obtained from methylene chloride, however a detailed discussion of the results obtained from the solution of the latter compound is precluded due to poor X-ray data. Fortunately, due to the insolubility of **3.7** in aromatic solvents such as benzene or toluene, it is efficiently separated from **3.6** by filtration. Isolation and characterization of **3.7** offered initial evidence that the aryl phosphine was not being sufficiently purified to remove the ammonium salt. NMR data, however, also provided distinction between the two products ($^{31}P\{^{1}H\}$in C_6D_6 and CD_2Cl_2, respectively δ: 48.2 (**3.6**), 64.3 (**3.7**)).

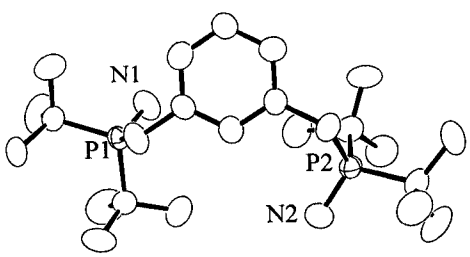

Figure 3.5: ORTEP drawing of *m*-$(CH_2P^tBu_2NH)_2C_6H_4$ (**3.6**) (50% thermal ellipsoids).

Previously, Dr. Jeffrey C. Stewart observed that reaction of *m*-$(CH_2P^tBu_2NSiMe_3)_2C_6H_4$ (**3.4**) with $TiCl_4$ afforded Ti[*m*-$(CH_2P^tBu_2N)_2C_6H_4]Cl_2$ in good yield.[266] Replication of this procedure using **3.4** or the cyclohexyl derivative **3.5** afforded the desired $TiLCl_2$ complexes only in low yields after recrystallization (< 30%). Crystals suitable for X-ray diffraction were obtained by this route, although only the X-ray data obtained from analysis of Ti[*m*-$(CH_2PCy_2N)_2C_6H_4]Cl_2$ (**3.14**) were suitable for a detailed report of the metrical parameters. These low yields may be attributed to an unreliable route due to the methylene protons, which Bochmann and co-workers have demonstrated to be relatively acidic in related *bis*(phosphinimine) ligands derived from diphenylphosphinoethane (dppe) (Figure 3.6).[24] It is noteworthy that Siemeling and co-workers have circumvented this unwanted side reaction to successfully isolate a TiL_2Cl_2 derivative by dropwise addition of the related ligand $[^tBu_2P(NSiMe_3)CH_2]_2CH_2$ to $TiCl_4$ in hot solvent.[270]

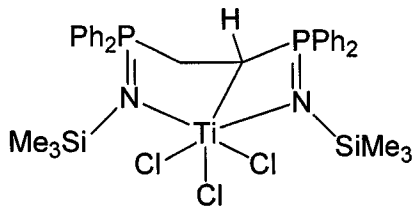

Figure 3.6: The product of C-H activation of a phosphinimine ligand by $TiCl_4$.[24]

Reaction of *m*-$(CH_2PR_2NH)_2C_6H_4$ (R = ^{t}Bu (**3.6**), Cy (**3.8**)) with $Ti(NMe_2)_4$ provided a more reliable procedure to the desired titanium complexes Ti[*m*-$(CH_2PR_2N)_2C_6H_4](NMe_2)_2$ (R = ^{t}Bu (**3.9**), Cy (**3.11**)). These syntheses were performed reproducibly in reasonable yields when the parent phosphinimines were free of ammonium salt contaminants (Figure 3.7). When the ligand precursor is impure, mixtures of **3.9** and the dissymmetric species Ti[*m*-$(CH_2P^tBu_2N)_2C_6H_4]Br(NMe_2)$ (**3.10**) were obtained. Fortunately, separation of the majority of the bromo amide derivative from the corresponding *bis*(amide) version is relatively straightforward due to the high solubility of the latter compound in pentanes. $^{31}P\{^1H\}$ NMR spectroscopy readily distinguishes between **3.9** and **3.10**, with chemical shifts at 12.7 and 17.2 ppm, respectively. Interestingly, the $^{31}P\{^1H\}$ spectrum for **3.10** only exhibits one signal, while

the methylene fragments of the ligand are inequivalent in the ^{1}H and $^{13}C\{^{1}H\}$ NMR spectra.

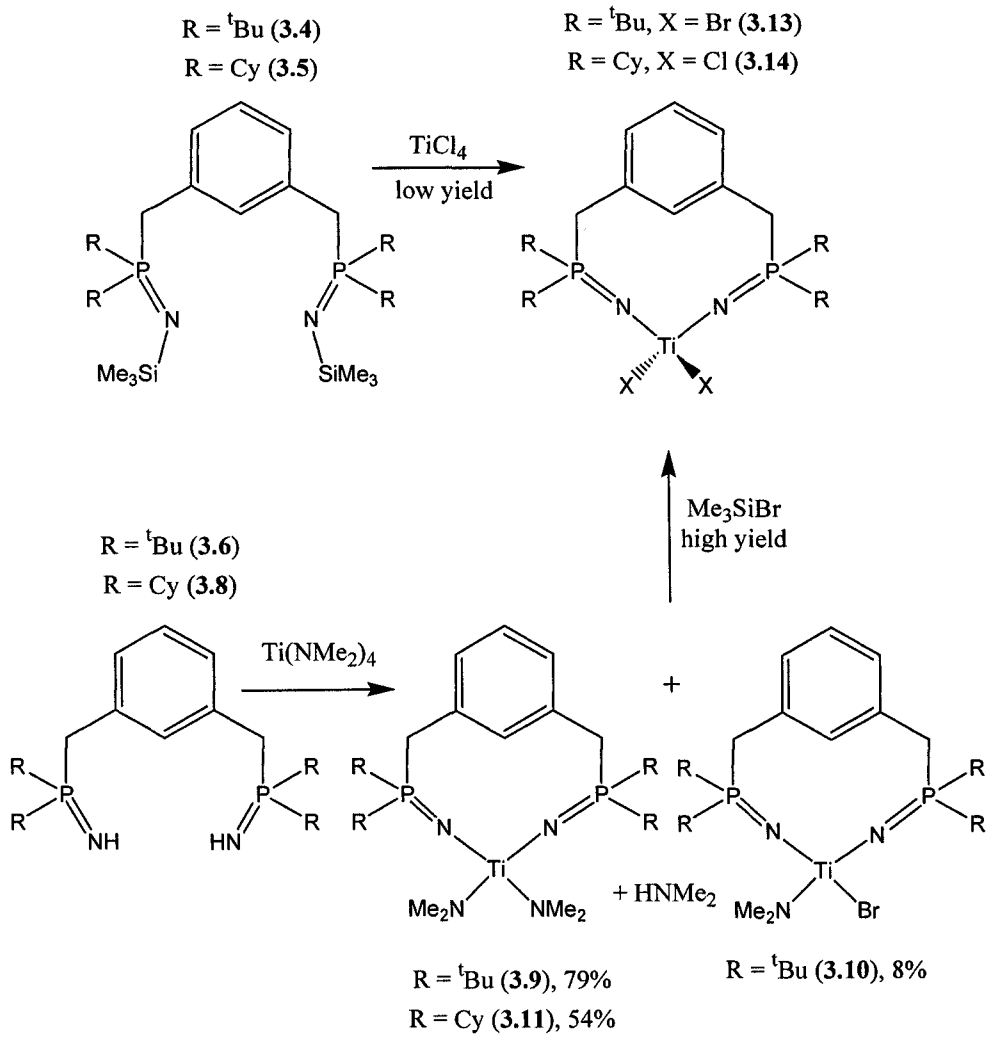

Figure 3.7: Synthesis of *bis*(phosphinimide) titanium complexes.

The derivatives **3.10**, **3.11**, **3.13** and **3.14** were further characterized by X-ray crystallography, although poor quality of the data obtained for **3.13** precludes a detailed discussion. Comparison of the metal-nitrogen bond distances of the phosphinimide ligands in Ti[*m*-$(CH_2P^tBu_2N)_2C_6H_4$]Br(NMe_2) (**3.10**) and Ti[*m*-$(CH_2PCy_2N)_2C_6H_4$](NMe_2)$_2$ (**3.11**) revealed that the Ti-N phosphinimide bond lengthens upon substitution of the bromide ligand with an amide ligand (Table 3.3). This is

accompanied by a shortening of the N-P bond length. This may represent an increase of donation of electron density from the phosphinimide ligand to accommodate the electron-withdrawing bromide ligand, or steric influences. The most significant difference is the decrease of the titanium-NP bond angle from approximately linear (*ca.* 170°) for **3.10**, to 151.3(3)° and 157.7(3)° for **3.11**.

Table 3.3: Key bond distances and angles for available data of X-ray analyses of chelate complexes of the form $TiLX_2$.

Compound	Ti-NP Å	N-P Å	Ti-NP °
Ti[*m*-$(CH_2P^tBu_2N)_2C_6H_4$]Br(NMe_2) (**3.10**)	1.818(4) 1.827(4)	1.578(5) 1.570(5)	170.9(3) 172.3(3)
Ti[*m*-$(CH_2PCy_2N)_2C_6H_4$](NMe_2)$_2$ (**3.11**)	1.866(4) 1.879(5)	1.553(4) 1.567(4)	151.3(3) 157.7(3)
Ti[*m*-$(CH_2PCy_2N)_2C_6H_4$]Cl_2 (**3.14**)	1.78(1) 1.82(1)	1.57(1) 1.59(1)	160.9(9) 170.2(9)

The analogous chemistry may be performed using zirconium in the place of titanium. Initially however, *m*-$(CH_2P^tBu_2NH)_2C_6H_4$ (**3.6**) was treated with $ZrBn_4$ in a 1:1 ratio, resulting in the loss of four equivalents of toluene to afford the presumed monomeric product Zr[*m*-$(CH_2P^tBu_2N)_2C_6H_4]_2$ (**3.20**) (Figure 3.8). This phenomenon has also been observed upon reaction of $ZrBn_4$ with 1,1'-*N*-substituted ferrocenediyl ligands without rationalization.[280] A possible explanation is that the transient compound Zr[*m*-$(CH_2P^tBu_2N)_2C_6H_4$]Bn_2 is more soluble in benzene than $ZrBn_4$, and therefore reacts more readily with the *bis*(phosphinimine) (or *bis*(amine)) ligand in solution. To circumvent this, *m*-$(CH_2P^tBu_2NH)_2C_6H_4$ (**3.6**) was reacted with $Zr(NEt_2)_4$ to provide Zr[*m*-$(CH_2P^tBu_2N)_2C_6H_4$](NEt_2)$_2$ (**3.12**) in good yield (87%). Subsequent conversion to Zr[*m*-$(CH_2P^tBu_2N)_2C_6H_4$]Cl_2 (**3.15**) was achieved by reaction of **3.12** with Me_3SiCl; NMR spectroscopy confirmed that the phosphinimide ligand remained intact upon selective cleavage of the amide groups. Conversely, an attempt to prepare the

corresponding dimethyl compound from reaction of Zr[*m*-$(CH_2P^tBu_2N)_2C_6H_4$]$(NEt_2)_2$ (**3.12**) with TMA, in a similar manner as performed by Gibson and co-workers, was unsuccessful.[256] This is perhaps not surprising considering the susceptibility of titanium or zirconium phosphinimide complexes to attack of the nitrogen atom by TMA.[12,16,18,234]

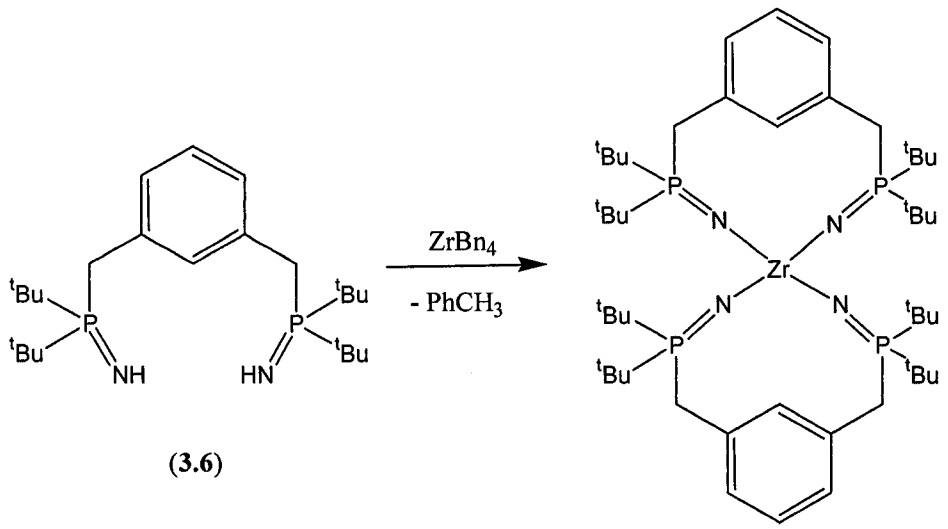

(**3.6**)

(**3.20**), 47%

Figure 3.8: Loss of four equivalents of toluene to give the presumed monomeric product Zr[*m*-$(CH_2P^tBu_2N)_2C_6H_4]_2$ (**3.20**).

Alkylation of Ti[*m*-$(CH_2P^tBu_2N)_2C_6H_4$]Br_2 (**3.13**) with precise control of the stoichiometry of MeMgBr or BnMgCl provided Ti[*m*-$(CH_2P^tBu_2N)_2C_6H_4$]R_2 (R = Me (**3.16**), R = Bn (**3.17**)) in reasonable yields (50-74%).[266] These were prepared expressly for the purpose of determining their ethylene polymerization activities upon reaction with well-defined co-catalysts such as $B(C_6F_5)_3$ or $[Ph_3C][B(C_6F_5)_4]$.

Utility as Ethylene Polymerization Catalysts

Prior to testing the chelated *bis*(phosphinimide) titanium complexes as olefin polymerization catalysts, the procedure was optimized using $Ti(NP^tBu_3)_2X_2$ (X = Cl, Me) as a standard due to its relative ease of synthesis. In addition, they were compared to the industrially accepted standard $ZrCp_2X_2$ (X = Cl, Me). A more detailed description of the polymerization method and collection of polymer is provided in Section 4.3. Previously, it was reported that an activity of 62,310 g $mmol^{-1}h^{-1}$ was achieved when $Ti(NP^tBu_3)_2Me_2$ was reacted with $[Ph_3C][B(C_6F_5)_4]$ under commercially relevant solution polymerization conditions. This experiment was performed at high temperature (160°C), and high monomer pressure (228 atm) in cyclohexane under solution flow conditions (catalyst and ethylene were continuously loaded into the reactor while polymer product was continuously removed).[7] When the temperature and pressure is substantially reduced to 30°C and 1.82 atm, as in laboratory conditions in a Büchi reactor, it is apparent that the polymerization activity is dramatically different (Table 3.4).

Table 3.4: Optimization of ethylene polymerization conditions using $Ti(NP^tBu_3)_2Me_2$ as a standard.[a]

Precursor	Al (eq)	Borane Reagent	Activity	M_n	M_w	PDI
$Ti(NP^tBu_3)_2Me_2$[b]	20	$B(C_6F_5)_3$	Trace	-	-	-
$Ti(NP^tBu_3)_2Me_2$	20	$B(C_6F_5)_3$	84	65,700	326,400	4.97
$Ti(NP^tBu_3)_2Me_2$	0	$B(C_6F_5)_3$	20	31,400	38,500	1.23
$Ti(NP^tBu_3)_2Me_2$[c]	20	$[Ph_3C][B(C_6F_5)_4]$	4	22,200	281,200	12.67
$Ti(NP^tBu_3)_2Me_2$[d]	20	$[Ph_3C][B(C_6F_5)_4]$	75	77,200	510,400	6.61
$Ti(NP^tBu_3)_2Me_2$	20	$[Ph_3C][B(C_6F_5)_4]$	185	149,800	654,600	4.37
$Ti(NP^tBu_3)_2Me_2$	10	$[Ph_3C][B(C_6F_5)_4]$	145	582,800	983,500	1.69
$Ti(NP^tBu_3)_2Me_2$	0	$[Ph_3C][B(C_6F_5)_4]$	155	170,800	479,600	2.81
$ZrCp_2Me_2$	20	$B(C_6F_5)_3$	1740	69,500	192,300	2.77
$ZrCp_2Me_2$	20	$[Ph_3C][B(C_6F_5)_4]$	1010	171,000	334,800	1.96

a) T^iBAl scrubber reported in number of equivalents of Al relative to Ti/Zr, Ti/Zr:B ratio 1:2, PhMe solvent, 30°C, 1.82 atm C_2, 50 μM precatalyst, 10 min. Activity reported in g $mmol^{-1}h^{-1}atm^{-1}$, M_n and M_w in g mol^{-1}.

b) Ti:B ratio 1:1.

c) Hexanes solvent instead of PhMe.

d) Reverse order of catalyst loading: i.e. the solution of $[Ph_3C][B(C_6F_5)_4]$ was injected, followed immediately by a solution of the catalyst precursor.

Several factors were varied to determine the best possible conditions to test and compare the chelated *bis*(phosphinimide) titanium precatalysts, including varying the catalyst loading method, type and ratio of Lewis acid activator, the solvent, and the aluminum (scrubber) concentration. Traditionally, when a polymerization is performed, the best results are obtained when the scrubber is injected into the reactor and the solution is stirred for five minutes.[21] This effectively removes any trace impurities which may remain in the solvent from the purification columns, or walls of the reactor. Next, the catalyst precursor is injected, followed immediately by the activator. The order of catalyst-activator addition is particularly important when $Ti(NP^tBu_3)_2Me_2$ is activated

with two equivalents of $[Ph_3C][B(C_6F_5)_4]$; the polymerization activity was reduced in half when the co-catalyst was added before the precatalyst (75 *vs.* 185 g $mmol^{-1}h^{-1}atm^{-1}$). This is likely the result of formation of a dicationic species, which was determined to be inactive for the polymerization of ethylene.[214]

It was determined that $[Ph_3C][B(C_6F_5)_4]$ was a more efficient activator of $Ti(NP^tBu_3)_2Me_2$ than $B(C_6F_5)_3$, providing twice as much polymer product per mole of precatalyst under otherwise identical conditions (84 *vs.* 185 g $mmol^{-1}h^{-1}atm^{-1}$). Furthermore, the resulting polymer produced by activation with $B(C_6F_5)_3$ had a value of M_n (number averaged molecular weight) that halved from 150,000 g mol^{-1} from when $[Ph_3C][B(C_6F_5)_4]$ was used to 66,000 g mol^{-1}. When only one equivalent of $B(C_6F_5)_3$ was used as activator, very little polymer was isolated. This indicated that two equivalents of $B(C_6F_5)_3$ were required to produce measurable amounts of polymer. In addition, toluene was determined to be a better solvent than hexanes, since when the latter solvent was used, only a negligible amount of plastic was produced under otherwise optimized conditions. Upon analysis of the polymer formed in the hexanes solvent, the polydispersity index (PDI) was 12.67, which indicates that the polymer was not produced from a well-behaved single-site catalyst.

Finally, varying the scrubber (tri*iso*butylaluminum, T^iBAl) concentration had a dramatic effect on the polymerization, depending on the activating agent employed. For the majority of polymerization experiments, a ratio of 1:20 is employed for the ratio of titanium precatalyst:aluminum purifying agent. When $B(C_6F_5)_3$ is used as an activator, as the aluminum concentration is reduced to zero, the polymerization activity drops from 84 to 20 g $mmol^{-1}h^{-1}atm^{-1}$. Even more interesting are the properties of the polymer that is produced: as the aluminum concentration drops, so does the molecular weight of the polymer. In addition, the PDI value decreased from 4.97 to 1.23 as the aluminum concentration is reduced from 20 to zero equivalents. This may indicate that at higher aluminum concentrations, the catalyst produces higher molecular weight polymer before undergoing a number of processes (chain transfer of the polymer chain to the aluminum centre, decomposition, β-H transfer or elimination) which ultimately broaden the PDI value. Conversely, without the presence of the aluminum reagent, the catalyst encounters

impurities more readily therefore quenching the active species. The mechanism of polymer transfer to aluminum is also eliminated.

These effects of varying the T^iBAl concentration are not nearly as predictable when $[Ph_3C][B(C_6F_5)_4]$ is used as an activator. Although the polymerization activity does decrease when the aluminum concentration is reduced from 20 to 10 equivalents (185 to 145 g $mmol^{-1}h^{-1}atm^{-1}$), it does not decrease further as the scrubber concentration is reduced to zero. Rather, the activity seems to stabilize within experimental error to a value of 150 g $mmol^{-1}h^{-1}atm^{-1}$. Furthermore, the polymer molecular weights and polydispersities are not linearly dependent on the aluminum concentration. For example, the polymer molecular weight decreases as the aluminum concentration is lowered from 20 equivalents to zero, but when 10 equivalents are employed, the molecular weight increases while the polydispersity decreases. Since these observations are consistent as long as the conditions are reproduced exactly, this illustrates that competing processes of the polymerization mechanism cannot be exactly deduced from the polymer properties.

From these observations, it is clear that varying the polymerization technique is essential for determining optimal conditions. Polymerization activities using $Ti(NP^tBu_3)_2Me_2$ as a precatalyst fluctuate from trace isolation of polymer to 185 g $mmol^{-1}h^{-1}atm^{-1}$, however, it is clear that this class of catalyst precursor is not effective for polymerization employing standard laboratory practices. To put these values in perspective, they were compared to the accepted standard precursor $ZrCp_2Me_2$, which produced polymer with activities of 1740 and 1010 g $mmol^{-1}h^{-1}atm^{-1}$, depending on whether $B(C_6F_5)_3$ or $[Ph_3C][B(C_6F_5)_4]$ was used as an activating agent.

Initially, polymerization testing of the precursors $Ti[m\text{-}(CH_2PR_2N)_2C_6H_4]X_2$ (R = ^{t}Bu, X = NMe_2 (**3.9**), Br (**3.13**), Me (**3.16**); R = Cy, X = NMe_2 (**3.11**), Cl (**3.14**)) and $Zr[m\text{-}(CH_2P^tBu_2N)_2C_6H_4]Cl_2$ (**3.15**) was performed using MAO as an activator. Although it has been established that MAO is an ineffective activator for $Ti(NP^tBu_3)_2X_2$ (X = Cl, Me) since it induces catalyst decomposition (using TMA as a model),[7,18] these experiments were performed to determine if the chelated *bis*(phosphinimide) ligand provided a titanium centre that displayed similar polymerization behaviour. All precursors produced polyethylene with low to moderate activities (Table 3.5, and see Table 4.4 for activity nomenclature). Only the precatalysts that have ^{t}Bu groups on the

phosphorus atom such as $Ti(NP^tBu_3)_2Cl_2$ or the chelated version $Ti[m\text{-}(CH_2P^tBu_2N)_2C_6H_4]Br_2$ (**3.13**) produced sufficient plastic to determine polymerization activities of 60 and 75 g $mmol^{-1}h^{-1}atm^{-1}$, respectively. The precursor $Zr[m\text{-}(CH_2P^tBu_2N)_2C_6H_4]Cl_2$ (**3.15**) fared even worse as a catalyst precursor; a polymerization activity of only 40 g $mmol^{-1}h^{-1}atm^{-1}$ was obtained. Unfortunately, the polymer produced by the catalyst derived from $Ti[m\text{-}(CH_2P^tBu_2N)_2C_6H_4]Br_2$ (**3.13**) was not soluble enough to perform a GPC analysis, thus a comparison of the polymer properties could not be made. It is clear, however, that under these conditions the *bis*(phosphinimide) Group IV class of precursors are not useful olefin polymerization catalysts.

Table 3.5: Comparison of the polymerization activities using $Ti[m\text{-}(CH_2PR_2N)_2C_6H_4]X_2$ (R = ^{t}Bu, X = NMe_2 (**3.9**), Br (**3.13**), Me (**3.16**); R = Cy, X = NMe_2 (**3.11**), Cl (**3.14**)) or $Ti(NP^tBu_3)_2X_2$ (X = Cl, Me) as a precursor with activation by MAO.[a]

Precursor	Activity	M_n	M_w	PDI
$Ti(NP^tBu_3)_2Cl_2$	60	37,300	428,800	11.44
$Ti[m\text{-}(CH_2P^tBu_2N)_2C_6H_4](NMe_2)_2$ (**3.9**)	Trace	b	b	b
$Ti[m\text{-}(CH_2PCy_2N)_2C_6H_4](NMe_2)_2$ (**3.11**)	Trace	91,700	634,900	6.92
$Ti[m\text{-}(CH_2P^tBu_2N)_2C_6H_4]Br_2$ (**3.13**)	75	c	c	c
$Ti[m\text{-}(CH_2PCy_2N)_2C_6H_4]Cl_2$ (**3.14**)	Trace	b	b	b
$Zr[m\text{-}(CH_2P^tBu_2N)_2C_6H_4]Cl_2$ (**3.15**)	40	13,900	92,500	6.65
$Ti(NP^tBu_3)_2Me_2$	Trace	b	b	b
$Ti[m\text{-}(CH_2P^tBu_2N)_2C_6H_4]Me_2$ (**3.16**)	Trace	b	b	b
$ZrCp_2Cl_2$	1830	95,100	293,300	3.08
$ZrCp_2Me_2$	1700	78,200	201,500	2.58

a) MAO activation, Ti/Zr:Al ratio 1:500, PhMe solvent, 30°C, 1.82 atm C_2, 50 μM precatalyst, 10 min, Activity reported in g $mmol^{-1}h^{-1}atm^{-1}$, M_n and M_w in g mol^{-1}.

b) Too little polymer to analyze.

c) Polymer formed a gel that would not dissolve in 1,2,4-trichlorobenzene.

Slightly elevated polymerization activities were observed when $Ti(NP^tBu_3)_2Me_2$ was activated by boron-based co-catalysts (Table 3.4), therefore the chelated *bis*(phosphinimide) titanium precatalyst $Ti[m\text{-}(CH_2P^tBu_2N)_2C_6H_4]Me_2$ (**3.16**) was subjected to the same conditions. The precursor $Ti[m\text{-}(CH_2P^tBu_2N)_2C_6H_4]Me_2$ (**3.16**) displayed lower polymerization activities relative to $Ti(NP^tBu_3)_2Me_2$ upon activation with $B(C_6F_5)_3$ or $[Ph_3C][B(C_6F_5)_4]$ using the optimized polymerization conditions (Table 3.6). This may be rationalized by a steric argument: rather than three ^{t}Bu groups on the phosphorus atom, there is (essentially) a di-^{t}Bu benzyl group. It is apparent that the chelated *bis*(phosphinimide) titanium precatalysts are not adequate substitutes for $Ti(NP^tBu_3)_2X_2$ using these polymerization conditions.

Table 3.6: Comparison of the polymerization activities using $Ti[m\text{-}(CH_2P^tBu_2N)_2C_6H_4]Me_2$ (**3.16**) or $Ti(NP^tBu_3)_2Me_2$ as a precursor while activated by $B(C_6F_5)_3$ or $[Ph_3C][B(C_6F_5)_4]$ (TB).[a]

Precursor	Activator	Activity	M_n	M_w	PDI
$Ti(NP^tBu_3)_2Me_2$	$B(C_6F_5)_3$	94	65,700	326,400	4.97
$Ti[m\text{-}(CH_2P^tBu_2N)_2C_6H_4]Me_2$ **(3.16)**	$B(C_6F_5)_3$	6	24,100	189,400	7.86
$ZrCp_2Me_2$	$B(C_6F_5)_3$	1760	69,500	192,300	2.77
$Ti(NP^tBu_3)_2Me_2$	TB	205	149,800	654,600	4.37
$Ti[m\text{-}(CH_2P^tBu_2N)_2C_6H_4]Me_2$ **(3.16)**	TB	26	60,800	360,600	5.93
$ZrCp_2Me_2$	TB	1030	171,000	334,800	1.96

a) Ti/Zr:B ratio 1:2, Ti/Zr:Al ratio 1:500, PhMe solvent, 30°C, 1.82 atm C_2, 50 μM precatalyst, 10 min, Activity reported in g $mmol^{-1}h^{-1}atm^{-1}$, M_n and M_w in g mol^{-1}.

3.4 Summary

A reliable synthetic route to the *bis*(phosphinimine) ligands *m*-$(CH_2PR_2NH)_2C_6H_4$ (R = ^tBu (**3.6**), Cy (**3.8**)), and their corresponding titanium complexes Ti[*m*-$(CH_2PR_2N)_2C_6H_4]X_2$ has been established. The majority of complications in these preparations may be avoided simply by rigorously purifying the initial phosphines. The methodology was further extended to include the zirconium derivatives Zr[*m*-$(CH_2P^tBu_2N)_2C_6H_4]X_2$ (X = NEt_2 (**3.12**), Cl (**3.15**)). Alternatively, reaction of the neutral ligand *m*-$(CH_2P^tBu_2NH)_2C_6H_4$ (**3.6**) in a 1:1 ratio with $ZrBn_4$ produced Zr[*m*-$(CH_2P^tBu_2N)_2C_6H_4]_2$ (**3.20**).

It is evident that the present chelating *bis*(phosphinimide) scaffold does not provide an active titanium olefin polymerization catalyst under the polymerization conditions attempted throughout the course of this work. Rather, it has demonstrated that the Group IV *bis*(phosphinimide) complexes react in an entirely different manner than their corresponding MCp_2X_2 analogues, even although the phosphinimide ligand is arguably similar to the cyclopentadienide ligand based on steric and electronic rationalizations.[21]

4 Bimetallic Titanium Phosphinimide Complexes

4.1 Introduction

The use of single-site homogeneous catalysts to produce polymer materials that possess narrow polydispersities is prevalent in the scientific literature, particularly with reference to living catalyst systems.[206,209,281-286] Resins of narrow polydispersity are of academic interest, since they tend to support a well-defined polymerization mechanism with one active catalytic site. To maximize processing efficiency, industrial applications favour materials that consist of a broader molecular weight distribution, while still defining specific molecular weight ranges.[158,159] Typically, broad molecular weight products are generated by modifying the engineering process of the polymerization rather than employing unusual catalyst precursors. Regulating factors such as pressure or temperature (and consequently the phase)[287] of the polymerization, or simply the addition of hydrogen,[288-293] co-monomer,[287] carbon dioxide or water[294] have a dramatic influence on the polymer materials that are formed. Alternatively, multimodal polymers may be formed by the use of specific ratios of several precatalysts[295-301] or activators[302] in a single reactor while effecting the polymerization. By employing several single-site catalyst precursors or differing activators in the same reactor, assorted well-defined polymers are in essence combined together to provide a product that ultimately possesses a broader molecular weight distribution. The same effect may also be achieved by employing two different catalyst systems in tandem reactors, followed by a mechanical blending to produce the desired products.[303,304]

More recently, an increasingly sophisticated approach involves the use of cooperative catalysts and only ethylene as a feedstock to produce highly branched materials.[305,306] From a practical perspective, however, it would be advantageous to use a single precatalyst in a single reactor to produce the desired multimodal materials. This ultimately requires a catalyst that possesses two or more distinct polymerization-active sites.[307] An elegant demonstration of this criterion is illustrated by the active binuclear catalysts (e.g. (μ-CH_2CH_2-3,3')[1-(Me_2SiN^tBu)$InTiMe_2$]$_2$)[161,308] or co-catalysts (e.g.

$[Ph_3C]_2[((C_6F_5)_3B)_2C_6F_4]$[308-310] reported by Marks and co-workers. These systems are particularly desirable, since modifying the catalyst to co-catalyst ratio provides polymers that range from essentially monodisperse (PDI 1.1-1.2) to materials that possess extremely broad molecular weight distributions.

Given these fresh perspectives of tailoring either the cationic (catalyst) or the anionic (co-catalyst) portion of the polymerization site to produce specific polymer products, a series of bimetallic titanium phosphinimide complexes and their corresponding monometallic derivatives were targeted. A description of the catalyst preparation, subsequent polymerization testing and polymer analysis will be detailed.

4.2 Experimental

4.2.1 General Considerations

The synthetic protocol, and characterization of the complexes or polymer products by multinuclear NMR spectroscopy, X-ray crystallography, GPC and microanalysis are analogous to those described in Sections 2.2.1 and 3.2.1.

4.2.2 Solvents

All solvents, including deuterated solvents used for NMR experiments, were purified using the methods described in Sections 2.2.2 and 3.2.2.

4.2.3 Reagents

$TiCpCl_3$ was prepared according to a literature method[244,245] and the phosphines R_2BnP (R = ^{t}Bu (**4.3**), Cy (**4.4**))[311] and *p*-$(CH_2PR_2)_2C_6H_4$ (R = ^{t}Bu (**4.5**), Cy (**4.6**))[271] were prepared via modification of literature procedures. The improved synthesis of HP^tBu_2

(**3.1**) is detailed in Section 3.2.4. Indene was purchased from Aldrich Chemical Co., and was dried over NaOH prior to vacuum distillation. Lithium indenide was freshly prepared and isolated as a solid from an equimolar amount of indene and ^{n}BuLi prior to use. The reagents MeMgBr, BnMgCl, ^{n}BuLi, Me_3SiN_3, Me_3SiCl, $ClP^{t}Bu_2$, $ClPCy_2$ and α,α'-dibromo-*p*-xylene were purchased from Aldrich Chemical Co., and $HPCy_2$, and $TiCp^*Cl_3$ were purchased from Strem Chemical Co.; all were used without further purification.

4.2.4 Organic Syntheses

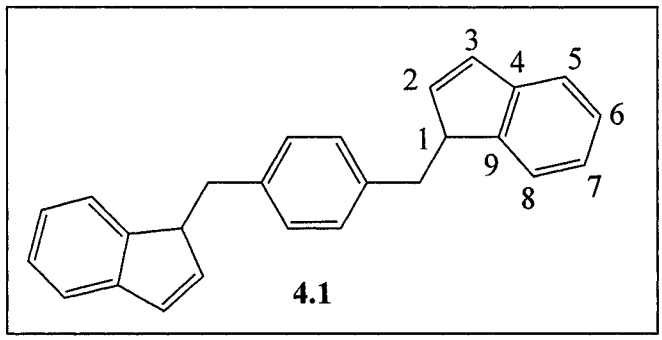

4.1

1,4-*bis*-(1-methyl-1*H*-indenyl)benzene (*p*-$(CH_2C_9H_7)_2C_6H_4$, **4.1**): α,α'-dibromo-*p*-xylene (1.69 g, 6.4 mmol) was slurried in Et_2O (80 mL) and a clear pink solution of indenyl lithium (1.56 g, 12.8 mmol) in Et_2O (20 mL) was added dropwise at RT. The solution was stirred for 12 h, after which time the solvent was removed *in vacuo*. The product was extracted with PhH (3 x 30 mL), and the extracts were filtered through Celite. The solvent was concentrated *in vacuo* to *ca.* 20 mL, and the product was precipitated with pentanes (*ca.* 10 mL). The white solid was filtered, washed with pentanes (3 x 10 mL) and dried. A second crop of material was isolated from the mother liquor in the same manner; no degradation in purity was evident by ^{1}H NMR spectroscopy. Combined yield: 1.84 g (86%). ^{1}H NMR (500 MHz, C_6D_6): 7.44 (d, 2H, $^3J_{H\text{-}H}$ = 7 Hz, $C_9\mathbf{H}_7$ (H-5)), 7.35 (pseudo t, 2H, $^3J_{H\text{-}H}$ = 7 Hz, $C_9\mathbf{H}_7$ (H-7)), 7.32 (d, 2H, $^3J_{H\text{-}H}$ = 8 Hz, $C_9\mathbf{H}_7$ (H-8)), 7.27 (s, 4H, $C_6\mathbf{H}_4$), 7.25 (pseudo t, 2H, $^3J_{H\text{-}H}$ = 8 Hz, $C_9\mathbf{H}_7$ (H-6)), 6.88 (d, 2H, $^3J_{H\text{-}H}$ = 5 Hz, $C_9\mathbf{H}_7$ (H-3)), 6.54 (dd, 2H, $^3J_{H\text{-}H}$ = 5 Hz, $^4J_{H\text{-}H}$ = 1 Hz, $C_9\mathbf{H}_7$ (H-2)), 3.81 (pseudo t, 2H, $^3J_{H\text{-}H}$ = 7 Hz, $C_9\mathbf{H}_7$ (H-1)), 3.16 (dd, 2H, $^2J_{H\text{-}H}$ = 13.5 Hz, $^3J_{H\text{-}H}$ = 7 Hz (*cis*), $C_6H_4C\mathbf{H}_2$), 2.83 (dd, 2H, $^2J_{H\text{-}H}$ = 13.5 Hz, $^3J_{H\text{-}H}$ = 9 Hz (*trans*), $C_6H_4C\mathbf{H}_2$). $^{13}C\{^1H\}$ NMR (75.5 MHz, C_6D_6) δ: 147.3 (s, $\mathbf{C}_9H_7$

(C-9)), 144.5 (s, C_6H_4 (*ipso*-C)), 139.2 (s, C_9H_7 (C-2)), 138.4 (s, C_9H_7 (C-4)), 131.1 (s, C_9H_7 (C-3)), 129.2 (s, C_6H_4 (*o*-C)), 126.9 (s, C_9H_7 (C-7)), 124.8 (s, C_9H_7 (C-6)), 123.4 (s, C_9H_7 (C-8)), 121.3 (s, C_9H_7 (C-5)), 52.1 (s, C_9H_7 (C-1)), 37.8 (s, $C_6H_4CH_2$). Anal. Calc'd for $C_{26}H_{22}$: C, 93.37; H, 6.63; N, 0.00. Found: C, 92.82; H, 6.74; N, 0.03.

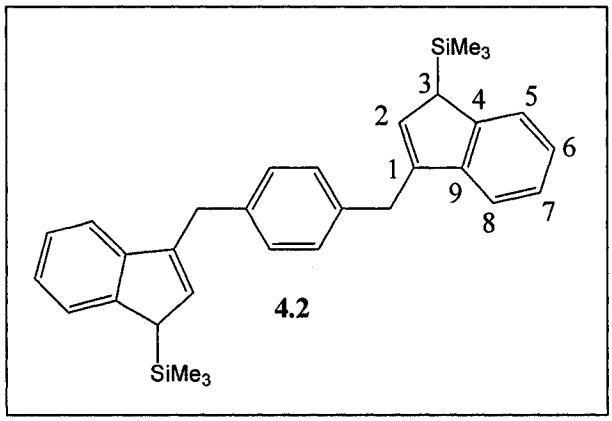

4.2

1,4-*bis*-(3-methyl-1*H*-1-(trimethylsilyl)inden-1-yl)benzene (*p*-$(CH_2C_9H_6SiMe_3)_2C_6H_4$, **4.2**): A slurry of *p*-$(CH_2C_9H_7)_2C_6H_4$ (**4.1**) (216 mg, 0.64 mmol) in Et_2O (20 mL) was cooled to -35°C, and ^nBuLi (0.65 mL, 0.13 mmol) was added dropwise via syringe over a 15 min period. The solution was gradually warmed to RT and was stirred for 5 h, during which time the mixture became homogeneous. The solution was re-cooled to -35°C and Me_3SiCl (0.17 mL, 0.13 mmol) was added dropwise via syringe over a 5 min period. The solution was warmed to RT, and stirred for an additional 16 h. The solvent was removed *in vacuo*, and the product was extracted with pentanes (3 x 15 mL). Following filtration through Celite, the solvent was removed *in vacuo* to afford a white solid (193 mg, 63%). ^1H NMR (500 MHz, C_6D_6): 7.38 (pseudo t, 4H, $C_9\mathbf{H}_7$ (H-5,7)), 7.20 (s, 4H, $C_6\mathbf{H}_4$), 7.18 (dd, 2H, $^3J_{H\text{-}H}$ = 6 Hz, $^4J_{H\text{-}H}$ = 1 Hz, $C_9\mathbf{H}_7$ (H-8)), 7.16 (m, $C_9\mathbf{H}_7$ (H-6)), 6.16 (s, $C_9\mathbf{H}_7$ (H-2)), 3.85 (s, 4H, $C_6H_4C\mathbf{H}_2$), 3.23 (s, 2H, $C_9\mathbf{H}_7$ (H-3)), -0.15 (s, 18H, $Si(C\mathbf{H}_3)_3$). $^{13}C\{^1H\}$ NMR (75.5 MHz, C_6D_6) δ: 146.6 (s, C_9H_7 (C-1)), 144.6 (s, C_6H_4 (C-9)), 141.4 (s, C_9H_7 (C-4)), 138.1 (s, C_6H_4 (*ipso*-C)), 131.9 (s, C_9H_7 (C-5)), 129.2 (s, C_9H_7 (*o*-C)), 125.1 (s, C_9H_7 (C-6)), 124.2 (s, C_9H_7 (C-8)), 123.0 (s, C_9H_7 (C-7)), 120.0 (s, C_9H_7 (C-2)), 44.7 (s, C_9H_7 (C-3)), 34.4 (s, $C_6H_4CH_2$), -3.4 (s, $Si(CH_3)_3$). Anal. Calc'd for $C_{32}H_{38}Si_2$: C, 80.27; H, 8.00; N, 0.00. Found: C, 80.01; H, 8.42; N, 0.03.

4.2.5 Phosphine Syntheses

Di-*tert*-butylbenzylphosphine ($^tBu_2BnP$, **4.3**):[311] ClP^tBu_2 (1.90 g, 10.53 mmol) was dissolved in Et_2O (50 mL), and a 1.0 M solution of BnMgCl in Et_2O (7.90 mL, 15.80 mmol) was added dropwise via syringe at -78°C over a 30 min period. The solution was stirred at -78°C for 5 h, then gradually warmed to RT. After stirring for an additional 48 h, a precipitate had formed. The solvent was removed *in vacuo*, and the product was extracted with pentanes (3 x 25 mL). Following filtration through Celite, the solvent was removed *in vacuo*, affording a viscous oil. To remove residual BnMgCl, the crude mixture was dissolved in a minimum amount of pentanes (*ca.* 2 mL), and cooled to -35°C. The slurry was filtered while cold, and the solvent was removed *in vacuo* to afford a colourless liquid that solidified to a gel. The phosphine was used without further purification, and spectroscopic data were consistent with literature values.[311,312] Yield: 1.98 g, 80%. ^{1}H NMR (500 MHz, C_6D_6) δ: 7.40 (d, 2H, $^3J_{H-H}$ = 8 Hz, $C_6\mathbf{H}_5$ (*o*-H)), 7.19 (pseudo t, 2H, $^3J_{H-H}$ = 8 Hz, $C_6\mathbf{H}_5$ (*m*-H)), 7.06 (t, 1H, $^3J_{H-H}$ = 8 Hz, $C_6\mathbf{H}_5$ (*p*-H)), 2.76 (d, 2H, $^2J_{P-H}$ = 2 Hz, $C\mathbf{H}_2Ph$), 1.09 (d, 18H, $^3J_{P-H}$ = 11 Hz, $C(C\mathbf{H}_3)_3$). $^{13}C\{^1H\}$ NMR (75.5 MHz, C_6D_6) δ: 142.0 (s, $\mathbf{C}_6H_5$ (*ipso*-C)), 130.0 (s, $\mathbf{C}_6H_5$ (*o*-C)), 127.8 (s, $\mathbf{C}_6H_5$ (*m*-C)), 125.6 (s, $\mathbf{C}_6H_5$ (*p*-C)), 31.7 (d, $^1J_{P-C}$ = 24 Hz, $\mathbf{C}(CH_3)_3$), 30.9 (d, $^2J_{P-C}$ = 14 Hz, $C(\mathbf{C}H_3)_3$), 29.0 (d, $^1J_{P-C}$ = 26 Hz, $\mathbf{C}H_2P^tBu_2$). $^{31}P\{^1H\}$ NMR (121.5 MHz, C_6D_6) δ: 34.1 (s).

Dicyclohexylbenzylphosphine (Cy_2BnP, **4.4**):[313] $ClPCy_2$ (6.02 g, 25.9 mmol) was dissolved in Et_2O (100 mL), and a 1.0 M solution of BnMgCl in Et_2O (13 mL, 25.9 mmol) was added dropwise via syringe at -78°C over a 30 min period. The solution was stirred at -78°C for 5 h, then gradually warmed to RT and stirred for an additional 16 h during which time a precipitate formed. The solvent was removed *in vacuo*, and the product was extracted with pentanes (3 x 25 mL). Following filtration through Celite, the solvent was removed *in vacuo*, affording a white solid. Spectroscopic data were consistent with literature values.[313] Yield: 4.21 g, 56%. ^{1}H NMR (500 MHz, C_6D_6) δ: 7.33 (d, 2H, $^3J_{H-H}$ = 8 Hz, $C_6\mathbf{H}_5$ (*o*-H)), 7.17 (pseudo t, 2H, $^3J_{H-H}$ = 8 Hz, $C_6\mathbf{H}_5$ (*m*-H)), 7.03 (t, 1H, $^3J_{H-H}$ = 8 Hz, $C_6\mathbf{H}_5$ (*p*-H)), 2.71 (s, 2H, $C\mathbf{H}_2Ph$), 1.80-1.10 (m, 22H,

$P(C_6\mathbf{H}_{11})_2$). $^{13}C\{^1H\}$ NMR (75.5 MHz, C_6D_6) δ: 140.9 (s, $\mathbf{C}_6H_5$ (*ipso*-C)), 129.8 (s, $\mathbf{C}_6H_5$ (*o*-C)), 128.6 (s, $\mathbf{C}_6H_5$ (*m*-C)), 125.7 (s, $\mathbf{C}_6H_5$ (*p*-C)), 34.0 (d, $^1J_{P\text{-}C}$ = 10 Hz, $P(\mathbf{C}_6H_{11})_2$ (*ipso*-C)), 30.2 (d, $^1J_{P\text{-}C}$ = 8 Hz, $\mathbf{C}H_2PCy_2$), 29.7 (d, $^2J_{P\text{-}C}$ = 6 Hz, $P(\mathbf{C}_6H_{11})_2$ (*o*-C)), 26.6 (s, $P(\mathbf{C}_6H_{11})_2$ (*m*-C)), 26.8 (s, $P(\mathbf{C}_6H_{11})_2$ (*p*-C)). $^{31}P\{^1H\}$ NMR (121.5 MHz, C_6D_6) δ: 2.5 (s).

1,4-*bis*-[(di-*tert*-butylphosphinyl)methyl]benzene (*p*-$(CH_2P^tBu_2)_2C_6H_4$, **4.5**):[271] α,α′-dibromo-*p*-xylene (0.88 g, 3.3 mmol) was slurried in MeOH (35 mL) and HP^tBu_2 (1.08 g, 7.3 mmol) was added via syringe. The mixture was stirred at RT for 16 h, during which time the solution became homogeneous. NEt_3 was added via syringe (0.74 g, 7.3 mmol), and **4.5** precipitated as a fine white solid from solution. The solid was isolated by filtration, washed with MeOH (3 x 10 mL), and dried *in vacuo* for 5 h. A second crop of **4.5** was obtained by concentrating the mother liquor, and precipitating the product with degassed water; no degradation in purity was evident upon examination of the ^1H NMR spectrum. Combined yield: 1.16 g (88%). ^1H NMR (500 MHz, C_6D_6): 7.38 (s, 4H, $C_6\mathbf{H}_4$), 2.73 (s, 4H, $C\mathbf{H}_2P^tBu_2$), 1.06 (d, 36H, $^3J_{P\text{-}H}$ = 10 Hz, $C(C\mathbf{H}_3)_3$). $^{13}C\{^1H\}$ NMR (75.5 MHz, C_6D_6) δ: 138.4 (s, $\mathbf{C}_6H_4$ (*ipso*-C)), 130.1 (s, $\mathbf{C}_6H_4$ (*o*-C)), 32.1 (d, $^1J_{P\text{-}C}$ = 54 Hz, $\mathbf{C}(CH_3)_3$), 30.1 (s, $C(\mathbf{C}H_3)_3$), 29.0 (d, $^1J_{P\text{-}C}$ = 48 Hz, $\mathbf{C}H_2P^tBu_2$). $^{31}P\{^1H\}$ NMR (121.5 MHz, C_6D_6) δ: 33.4 (s). Anal. Calc'd for $C_{24}H_{44}P_2$: C, 73.06; H, 11.24; N, 0.00. Found: C, 72.36; H, 11.05; N, 0.08. Colourless crystals suitable for X-ray diffraction were grown by slow evaporation from PhH.

1,4-*bis*-[(dicyclohexylphosphinyl)methyl]benzene (*p*-$(CH_2PCy_2)_2C_6H_4$, **4.6**):[271] This was prepared by an analogous method as described for the synthesis of **4.5** to afford a white solid (4.23 g, 85%). ^1H NMR (500 MHz, C_6D_6) δ: 7.33 (s, 4H, $C_6\mathbf{H}_4$), 2.72 (s, 4H, $C\mathbf{H}_2PCy_2$), 1.80-1.12 (m, 44H, $CH_2P(C_6\mathbf{H}_{11})_2$). $^{13}C\{^1H\}$ NMR (75.5 MHz, C_6D_6) δ: 137.9 (s, $\mathbf{C}_6H_4$ (*ipso*-C)), 129.7 (s, $\mathbf{C}_6H_4$ (*o*-C)), 34.0 (d, $^1J_{P\text{-}C}$ = 17 Hz, $P(\mathbf{C}_6H_{11})_2$ (*ipso*-C)), 30.3 (d, $^1J_{P\text{-}C}$ = 14 Hz, $\mathbf{C}H_2PCy_2$), 29.7 (d, $^2J_{P\text{-}C}$ = 10 Hz, $P(\mathbf{C}_6H_{11})_2$ (*o*-C)), 27.6 (s, $P(\mathbf{C}_6H_{11})_2$ (*m*-C)), 26.9 (s, $P(\mathbf{C}_6H_{11})_2$ (*p*-C)). $^{31}P\{^1H\}$ NMR (121.5 MHz, C_6D_6) δ: 1.2 (s). Anal. Calc'd for $C_{32}H_{52}P_2$: C, 77.07; H, 10.51; N, 0.00. Found: C, 76.26; H, 10.59; N, 0.09.

4.2.6 Phosphinimine Syntheses[274]

$^{t}Bu_2BnPNSiMe_3$ (**4.7**): Liquid $^{t}Bu_2BnP$ (590 mg, 2.5 mmol) was dissolved in PhMe (10 mL) to give a clear, colourless solution. Me_3SiN_3 (0.38 mL, 2.8 mmol) was added at RT, and the solution was heated at 45°C for 18 h. The foggy solution was filtered through Celite, and the solvent was removed *in vacuo*, affording a colourless liquid (489 mg, 60%). ^{1}H NMR (500 MHz, C_6D_6) δ: 7.35 (d, 2H, $^{3}J_{H-H}$ = 8 Hz, $C_6\mathbf{H}_5$ (*o*-H)), 7.19 (pseudo t, 2H, $^{3}J_{H-H}$ = 8 Hz, $C_6\mathbf{H}_5$ (*m*-H)), 7.06 (t, 1H, $^{3}J_{H-H}$ = 8 Hz, $C_6\mathbf{H}_5$ (*p*-H)), 2.74 (d, 2H, $^{2}J_{P-H}$ = 10 Hz, $C\mathbf{H}_2Ph$), 0.99 (d, 18H, $^{3}J_{P-H}$ = 14 Hz, $C(C\mathbf{H}_3)_3$), 0.31 (s, 9H, $Si(C\mathbf{H}_3)_3$). $^{13}C\{^{1}H\}$ NMR (75.5 MHz, C_6D_6) δ: 135.7 (d, $^{1}J_{P-C}$ = 5 Hz, $\mathbf{C}_6H_5$ (*ipso*-C)), 130.9 (d, $^{1}J_{P-C}$ = 3 Hz, $\mathbf{C}_6H_5$ (*o*-C)), 128.5 (s, $\mathbf{C}_6H_5$ (*m*-C)), 126.2 (s, $\mathbf{C}_6H_5$ (*p*-C)), 37.1 (d, $^{1}J_{P-C}$ = 36 Hz, $\mathbf{C}(CH_3)_3$), 30.8 (d, $^{1}J_{P-C}$ = 33 Hz, $\mathbf{C}H_2P^{t}Bu_2$), 27.6 (s, $C(\mathbf{C}H_3)_3$), 4.7 (s, $Si(\mathbf{C}H_3)_3$). $^{31}P\{^{1}H\}$ NMR (121.5 MHz, C_6D_6) δ: 24.6 (s).

$Cy_2BnPNSiMe_3$ (**4.8**): Solid Cy_2BnP (4.21 g, 14.6 mmol) was dissolved in PhMe (30 mL) to give a clear, colourless solution. Me_3SiN_3 (1.93 mL, 14.6 mmol) was added at RT, and the solution was heated at 70°C for 18 h. The solvent was removed *in vacuo*, and the residue was washed with cold pentanes (3 x 10 mL) to afford a white solid (5.24 g, 96%). ^{1}H NMR (500 MHz, C_6D_6) δ: 7.32 (d, 2H, $^{3}J_{H-H}$ = 8 Hz, $C_6\mathbf{H}_5$ (*o*-H)), 7.19 (pseudo t, 2H, $^{3}J_{H-H}$ = 8 Hz, $C_6\mathbf{H}_5$ (*m*-H)), 7.08 (t, 1H, $^{3}J_{H-H}$ = 8 Hz, $C_6\mathbf{H}_5$ (*p*-H)), 2.68 (d, 2H, $^{2}J_{P-H}$ = 12 Hz, $C\mathbf{H}_2Ph$), 1.78-1.01 (m, 44H, $P(C_6\mathbf{H}_{11})_2$), 0.39 (s, 9H, $Si(C\mathbf{H}_3)_3$). $^{13}C\{^{1}H\}$ NMR (75.5 MHz, C_6D_6) δ: 135.1 (s, $\mathbf{C}_6H_5$ (*ipso*-C)), 130.3 (s, $\mathbf{C}_6H_5$ (*o*-C)), 128.3 (s, $\mathbf{C}_6H_5$ (*m*-C)), 126.4 (s, $\mathbf{C}_6H_5$ (*p*-C)), 37.6 (d, $^{1}J_{P-C}$ = 65 Hz, $P(\mathbf{C}_6H_{11})_2$ (*ipso*-C)), 34.2 (d, $^{1}J_{P-C}$ = 59 Hz, $\mathbf{C}H_2PCy_2$), 27.0 (d, $^{2}J_{P-C}$ = 12 Hz, $P(\mathbf{C}_6H_{11})_2$ (*o*-C)), 26.5 (s, $P(\mathbf{C}_6H_{11})_2$ (*m*-C)), 25.5 (s, $P(\mathbf{C}_6H_{11})_2$ (*p*-C)), 5.1 (s, $Si(\mathbf{C}H_3)_3$). $^{31}P\{^{1}H\}$ NMR (121.5 MHz, C_6D_6) δ: 13.8 (s). Anal. Calc'd for $C_{22}H_{38}NPSi$: C, 70.35; H, 10.20; N, 3.73. Found: C, 70.39; H, 10.50; N, 3.80. Colourless crystals suitable for X-ray diffraction were grown by slow evaporation from pentanes.

p-$(CH_2P^{t}Bu_2NSiMe_3)_2C_6H_4$ (**4.9**): Solid *p*-$(CH_2P^{t}Bu_2)_2C_6H_4$ (**4.5**) (690 mg, 1.7 mmol) and Me_3SiN_3 (1.00 g, 8.7 mmol) were combined at RT to generate a slurry. The mixture

was heated at reflux for 15 h, after which time the excess Me_3SiN_3 was removed *in vacuo*. The beige solid was crushed with a mortar and pestle into a fine powder, washed with hexanes (3 x 10 mL) and dried *in vacuo* for an additional 5 h to afford a white powder (0.88 g, 88%). ^{1}H NMR (500 MHz, C_6D_6) δ: 7.39 (s, 4H, $C_6\mathbf{H}_4$), 2.73 (d, 4H, $^2J_{P-H}$ = 10 Hz, $C\mathbf{H}_2P^tBu_2$), 0.99 (d, 36H, $^3J_{P-H}$ = 13 Hz, $C(C\mathbf{H}_3)_3$), 0.35 (s, 18H, $Si(C\mathbf{H}_3)_3$). $^{13}C\{^1H\}$ NMR (75.5 MHz, C_6D_6) δ: 133.4 (s, $\mathbf{C}_6H_4$ (*ipso*-C)), 130.4 (s, $\mathbf{C}_6H_4$ (*o*-C)), 37.1 (d, $^1J_{P-C}$ = 60 Hz, $\mathbf{C}(CH_3)_3$), 30.1 (d, $^1J_{P-C}$ = 57 Hz, $\mathbf{C}H_2P^tBu_2$), 27.6 (s, $C(\mathbf{C}H_3)_3$), 1.4 (s, $Si(\mathbf{C}H_3)_3$). $^{31}P\{^1H\}$ NMR (121.5 MHz, C_6D_6) δ: 24.6 (s). Anal. Calc'd for $C_{30}H_{62}N_2P_2Si_2$: C, 63.33; H, 10.98; N, 4.92. Found: C, 63.34; H, 10.36; N, 4.93.

p-$(CH_2PCy_2NSiMe_3)_2C_6H_4$ (**4.10**): This was prepared by an analogous method described for the synthesis of **4.9** to afford a white solid (2.77 g, 94%). ^{1}H NMR (500 MHz, C_6D_6) δ: 7.34 (s, 4H, $C_6\mathbf{H}_4$), 2.67 (d, 4H, $^2J_{P-H}$ = 12 Hz, $C\mathbf{H}_2PCy_2$), 1.78-1.07 (m, 44H, $CH_2P(C_6\mathbf{H}_{11})_2$), 0.41 (s, 18H, $Si(C\mathbf{H}_3)_3$). $^{13}C\{^1H\}$ NMR (75.5 MHz, C_6D_6) δ: 132.9 (s, $\mathbf{C}_6H_4$ (*ipso*-C)), 130.1 (s, $\mathbf{C}_6H_4$ (*o*-C)), 37.6 (d, $^1J_{P-C}$ = 65 Hz, $P(\mathbf{C}_6H_{11})_2$ (*ipso*-C)), 33.7 (d, $^1J_{P-C}$ = 60 Hz, $\mathbf{C}H_2PCy_2$), 27.2 (d, $^2J_{P-C}$ = 13 Hz, $P(\mathbf{C}_6H_{11})_2$ (*o*-C)), 26.5 (s, $P(\mathbf{C}_6H_{11})_2$ (*m*-C)), 26.2 (s, $P(\mathbf{C}_6H_{11})_2$ (*p*-C)), 5.2 (s, $Si(\mathbf{C}H_3)_3$). $^{31}P\{^1H\}$ NMR (121.5 MHz, C_6D_6) δ: 13.5 (s). Anal. Calc'd for $C_{38}H_{70}N_2P_2Si_2$: C, 67.81; H, 10.48; N, 4.16. Found: C, 68.08; H, 10.85; N, 3.89. Colourless crystals suitable for X-ray diffraction were grown by slow evaporation from hexanes.

p-$(CH_2P^tBu_2NH)_2C_6H_4$ (**4.11**): Solid *p*-$(CH_2P^tBu_2NSiMe_3)_2C_6H_4$ (**4.9**) (1.21 g, 2.2 mmol) and MeOH (50 mL) were heated at reflux for 16 h, after which time the volatile products were removed *in vacuo*. The oily residue was washed with hexanes (3 x 10 mL) to afford a fine white powder (0.79 g, 87%). ^{1}H NMR (500 MHz, CD_2Cl_2) δ: 7.33 (s, 4H, $C_6\mathbf{H}_4$), 3.12 (d, 4H, $^2J_{P-H}$ = 11 Hz, $C\mathbf{H}_2P^tBu_2$), 1.21 (d, 36H, $^3J_{P-H}$ = 13 Hz, $C(C\mathbf{H}_3)_3$). $^{13}C\{^1H\}$ NMR (75.5 MHz, CD_2Cl_2) δ: 135.5 (s, $\mathbf{C}_6H_4$ (*ipso*-C)), 130.6 (s, $\mathbf{C}_6H_4$ (*o*-C)), 36.5 (d, $^1J_{P-C}$ = 56 Hz, $\mathbf{C}(CH_3)_3$), 29.9 (d, $^1J_{P-C}$ = 40 Hz, $\mathbf{C}H_2P^tBu_2$), 27.8 (s, $C(\mathbf{C}H_3)_3$). $^{31}P\{^1H\}$ NMR (121.5 MHz, CD_2Cl_2) δ: 51.7 (s). Anal. Calc'd for $C_{24}H_{46}N_2P_2$: C, 67.89; H, 10.92; N, 6.60. Found: C, 67.17; H, 10.93; N, 6.67.

p-($CH_2PCy_2NH)_2C_6H_4$ (**4.12**): Solid *p*-($CH_2PCy_2NSiMe_3)_2C_6H_4$ (**4.10**) (1.97 g, 2.9 mmol) and ^iPrOH (50mL) were heated at reflux for 16 h. Removal of the volatile products *in vacuo* afforded a white, oily solid (1.47 g, 95%). ^1H NMR (500 MHz, CD_2Cl_2) δ: 7.34 (s, 4H, $C_6\mathbf{H}_4$), 3.24 (d, 4H, $^2J_{P\text{-}H}$ = 13 Hz, $C\mathbf{H}_2PCy_2$), 2.85 (br, 2H, N**H**), 1.93-1.15 (m, 44H, $P(C_6\mathbf{H}_{11})_2$). $^{13}C\{^1H\}$ NMR (75.5 MHz, CD_2Cl_2) δ: 131.4 (s, $\mathbf{C}_6H_4$ (*ipso*-C)), 130.9 (s, $\mathbf{C}_6H_4$ (*o*-C)), 35.6 (d, $^1J_{P\text{-}C}$ = 60 Hz, $P(\mathbf{C}_6H_{11})_2$ (*ipso*-C)), 31.5 (d, $^1J_{P\text{-}C}$ = 48 Hz, $\mathbf{C}H_2PCy_2$), 27.2 (d, $^2J_{P\text{-}C}$ = 13 Hz, $P(\mathbf{C}_6H_{11})_2$ (*o*-C)), 26.4 (br, $P(\mathbf{C}_6H_{11})_2$ (*m*-C)), 26.4 (br, $P(\mathbf{C}_6H_{11})_2$ (*p*-C)). $^{31}P\{^1H\}$ NMR (121.5 MHz, CD_2Cl_2) δ: 36.2 (s).

4.2.7 Organometallic Syntheses[131,314]

$TiCp^*(NP^tBu_2Bn)Cl_2$ (**4.13**): The metal complexes **4.13-4.16** were prepared in a comparable fashion, thus only a representative experiment is described. Solid $TiCp^*Cl_3$ (1.12 g, 3.8 mmol) was dissolved in PhMe (100 mL) to give a clear, red solution. $^tBu_2BnPNSiMe_3$ (**4.7**) (1.24 g, 3.8 mmol) was dissolved in PhMe (10 mL), and was added dropwise at RT to the solution containing the titanium reagent. The suspension was stirred for 24 h, after which time the volatile products were removed *in vacuo*. The bright orange solid was washed with hexanes (3 x 10 mL) and dried. Yield: 1.73 g (91%). ^1H NMR (500 MHz, C_6D_6) δ: 7.39 (d, 2H, $^3J_{H\text{-}H}$ = 8 Hz, $C_6\mathbf{H}_5$ (*o*-H)), 7.19 (pseudo t, 2H, $^3J_{H\text{-}H}$ = 8 Hz, $C_6\mathbf{H}_5$ (*m*-H)), 7.08 (t, 1H, $^3J_{H\text{-}H}$ = 8 Hz, $C_6\mathbf{H}_5$ (*p*-H)), 2.92 (d, 2H, $^2J_{P\text{-}H}$ = 12 Hz, $C\mathbf{H}_2Ph$), 2.21 (s, 15H, $C_5(C\mathbf{H}_3)_5$), 1.10 (d, 18H, $^3J_{P\text{-}H}$ = 14 Hz, $C(C\mathbf{H}_3)_3$). $^{13}C\{^1H\}$ NMR (75.5 MHz, C_6D_6) δ: 140.8 (s, $\mathbf{C}_6H_5$ (*ipso*-C)), 131.2 (s, $\mathbf{C}_6H_5$ (*o*-C)), 128.7 (s, $\mathbf{C}_6H_5$ (*m*-C)), 127.1 (s, $\mathbf{C}_6H_5$ (*p*-C)), 125.9 (s, $\mathbf{C}_5(CH_3)_5$), 39.6 (d, $^1J_{P\text{-}C}$ = 52 Hz, $\mathbf{C}(CH_3)_3$), 30.9 (d, $^1J_{P\text{-}C}$ = 48 Hz, $\mathbf{C}H_2Ph$), 27.8 (s, $C(\mathbf{C}H_3)_3$), 13.1 (s, $C_5(\mathbf{C}H_3)_5$). $^{31}P\{^1H\}$ NMR (121.5 MHz, C_6D_6) δ: 35.3 (s). Anal. Calc'd for $C_{24}H_{38}Cl_2NPTi$: C, 59.54; H, 7.99; N, 2.78. Found: C, 59.07; H, 8.08; N, 2.60. Bright orange crystals suitable for X-ray diffraction were grown by slow evaporation from PhH.

$TiCp^*(NPCy_2Bn)Cl_2$ (**4.14**): Bright orange solid (580 mg, 93%). ^1H NMR (500 MHz, C_6D_6) δ: 7.20 (d, 2H, $^3J_{H\text{-}H}$ = 8 Hz, $C_6\mathbf{H}_5$ (*o*-H)), 7.15 (pseudo t, 2H, $^3J_{H\text{-}H}$ = 8 Hz, $C_6\mathbf{H}_5$

(*m*-H)), 7.04 (t, 1H, $^{3}J_{H-H}$ = 8 Hz, $C_6\mathbf{H}_5$ (*p*-H)), 3.01 (d, 2H, $^{2}J_{P-H}$ = 14 Hz, $C\mathbf{H}_2Ph$), 2.20 (s, 15H, $C_5(C\mathbf{H}_3)_3$), 1.71-0.96 (m, 22H, $P(C_6\mathbf{H}_{11})_2$). $^{13}C\{^{1}H\}$ NMR (75.5 MHz, C_6D_6) δ: 132.6 (d, $^{2}J_{P-C}$ = 7 Hz, $\mathbf{C}_6H_5$ (*ipso*-C)), 130.5 (d, $^{3}J_{P-C}$ = 5 Hz, $\mathbf{C}_6H_5$ (*o*-C)), 128.9 (s, $\mathbf{C}_6H_5$ (*m*-C)), 127.2 (s, $\mathbf{C}_6H_5$ (*p*-C)), 125.9 (s, $\mathbf{C}_5(CH_3)_5$), 37.2 (d, $^{1}J_{P-C}$ = 59 Hz, $P(\mathbf{C}_6H_{11})_2$ (*ipso*-C)), 32.2 (d, $^{1}J_{P-C}$ = 52 Hz, $\mathbf{C}H_2PCy_2$), 26.8 (d, $^{2}J_{P-C}$ = 12 Hz, $P(\mathbf{C}_6H_{11})_2$ (*o*-C)), 26.7 (d, $^{2}J_{P-C}$ = 12 Hz, $P(\mathbf{C}_6H_{11})_2$ (*o*-C)), 26.1 (s, $P(\mathbf{C}_6H_{11})_2$ (*m*-C)), 26.0 (s, $P(\mathbf{C}_6H_{11})_2$ (*p*-C)), 13.2 (s, $C_5(\mathbf{C}H_3)_5$). $^{31}P\{^{1}H\}$ NMR (121.5 MHz, C_6D_6) δ: 23.0 (s). Anal. Calc'd for $C_{29}H_{44}Cl_2NPTi$: C, 62.60; H, 7.97; N, 2.52. Found: C, 62.29; H, 8.27; N, 2.45. Orange crystals suitable for X-ray diffraction were grown by slow diffusion of pentanes/hexanes into PhH.

$TiCp(NP^{t}Bu_2Bn)Cl_2$ (**4.15**): Bright yellow solid (393 mg, 77%). ^{1}H NMR (500 MHz, C_6D_6) δ: 7.26 (d, 2H, $^{3}J_{H-H}$ = 8 Hz, $C_6\mathbf{H}_5$ (*o*-H)), 7.20 (pseudo t, 2H, $^{3}J_{H-H}$ = 8 Hz, $C_6\mathbf{H}_5$ (*m*-H)), 7.07 (t, 1H, $^{3}J_{H-H}$ = 8 Hz, $C_6\mathbf{H}_5$ (*p*-H)), 6.22 (s, 5H, $C_5\mathbf{H}_5$), 2.61 (d, 2H, $^{2}J_{P-H}$ = 10 Hz, $C\mathbf{H}_2Ph$), 1.04 (d, 18H, $^{3}J_{P-H}$ = 15 Hz, $C(C\mathbf{H}_3)_3$). $^{13}C\{^{1}H\}$ NMR (75.5 MHz, C_6D_6) δ: 131.5 (d, $^{2}J_{P-C}$ = 5 Hz, (*ipso*-C)), 128.7 (d, $^{3}J_{P-C}$ = 5 Hz, (*o*-C)), 128.6 (s, $\mathbf{C}_6H_5$ (*m*-C)), 128.3 (s, $\mathbf{C}_6H_5$ (*p*-C)), 115.5 (s, $\mathbf{C}_5H_5$), 39.3 (d, $^{1}J_{P-C}$ = 51 Hz, $\mathbf{C}(CH_3)_3$), 28.9 (d, $^{1}J_{P-C}$ = 47 Hz, $\mathbf{C}H_2Ph$), 27.2 (s, $C(\mathbf{C}H_3)_3$). $^{31}P\{^{1}H\}$ NMR (121.5 MHz, C_6D_6) δ: 34.9 (s). Anal. Calc'd for $C_{20}H_{30}Cl_2NPTi$: C, 55.32; H, 6.96; N, 3.23. Found: C, 55.49; H, 7.14; N, 3.19.

$TiCp(NPCy_2Bn)Cl_2$ (**4.16**): Bright yellow solid (685 mg, 92%). ^{1}H NMR (500 MHz, C_6D_6) δ: 7.27 (d, 2H, $^{3}J_{H-H}$ = 8 Hz, $C_6\mathbf{H}_5$ (*o*-H)), 7.18 (pseudo t, 2H, $^{3}J_{H-H}$ = 8 Hz, $C_6\mathbf{H}_5$ (*m*-H)), 7.06 (t, 1H, $^{3}J_{H-H}$ = 8 Hz, $C_6\mathbf{H}_5$ (*p*-H)), 6.38 (s, 5H, $C_5\mathbf{H}_5$), 2.65 (d, 2H, $^{2}J_{P-H}$ = 13 Hz, $C\mathbf{H}_2Ph$), 1.74-0.84 (m, 22H, $P(C_6\mathbf{H}_{11})_2$). $^{13}C\{^{1}H\}$ NMR (75.5 MHz, C_6D_6) δ: 131.6 (d, $^{2}J_{P-C}$ = 8 Hz, $\mathbf{C}_6H_5$ (*ipso*-C)), 130.8 (d, $^{3}J_{P-C}$ = 5 Hz, $\mathbf{C}_6H_5$ (*o*-C)), 128.9 (s, $\mathbf{C}_6H_5$ (*m*-C)), 128.5 (s, $\mathbf{C}_6H_5$ (*p*-C)), 115.2 (s, $\mathbf{C}_5H_5$), 36.6 (d, $^{1}J_{P-C}$ = 58 Hz, $P(\mathbf{C}_6H_{11})_2$ (*ipso*-C)), 30.9 (d, $^{1}J_{P-C}$ = 52 Hz, $\mathbf{C}H_2PCy_2$), 26.6 (d, $^{2}J_{P-C}$ = 13 Hz, $P(\mathbf{C}_6H_{11})_2$ (*o*-C)), 25.9 (s, $P(\mathbf{C}_6H_{11})_2$ (*m*-C)), 25.7 (s, $P(\mathbf{C}_6H_{11})_2$ (*p*-C)). $^{31}P\{^{1}H\}$ NMR (121.5 MHz, C_6D_6) δ: 24.3 (s). Anal. Calc'd for $C_{24}H_{44}Cl_2NPTi$: C, 59.28; H, 7.05; N, 2.88. Found: C, 59.68; H, 7.28; N, 2.82. Yellow crystals suitable for X-ray diffraction were grown by slow diffusion of pentanes/hexanes into PhH.

p-($CH_2P^tBu_2NTiCp^*Cl_2)_2C_6H_4$ (**4.17**): The bimetallic metal complexes **4.17-4.20** were prepared in a similar fashion, thus a representative experiment is described. *p*-($CH_2P^tBu_2NSiMe_3)_2C_6H_4$ (**4.9**) (810 mg, 1.2 mmol) and Cp^*TiCl_3 (700 mg, 2.4 mmol) were slurried in PhMe (80 mL) to afford a bright orange suspension. The mixture was heated at reflux for 15 h, after which time it was filtered through Celite. The filtrate was concentrated to *ca.* 20 mL, and the bright orange powder that precipitated was isolated by filtration, washed with PhH (3 x 15 mL) and dried *in vacuo*. Yield: 1.06 g (95%). ^{1}H NMR (500 MHz, CD_2Cl_2) δ: 7.48 (s, 4H, $C_6\mathbf{H}_4$), 3.38 (d, 4H, $^2J_{P-H}$ = 12 Hz, $C\mathbf{H}_2P^tBu_2$), 2.14 (s, 30H, $C_5(C\mathbf{H}_3)_5$), 1.34 (d, 36H, $^3J_{P-H}$ = 15 Hz, $C(C\mathbf{H}_3)_3$). $^{13}C\{^1H\}$ NMR (75.5 MHz, CD_2Cl_2) δ: 133.4 (s, $\mathbf{C}_6H_4$ (*ipso*-C)), 131.5 (s, $\mathbf{C}_6H_4$ (*o*-C)), 123.2 (s, $\mathbf{C}_5(CH_3)_5$), 40.6 (s, $\mathbf{C}H_2P^tBu_2$), 39.8 (d, $^1J_{P-C}$ = 55 Hz, $\mathbf{C}(CH_3)_3$), 28.3 (s, $C(\mathbf{C}H_3)_3$), 8.9 (s, $C_5(\mathbf{C}H_3)_5$). $^{31}P\{^1H\}$ NMR (121.5 MHz, CD_2Cl_2) δ: 37.2 (s). Anal. Calc'd for $C_{44}H_{74}Cl_4N_2P_2Ti_2$: C, 56.79; H, 8.02; N, 3.01. Found: C, 54.92; H, 8.16; N, 3.35.

p-($CH_2PCy_2NTiCp^*Cl_2)_2C_6H_4$ (**4.18**): Bright orange solid (980 mg, 79%). ^{1}H NMR (500 MHz, C_6D_6) δ: 7.36 (s, 4H, $C_6\mathbf{H}_4$), 3.01 (d, 4H, $^2J_{P-H}$ = 13 Hz, $C\mathbf{H}_2PCy_2$), 2.24 (s, 30H, $C_5(C\mathbf{H}_3)_5$), 1.71-1.03 (m, 44H, $P(C_6\mathbf{H}_{11})_2$). $^{13}C\{^1H\}$ NMR (75.5 MHz, C_6D_6) δ: 137.4 (s, $\mathbf{C}_6H_4$ (*ipso*-C)), 131.0 (s, $\mathbf{C}_6H_4$ (*o*-C)), 125.8 (s, $\mathbf{C}_5(CH_3)_5$), 37.2 (d, $^1J_{P-C}$ = 59 Hz, $P(\mathbf{C}_6H_{11})_2$ (*ipso*-C)), 31.9 (d, $^1J_{P-C}$ = 52 Hz, $\mathbf{C}H_2PCy_2$), 26.8 (d, $^2J_{P-C}$ = 12 Hz, $P(\mathbf{C}_6H_{11})_2$ (*o*-C)), 26.1 (s, $P(\mathbf{C}_6H_{11})_2$ (*m*-C)), 26.1 (s, $P(\mathbf{C}_6H_{11})_2$ (*p*-C)), 13.2 (s, $C_5(\mathbf{C}H_3)_5$). $^{31}P\{^1H\}$ NMR (121.5 MHz, C_6D_6) δ: 22.4 (s). Anal. Calc'd for $C_{52}H_{82}Cl_4N_2P_2Ti_2$: C, 60.36; H, 7.99; N, 2.71. Found: C, 60.20; H, 8.19; N, 2.76. Bright orange crystals suitable for X-ray diffraction were grown by slow evaporation from PhMe.

p-($CH_2P^tBu_2NTiCpCl_2)_2C_6H_4$ (**4.19**): Bright yellow solid (2.34 g, 95%). ^{1}H NMR (500 MHz, CD_2Cl_2) δ: 7.54 (s, 4H, $C_6\mathbf{H}_4$), 6.29 (s, 10H, $C_5\mathbf{H}_5$), 3.31 (d, 4H, $^2J_{P-H}$ = 10 Hz, $C\mathbf{H}_2P^tBu_2$), 1.40 (d, 36H, $^3J_{P-H}$ = 13 Hz, $C(C\mathbf{H}_3)_3$). $^{13}C\{^1H\}$ NMR (75.5 MHz, , CD_2Cl_2) δ: 132.7 (s, $\mathbf{C}_6H_4$ (*ipso*-C)), 132.0 (s, $\mathbf{C}_6H_4$ (*o*-C)), 116.0 (s, $\mathbf{C}_5H_5$), 46.4 (s, $\mathbf{C}H_2P^tBu_2$), 40.0 (d, $^1J_{P-C}$ = 51 Hz, $\mathbf{C}(CH_3)_3$), 27.8 (s, $C(\mathbf{C}H_3)_3$). $^{31}P\{^1H\}$ NMR (121.5 MHz,

CD_2Cl_2) δ: 38.7 (s). Anal. Calc'd for $C_{34}H_{54}Cl_4N_2P_2Ti_2$: C, 51.67; H, 6.89; N, 3.54. Found: C, 52.65; H, 7.64; N, 3.45.

p-$(CH_2PCy_2NTiCpCl_2)_2C_6H_4$ (**4.20**): Bright yellow solid (1.36 g, 95%). ^1H NMR (500 MHz, C_6D_6) δ: 7.46 (s, 4H, $C_6\mathbf{H}_4$), 6.39 (s, 10H, $C_5\mathbf{H}_5$), 3.21 (d, 4H, $^2J_{P-H}$ = 12 Hz, $C\mathbf{H}_2PCy_2$), 1.96-1.27 (m, 44H, $P(C_6\mathbf{H}_{11})_2$). $^{13}C\{^1H\}$ NMR (75.5 MHz, C_6D_6) δ: 131.8 (s, $\mathbf{C}_6H_4$ (*ipso*-C)), 131.5 (s, $\mathbf{C}_6H_4$ (*o*-C)), 115.7 (s, $\mathbf{C}_5H_5$), 37.1 (d, $^1J_{P-C}$ = 58 Hz, $P(\mathbf{C}_6H_{11})_2$ (*ipso*-C)), 31.1 (d, $^1J_{P-C}$ = 53 Hz, $\mathbf{C}H_2PCy_2$), 27.0 (d, $^2J_{P-C}$ = 13 Hz, $P(\mathbf{C}_6H_{11})_2$ (*o*-C)), 26.3 (s, $P(\mathbf{C}_6H_{11})_2$ (*m*-C)), 26.3 (s, $P(\mathbf{C}_6H_{11})_2$ (*p*-C)). $^{31}P\{^1H\}$ NMR (121.5 MHz, C_6D_6) δ: 27.0 (s). Anal. Calc'd for $C_{42}H_{62}Cl_4N_2P_2Ti_2$: C, 56.40; H, 6.99; N, 3.13. Found: C, 56.23; H, 7.00; N, 3.36. Bright yellow crystals suitable for X-ray diffraction were grown by slow evaporation from CD_2Cl_2.

$TiCp^*(NP^tBu_2Bn)Me_2$ (**4.21**): The alkyl derivatives **4.21-4.24** were prepared in a comparable fashion, thus only a representative experiment is described. $TiCp^*(NP^tBu_2Bn)Cl_2$ (160 mg, 0.32 mmol) was slurried in Et_2O (15 mL), and a 3.0 M solution of MeMgBr in the same solvent (2.24 mL, 0.67 mmol) was added dropwise via syringe at RT. The slurry was stirred for 15 h, after which time the solvent was removed *in vacuo*. Extraction with hexanes (3 x 10 mL) and filtration through Celite afforded a bright yellow solution. Subsequent removal of the solvent *in vacuo* generated bright yellow crystals (122 mg, 83%). ^1H NMR (500 MHz, C_6D_6) δ: 7.38 (d, 2H, $^3J_{H-H}$ = 8 Hz, $C_6\mathbf{H}_5$ (*o*-H)), 7.15 (pseudo t, 2H, $^3J_{H-H}$ = 8 Hz, $C_6\mathbf{H}_5$ (*m*-H)), 7.08 (t, 1H, $^3J_{H-H}$ = 8 Hz, $C_6\mathbf{H}_5$ (*p*-H)), 2.90 (d, 2H, $^2J_{P-H}$ = 12 Hz, $C\mathbf{H}_2Ph$), 2.03 (s, 15H, $C_5(C\mathbf{H}_3)_5$), 1.16 (d, 18H, $^3J_{P-H}$ = 14 Hz, $C(C\mathbf{H}_3)_3$), 0.39 (s, 6H, Ti-$C\mathbf{H}_3$). $^{13}C\{^1H\}$ NMR (75.5 MHz, C_6D_6) δ: 135.0 (d, $^2J_{P-C}$ = 7 Hz, $\mathbf{C}_6H_5$ (*ipso*-C)), 130.9 (d, $^3J_{P-C}$ = 5 Hz, $\mathbf{C}_6H_5$ (*o*-C)), 128.3 (s, $\mathbf{C}_6H_5$ (*m*-C)), 126.7 (s, $\mathbf{C}_6H_5$ (*p*-C)), 118.5 (s, $\mathbf{C}_5(CH_3)_5$), 44.4 (s, Ti-$\mathbf{C}H_3$), 39.0 (d, $^1J_{P-C}$ = 54 Hz, $C(CH_3)_3$), 31.6 (d, $^1J_{P-C}$ = 48 Hz, $\mathbf{C}H_2Ph$), 28.0 (s, $C(\mathbf{C}H_3)_3$), 12.2 (s, $C_5(\mathbf{C}H_3)_5$). $^{31}P\{^1H\}$ NMR (121.5 MHz, C_6D_6) δ: 21.4 (s). Anal. Calc'd for $C_{27}H_{46}NPTi$: C, 69.96; H, 10.00; N, 3.02. Found: C, 69.59; H, 10.03; N, 3.02. Yellow crystals suitable for X-ray diffraction were grown by slow evaporation from hexanes.

TiCp*(NPCy$_2$Bn)Me$_2$ (**4.22**): Light yellow solid (100 mg, 47%). ^{1}H NMR (500 MHz, C_6D_6) δ: 7.28 (d, 2H, $^3J_{H\text{-}H}$ = 8 Hz, $C_6\mathbf{H}_5$ (*o*-H)), 7.17 (pseudo t, 2H, $^3J_{H\text{-}H}$ = 8 Hz, $C_6\mathbf{H}_5$ (*m*-H)), 7.06 (t, 1H, $^3J_{H\text{-}H}$ = 8 Hz, $C_6\mathbf{H}_5$ (*p*-H)), 2.93 (d, 2H, $^2J_{P\text{-}H}$ = 13 Hz, $C\mathbf{H}_2Ph$), 2.08 (s, 15H, $C_5(C\mathbf{H}_3)_5$), 1.91-1.03 (m, 22H, $P(C_6\mathbf{H}_{11})_2$), 0.45 (s, 6H, Ti-$C\mathbf{H}_3$). $^{13}C\{^1H\}$ NMR (75.5 MHz, C_6D_6) δ: 134.2 (d, $^2J_{P\text{-}C}$ = 7 Hz, $\mathbf{C}_6H_5$ (*ipso*-C)), 130.3 (d, $^3J_{P\text{-}C}$ = 5 Hz, $\mathbf{C}_6H_5$ (*o*-C)), 128.6 (s, $\mathbf{C}_6H_5$ (*m*-C)), 126.8 (s, $\mathbf{C}_6H_5$ (*p*-C)), 118.5 (s, $\mathbf{C}_5(CH_3)_5$), 42.6 (s, Ti-$\mathbf{C}H_3$), 38.1 (d, $^1J_{P\text{-}C}$ = 60 Hz, $P(\mathbf{C}_6H_{11})_2$ (*ipso*-C)), 34.4 (d, $^1J_{P\text{-}C}$ = 52 Hz, $\mathbf{C}H_2PCy_2$), 27.0 (d, $^2J_{P\text{-}C}$ = 3 Hz, $P(\mathbf{C}_6H_{11})_2$ (*o*-C)), 26.8 (d, $^2J_{P\text{-}C}$ = 3 Hz, $P(\mathbf{C}_6H_{11})_2$ (*o*-C)), 26.4 (s, $P(\mathbf{C}_6H_{11})_2$ (*m*-C)), 26.3 (s, $P(\mathbf{C}_6H_{11})_2$ (*p*-C)), 12.3 (s, $C_5(\mathbf{C}H_3)_5$). $^{31}P\{^1H\}$ NMR (121.5 MHz, C_6D_6) δ: 8.4 (s). Anal. Calc'd for $C_{31}H_{50}NPTi$: C, 72.22; H, 9.77; N, 2.72. Found: C, 71.93; H, 10.10; N, 2.52. Yellow-orange crystals suitable for X-ray diffraction were grown by slow evaporation from pentanes.

TiCp(NP^{t}Bu$_2$Bn)Me$_2$ (**4.23**): Beige solid (74 mg, 78%). ^{1}H NMR (500 MHz, C_6D_6) δ: 7.32 (d, 2H, $^3J_{H\text{-}H}$ = 7 Hz, $C_6\mathbf{H}_5$ (*o*-H)), 7.16 (pseudo t, 2H, $^3J_{H\text{-}H}$ = 7 Hz, $C_6\mathbf{H}_5$ (*m*-H)), 7.05 (t, 1H, $^3J_{H\text{-}H}$ = 7 Hz, $C_6\mathbf{H}_5$ (*p*-H)), 6.08 (s, 5H, $C_5\mathbf{H}_5$), 2.74 (d, 2H, $^2J_{P\text{-}H}$ = 11 Hz, $C\mathbf{H}_2Ph$), 1.06 (d, 18H, $^3J_{P\text{-}H}$ = 14 Hz, $C(C\mathbf{H}_3)_3$), 0.70 (s, 6H, Ti-$C\mathbf{H}_3$). $^{13}C\{^1H\}$ NMR (75.5 MHz, C_6D_6) δ: 134.0 (s, $\mathbf{C}_6H_5$ (*ipso*-C)), 131.1 (d, $^3J_{P\text{-}C}$ = 4 Hz, $\mathbf{C}_6H_5$ (*o*-C)), 128.4 (s, $\mathbf{C}_6H_5$ (*m*-C)), 126.8 (s, $\mathbf{C}_6H_5$ (*p*-C)), 111.1 (s, $\mathbf{C}_5H_5$), 41.4 (s, Ti-$\mathbf{C}H_3$), 38.5 (d, $^1J_{P\text{-}C}$ = 54 Hz, $\mathbf{C}(CH_3)_3$), 30.2 (d, $^1J_{P\text{-}C}$ = 48 Hz, $\mathbf{C}H_2Ph$), 27.5 (s, $C(\mathbf{C}H_3)_3$). $^{31}P\{^1H\}$ NMR (121.5 MHz, C_6D_6) δ: 21.6 (s).

TiCp(NPCy$_2$Bn)Me$_2$ (**4.24**): Beige solid (230 mg, 46%). ^{1}H NMR (500 MHz, C_6D_6) δ: 7.33 (d, 2H, $^3J_{H\text{-}H}$ = 8 Hz, $C_6\mathbf{H}_5$ (*o*-H)), 7.18 (pseudo t, 2H, $^3J_{H\text{-}H}$ = 8 Hz, $C_6\mathbf{H}_5$ (*m*-H)), 7.06 (t, 1H, $^3J_{H\text{-}H}$ = 8 Hz, $C_6\mathbf{H}_5$ (*p*-H)), 6.18 (s, 5H, $C_5\mathbf{H}_5$), 2.71 (d, 2H, $^2J_{P\text{-}H}$ = 13 Hz, $C\mathbf{H}_2Ph$), 1.62-0.98 (m, 22H, $P(C_6\mathbf{H}_{11})_2$), 0.73 (s, 6H, Ti-$C\mathbf{H}_3$). $^{13}C\{^1H\}$ NMR (75.5 MHz, C_6D_6) δ: 133.5 (d, $^2J_{P\text{-}C}$ = 7 Hz, $\mathbf{C}_6H_5$ (*ipso*-C)), 130.5 (d, $^3J_{P\text{-}C}$ = 5 Hz, $\mathbf{C}_6H_5$ (*o*-C)), 128.5 (s, $\mathbf{C}_6H_5$ (*m*-C)), 127.0 (s, $\mathbf{C}_6H_5$ (*p*-C)), 110.8 (s, $\mathbf{C}_5H_5$), 40.7 (s, Ti-$\mathbf{C}H_3$), 37.6 (d, $^1J_{P\text{-}C}$ = 60 Hz, $P(\mathbf{C}_6H_{11})_2$ (*ipso*-C)), 32.9 (d, $^1J_{P\text{-}C}$ = 53 Hz, $\mathbf{C}H_2PCy_2$), 26.8 (d, $^2J_{P\text{-}C}$ = 12 Hz, $P(\mathbf{C}_6H_{11})_2$ (*o*-C)), 26.3 (s, $P(\mathbf{C}_6H_{11})_2$ (*p*-C)), 26.0 (d, $^3J_{P\text{-}C}$ = 8 Hz, $P(\mathbf{C}_6H_{11})_2$ (*m*-C)). $^{31}P\{^1H\}$ NMR (121.5 MHz, C_6D_6) δ: 10.2 (s). Anal. Calc'd for $C_{26}H_{40}NPTi$: C, 70.11; H,

9.05; N, 3.14. Found: C, 69.03; H, 9.20; N, 3.08. Yellow crystals suitable for X-ray diffraction were grown by slow evaporation from pentanes.

p-($CH_2P^tBu_2NTiCp^*Me_2)_2C_6H_4$ (**4.25**): The alkyl bimetallic derivatives **4.25-4.28** were prepared in a comparable fashion, thus only a representative experiment is described. *p*-($CH_2P^tBu_2NTiCp^*Cl_2)_2C_6H_4$ (210 mg, 0.27 mmol) was slurried in Et_2O (25 mL), and a 3.0 M solution of MeMgBr in the same solvent (0.84 mL, 1.4 mmol) was added dropwise via syringe at RT. The slurry was stirred for 15 h, after which time the solvent was removed *in vacuo*. Extraction with hexanes (3 x 10 mL) and filtration through Celite afforded a colourless solution. Removal of the solvent *in vacuo* generated a white solid (230 mg, 77%). ^{1}H NMR (500 MHz, C_6D_6) δ: 7.50 (s, 4H, $C_6\mathbf{H}_4$), 2.96 (d, 4H, $^2J_{P-H}$ = 11 Hz, $C\mathbf{H}_2P^tBu_2$), 2.12 (s, 30H, $C_5(C\mathbf{H}_3)_5$), 1.17 (d, 36H, $^3J_{P-H}$ = 14 Hz, $C(C\mathbf{H}_3)_3$,), 0.46 (s, 12H, Ti-$C\mathbf{H}_3$). $^{13}C\{^1H\}$ NMR (75.5 MHz, C_6D_6) δ: 133.4 (s, $\mathbf{C}_6H_4$ (*ipso*-C)), 130.8 (s, $\mathbf{C}_6H_4$ (*o*-C)), 118.4 (s, $\mathbf{C}_5(CH_3)_5$), 44.4 (s, Ti-$\mathbf{C}H_3$), 38.9 (d, $^1J_{P-C}$ = 54 Hz, $\mathbf{C}(CH_3)_3$), 31.6 (d, $^1J_{P-C}$ = 48 Hz, $\mathbf{C}H_2P^tBu_2$), 28.0 (s, $C(\mathbf{C}H_3)_3$), 12.3 (s, $C_5(\mathbf{C}H_3)_5$). $^{31}P\{^1H\}$ NMR (121.5 MHz, C_6D_6) δ: 22.0 (s). Anal. Calc'd for $C_{48}H_{86}N_2P_2Ti_2$: C, 67.91; H, 10.21; N, 3.30. Found: C, 60.51; H, 8.96; N, 2.95.

p-($CH_2PCy_2NTiCp^*Me_2)_2C_6H_4$ (**4.26**): Yellow solid (410 mg, 73%). ^{1}H NMR (500 MHz, C_6D_6) δ: 7.35 (s, 4H, $C_6\mathbf{H}_4$), 2.92 (d, 4H, $^2J_{P-H}$ = 13 Hz, $C\mathbf{H}_2PCy_2$), 2.10 (s, 30H, $C_5(C\mathbf{H}_3)_5$), 1.81-1.10 (m, 44H, $P(C_6\mathbf{H}_{11})_2$), 0.43 (s, 12H, Ti-$C\mathbf{H}_3$). $^{13}C\{^1H\}$ NMR (75.5 MHz, C_6D_6) δ: 132.5 (s, $\mathbf{C}_6H_4$ (*ipso*-C)), 130.5 (s, $\mathbf{C}_6H_4$ (*o*-C)), 122.3 (s, $\mathbf{C}_5(CH_3)_5$), 42.7 (s, Ti-$\mathbf{C}H_3$), 38.2 (d, $^1J_{P-C}$ = 61 Hz, $P(\mathbf{C}_6H_{11})_2$ (*ipso*-C)), 34.0 (d, $^1J_{P-C}$ = 52 Hz, $\mathbf{C}H_2PCy_2$), 27.1 (d, $^2J_{P-C}$ = 12 Hz, $P(\mathbf{C}_6H_{11})_2$ (*o*-C)), 26.5 (d, $^3J_{P-C}$ = 6 Hz, $P(\mathbf{C}_6H_{11})_2$ (*m*-C)), 26.4 (s, $P(\mathbf{C}_6H_{11})_2$ (*p*-C)), 11.9 (s, $C_5(\mathbf{C}H_3)_5$). $^{31}P\{^1H\}$ NMR (121.5 MHz, C_6D_6) δ: 8.0 (s). Anal. Calc'd for $C_{56}H_{94}N_2P_2Ti_2$: C, 70.57; H, 9.94; N, 2.94. Found: C, 67.06; H, 9.29; N, 2.63. Yellow crystals suitable for X-ray diffraction were grown by slow evaporation from pentanes.

p-($CH_2P^tBu_2NTiCpMe_2)_2C_6H_4$ (**4.27**): Colourless block crystals (160 mg, 83%). ^{1}H NMR (500 MHz, C_6D_6) δ: 7.48 (s, 4H, $C_6\mathbf{H}_4$), 6.18 (s, 10H, $C_5\mathbf{H}_5$), 2.80 (d, 4H, $^2J_{P-H}$ =

10 Hz, $CH_2P^tBu_2$), 1.06 (d, 36H, $^3J_{P-H}$ = 14 Hz, $C(CH_3)_3$), 0.72 (s, 12H, Ti-CH_3). $^{13}C\{^1H\}$ NMR (75.5 MHz, C_6D_6) δ: 132.5 (s, C_6H_4 (*ipso*-C)), 130.8 (s, C_6H_4 (*o*-C)), 110.9 (s, C_5H_5), 41.3 (s, $CH_2P^tBu_2$), 38.4 (d, $^1J_{P-C}$ = 54 Hz, $C(CH_3)_3$), 31.7 (s, Ti-CH_3), 27.4 (s, $C(CH_3)_3$). $^{31}P\{^1H\}$ NMR (121.5 MHz, C_6D_6) δ: 22.6 (s). Anal. Calc'd for $C_{38}H_{66}N_2P_2Ti_2$: C, 64.41; H, 9.39; N, 3.95. Found: C, 65.15; H, 9.39; N, 3.47. Colourless crystals suitable for X-ray diffraction were grown by slow evaporation from PhMe.

p-$(CH_2PCy_2NTiCpMe_2)_2C_6H_4$ (**4.28**): Yellow needle-like crystals (450 mg, 77%). ^1H NMR (500 MHz, C_6D_6) δ: 7.48 (s, 4H, C_6H_4), 6.22 (s, 10H, C_5H_5), 2.70 (d, 4H, $^2J_{P-H}$ = 12 Hz, CH_2PCy_2), 1.65-1.06 (m, 44H, $P(C_6H_{11})_2$), 0.74 (s, 12H, Ti-CH_3). $^{13}C\{^1H\}$ NMR (75.5 MHz, C_6D_6) δ: 132.1 (s, C_6H_4 (*ipso*-C)), 130.6 (s, C_6H_4 (*o*-C)), 110.8 (s, C_5H_5), 40.8 (s, Ti-CH_3), 37.6 (d, $^1J_{P-C}$ = 60 Hz, $P(C_6H_{11})_2$ (*ipso*-C)), 32.4 (d, $^1J_{P-C}$ = 53 Hz, CH_2PCy_2), 26.9 (d, $^2J_{P-C}$ = 12 Hz, $P(C_6H_{11})_2$ (*o*-C)), 26.3 (s, $P(C_6H_{11})_2$ (*m*-C)), 26.1 (s, $P(C_6H_{11})_2$ (*p*-C)). $^{31}P\{^1H\}$ NMR (121.5 MHz, C_6D_6) δ: 10.1 (s). Anal. Calc'd for $C_{46}H_{74}N_2P_2Ti_2$: C, 67.98; H, 9.18; N, 3.45. Found: C, 68.30; H, 9.45; N, 3.06. Yellow crystals suitable for X-ray diffraction were grown by slow evaporation from PhH.

4.2.8 Reactions with Borane Reagents

[TiCp*$(NP^tBu_2Bn)Me$][$MeB(C_6F_5)_3$] (**4.29**): Solid TiCp*$(NP^tBu_2Bn)Me_2$ (14 mg, 0.030 mmol) and $B(C_6F_5)_3$ (15 mg, 0.030 mmol) were dissolved separately in CH_2Cl_2 (2 mL each) to give clear solutions. They were combined rapidly at RT, and the solution remained clear, although changed colour from yellow to red-orange. After stirring for 10 min, the solvent was removed *in vacuo*. The residue was washed with pentanes (2 x 2 mL) and dried exhaustively *in vacuo* to obtain a yellow foam (22 mg, 76%). Decomposition (*ca.* 40%) was observed at RT in CD_2Cl_2 solution over a 24 h period. ^1H NMR (500 MHz, CD_2Cl_2) δ: 7.39 (br, 1H, C_6H_5 (*p*-H)), 7.34 (br, 2H, C_6H_5 (*m*-H)), 7.30 (br, 2H, C_6H_5 (*o*-H)), 2.37 (d, 1H, $^2J_{P-H}$ = 13 Hz, CH_2Ph), 2.35 (d, 1H, $^2J_{P-H}$ = 13 Hz, CH_2Ph), 2.03 (s, 15H, $C_5(CH_3)_3$), 1.31 (d, 9H, $^3J_{P-H}$ = 20 Hz, $C(CH_3)_3$), 1.30 (d, 9H, $^3J_{P-H}$

= 20 Hz, C($\mathbf{CH_3}$)$_3$), 0.89 (s, 3H, Ti-$\mathbf{CH_3}$), 0.48 (br s, 3H, $\mathbf{H_3}$CB(C_6F_5)$_3$). $^{13}C\{^1H\}$ NMR (75.5 MHz, CD_2Cl_2) δ: 148.8 (d(br), $^1J_{C\text{-}F}$ = 255 Hz, $\mathbf{C_6F_5}$ (*o*-C)), 138.0 (d(br), $^1J_{C\text{-}F}$ = 240 Hz, $\mathbf{C_6F_5}$ (*p*-C)), 137.0 (d(br), $^1J_{C\text{-}F}$ = 220 Hz, $\mathbf{C_6F_5}$ (*m*-C)), 132.4 (br, $\mathbf{C_6F_5}$ (*ipso*)), 130.2 (s, $\mathbf{C_6H_5}$ (*ipso*-C)), 129.5 (s, $\mathbf{C_6H_5}$ (*o*-C)), 129.4 (s, $\mathbf{C_6H_5}$ (*m*-C)), 128.7 (s, $\mathbf{C_6H_5}$ (*p*-C)), 125.8 (s, $\mathbf{C_5}(CH_3)_5$), 41.2 (s, Ti-$\mathbf{CH_3}$), 40.3 (d, $^1J_{P\text{-}C}$ = 50 Hz, $\mathbf{C}(CH_3)_3$), 39.3 (d, $^1J_{P\text{-}C}$ = 50 Hz, $\mathbf{C}(CH_3)_3$), 32.3 (d, $^1J_{P\text{-}C}$ = 26 Hz, $\mathbf{CH_2}$Ph), 28.2 (s, C($\mathbf{CH_3}$)$_3$), 13.7 (s, $C_5(\mathbf{CH_3})_5$), 10.3 (br, $H_3\mathbf{C}B(C_6F_5)_3$). $^{11}B\{^1H\}$ NMR (96.25 MHz, CD_2Cl_2) δ: -15.2 (s). ^{19}F NMR (282.34 MHz, CD_2Cl_2) δ: -133.50 (d, 6F, $^3J_{F\text{-}F}$ = 23 Hz, $C_6\mathbf{F_5}$ (*o*-F)), -165.64 (br, 3F, $C_6\mathbf{F_5}$ (*p*-F)), -168.20 (br, 6F, $C_6\mathbf{F_5}$ (*m*-F)). $^{31}P\{^1H\}$ NMR (121.5 MHz, CD_2Cl_2) δ: 37.8 (s). Anal. Calc'd for $C_{45}H_{46}BF_{15}NPTi$: C, 55.41; H, 4.75; N, 1.44. Found: C, 55.15; H, 5.12; N, 1.10.

4.2.9 X-Ray Experimental

X-ray structural solutions of *p*-$(CH_2P^tBu_2)_2C_6H_4$ (**4.5**), $Cy_2BnPNSiMe_3$ (**4.8**), *p*-$(CH_2PCy_2NSiMe_3)_2C_6H_4$ (**4.10**), TiCp*$(NP^tBu_2Bn)Cl_2$ (**4.13**), TiCp*$(NPCy_2Bn)Cl_2$ (**4.14**), TiCp$(NPCy_2Bn)Cl_2$ (**4.16**), *p*-$(CH_2PCy_2NTiCp^*Cl_2)_2C_6H_4$ (**4.18**), *p*-$(CH_2PCy_2NTiCpCl_2)_2C_6H_4$ (**4.20**), TiCp*$(NPCy_2Bn)Me_2$ (**4.22**), TiCp$(NPCy_2Bn)Me_2$ (**4.24**), *p*-$(CH_2PCy_2NTiCp^*Me_2)_2C_6H_4$ (**4.26**), *p*-$(CH_2P^tBu_2NTiCpMe_2)_2C_6H_4$ (**4.27**), *p*-$(CH_2PCy_2NTiCpMe_2)_2C_6H_4$ (**4.28**) were obtained using direct methods, while TiCp*$(NP^tBu_2Bn)Me_2$ (**4.21**) was solved using a Patterson map. Cell parameters, R, R_w and GoF values are located in Table 4.1, while detailed structural parameters have been included as an appendix on CD. The solutions for structures **4.5**, **4.20**, **4.26** and **4.28** included solvent molecules: **4.20** had a molecule of CD_2Cl_2 in the cell, while the other three solutions included a molecule of C_6H_6. The additional atoms due to the presence of solvent were refined anisotropically. No residual electron density remained in any of the solutions that was of any chemical significance. Representative ORTEP drawings of **4.5**, **4.8**, **4.10**, **4.16** and **4.20** are depicted in Figures 4.2 and 4.4, while select bond distances and angles are provided in Table 4.2 and in the text.

Table 4.1: Crystallographic parameters for *p*-$(CH_2P^tBu_2)_2C_6H_4$ (**4.5**), $Cy_2BnPNSiMe_3$ (**4.8**), *p*-$(CH_2PCy_2NSiMe_3)_2C_6H_4$ (**4.10**).

	4.5	**4.8**	**4.10**
Molecular formula	$C_{24}H_{44}P_2$	$C_{22}H_{38}NPSi$	$C_{38}H_{70}N_2P_2Si_2$
Formula weight	394.53	375.60	673.08
a(Å)	6.1600(2)	9.107(5)	9.453(6)
b(Å)	8.2564(3)	34.51(2)	14.566(8)
c(Å)	13.5269(6)	14.996(8)	17.62(1)
α(°)	80.190(1)	90.00	106.25(1)
β(°)	79.053(1)	96.75 (1)	104.112(9)
γ (°)	71.074(1)	90.00	103.76(1)
Crystal system	Triclinic	Monoclinic	Triclinic
Space group	P-1	$P2_1/n$	P-1
Volume ($Å^3$)	634.54(4)	4680(4)	2133(2)
D_{calc} (gcm^{-3})	1.032	1.066	1.048
Z	1	4	2
Abs coeff, μ, mm^{-1}	0.177	0.174	0.184
θ range (°)	1.54-24.99	1.18-23.18	1.61-23.27
Reflections collected	3184	19794	9172
Data $F_o^2 > 3\sigma(F_o^2)$	1726	3826	4385
Parameters	124	451	397
R(%)	0.0674	0.0411	0.0371
R_w(%)	0.2067	0.0815	0.0979
Goodness of Fit	0.913	1.056	0.902

The data was collected at 20°C with Mo Kα radiation (λ = 0.71069 Å)

$R = \Sigma \, | \, |F_o| - |F_c| \, | \, / \, \Sigma \, |F_o|$, $R_w = [\Sigma(|F_o| - |F_c|)^2 / \Sigma \, |F_o|^2]^{0.5}$

Table 4.1 (continued): Crystallographic parameters for $TiCp^*(NP^tBu_2Bn)Cl_2$ (**4.13**), $TiCp^*(NPCy_2Bn)Cl_2$ (**4.14**), $TiCp(NPCy_2Bn)Cl_2$ (**4.16**).

	4.13	**4.14**	**4.16**
Molecular formula	$C_{25}H_{40}Cl_2NPTi$	$C_{29}H_{44}Cl_2NPTi$	$C_{24}H_{34}Cl_2NPTi$
Formula weight	504.35	556.42	486.28
a(Å)	9.743(6)	11.359(7)	11.660(6)
b(Å)	17.53(1)	16.38(1)	13.481(7)
c(Å)	16.13(1)	16.44(1)	15.984(8)
α(°)	90.00	90.00	90.00
β(°)	98.57(1)	103.67(1)	90.00
γ (°)	90.00	90.00	90.00
Crystal system	Monoclinic	Monoclinic	Orthorhombic
Space group	$P2_1/c$	$P2_1/c$	$P2_12_12_1$
Volume ($Å^3$)	2724(3)	2985(3)	2512(2)
D_{calc} (gcm^{-3})	1.230	1.238	1.286
Z	4	4	4
Abs coeff, μ, mm^{-1}	0.581	0.537	0.628
θ range (°)	2.32-23.19	2.22-23.34	1.98-23.21
Reflections collected	11282	12502	10691
Data $F_o^2 > 3\sigma(F_o^2)$	3307	3191	3219
Parameters	271	307	262
R(%)	0.0394	0.0331	0.0233
R_w(%)	0.1213	0.0878	0.0555
Goodness of Fit	1.114	1.015	0.982

The data was collected at 20°C with Mo Kα radiation (λ = 0.71069 Å)

$R = \Sigma \, | \, |F_o| - |F_c| \, | \, / \, \Sigma \, |F_o|$, $R_w = [\Sigma(|F_o| - |F_c|)^2 / \Sigma \, |F_o|^2]^{0.5}$

Table 4.1 (continued): Crystallographic parameters for *p*-$(CH_2PCy_2NTiCp^*Cl_2)_2C_6H_4$ (**4.18**), *p*-$(CH_2PCy_2NTiCpCl_2)_2C_6H_4$ (**4.20**), $TiCp^*(NP^tBu_2Bn)Me_2$ (**4.21**).

	4.18	**4.20**	**4.21**
Molecular formula	$C_{52}H_{82}Cl_4N_2P_2Ti_2$	$C_{44}H_{62}Cl_8D_4N_2P_2Ti_2$	$C_{27}H_{46}NPTi$
Formula weight	1034.714	1068.33	463.52
a(Å)	15.218(9)	8.974(5)	10.037(5)
b(Å)	24.24(1)	11.490(6)	19.06(1)
c(Å)	15.996(9)	14.905(8)	15.059(8)
α(°)	90.00	96.09(1)	90.00
β(°)	110.39(1)	105.085(9)	104.05(1)
γ (°)	90.00	112.20(1)	90.00
Crystal system	Monoclinic	Triclinic	Monoclinic
Space group	$P2_1/c$	P-1	$P2_1/c$
Volume ($Å^3$)	5530(5)	1337(1)	2794(3)
D_{calc} (gcm^{-3})	1.243	1.322	1.102
Z	4	2	4
Abs coeff, μ, mm^{-1}	0.574	0.789	0.376
θ range (°)	1.60-23.21	2.16-23.27	1.76-23.24
Reflections collected	22618	5717	11755
Data $F_o^2 > 3\sigma(F_o^2)$	5218	3019	3214
Parameters	559	262	271
R(%)	0.0546	0.0461	0.0408
R_w(%)	0.1515	0.1317	0.1209
Goodness of Fit	0.859	1.062	1.056

The data was collected at 20°C with Mo Kα radiation (λ = 0.71069 Å)

$R = \Sigma \, | \, |F_o| - |F_c| \, | \, / \, \Sigma \, |F_o|$, $R_w = [\Sigma(|F_o| - |F_c|)^2 / \Sigma \, |F_o|^2]^{0.5}$

Table 4.1 (continued): Crystallographic parameters for $TiCp^*(NPCy_2Bn)Me_2$ (**4.22**), $TiCp(NPCy_2Bn)Me_2$ (**4.24**), *p*-$(CH_2PCy_2NTiCp^*Me_2)_2C_6H_4$ (**4.26**).

	4.22	**4.24**	**4.26**
Molecular formula	$C_{31}H_{51}NPTi$	$C_{26}H_{40}NPTi$	$C_{68}H_{106}N_2P_2Ti_2$
Formula weight	516.60	445.46	1109.29
a(Å)	11.613(6)	11.729(7)	16.53(1)
b(Å)	16.468(8)	13.616(8)	17.11(1)
c(Å)	16.287(8)	16.206(9)	24.45(1)
α(°)	90.00	90.00	90.00
β(°)	102.618(9)	90.00	106.22(1)
γ (°)	90.00	90.00	90.00
Crystal system	Monoclinic	Orthorhombic	Monoclinic
Space group	$P2_1/c$	$P2_12_12_1$	$P2_1/c$
Volume ($Å^3$)	3040(3)	2588(3)	6639(7)
D_{calc} (gcm^{-3})	1.129	1.143	1.110
Z	4	4	4
Abs coeff, μ, mm^{-1}	0.352	0.404	0.327
θ range (°)	2.32-23.35	1.95-23.22	1.28-23.21
Reflections collected	12840	10620	27145
Data $F_o^2 > 3\sigma(F_o^2)$	3036	3103	2660
Parameters	307	262	667
R(%)	0.0417	0.0595	0.0510
R_w(%)	0.1119	0.1196	0.1084
Goodness of Fit	0.927	1.199	0.693

The data was collected at 20°C with Mo Kα radiation (λ = 0.71069 Å)

$R = \Sigma \, | \, |F_o| - |F_c| \, | \, / \, \Sigma \, |F_o|$, $R_w = [\Sigma(|F_o| - |F_c|)^2 / \Sigma \, |F_o|^2]^{0.5}$

Table 4.1 (continued): Crystallographic parameters for *p*-$(CH_2P^tBu_2NTiCpMe_2)_2C_6H_4$ (**4.27**), *p*-$(CH_2PCy_2NTiCpMe_2)_2C_6H_4$ (**4.28**·).

	4.27	**4.28**
Molecular formula	$C_{38}H_{66}N_2P_2Ti_2$	$C_{52}H_{80}N_2P_2Ti_2$
Formula weight	708.67	890.92
a(Å)	16.290(9)	8.794(5)
b(Å)	16.455(9)	9.772(5)
c(Å)	15.594(8)	16.678(9)
α(°)	90.00	77.21(1)
β(°)	100.86(1)	79.91(1)
γ (°)	90.00	68.50(9)
Crystal system	Monoclinic	Triclinic
Space group	$P2_1/c$	P-1
Volume ($Å^3$)	4105(4)	1293(1)
D_{calc} (gcm^{-3})	1.147	1.144
Z	4	1
Abs coeff, μ, mm^{-1}	0.493	0.404
θ range (°)	1.78-23.25	2.27-23.26
Reflections collected	17348	5554
Data $F_o^2 > 3\sigma(F_o^2)$	4621	3034
Parameters	397	262
R(%)	0.0378	0.0379
R_w(%)	0.1081	0.1080
Goodness of Fit	1.008	1.033

The data was collected at 20°C with Mo Kα radiation (λ = 0.71069 Å)

$R = \Sigma \, | \, |F_o| - |F_c| \, | \, / \, \Sigma \, |F_o|$, $R_w = [\Sigma(|F_o| - |F_c|)^2 / \Sigma \, |F_o|^2]^{0.5}$

4.2.10 Polymerization Protocol

Purification of reagents used in the polymerizations and a brief description of the reactor are detailed in Section 3.2.9.

(i-Procedure using a Schlenk flask apparatus with MAO activation) A Schlenk flask was charged with PhMe (50 mL) and MAO (500:1 Al:Ti ratio in PhMe), and the solution was presaturated with the monomer by briefly evacuating/backfilling (x 4) and then stirring under an atmosphere of C_2H_4 for 5 min. A PhMe solution of the catalyst precursor such that the resultant catalyst concentration was 350 μmol L^{-1} was injected, and the mixture was stirred at RT for 30 min. The reaction was quenched with 1 M HCl in MeOH, and the precipitated polymer was subsequently washed with HCl, HCl/MeOH and PhMe before drying at 50°C for at least 48 h prior to weighing.

(ii-Procedure using a Büchi reactor apparatus with MAO activation) A 1L Büchi glass autoclave was dried *in vacuo* (10^{-2} mmHg) for several hours. PhMe (500 mL) was transferred into the vessel under a positive pressure of N_2 and was heated to 30°C for at least 30 min. The temperature was controlled (to *ca.* ±2°C) with an external heating/cooling bath and was monitored by a jacketed thermocouple that extended into the polymerization vessel. The vessel was vented of N_2 and then pressurized with C_2H_4 (1.82 atm) while the solvent stirred at a rate of 1000 rpm. A solution of MAO (500:1 Al:Ti ratio in PhMe) was injected and the mixture was stirred for 5 min. A PhMe solution of the precatalyst such that the resultant catalyst concentration was 50 μmol L^{-1} was injected and the solution was stirred for the desired amount of time. Any recorded exotherm was within the allowed temperature differential of the heating/cooling system. The reaction was quenched by emptying the contents of the autoclave into *ca.* 200 mL of 1 M HCl in MeOH. The collection/treatment of the polymer was as described above.

(iii-Procedure using a Büchi reactor apparatus with $[Ph_3C][B(C_6F_5)_4]$ activation) The polymerization experiment was conducted in the same manner as described for MAO activation with the following modifications: a solution of T^iBAl (10:1 Al:Ti ratio in

PhMe) was injected and the mixture was stirred for 5 min. A PhMe solution of the precatalyst such that the resultant catalyst concentration was 50 μmol L^{-1} was injected, followed immediately by a PhMe solution of the activator (1, 2 or 4 equivalents), and the solution was stirred for the desired amount of time. Recorded exotherms were significant enough that they could not be adequately controlled using the heating/cooling system (typical temperature spikes *ca.* 10°C). The reaction was quenched by emptying the contents of the autoclave into *ca.* 200 mL of 1 M HCl in MeOH. The collection/treatment of the polymer was as described above.

The masses of reagents and polyethylene, in addition to the raw GPC data, may be viewed in Appendix D (on CD).

4.3 Results and Discussion

The phosphines R_2BnP (R = ^{t}Bu (**4.3**), Cy (**4.4**)) were prepared via a modification of a literature procedure[311] from the reaction of BnMgCl with $ClPR_2$ at low temperature (Figure 4.1). The related *para*-substituted aryl phosphines *p*-$(CH_2PR_2)_2C_6H_4$ (R = ^{t}Bu (**4.5**), Cy (**4.6**)) were prepared in good yields (typically 80-90%) in a similar manner to the *meta*-substituted versions as described in Section 3.2.4 (Figure 4.1),[271] without the impediment of the persistent by-product NEt_3·HBr (*vide supra*). Spectroscopic data confirmed the presence of the desired products, and *p*-$(CH_2P^tBu_2)_2C_6H_4$ (**4.5**) was further characterized by X-ray crystallography (Figure 4.2). All phosphines were readily oxidized to the corresponding trimethylsilyl-phosphinimines from reaction with excess Me_3SiN_3 (Figure 4.1). The phosphinimines were characterized spectroscopically, and in both cases where R = ^{t}Bu, an upfield shift in the $^{31}P\{^1H\}$ NMR spectra of *ca.* 10 ppm was observed relative to the parent phosphines, in contrast to a downfield shift of *ca.* 10 ppm where R = Cy. X-ray crystallographic analyses of the cyclohexyl derivatives also confirmed the successful oxidation (Figure 4.2). The P-N bond distances of 1.543(2), 1.540(2) and 1.544(2) Å, and the Si-N bond distances of 1.658(2), 1.656(2) and 1.669(2) Å for $Cy_2BnPNSiMe_3$ (**4.8**) and *p*-$(CH_2PCy_2NSiMe_3)_2C_6H_4$ (**4.10**) (latter 2 values),

respectively, are representative of typical trimethylsilyl-phosphinimine compounds.[315,316] The syntheses of *p*-$(CH_2PR_2NH)_2C_6H_4$ (R = ^{t}Bu (**4.11**), Cy (**4.12**)) from reaction of the appropriate trimethylsilyl-phosphinimine precursor with methanol was also feasible, although where R = Cy, isopropanol proved to be a better choice of reagent to avoid oxide impurities.

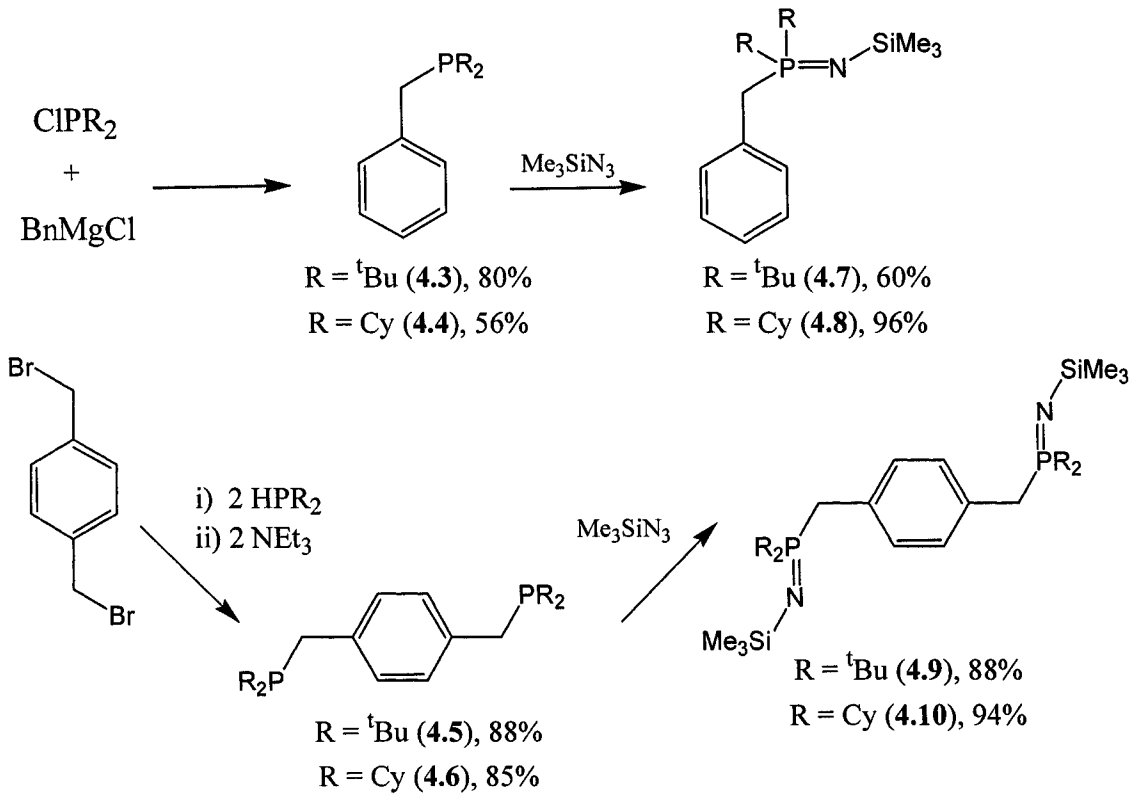

Figure 4.1: Synthesis of R_2BnP and *p*-$(CH_2PR_2)_2C_6H_4$, and their trimethylsilyl-phosphinimine derivatives.

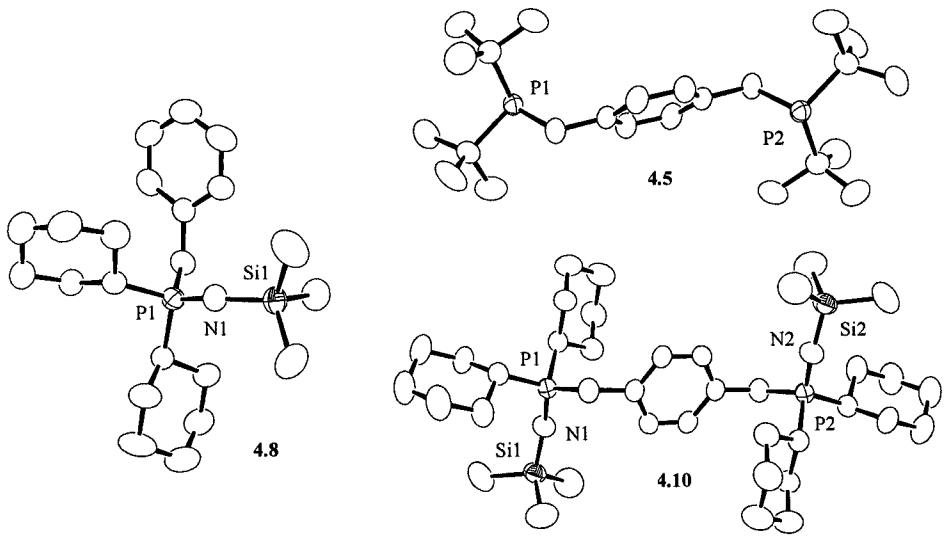

Figure 4.2: ORTEP drawings of *p*-$(CH_2P^tBu_2)_2C_6H_4$ (**4.5**), $Cy_2BnPNSiMe_3$ (**4.8**) and *p*-$(CH_2PCy_2NSiMe_3)_2C_6H_4$ (**4.10**) (50% thermal ellipsoids).

The bimetallic titanium complexes *p*-$(CH_2PR_2NTiCp'Cl_2)_2C_6H_4$ (Cp' = C_5Me_5 (Cp*), R = ^{t}Bu (**4.17**), Cy (**4.18**); Cp' = C_5H_5 (Cp), R = ^{t}Bu (**4.19**), Cy (**4.20**)) were attained upon liberation of Me_3SiCl by metathesis of the trimethylsilyl-phosphinimines with two equivalents of the appropriate $TiCp'Cl_3$ precursor (Figure 4.3).[131] A similar approach was exploited by Bochmann and co-workers to prepare the related bimetallic complexes *m*-$(PPh_2NTiCp^*Cl_2)_2C_5H_3N$ (**I**) and $(CH_2PPh_2NTiCp^*Cl_2)_2$ (**II**),[24] and by Cavell and co-workers to prepare $CH_2(PR_2NTiCp^*Cl_2)_2$ (R = Me, Ph, Cy, **III**) (Figure 4.4).[269] The bimetallic tetrachloride complexes **4.17-4.20** were relatively insoluble in aromatic solvents such as benzene or toluene, which necessitated spectroscopic characterization to be performed in CD_2Cl_2 solvent in several cases. The solubility increases if Cp* is replaced by Cp, or if cyclohexyl groups replace the *t*-butyl groups. For all derivatives, only one set of signals is observed in the ^{1}H NMR spectrum representing each of the aryl, Cp, benzyl and alkyl protons. This is as expected, due to the inherent symmetry of the molecule in solution, in addition to the freedom of rotation of the benzyl portion of the compounds. X-ray crystallography confirmed the bimetallic nature of the cyclohexyl derivatives (see Figure 4.5 for an ORTEP depiction of one

example), although attempts to grow X-ray quality crystals of the *t*-butyl analogues were unfortunately unsuccessful. Key bond distances and angles are summarized in Table 4.2.

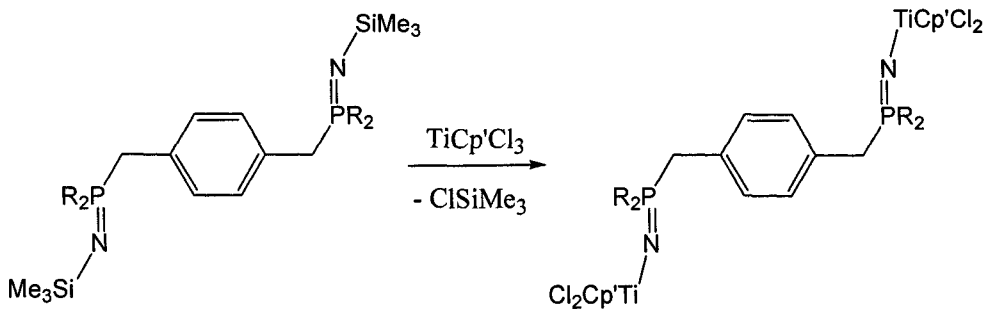

R = ^{t}Bu (**4.9**)
R = Cy (**4.10**)

Cp' = Cp*
R = ^{t}Bu (**4.17**), 95%; Cy (**4.18**), 79%
Cp' = Cp
R = ^{t}Bu (**4.19**), 95%; Cy (**4.20**), 95%

Figure 4.3: Synthesis of bimetallic titanium complexes, *p*-$(CH_2PR_2NTiCp'Cl_2)_2C_6H_4$.

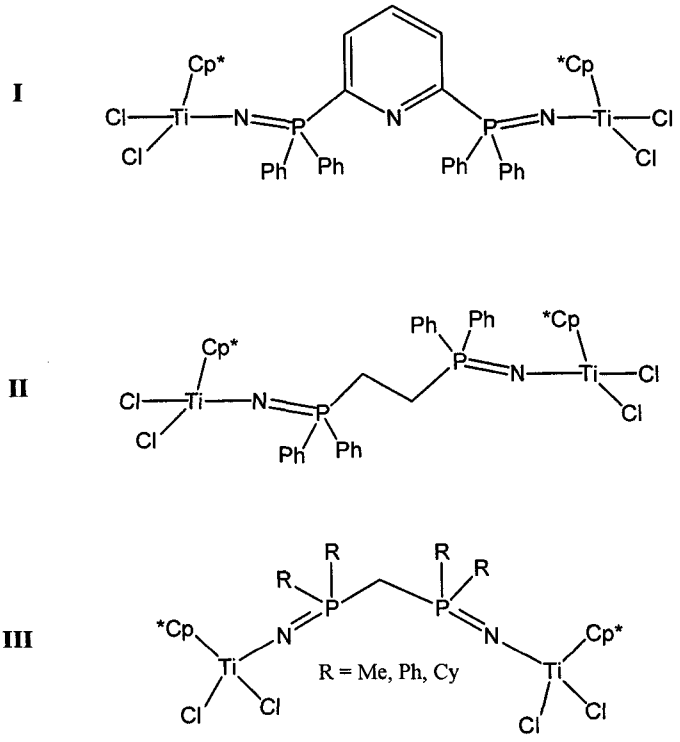

Figure 4.4: Related bimetallic phosphinimide complexes.[24,269]

The monometallic versions, $TiCp'(NPR_2Bn)Cl_2$ (Cp' = Cp*, R = ^{t}Bu (**4.13**), Cy (**4.14**); Cp' = Cp, R = ^{t}Bu (**4.15**), Cy (**4.16**)), were synthesized using the desired trimethylsilyl-phosphinimine precursor in high yields (77-93%), but conveniently, heating was not required to ensure complete reaction. Spectroscopy and X-ray data confirmed the formulated structures for all cases. It must be noted that the crystal structure of $TiCp(NP^tBu_2Bn)Cl_2$ (**4.15**) was previously determined by Dr. Fred Guérin in collaboration with NOVA Chemicals Inc. All key bond distances and angles were similar to those obtained from the comparable bimetallic derivatives (Table 4.2, see Figure 4.5 for an ORTEP depiction of one example), and related structures previously reported in the literature.[8,24,131,138]

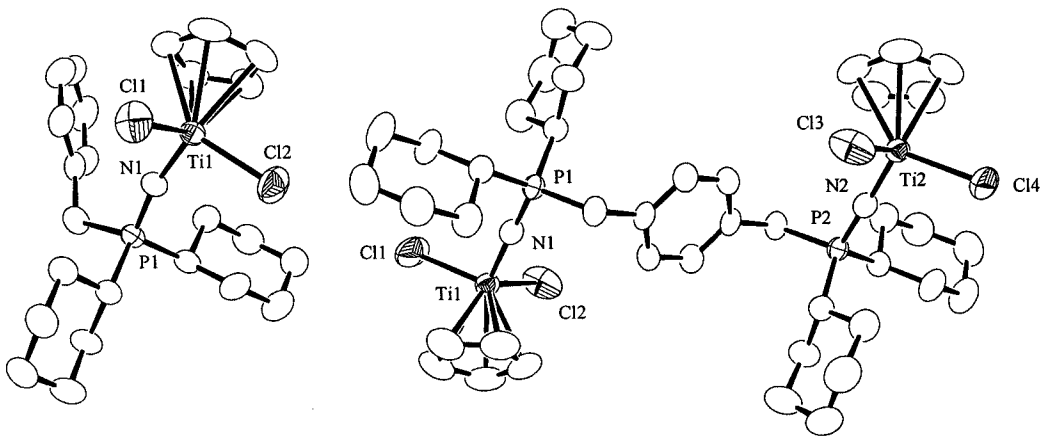

4.16 **4.20**

Figure 4.5: ORTEP illustrations of $TiCp(NPCy_2Bn)Cl_2$ (**4.16**) and *p*-$(CH_2PCy_2NTiCpCl_2)_2C_6H_4$ (**4.20**) (CH_2Cl_2 molecule omitted for clarity), representative of a bimetallic complex and its related monometallic analogue (50% thermal ellipsoids).

Table 4.2: Key bond distances and angles for available data from X-ray analysis of *p*-$(CH_2PR_2NTiCp'X_2)_2C_6H_4$ and $TiCp'(NPR_2Bn)X_2$.

Compound	Ti-X Å	Ti-N Å	N-P Å	Ti-NP °
$TiCp^*(NP^tBu_2Bn)Cl_2$ (**4.13**)	2.322(1) 2.324(1)	1.786(2)	1.598(2)	167.6(1)
$TiCp^*(NPCy_2Bn)Cl_2$ (**4.14**)	2.317(1) 2.309(1)	1.776(2)	1.594(2)	157.3(1)
$TiCp(NP^tBu_2Bn)Cl_2$ (**4.15**)[a]	2.3072(9) 2.3091(8)	1.760(2)	1.599(2)	175.2(1)
$TiCp(NPCy_2Bn)Cl_2$ (**4.16**)	2.312(1) 2.314(1)	1.765(2)	1.607(2)	168.4(1)
p-$(CH_2PCy_2NTiCp^*Cl_2)_2C_6H_4$ (**4.18**)	2.312(2) 2.328(2) 2.305(2) 2.317(2)	1.786(5) 1.768(5)	1.589(5) 1.602(5)	157.1(3) 162.6(3)
p-$(CH_2PCy_2NTiCpCl_2)_2C_6H_4$ (**4.20**)	2.303(2) 2.323(1)	1.764(3)	1.608(3)	172.7(2)
$TiCp^*(NP^tBu_2Bn)Me_2$ (**4.21**)	2.164(3) 2.228(3)	1.830(2)	1.580(2)	172.6(2)
$TiCp^*(NPCy_2Bn)Me_2$ (**4.22**)	2.136(3) 2.152(3)	1.811(2)	1.570(2)	162.8(2)
$TiCp(NPCy_2Bn)Me_2$ (**4.24**)	2.131(6) 2.130(6)	1.804(4)	1.579(4)	168.1(3)
p-$(CH_2PCy_2NTiCp^*Me_2)_2C_6H_4$ (**4.26**)	2.119(7) 2.145(6) 2.160(6) 2.155(6)	1.829(5) 1.813(5)	1.573(5) 1.582(5)	163.4(4) 161.5(4)
p-$(CH_2P^tBu_2NTiCpMe_2)_2C_6H_4$ (**4.27**)	2.137(3) 2.143(3) 2.124(3) 2.130(4)	1.806(2) 1.802(2)	1.582(2) 1.581(2)	171.0(1) 173.9(2)
p-$(CH_2PCy_2NTiCpMe_2)_2C_6H_4$ (**4.28**)	2.160(3) 2.191(3)	1.806(2)	1.580(2)	167.8(1)

a) Structure was determined by Dr. Fred Guérin in collaboration with NOVA Chemicals Inc.

Methylation of all the titanium chloride complexes was readily achieved from the use of MeMgBr at ambient temperature. In this manner, $TiCp'(NPR_2Bn)Me_2$ (Cp' = Cp*, R = ^{t}Bu (**4.21**), Cy (**4.22**); Cp' = Cp, R = ^{t}Bu (**4.23**), Cy (**4.24**)) and *p*-$(CH_2PR_2NTiCp'Me_2)_2C_6H_4$ (Cp' = Cp*, R = ^{t}Bu (**4.25**), Cy (**4.26**); Cp' = Cp, R = ^{t}Bu

(**4.27**), Cy (**4.28**)) were prepared in moderate to good yields (Figure 4.6). Without exception, methylation of the titanium centre(s) resulted in an upfield shift of the signal in the ^{31}P NMR spectra relative to the di- or tetrachloride precursors, and an upfield shift for the Cp ligand ^{1}H and $^{13}C\{^{1}H\}$ resonances (Table 4.3). This correlates well with increased electron density at the titanium centre(s) upon exchange of chloride ligands for methyl groups. Several of the methyl derivatives were characterized by X-ray crystallography (Table 4.2). In all cases, the titanium-nitrogen phosphinimide bond length increased upon substitution with methyl groups, which is also consistent with a more electron-rich metal centre; this observation may be interpreted as the phosphinimide ligand donating slightly less electron density to the titanium atom.[138,315]

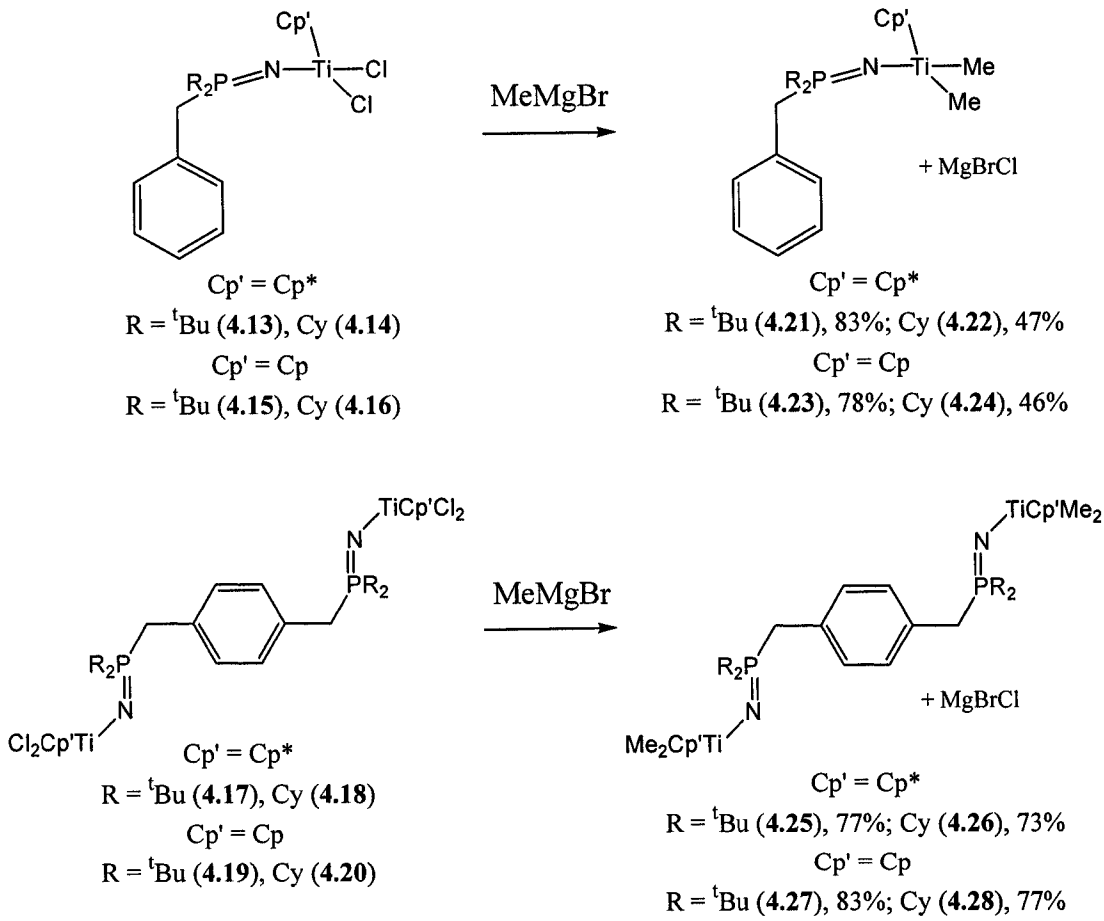

Figure 4.6: Syntheses of *p*-$(CH_2PR_2NTiCp'Me_2)_2C_6H_4$ and $TiCp'(NPR_2Bn)Me_2$.

Table 4.3: Comparison of NMR shifts (ppm) for *p*-$(CH_2PR_2NTiCp'X_2)_2C_6H_4$ and $TiCp'(NPR_2Bn)X_2$.[a]

Compound	Cp ^1H	Cp $^{13}C\{^1H\}$	$^{31}P\{^1H\}$
$TiCp^*(NP^tBu_2Bn)Cl_2$ (**4.13**)	2.21	125.9, 13.1	35.3
$TiCp^*(NPCy_2Bn)Cl_2$ (**4.14**)	2.20	125.9, 13.2	23.0
$TiCp(NP^tBu_2Bn)Cl_2$ (**4.15**)	6.22	115.5	34.9
$TiCp(NPCy_2Bn)Cl_2$ (**4.16**)	6.38	115.2	24.3
p-$(CH_2P^tBu_2NTiCp^*Cl_2)_2C_6H_4$ (**4.17**)	2.14[b]	123.2, 8.9[b]	37.2[b]
p-$(CH_2PCy_2NTiCp^*Cl_2)_2C_6H_4$ (**4.18**)	2.24	125.8, 13.2	22.4
p-$(CH_2P^tBu_2NTiCpCl_2)_2C_6H_4$ (**4.19**)	6.29[b]	116.0[b]	38.7[b]
p-$(CH_2PCy_2NTiCpCl_2)_2C_6H_4$ (**4.20**)	6.39	115.7	27.0
$TiCp^*(NP^tBu_2Bn)Me_2$ (**4.21**)	2.03	118.5, 12.2	21.4
$TiCp^*(NPCy_2Bn)Me_2$ (**4.22**)	2.08	118.5, 12.3	8.4
$TiCp(NP^tBu_2Bn)Me_2$ (**4.23**)	6.08	111.1	21.6
$TiCp(NPCy_2Bn)Me_2$ (**4.24**)	6.18	110.8	10.2
p-$(CH_2P^tBu_2NTiCp^*Me_2)_2C_6H_4$ (**4.25**)	2.12	118.4, 12.3	22.0
p-$(CH_2PCy_2NTiCp^*Me_2)_2C_6H_4$ (**4.26**)	2.10	122.3, 11.9	8.0
p-$(CH_2P^tBu_2NTiCpMe_2)_2C_6H_4$ (**4.27**)	6.18	110.9	22.6
p-$(CH_2PCy_2NTiCpMe_2)_2C_6H_4$ (**4.28**)	6.22	110.8	10.0

a) C_6D_6 solvent unless otherwise noted.

b) CD_2Cl_2 solvent.

Generation of the zwitterion $[TiCp^*(NP^tBu_2Bn)Me][MeB(C_6F_5)_3]$ (**4.29**) was achieved by reaction of an equimolar amount of the dimethyl precursor with the strong Lewis acid $B(C_6F_5)_3$. When this synthesis is performed, it is key that the two precursors are dissolved in meticulously dry solvent *separately* to give clear solutions. Upon combining at ambient temperature, the desired product is occasionally plagued by persistent side-products, reflecting the extreme sensitivity of this zwitterion to the reaction conditions. Further, the cation decomposes (*ca.* 40% in 12 hours) to unidentified

products if left in methylene chloride solution under an inert atmosphere. Interestingly, the signals of the benzyl aromatic ring broadened in the ^{1}H NMR spectrum relative to the titanium dimethyl precursor, and the two *t*-butyl groups gave rise to individual doublets upon formation of the tight ion-pair. In addition, two distinct signals for Ti-C**H**$_3$ (0.89 ppm) and Ti-C**H**$_3$-B(C_6F_5)$_3$ (0.48 ppm) were observed in the ^{1}H NMR spectrum, a phenomenon that has been observed in the related complex [TiCp(NP^{t}Bu$_2$$C_6H_4$*o*Ph)Me][MeB($C_6F_5$)$_3$], but not [TiCp(NP^{t}Bu$_3$)Me][MeB(C_6F_5)$_3$].[8, xi] A satisfactory CHN microanalysis of the yellow foam attested to its purity, since X-ray quality crystals were unfortunately not obtained. All attempts to prepare mono- or di-zwitterionic complexes from the bimetallic titanium precursors were unsuccessful, resulting only in intractable mixtures.

Utility as Ethylene Polymerization Catalysts

Initially, polymerization experiments were conducted employing Schlenk-line conditions, namely using an atmospheric pressure of ethylene, room temperature and 50 mL of toluene in a Schlenk flask. By performing the polymerization experiments over a 30 minute period, it was possible to obtain a catalyst activity that reflected the polymerization behaviour over time, rather than just the first few minutes, which often gives artificially high values. All polymerization experiments were performed at least in duplicate until the activities were within reasonable experimental error. The polymer yields were obtained by precipitating the product with hydrogen chloride solution in methanol, and drying the polymer to a constant weight.

Several factors must be taken into consideration when examining these, or any, polymerization results. It is imperative that the activity units are carefully scrutinized, since they may be easily manipulated to obtain seemingly high polymerization activities. For example, if higher pressures of ethylene gas are used and not accounted for, inflated polymerization activities will result. For this reason, all activities in this thesis are reported in grams of polymer that are obtained per millimole of precatalyst, per hour, per

[xi] J. E. Kickham, unpublished results.

atmosphere of ethylene (g $mmol^{-1}$ h^{-1} atm^{-1}, Equation 4.1). For convention, the catalytic activity will be rated relative to Gibson's scale (Table 4.4).[32] Other factors that influence polymerization activity include the rate of stirring, temperature, solvent employed, size of the vessel, and most importantly, the selection and concentration of scrubber and/or activator.[xii, 40,317] In particular, even if the same source of aluminum reagent (MAO, methylaluminoxane) is employed, the age of the activator influences the polymerization numbers obtained, since MAO is notorious for decomposing during storage over time.[40,318,319] In addition, since the exact composition of MAO remains to be unequivocally identified,[95] even different batches from the same company may possess slightly different properties.[319] Thus, the reader is cautioned that although exhaustive efforts have been undertaken to acquire strictly reproducible results, this is not always possible, and the values reported herein represent an average description of polymerization activity and polymer product. In all cases, the activity is compared to the industrially accepted standard, zirconocene dichloride or dimethyl. This is a common practice since it is commercially available or readily synthesized, and acts as a very active olefin polymerization catalyst upon activation with many Lewis acids, including MAO, $B(C_6F_5)_3$, $[Ph_3C][B(C_6F_5)_4]$, and other similar reagents.

Table 4.4: Gibson's rating for catalytic performance of ethylene polymerization catalysts.[32]

Catalyst Evaluation	**Activity (g $mmol^{-1}$ h^{-1} atm^{-1})**
Very low	<1
Low	1-10
Moderate	10-100
High	100-1000
Very High	>1000

[xii] C. L. Beddie, unpublished results.

$$\text{Polymerization Activity} = \frac{\text{g polymer}}{\text{(mmol catalyst) (hour) (atm ethylene)}} = \text{g mmol}^{-1}\text{h}^{-1}\text{atm}^{-1}$$

Equation 4.1: Polymerization activity units.

Initial results from the Schlenk-line polymerizations indicate that *p*-$(CH_2PR_2NTiCp'X_2)_2C_6H_4$ and $TiCp'(NPR_2Bn)X_2$ display moderate to high catalytic activity for ethylene polymerization upon activation with MAO (Table 4.5). The polymerization activity is directly proportional to the size of the phosphinimide ligand; more polymer is generated upon increasing the size of the groups on the phosphorus atom. This result is in agreement with other cases that exploit increased steric bulk on the phosphinimide ligand to afford more active Group IV olefin polymerization catalysts upon activation with MAO.[12,21] In addition, as Cp is changed to Cp*, the activity also increases for each ligand set. This is consistent with calculations and experimental observations that demonstrate increased electron density provided by a Cp* group effects an increase in polymerization rate.[105,320-323] Finally, the monomeric analogues are more active than their bimetallic counterparts. Possible explanations for this observation are that the bimetallic derivatives are less soluble in toluene, or that they are more prone to entanglement in the growing polymer chain. Unfortunately, the precise reasons remain unclear.

Table 4.5: Schlenk-line polymerization results.[a]

Precatalyst	Activity	M_n	M_w	PDI[b]
$TiCp^*(NP^tBu_2Bn)Cl_2$ (**4.13**)	42	53,800	234,100	4.35
p-$(CH_2P^tBu_2NCp^*TiCl_2)_2C_6H_4$ (**4.17**)	18	24,200	131,100	5.42
p-$(CH_2PCy_2NCp^*TiCl_2)_2C_6H_4$ (**4.18**)	<1	c	c	c
p-$(CH_2P^tBu_2NCpTiCl_2)_2C_6H_4$ (**4.19**)	10	3,150	15,200	4.83
p-$(CH_2PCy_2NCpTiCl_2)_2C_6H_4$ (**4.20**)	<1	c	c	c
$TiCp^*(NP^tBu_2Bn)Me_2$ (**4.21**)	165	58,000	117,400	2.02
p-$(CH_2P^tBu_2NCp^*TiMe_2)_2C_6H_4$ (**4.25**)	48	84,400	138,700	1.64
p-$(CH_2PCy_2NCp^*TiMe_2)_2C_6H_4$ (**4.26**)	34	d	d	d
p-$(CH_2P^tBu_2NCpTiMe_2)_2C_6H_4$ (**4.27**)	20	17,600	38,100	2.16
p-$(CH_2PCy_2NCpTiMe_2)_2C_6H_4$ (**4.28**)	6	270,600	536,500	1.98
$ZrCp_2Cl_2$	200	14,000	35,600	2.54
$ZrCp_2Me_2$	470	18,500	55,800	3.02

a) MAO activation, Ti/Zr:Al ratio 1:500, PhMe solvent, 25°C, 1 atm C_2, 350 μM precatalyst, 30 min, M_n and M_w in g mol^{-1}, Activity in units of g $mmol \cdot Ti^{-1}h^{-1}atm^{-1}$.

b) Average PDI reported.

c) Too little polymer to analyze.

d) Polymer would not dissolve in 1,2,4-trichlorobenzene.

In order to determine the polymerization activities under more controlled polymerization conditions, the experiments were repeated in a Büchi reactor. The temperature was maintained at 30 ±2°C, and the polymerizations were conducted under more dilute concentrations (50 μmol L^{-1}), and higher ethylene pressure (1.82 atm; *vide infra*). Even when the additional ethylene pressure is taken into consideration (Equation 4.1), all polymerization activities are higher, probably a reflection of the lower precatalyst concentrations. The same general trends occur as for the Schlenk-line experiments: namely that the Cp* complexes are more active than the corresponding Cp derivatives, and the *t*-butyl groups on the phosphorus atom generate more active species then the cyclohexyl versions (Table 4.6). These results compare well relative to

$(CH_2PPh_2NTiCp^*Cl_2)_2$, which displays only moderate activity when activated with MAO.[24] Perhaps the most interesting feature of these systems became evident upon gel permeation chromatography (GPC) analysis of the polymer products.

Table 4.6: Büchi reactor polymerization results.[a]

Precatalyst	Activity[b]	M_n	M_w	PDI[c]
$TiCp^*(NP^tBu_2Bn)Cl_2$ (**4.13**)	142	85,700	239,800	2.80
p-$(CH_2P^tBu_2NCp^*TiCl_2)_2C_6H_4$ (**4.17**)	75	101,000	319,200	3.16
p-$(CH_2PCy_2NCp^*TiCl_2)_2C_6H_4$ (**4.18**)	14	d	d	d
p-$(CH_2P^tBu_2NCpTiCl_2)_2C_6H_4$ (**4.19**)	23	30,100	143,300	4.76
p-$(CH_2PCy_2NCpTiCl_2)_2C_6H_4$ (**4.20**)	13	568,800	1,104,000	1.94
$TiCp^*(NP^tBu_2Bn)Me_2$ (**4.21**)	276	197,100	628,400	3.19
p-$(CH_2P^tBu_2NCp^*TiMe_2)_2C_6H_4$ (**4.25**)	43	241,900	468,600	1.94
p-$(CH_2PCy_2NCp^*TiMe_2)_2C_6H_4$ (**4.26**)	46	d	d	d
p-$(CH_2P^tBu_2NCpTiMe_2)_2C_6H_4$ (**4.27**)	23	19,500	195,200	10.01
p-$(CH_2PCy_2NCpTiMe_2)_2C_6H_4$ (**4.28**)	10	420,300	1,416,000	3.37
$ZrCp_2Cl_2$	610	161,100	340,800	2.12

a) MAO activation, Ti/Zr:Al ratio 1:500, PhMe solvent, 30°C, 1.82 atm C_2[b], 50 μM precatalyst, 30 min, M_n and M_w in g mol^{-1}.

b) Normally, the activity would be reported in units of g $mmol{\cdot}Ti^{-1}h^{-1}atm^{-1}$. Due to a clogged purification column, the steady-state pressure of ethylene was likely not 1.82 atm (*vide infra*), and these numbers are likely underestimated. These results, including the standard $ZrCp_2Cl_2$, were reproducible prior to maintenance of the column and therefore the *relative* activities are still valid.

c) Average PDI reported.

d) Polymer would not dissolve in 1,2,4-trichlorobenzene.

It is advantageous at this time to briefly summarize the information that can be gleaned from GPC analysis of polymer materials. All samples were prepared by obtaining a homogeneous fraction of polymer. The sample is dissolved in 1,2,4-trichlorobenzene at high temperatures, filtered, and processed through the GPC

instrument. As indicated in Table 4.5 and 4.6, some of the polymer samples could not be handled by this method. During the chromatography, the larger polymer molecules elute first, since the smaller molecules take a longer period of time to pass through the column. The elution times are compared to a standard graph that is generated using samples of precise molecular weight. The ultimate result is a graph (Figure 4.7) that exhibits the logarithm of the molecular weight *vs.* the change of the polymer weight divided by the change of the logarithm of the molecular weight. Recall that the purpose of this analysis is to determine several features of the polymer distribution; in particular, number molecular weight (M_n in g mol^{-1}), weight averaged molecular weight (M_w in g mol^{-1}), and polydispersity index (PDI) (Equations 4.2.a-c). The PDI, a value which may not be lower than 1.00, is an indication of how monodisperse the polymer sample is. Typically, single-site catalysts produce polymer materials that possess narrow polydispersities (*ca.* 2),[145] although often multimodal products are desired for their relative ease of processing or distinct physical properties.

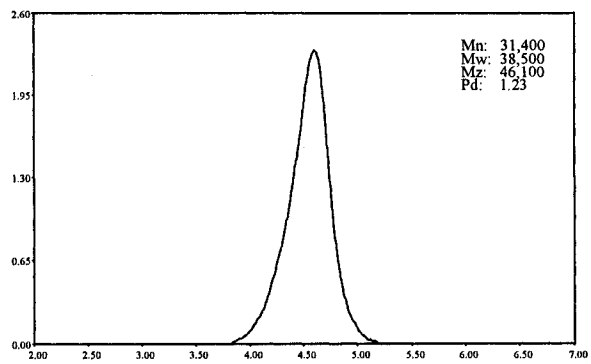

Figure 4.7: Differential molecular weight distribution of a monodisperse polymer sample.

$$M_n = \frac{\Sigma N_i M_i}{\Sigma N_i} \qquad M_w = \frac{\Sigma N_i M_i M_i}{\Sigma N_i M_i} \qquad PDI = \frac{M_w}{M_n}$$

N_i number of molecules of fraction i

M_i mass of molecules of fraction i

Equation 4.2.a-c: Statistical equations for M_n, M_w (g mol^{-1}) and PDI.

Inspection of the results from the GPC data indicated several features about this series of catalyst systems (Table 4.5 and 4.6). The bimetallic precatalysts *p*-$(CH_2PCy_2NTiCp'X_2)_2C_6H_4$ (**4.18**, **4.20**, **4.26**, **4.28**) generated very high molecular weight polyethylene (M_w = 500,000 – 1,100,000 g mol^{-1}) upon activation with MAO. The PDI values are narrow (< 2) relative to the other bimetallic catalysts that have *t*-butyl groups on the phosphorus atom. In several cases, the polymer could not be dissolved in the mobile phase for analysis, which may indicate that the materials possess extremely high molecular weights. Given the relatively low polymerization activities relative to the other catalysts, this data is characteristic, since poor ethylene polymerization catalysts often give high molecular weight polymer. Whether this is the result of a single catalytic titanium centre, or two centres that have been simultaneously activated remains unclear.

When the data from the Büchi reactor are compared to the data obtained from the Schlenk experiments, all of the polymerization activities and the molecular weights are higher. A number of factors may account for this difference in activity: in the Büchi reactor, the temperature and ethylene pressure was higher, and the catalyst concentration greatly reduced (from 350 to 50 μmol L^{-1}). In addition, it is important to note that the polymerization activities for $TiCp^*(NP^tBu_2Bn)X_2$, 100-200 g $mmol^{-1}h^{-1}atm^{-1}$, relative to $ZrCp_2X_2$, 600-700 g $mmol^{-1}h^{-1}atm^{-1}$, (X = Cl, Me) seem respectable, however, it is likely that the zirconocene standards possess polymerization rates that are ethylene diffusion limited at these catalyst concentrations. A flow of ethylene was noted for the zirconocene standards over the entire 30 minute period of the experiment, however, no ethylene flow was observed after a 5-10 minute period when the titanium phosphinimide

complexes were used. Therefore, initial polymerization rates for these catalysts are likely much higher, although the reported activities reflect their overall effectiveness over an extended period of time.

In several cases, large average PDI values of 5-10 were observed. Simple visual inspection (Figure 4.8) of the GPC trace confirms that the polymer has a bimodal molecular weight distribution when *p*-$(CH_2P^tBu_2NTiCpMe_2)_2C_6H_4$ (**4.27**) was employed as a catalyst precursor. This is an interesting result, since in some cases, it is highly desirable to produce materials that possess a bimodal molecular weight distribution. A variety of methods have been reported by other research groups to achieve this result.[159,287-301] Based on these results, it appears that employing a bimetallic catalyst precursor could be a beneficial approach to producing these types of polymer materials, since ideally, no additional engineering tasks such as the use of tandem reactors, addition of hydrogen or mechanical blending would be required.

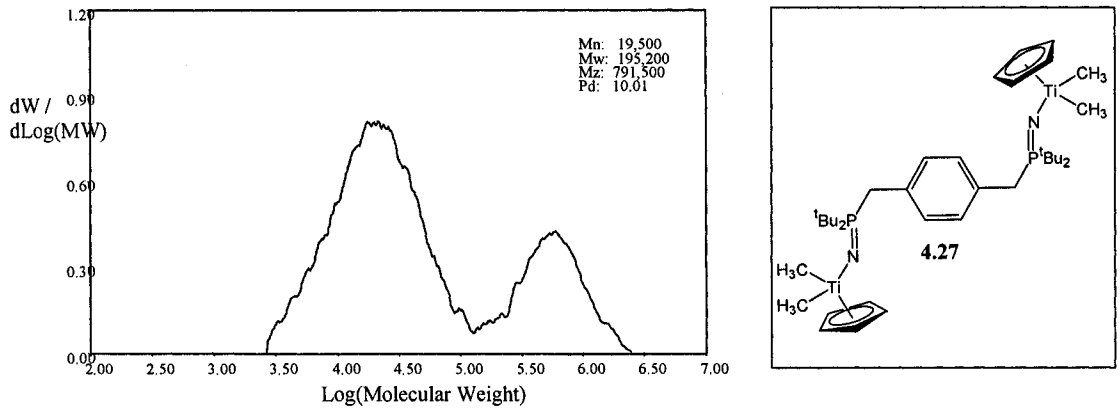

Figure 4.8: Bimodal distribution of polymer generated from MAO activation of *p*-$(CH_2P^tBu_2NTiCpMe_2)_2C_6H_4$ (**4.27**).

Not all of the polymeric materials produced displayed such an obvious distribution of molecular weights. When the plastic that was produced from the most active bimetallic complex of the series, *p*-$(CH_2P^tBu_2NTiCp^*Cl_2)_2C_6H_4$ (**4.17**), was assessed by GPC, a more subtle bimodal molecular weight distribution was observed (blue trace, Figure 4.9). Interestingly, the polymer derived from the related monometallic

derivative $TiCp^*(NP^tBu_2Bn)Cl_2$ (**4.13**) had a molecular weight distribution that appeared to be the same as one of the polymer distributions that was produced from the bimetallic analogue (red trace, Figure 4.9). This seems remarkable and offers a possible explanation for the observation of a bimodal distribution when the bimetallic catalysts are used. A straightforward explanation could be that one of the titanium sites on the bimetallic precatalyst is being activated in a similar fashion to the titanium centre of the monometallic analogue. This appears to be responsible for the lower molecular weight fraction of the polymer. The second titanium centre of the bimetallic precursor would be activated under different conditions, namely before or after the other metal centre. If this theory is reasonable, it would seem likely the other titanium centre would be activated *after* the centre responsible for the lower molecular weight fraction. By having additional polymer around the other titanium centre, it may serve as a significantly large ligand (Figure 4.10), thus permitting the active catalyst to facilitate the production of higher molecular weight polymer. This rationale is based on the precedence that phosphinimide ligands tend to perform better on Group IV olefin polymerization catalysts when a larger scaffold exists, presumably to protect the nitrogen atom from attack and subsequent catalyst deactivation by the Lewis acid activators.[16,18,21,234]

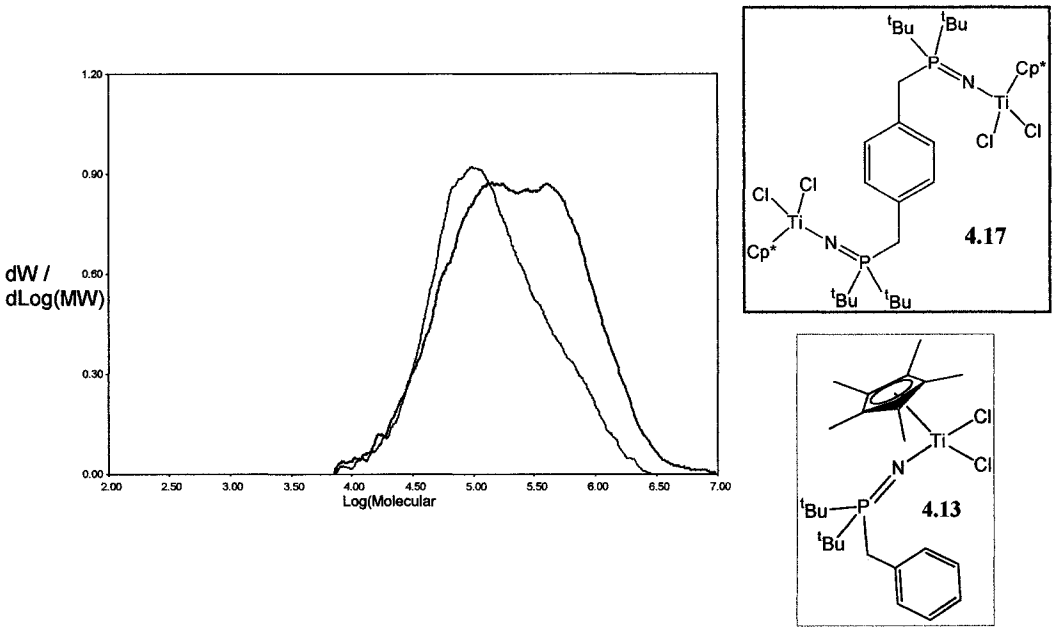

Figure 4.9: A comparison of the polymer that was produced from catalysts derived from *p*-$(CH_2P^tBu_2NTiCp^*Cl_2)_2C_6H_4$ (**4.17**) and its monometallic derivative $TiCp^*(NP^tBu_2Bn)Cl_2$ (**4.13**).

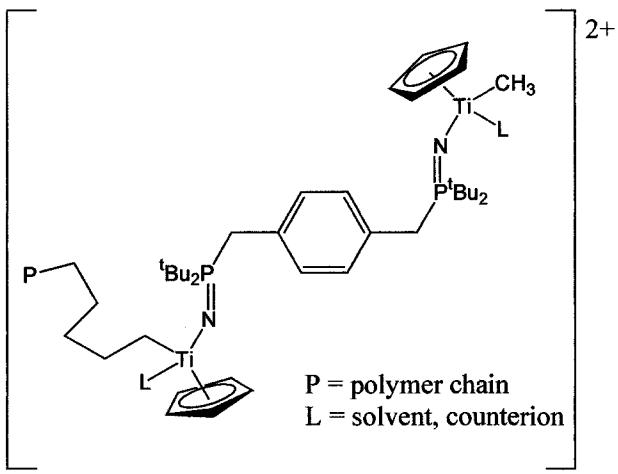

Figure 4.10: Possible scenario of the polymer functioning as a large ancillary ligand of an active titanium polymerization catalyst.

In an unfortunate demonstration of the sensitivity of the catalyst to polymerization conditions, subsequent reproduction of the polymerization experiments afforded different polymer products. The two factors that had been altered were the MAO source and the

ethylene flow. The ethylene flow, previously dampened by a clogged gas purification column, was increased to maintain the operating conditions at a steady-state pressure of 1.82 atmospheres. When the monometallic analogues were subjected to the "same" polymerization conditions, the result was a polymer that possessed a broader molecular weight distribution. These results were deemed reproducible under the altered conditions after several GPC analyses of polymers generated from several identical polymerization experiments were conducted. Of interest from this series of polymerization testing results was the initial appearance of a higher molecular weight fraction that accumulated over time (Figure 4.11). This behaviour is remarkably similar to the pattern that is produced by the bimetallic analogues, and may suggest that the active catalyst undergoes some sort of transformation through the course of the polymerization. For example, Bochmann and co-workers have observed that the methylene protons of $(CH_2PPh_2NTiCp^*Cl_2)_2$ are acidic enough to be activated by the titanium centre.[24] It is probable that the benzylic protons are subject to similar pathways, even if by an intermolecular process. This process may account for the bimodal polymer distributions generated from the monometallic or bimetallic catalyst precursors.

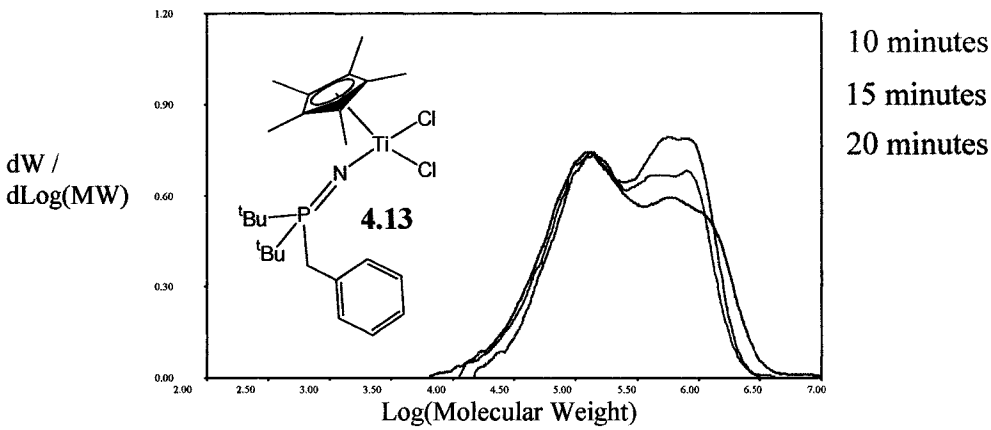

Figure 4.11: Monitoring the molecular weight distribution over time of the polymer produced by $TiCp^*(NP^tBu_2Bn)Cl_2$ (**4.13**) upon activation with MAO.

The Büchi polymerization experiments for $TiCp^*(NP^tBu_2Bn)X_2$ (X = Cl (**4.13**), Me (**4.21**)) were also monitored over time for relative activity (Table 4.7). It appears as although the activities are nearly the same whether the dimethyl or dichloride precursors are employed. This indicates that methyl-for-chloride exchange of the dichloride precursor occurs rapidly with MAO. In addition, as the polymerization progresses over time, the rate of polymerization decelerates. Due to the amount of polymer material that was recovered (in excess of 10 grams), it is possible that the catalyst is not being sufficiently saturated with ethylene, since when large polymer masses are produced in the Büchi reactor, a polymer film can form, which precludes ethylene from entering the solvent phase. The most probable explanation is that some of the active polymerization species has decomposed.

One important observation is that the activity after 10 minutes is in the same order of magnitude of the activity obtained using the industrially accepted standard, $ZrCp_2X_2$ (X = Cl, Me). Consider that when $TiCp(NP^tBu_3)Cl_2$ is employed as a catalyst precursor, upon activation with MAO, the resulting catalyst is extremely active and produces polymers with low PDI values (< 2).[8,20] However, when one of the *t*-butyl groups on the phosphorus atom is substituted with a benzyl group, the catalyst formed upon activation with MAO is still highly active, but instead produces polydisperse polymer materials. This result may be industrially significant, since the catalyst boasts respectable polymerization activities, while producing materials that are commercially relevant. This consequence also suggests that the role of the benzyl substituent on the phosphorus atom is key to the modification of the active catalyst site.

Table 4.7: Monitoring polymerization activity over time of the catalysts produced from activation of TiCp*(NP^{t}Bu$_2$Bn)X$_2$ (X = Cl (**4.13**), Me (**4.21**)) by MAO.[a]

Precatalyst	Time (min)	Polymer Yield (g)	Activity
TiCp*(NP^{t}Bu$_2$Bn)Cl$_2$ (**4.13**)	10	10.335	1360
TiCp*(NP^{t}Bu$_2$Bn)Cl$_2$ (**4.13**)	15	12.157	1070
TiCp*(NP^{t}Bu$_2$Bn)Cl$_2$ (**4.13**)	20	14.360	950
TiCp*(NP^{t}Bu$_2$Bn)Me$_2$ (**4.21**)	10	10.803	1440
TiCp*(NP^{t}Bu$_2$Bn)Me$_2$ (**4.21**)	15	12.952	1140
TiCp*(NP^{t}Bu$_2$Bn)Me$_2$ (**4.21**)	20	15.575	1030
TiCp*(NP^{t}Bu$_2$Bn)Me$_2$ (**4.21**)	30	15.902	700
ZrCp$_2$Cl$_2$	10	13.880	1830
ZrCp$_2$Me$_2$	10	12.856	1695

a) MAO activation, Ti/Zr:Al ratio 1:500, PhMe solvent, 30°C, 1.82 atm C_2, 50 μM precatalyst, activity in units of g mmol^{-1} h^{-1}atm^{-1}.

In an attempt to observe how multiple metal centres in a single catalyst precursor perform polymerization of ethylene, varying equivalents of [Ph$_3$C][B(C$_6$F$_5$)$_4$] were added to the *p*-(CH$_2$PCy$_2$NCp'TiMe$_2$)$_2$C$_6$H$_4$ (Cp' = Cp* (**4.26**), Cp (**4.28**)) precursors. The purpose of this series of experiments was to determine if one of the titanium centres could be selectively activated, and the difference (if any) when both metal centres were activated. Polymerization experiments were conducted using one, two and four equivalents of [Ph$_3$C][B(C$_6$F$_5$)$_4$] as the catalyst activator, which was selected specifically for its ability to activate a single catalytic site via irreversible alkyl abstraction.

The polymerization activities and polymer properties are summarized in Table 4.8, and several key observations may be noted. One of the most striking features is the dramatic difference in activity between the Cp* (**4.26**) and Cp (**4.28**) precursors. The bulkier Cp* analogue is *ca.* four times as active as the Cp derivative when four equivalents of [Ph$_3$C][B(C$_6$F$_5$)$_4$] are used, and *ca.* 50 times higher when one equivalent is used. As the equivalents of activator are increased from one to two, regardless of the

precatalyst employed, the polymerization activities also increase. Interestingly, all PDI values obtained upon analysis of the polymer were less than 4 and the GPC curves were monodisperse, indicative of predominantly single-site catalysis. This is in direct contrast to the results obtained when MAO was used as an activator. It appears likely that in order to obtain materials of higher polydispersity, two things are required: that the phosphinimide ligand is derived from a phosphine with two basic, bulky groups (e.g. *t*-butyl) and an "activatable" group (i.e. benzyl), and that MAO is employed as an activator. The MAO serves to modify the initial active catalyst, and generate another polymerization-active species that produces higher molecular weight polymer.

Table 4.8: Büchi reactor polymerization results using $[Ph_3C][B(C_6F_5)_4]$ as a discrete activator.[a]

Precatalyst	Eq.[b]	Activity	M_n	M_w	PDI
p-$(CH_2PCy_2NCp^*TiMe_2)_2C_6H_4$ (**4.26**)	1	568	213,600	566,400	2.65
p-$(CH_2PCy_2NCp^*TiMe_2)_2C_6H_4$ (**4.26**)	2	805	126,300	382,300	3.03
p-$(CH_2PCy_2NCp^*TiMe_2)_2C_6H_4$ (**4.26**)	4	470	252,200	718,000	2.85
p-$(CH_2PCy_2NCpTiMe_2)_2C_6H_4$ (**4.28**)	1	10	50,300	206,700	4.11
p-$(CH_2PCy_2NCpTiMe_2)_2C_6H_4$ (**4.28**)	2	87	628,900	1,270,000	2.02
p-$(CH_2PCy_2NCpTiMe_2)_2C_6H_4$ (**4.28**)	4	110	157,500	491,000	3.12
$ZrCp_2Me_2$[c]	2	1010	171,000	334,800	1.96

a) T^iBAl scrubber, Ti:Al ratio 1:5, Activator = $[Ph_3C][B(C_6F_5)_4]$, PhMe solvent, 30°C, 1.82 atm C_2, 50 μM precatalyst, 10 min, M_n and M_w in g mol^{-1}, activity in g $mmol(precatalyst)^{-1}h^{-1}atm^{-1}$.

b) Number of equivalents of $[Ph_3C][B(C_6F_5)_4]$.

c) Zr:Al ratio 1:20.

A Conceptual Extension of Bimetallic Titanium Phosphinimide Complexes

The main shortcoming of the bimetallic titanium phosphinimide complexes described herein is the relatively low polymerization activities relative to zirconocene standards when activated by MAO. Assessment of a series of active titanium catalysts of the general formula $TiCp(NPR_3)Cl_2$ indicate that the presence of the tri-*t*-butyl phosphinimide ligand is crucial to obtain high catalytic performance when discrete activators such as $[Ph_3C][B(C_6F_5)_4]$ are not employed.[20,21] Although other options, including bulky *tris*(amino)phosphinimide titanium complexes, show great promise,[xiii] it seems logical to envision a different series of bimetallic complexes that incorporate the NP^tBu_3 fragment to determine if MAO could be used as an activator to produce a highly active bimetallic catalyst system in the absence of the "activatable" group tethered to the phosphorus atom (Figure 4.12).

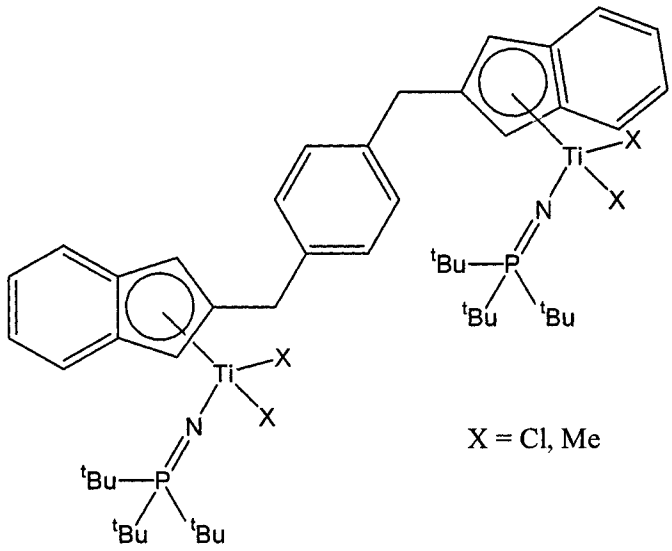

Figure 4.12: The proposed extension of bimetallic titanium phosphinimide complexes.

[xiii] C. L. Beddie, unpublished results. This new class of precatalysts are also sensitive to the activation conditions, and show only moderate activity upon activation with MAO.

For this reason, a new ligand that incorporated indenyl fragments was designed to tether two titanium centres. Thus, *p*-$(CH_2C_9H_7)_2C_6H_4$ (**4.1**) was prepared in high yield (86%) from the addition of two equivalents of lithium indenide to *p*-$(CH_2Br)_2C_6H_4$ at ambient temperature. Detailed ^1H, $^{13}C\{^1H\}$ and 2D NMR studies indicated that the isomer depicted in Section 4.2.4 was the only product. Attempts to prepare the cyclopentadienyl version were not pursued, due to the insolubility of the ligand in commonly employed organic solvents. Subsequently, *p*-$(CH_2C_9H_6SiMe_3)_2C_6H_4$ (**4.2**) was attained from the addition of ^{n}BuLi to the neutral *bis*(indenyl) ligand, which generated the dilithio salt *p*-$(CH_2LiC_9H_6)_2C_6H_4$ at -35°C, followed by *in situ* addition of Me_3SiCl. Unfortunately, prolonged thermolysis of *p*-$(CH_2C_9H_6SiMe_3)_2C_6H_4$ (**4.2**) with $Ti(NP^tBu_3)Cl_3$ resulted in no apparent reaction. Efforts to produce the desired titanium product from reaction of *p*-$(CH_2C_9H_7)_2C_6H_4$ (**4.1**) with $Ti(NMe_2)_4$, followed by addition of HNP^tBu_3 are ongoing.

4.4 Summary

A series of bimetallic titanium complexes of the general formula *p*-$(CH_2PR_2NTiCp'X_2)_2C_6H_4$ (Cp' = Cp, Cp*; R = ^{t}Bu, Cy; X = Cl, Me), and their monometallic counterparts, $TiCp(NPR_2Bn)X_2$, have been synthesized in generally good yields. All spectroscopic and crystallographic evidence indicate that the two families of compounds are structurally quite similar. Upon activation with MAO, the catalysts produce polyethylene with activities that range from essentially zero to being competitive with the common standard $ZrCp_2Cl_2$. Like related titanium phosphinimide complexes,[21] the polymerization activity increases upon addition of steric bulk both on the phosphinimide ligand itself, and through variation of the type of cyclopentadienyl group.

Perhaps the most interesting result is the type of polymer product that is being produced by this class of precursor. The materials possess bimodal molecular weight distributions, in addition to having high molecular weights in general, which may be of commercial significance.[158] Comparison of the polymer products to those produced by the related catalyst precursors $TiCp(NP^tBu_3)X_2$ indicates that the presence of the benzyl

group plays a considerable role in the formation of polydisperse polymer products. Studies that employ $[Ph_3C][B(C_6F_5)_4]$ as an activator also indicate that MAO plays a crucial role in the generation of the polydisperse materials. Efforts to extend the concept to highly active bimetallic catalysts upon activation by MAO include the design of *p*-$[CH_2C_9H_7Ti(NP^tBu_3)]_2C_6H_4$. Although it has not been successfully synthesized to date, it will likely be a good candidate as a highly active catalyst and could ultimately be used to perform insightful polymerization experiments to determine the effect, if any, of the second titanium centre.

5 Zirconium Half-Sandwich Phosphinimide Complexes

5.1 Introduction

Titanium and zirconium have both been used extensively in the production of olefin polymerization catalysts.[31,33,112,144] Recently, hafnium complexes have also demonstrated potential in polymerizing olefins with high activites.[324,325] Although active catalyst systems exist for all of the Group IV metals, it is difficult to predict which metal will produce the most active catalyst for a particular ligand. There are numerous examples in which the titanium complexes act as better catalysts than their zirconium analogues, or *vice versa*.[32,40] As a relatively recent example, McConville and co-workers have employed a chelating diamide ligand to prepare complexes of the form $M[CH_2(CH_2NAr)_2]X_2$ (M = Ti, Zr; Ar = (2,6-^{i}Pr$_2$)C_6H_3, (2,6-Me_2)C_6H_3; X = Cl, Me; Figure 5.1, **I**).[216,248] Although the titanium derivatives perform living polymerization of α-olefins upon activation with $B(C_6F_5)_3$[281] and produce extremely high activities when MAO is used as activator,[216] the zirconium analogues only act as moderate polymerization catalysts (Table 4.4).[248] Conversely, when M[^{t}BuNON]Me_2 (M = Ti, Zr; [^{t}BuNON] = (^{t}Bu-d_6-N-*o*-C_6H_4)$_2$O; Figure 5.1, **II**) were activated by $[NMe_2HPh][B(C_6F_5)_4]$, the titanium derivatives were inactive for olefin polymerization, while the zirconium derivatives polymerized 1-hexene in a living manner.[326]

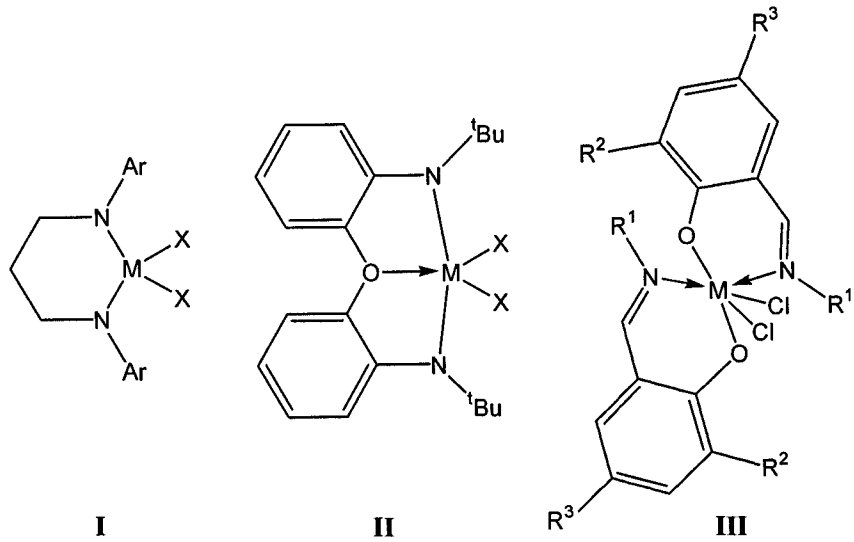

I II III

Figure 5.1: Group IV olefin polymerization precatalysts that show different catalytic activities upon activation, depending on the metal centre.

In some cases, judicious ligand design can provide for active titanium *and* zirconium olefin polymerization catalysts. The Mitsui Chemical Co. has divulged a series of complexes of the general formula ML_2Cl_2 (M = Ti, Zr; L = salicylaldehyde derivative; Figure 5.1, **III**) that polymerize ethylene with extremely high turnover frequencies (> 20 000 min^{-1} atm^{-1}) upon activation with MAO.[140,145] In this example, there still remains a difference between the activities of the two metal centres; the zirconium derivatives are at least twice as active as their titanium counterparts under similar polymerization conditions.

It is clear that it is challenging to predict which Group IV metal is the best candidate for an individual ligand system to produce the most active olefin polymerization catalyst. Previously, our research group has demonstrated the ability of titanium phosphinimide complexes to effect ethylene polymerization upon activation with an appropriate Lewis acid.[7,8,21] In this chapter, the synthesis of analogous zirconium phosphinimide complexes will be described and an investigation into their ability to polymerize ethylene will be detailed.

5.2 Experimental

5.2.1 General Considerations

The synthetic protocol, and characterization of the complexes or polymer products by multinuclear NMR spectroscopy, X-ray crystallography, GPC and microanalysis are analogous to those described in Section 2.2.1 and 3.2.1.

5.2.2 Solvents

All solvents, including deuterated solvents used for NMR experiments, were purified using the methods described in Sections 2.2.2 and 3.2.2.

5.2.3 Reagents

HNP^tBu_3, $LiNP^tBu_3$,[275] $ZrCp^*(NP^tBu_3)Cl_2$ and $ZrCp^*(NP^tBu_3)Me_2$[12] were prepared according to protocol established or modified in the Stephan laboratories. The reagents $^iPrNCN^iPr$, Al_2Me_6, MeMgBr, BnMgCl, PhMgBr, Me_3SiCH_2MgCl, C_6F_5MgBr, Me_3SiCl and $LiNMe_2$ were purchased from Aldrich Chemical Co., and $^tBu_3P$, $ZrCl_4$, $ZrCp_2HCl$, $[ZrCpCl_3]_n$ and $Zr(NEt_2)_4$ were purchased from Strem Chemical Co.; all were used without further purification except for $^iPrNCN^iPr$, which was dried over 3Å molecular sieves and freeze/pump/thaw degassed (x 4) before use. $B(C_6F_5)_3$, $[NMe_2HPh][B(C_6F_5)_4]$ and $[Ph_3C][B(C_6F_5)_4]$ were generously donated by NOVA Chemicals Corp., and were used as received.

5.2.4 Inorganic and Organometallic Syntheses

$Zr(NP^tBu_3)_2(NEt_2)_2$ (**5.1**): A suspension of HNP^tBu_3 (890 mg, 4.0 mmol) in PhMe (20 mL) was added dropwise to a clear solution of $Zr(NEt_2)_4$ (777 mg, 2.0 mmol) in the same solvent (50 mL). The clear mixture was heated at reflux for 12 h, after which time the volatile products were removed *in vacuo*. The product was purified by recrystallization in pentanes/Et_2O at -35°C to afford colourless crystals (1.24 g, 93%). ^1H NMR (500 MHz, C_6D_6) δ: 3.72 (q, 8H, $^3J_{H-H}$ = 7 Hz, $NC\mathbf{H}_2CH_3$), 1.36 (d, 54H, $^3J_{P-H}$ = 12 Hz, $C(C\mathbf{H}_3)_3$), 1.31 (t, 12H, $^3J_{H-H}$ = 7 Hz, $NCH_2C\mathbf{H}_3$). $^{13}C\{^1H\}$ NMR (75.5 MHz, C_6D_6) δ: 44.7 (s, $N\mathbf{C}H_2CH_3$), 40.2 (d, $^1J_{P-C}$ = 48 Hz, $\mathbf{C}(CH_3)_3$), 30.1 (s, $C(\mathbf{C}H_3)_3$), 16.6 (s, $NCH_2\mathbf{C}H_3$). $^{31}P\{^1H\}$ NMR (121.5 MHz, C_6D_6) δ: 28.5 (s). Anal. Calc'd for $C_{32}H_{74}N_4P_2Zr$: C, 57.53; H, 11.16; N, 8.39. Found: C, 55.95; H, 10.78; N, 8.60. Colourless crystals suitable for X-ray diffraction were grown by slow evaporation from pentanes.

$Zr(NP^tBu_3)_3(NMe_2)$ (**5.2**): $Zr(NP^tBu_3)_3Cl$ (**5.7**) (201 mg, 0.26 mmol) was dissolved in PhH (20 mL), and solid $LiNMe_2$ (41 mg, 0.79 mmol) was added at RT. The slurry was stirred for 20 h at RT, after which time it was filtered through Celite. The solvent was removed *in vacuo* to afford a white solid (124 mg, 61%). ^1H NMR (500 MHz, C_6D_6) δ: 3.53 (s, 6H, $N(C\mathbf{H}_3)_2$), 1.45 (s, 81H, $^3J_{P-H}$ = 12 Hz, $C(C\mathbf{H}_3)_3$). $^{13}C\{^1H\}$ NMR (75.5 MHz, C_6D_6) δ: 46.9 (s, $N(\mathbf{C}H_3)_2$), 40.2 (d, $^1J_{P-C}$ = 48 Hz, $\mathbf{C}(CH_3)_3$), 30.4 (s, $C(\mathbf{C}H_3)_3$). $^{31}P\{^1H\}$ NMR (121.5 MHz, C_6D_6) δ: 26.1 (s). Anal. Calc'd for $C_{38}H_{87}N_4P_3Zr$: C, 58.20; H, 11.18; N, 7.14. Found: C, 55.75; H, 10.85; N, 7.07. Colourless crystals suitable for X-ray diffraction were grown by slow evaporation from pentanes.

$ZrCp(NP^tBu_3)Cl_2$ (**5.3**): Solid $LiNP^tBu_3$ (160 mg, 0.72 mmol) was added in several portions over a 30 min period to a slurry of $[ZrCpCl_3]_n$ (180 mg, 0.72 mmol) in PhH (20 mL). The slurry was stirred for 48 h at RT, after which time it was filtered through Celite. Gradual removal of the solvent *in vacuo* afforded colourless crystals (260 mg, 81%). ^1H NMR (500 MHz, C_6D_6) δ: 6.40 (s, 5H, $C_5\mathbf{H}_5$), 1.10 (d, 27H, $^3J_{P-H}$ = 12 Hz,

$C(CH_3)_3$). $^{13}C\{^1H\}$ NMR (75.5 MHz, C_6D_6) δ: 113.8 (s, C_5H_5), 41.0 (d, $^1J_{P-C}$ = 28 Hz, $C(CH_3)_3$), 29.8 (s, $C(CH_3)_3$). $^{31}P\{^1H\}$ NMR (121.5 MHz, C_6D_6) δ: 40.7 (s). Anal. Calc'd for $C_{17}H_{32}Cl_2NPZr$: C, 46.04; H, 7.27; N, 3.16. Found: C, 46.21; H, 7.30; N, 3.16. Colourless crystals suitable for X-ray diffraction were grown by slow evaporation from PhH.

$ZrCp^*(NP^tBu_3)Cl_2$ (**5.4**): This compound was prepared according to a literature method.[12] Colourless crystals suitable for X-ray diffraction were grown from PhMe at -30°C.

$ZrCp(NP^tBu_3)_2Cl$ (**5.5**): Solid $LiNP^tBu_3$ (210 mg, 0.94 mmol) was added in several portions over a 10 min period to a slurry of $[ZrCpCl_3]_n$ (120 mg, 0.47 mmol) in PhH (20 mL). The mixture was stirred for 24 h at RT, after which time it was filtered through Celite. Gradual removal of the solvent *in vacuo* afforded colourless crystals (250 mg, 86%). ^1H NMR (500 MHz, C_6D_6) δ: 6.57 (s, 5H, C_5H_5), 1.27 (d, 54H, $^3J_{P-H}$ = 5 Hz, $C(CH_3)_3$). $^{13}C\{^1H\}$ NMR (75.5 MHz, C_6D_6) δ: 110.6 (s, C_5H_5), 40.6 (d, $^1J_{P-C}$ = 48 Hz, $C(CH_3)_3$), 29.9 (s, $C(CH_3)_3$). $^{31}P\{^1H\}$ NMR (121.5 MHz, C_6D_6) δ: 31.5 (s). Anal. Calc'd for $C_{29}H_{59}ClN_2P_2Zr$: C, 55.78; H, 9.52; N, 4.49. Found: C, 55.65; H, 9.80; N, 4.52. EA for the H_2O adduct (**5.5·H_2O**): Anal. Calc'd for $C_{29}H_{61}ClN_2OP_2Zr$: C, 54.22; H, 9.57; N, 4.36. Found: C, 54.24; H, 9.86; N, 4.38. Colourless crystals suitable for X-ray diffraction were grown by slow evaporation from PhH, and co-crystallized with the H_2O adduct. All attempts to deliberately prepare the H_2O adduct were unsuccessful.

$ZrCp_2(NP^tBu_3)Cl$ (**5.6**): $ZrCp_2HCl$ (320 mg, 1.2 mmol) was slurried in PhH (35 mL), and a suspension of HNP^tBu_3 (270 mg, 1.2 mmol) in the same solvent (5 mL) was added dropwise at RT. The slurry was stirred for 12 h, after which time the solvent was gradually removed *in vacuo*, affording colourless crystals (520 mg, 92%). ^1H NMR (500 MHz, C_6D_6) δ: 6.19 (s, 10H, C_5H_5), 1.16 (d, 27H, $^3J_{P-H}$ = 13 Hz, $C(CH_3)_3$). $^{13}C\{^1H\}$ NMR (75.5 MHz, C_6D_6) δ: 112.5 (s, C_5H_5), 40.8 (d, $^1J_{P-C}$ = 47 Hz, $C(CH_3)_3$), 29.9 (s, $C(CH_3)_3$). $^{31}P\{^1H\}$ NMR (121.5 MHz, C_6D_6) δ: 36.4 (s). Anal. Calc'd for $C_{22}H_{37}ClNPZr$: C, 55.84; H, 7.88; N, 2.96. Found: C, 54.58; H, 8.03; N, 2.92.

Colourless crystals suitable for X-ray diffraction were grown by slow evaporation from PhH.

$Zr(NP^tBu_3)_2Cl_2$ (**5.7**): Me_3SiCl (0.18 mL, 1.45 mmol) was added to a solution of $Zr(NP^tBu_3)_2(NEt_2)_2$ (464 mg, 0.69 mmol) in PhH (40 mL). The clear solution was stirred at RT for 20 h, after which time the volatile products were removed *in vacuo*. The solid was washed with pentanes (3 x 10 mL) and dried to afford a white solid (332 mg, 81%). ^1H NMR (500 MHz, C_6D_6) δ: 1.29 (d, 54H, $^3J_{P-H}$ = 13 Hz, $C(CH_3)_3$). $^{13}C\{^1H\}$ NMR (75.5 MHz, C_6D_6) δ: 40.5 (d, $^1J_{P-C}$ = 47 Hz, $C(CH_3)_3$), 29.7 (s, $C(CH_3)_3$). $^{31}P\{^1H\}$ NMR (121.5 MHz, C_6D_6) δ: 35.6 (s). Anal. Calc'd for $C_{24}H_{54}Cl_2N_2P_2Zr$: C, 48.46; H, 9.15; N, 4.71. Found: C, 48.02; H, 9.51; N, 4.62.

$Zr(NP^tBu_3)_3Cl$ (**5.8**): An improved synthesis for this previously reported compound[203] is described. Solid $ZrCl_4$ (183 mg, 0.79 mmol) was dissolved in THF (15 mL) at -35°C, and a clear solution of $LiNP^tBu_3$ (527 mg, 2.36 mmol) in the same solvent (10 mL) was added dropwise over a 10 min period. The solution was warmed to RT and stirred for 12 h during which time the yellow colour disappeared. The solvent was removed *in vacuo*, and the product was extracted with PhH (2 x 15 mL). Following filtration through Celite, the solvent was removed *in vacuo*, affording a white solid. Analytically pure product was obtained by recrystallizing the crude mixture from PhMe/pentanes at -35°C to ultimately afford colourless crystals (238 mg, 39%). The spectroscopic data agreed with literature values. ^1H NMR (500 MHz, C_6D_6) δ: 1.42 (d, 81H, $^3J_{P-H}$ = 12 Hz, $C(CH_3)_3$). $^{13}C\{^1H\}$ NMR (75.5 MHz, C_6D_6) δ: 40.0 (d, $^1J_{P-C}$ = 48 Hz, $C(CH_3)_3$), 29.8 (s, $C(CH_3)_3$). $^{31}P\{^1H\}$ NMR (121.5 MHz, C_6D_6) δ: 29.2 (s).

$ZrCp(NP^tBu_3)Me_2$ (**5.9**): A 3.0 M solution of MeMgBr in Et_2O (1.2 mL, 3.6 mmol) was added dropwise at RT to a slurry of $ZrCp(NP^tBu_3)Cl_2$ (**5.3**) (320 mg, 0.72 mmol) in the same solvent (30 mL). The mixture was stirred for 15 h, after which time the solvent was removed *in vacuo*. The product was extracted with hexanes (3 x 20 mL,) and the extracts were filtered through Celite. Removal of the solvent afforded a white solid (210 mg, 72%). ^1H NMR (500 MHz, C_6D_6) δ: 6.26 (s, 5H, C_5H_5), 1.16 (d, 27H, $^3J_{P-H}$ = 13 Hz,

$C(CH_3)_3$), 0.26 (s, 6H, Zr-CH_3). $^{13}C\{^1H\}$ NMR (75.5 MHz, C_6D_6) δ: 109.7 (s, C_5H_5), 40.2 (d, $^1J_{P-C}$ = 47 Hz, $C(CH_3)_3$), 29.5 (s, $C(CH_3)_3$), 28.1 (s, Zr-CH_3). $^{31}P\{^1H\}$ NMR (121.5 MHz, C_6D_6) δ: 33.4 (s). Anal. Calc'd for $C_{19}H_{38}NPZr$: C, 56.67; H, 9.51; N, 3.48. Found: C, 55.70; H, 9.42; N, 3.22.

The synthetic methodology for the compounds **5.10-5.17** is analogous to the protocol described above using the appropriate Grignard reagent (MeMgBr (3.0 M in Et_2O), BnMgCl (2.0 M in Et_2O), PhMgBr (3.0 M in Et_2O), Me_3SiCH_2MgCl (1.0 M in Et_2O)) and zirconium chloride precursor, thus only the spectroscopic data is included.

$ZrCp(NP^tBu_3)_2Me$ (**5.10**): White solid (235 mg, 85%). ^1H NMR (500 MHz, C_6D_6) δ: 6.41 (s, 5H, C_5H_5), 1.27 (d, 54H, $^3J_{P-H}$ = 12 Hz, $C(CH_3)_3$), 0.33 (s, 3H, Zr-CH_3). $^{13}C\{^1H\}$ NMR (75.5 MHz, C_6D_6) δ: 108.9 (s, C_5H_5), 40.4 (d, $^1J_{P-C}$ = 48 Hz, $C(CH_3)_3$), 30.0 (s, $C(CH_3)_3$), 29.5 (s, Zr-CH_3). $^{31}P\{^1H\}$ NMR (121.5 MHz, C_6D_6) δ: 28.5 (s). Anal. Calc'd for $C_{30}H_{62}N_2P_2Zr$: C, 59.66; H, 10.35; N, 4.64. Found: C, 54.24; H, 9.86; N, 4.38.

$ZrCp_2(NP^tBu_3)Me$ (**5.11**): Colourless crystals (112 mg, 82%). ^1H NMR (500 MHz, C_6D_6) δ: 5.97 (s, 10H, C_5H_5), 1.13 (d, 27H, $^3J_{P-H}$ = 12 Hz, $C(CH_3)_3$), 0.39 (s, 3H, Zr-CH_3). $^{13}C\{^1H\}$ NMR (75.5 MHz, C_6D_6) δ: 109.5 (s, C_5H_5), 40.5 (d, $^1J_{P-C}$ = 28 Hz, $C(CH_3)_3$), 29.9 (s, $C(CH_3)_3$), 16.6 (s, Zr-CH_3). $^{31}P\{^1H\}$ NMR (121.5 MHz, C_6D_6) δ: 33.0 (s). Calc'd for $C_{23}H_{40}NPZr$: C, 61.01; H, 8.90; N, 3.09. Found: C, 58.36; H, 8.65; N, 3.04.

$ZrCp(NP^tBu_3)Bn_2$ (**5.13**): Light brown solid when washed with Et_2O (133 mg, 80%). ^1H NMR (500 MHz, C_6D_6) δ: 7.22 (d, 4H, $^3J_{H-H}$ = 8 Hz, C_6H_5 (*o*-H)), 7.03 (pseudo t, 4H, $^3J_{H-H}$ = 8 Hz, C_6H_5 (*m*-H)), 6.93 (t, 2H, $^3J_{H-H}$ = 8 Hz, C_6H_5 (*p*-H)), 5.95 (s, 5H, C_5H_5), 2.48, 2.03 (ABq, 4H, $^2J_{H-H}$ = 10 Hz, $CH_2C_6H_5$), 1.09 (d, 27H, $^3J_{P-H}$ = 13 Hz, $C(CH_3)_3$). $^{13}C\{^1H\}$ NMR (75.5 MHz, C_6D_6) δ: 149.9 (s, C_6H_5 (*ipso*-C)), 130.0 (s, C_6H_5 (*o*-C)), 126.3 (s, C_6H_5 (*m*-C)), 120.7 (s, C_6H_5 (*p*-C)), 111.7 (s, C_5H_5), 56.5 (s, $CH_2C_6H_5$), 40.2 (d, $^1J_{P-C}$ = 45 Hz, $C(CH_3)_3$), 29.5 (s, $C(CH_3)_3$). $^{31}P\{^1H\}$ NMR (121.5 MHz, C_6D_6) δ:

35.4 (s). Colourless crystals suitable for X-ray diffraction were grown by slow evaporation from hexanes. Anal. Calc'd for $C_{31}H_{46}NPZr$: C, 67.10; H, 8.36; N, 2.52. Found: C, 65.74; H, 8.41; N, 2.29.

ZrCp*(NP^{t}Bu$_3$)Bn$_2$ (**5.14**): White solid when washed with hexanes (0.088 mg, 72%). ^{1}H NMR (500 MHz, C_6D_6) δ: 7.20 (d, 4H, $^3J_{H-H}$ = 7 Hz, $C_6\mathbf{H}_5$ (*o*-H)), 7.10 (pseudo t, 4H, $^3J_{H-H}$ = 7 Hz, $C_6\mathbf{H}_5$ (*m*-H)), 6.89 (t, 2H, $^3J_{H-H}$ = 7 Hz, $C_6\mathbf{H}_5$ (*p*-H)), 2.29, 2.13 (ABq, 4H, $^2J_{H-H}$ = 11 Hz, $C\mathbf{H}_2C_6H_5$), 1.93 (s, 15H, $C_5(C\mathbf{H}_3)_5$), 1.10 (d, 27H, $^3J_{P-H}$ = 13 Hz, $C(C\mathbf{H}_3)_3$). $^{13}C\{^1H\}$ NMR (75.5 MHz, C_6D_6) δ: 151.2 (s, $\mathbf{C}_6H_5$ (*ipso*-C)), 128.5 (s, $\mathbf{C}_6H_5$ (*o*-C)), 127.2 (s, $\mathbf{C}_6H_5$ (*m*-C)), 120.7 (s, $\mathbf{C}_6H_5$ (*p*-C)), 118.2 (s, $\mathbf{C}_5(CH_3)_5$), 62.1 (s, $\mathbf{C}H_2C_6H_5$), 40.2 (d, $^1J_{P-C}$ = 47 Hz, $\mathbf{C}(CH_3)_3$), 29.6 (s, $C(\mathbf{C}H_3)_3$), 11.7 (s, $C_5(\mathbf{C}H_3)_5$). $^{31}P\{^1H\}$ NMR (121.5 MHz, C_6D_6) δ: 36.6 (s).

ZrCp(NP^{t}Bu$_3$)$_2$Bn (**5.15**): Colourless crystals (156 mg, 89%). ^{1}H NMR (500 MHz, C_6D_6) δ: 7.38 (d, 2H, $^3J_{H-H}$ = 7Hz, $C_6\mathbf{H}_5$ (*o*-H)), 7.33 (pseudo t, 2H, $^3J_{H-H}$ = 7 Hz, $C_6\mathbf{H}_5$ (*m*-H)), 6.93 (t, 1H, $^3J_{H-H}$ = 7 Hz, $C_6\mathbf{H}_5$ (*p*-H)), 6.30 (s, 5H, $C_5\mathbf{H}_5$), 2.69 (s, 2H, $C\mathbf{H}_2C_6H_5$), 1.27 (d, 54H, $^3J_{P-H}$ = 12 Hz, $C(C\mathbf{H}_3)_3$). $^{13}C\{^1H\}$ NMR (75.5 MHz, C_6D_6) δ: 155.5 (s, $\mathbf{C}_6H_5$ (*ipso*-C)), 126.2 (s, $\mathbf{C}_6H_5$ (*o*-C)), 124.3 (s, $\mathbf{C}_6H_5$ (*m*-C)), 119.0 (s, $\mathbf{C}_6H_5$ (*p*-C)), 110.2 (s, $\mathbf{C}_5H_5$), 47.1 (s, $\mathbf{C}H_2C_6H_5$), 40.4 (d, $^1J_{P-C}$ = 47 Hz, $\mathbf{C}(CH_3)_3$), 30.0 (s, $C(\mathbf{C}H_3)_3$). $^{31}P\{^1H\}$ NMR (121.5 MHz, C_6D_6) δ: 29.7 (s). Calc'd for $C_{36}H_{66}N_2P_2Zr$: C, 63.58; H, 9.78; N, 4.12. Found: C, 62.53; H, 9.86; N, 4.38. Colourless crystals suitable for X-ray diffraction were grown by slow evaporation from hexanes.

ZrCp(NP^{t}Bu$_3$)[CH$_2$Si(CH$_3$)$_3$]$_2$ (**5.16**): White solid (232 mg, 77%). ^{1}H NMR (500 MHz, C_6D_6) δ: 6.35 (s, 5H, $C_5\mathbf{H}_5$), 1.15 (d, 27H, $^3J_{P-H}$ = 13 Hz, $C(C\mathbf{H}_3)_3$), 0.34 (s, 18H, $Si(C\mathbf{H}_3)_3$), 0.47, 0.07 (ABq, 4H, $^2J_{H-H}$ = 11 Hz, $C\mathbf{H}_2Si(CH_3)_3$). $^{13}C\{^1H\}$ NMR (75.5 MHz, C_6D_6) δ: 109.5 (s, $\mathbf{C}_5H_5$), 42.5 (s, $\mathbf{C}H_2Si(CH_3)_3$), 40.4 (d, $^1J_{P-C}$ = 47 Hz, $\mathbf{C}(CH_3)_3$), 29.6 (s, $C(\mathbf{C}H_3)_3$), 4.3 (s, $Si(\mathbf{C}H_3)_3$). $^{31}P\{^1H\}$ NMR (121.5 MHz, C_6D_6) δ: 34.0 (s).

ZrCp(NP^{t}Bu$_3$)Ph$_2$ (**5.17**): Light brown, crystalline solid (202 mg, 84%). ^{1}H NMR (500 MHz, C_6D_6) δ: 7.95 (d, 4H, $^3J_{H-H}$ = 7 Hz, $C_6\mathbf{H}_5$ (*o*-H)), 7.31 (pseudo t, 4H, $^3J_{H-H}$ = 7 Hz,

$C_6\mathbf{H}_5$ (*m*-H)), 7.21 (t, 2H, $^3J_{H\text{-}H}$ = 7 Hz $C_6\mathbf{H}_5$ (*p*-H)), 6.38 (s, 5H, $C_5\mathbf{H}_5$), 1.06 (d, 27H, $^3J_{P\text{-}H}$ = 6 Hz, $C(C\mathbf{H}_3)_3$). $^{13}C\{^1H\}$ NMR (75.5 MHz, C_6D_6) δ: 183.9 (s, $\mathbf{C}_6H_5$ (*ipso*-C)), 136.7 (s, $\mathbf{C}_6H_5$ (*o*-C)), 126.9 (s, $\mathbf{C}_6H_5$ (*m*-C)), 126.7 (s, $\mathbf{C}_6H_5$ (*p*-C)), 111.5 (s, $\mathbf{C}_5H_5$), 40.2 (d, $^1J_{P\text{-}C}$ = 46 Hz, $\mathbf{C}(CH_3)_3$), 23.0 (s, $C(\mathbf{C}H_3)_3$). $^{31}P\{^1H\}$ NMR (121.5 MHz, C_6D_6) δ: 35.4 (s).

$ZrCp(NP^tBu_3)(C_6F_5)_2$ (**5.18**) *Method 1*: A 0.5 M solution of C_6F_5MgBr in Et_2O (5.6 mL, 2.8 mmol) was added dropwise at RT to a slurry of $ZrCp(NP^tBu_3)Cl_2$ (250 mg, 0.56 mmol) in the same solvent (80 mL). The slurry was stirred for 15 h, after which time the solvent was removed *in vacuo*. The product was extracted with PhH (3 x 20mL) and the extracts were filtered through Celite. Following removal of the solvent, the brown residue was washed with hexanes (3 x 5 mL), filtered and dried *in vacuo* to afford a pale grey solid (320 mg, 81%). *Method 2*: Solid $ZrCp(NP^tBu_3)Me_2$ (36 mg, 0.089 mmol) and $B(C_6F_5)_3$ (46 mg, 0.089 mmol) were combined in a dry vial. Addition of PhH (2 mL) resulted in a foggy suspension that grew clear within 1 min. After stirring at RT for 30 min, the volatile products were removed *in vacuo*, and the residue was washed with hexanes (3 x 2 mL) before drying to afford a white solid (56 mg, 89%). ^1H NMR (500 MHz, C_6D_6) δ: 6.41 (s, 5H, $C_5\mathbf{H}_5$), 0.94 (d, 27H, $^3J_{P\text{-}H}$ = 6 Hz, $C(C\mathbf{H}_3)_3$). $^{13}C\{^1H\}$ NMR (75.5 MHz, C_6D_6) δ: 148.0 (dd, $^1J_{C\text{-}F}$ = 220 Hz, $^2J_{C\text{-}F}$ = 30 Hz, $\mathbf{C}_6F_5$ (*o*-C)), 140.6 (dd, $^1J_{C\text{-}F}$ = 240 Hz, $^2J_{C\text{-}F}$ = 15 Hz, $\mathbf{C}_6F_5$ (*p*-C)), 140.1 (s, $\mathbf{C}_6F_5$ (*ipso*-C)), 136.8 (ddd, $^1J_{C\text{-}F}$ = 260 Hz, $^2J_{C\text{-}F}$ = 30 Hz, $^2J_{C\text{-}F}$ = 15 Hz, $\mathbf{C}_6F_5$ (*m*-C)), 112.5 (s, $\mathbf{C}_5H_5$), 39.9 (d, $^1J_{P\text{-}C}$ = 45 Hz, $\mathbf{C}(CH_3)_3$), 28.9 (s, $C(\mathbf{C}H_3)_3$). $^{19}F\{^1H\}$ NMR (282.34 MHz, C_6D_6) δ: -118.73 (m, 4F, $C_6\mathbf{F}_5$ (*o*-F)), -154.46 (t, 2F, $^3J_{F\text{-}F}$ = 20 Hz, $C_6\mathbf{F}_5$ (*p*-F)), -161.49 (m, 4F, $C_6\mathbf{F}_5$ (*m*-F)). $^{31}P\{^1H\}$ NMR (121.5 MHz, C_6D_6) δ: 42.7 (s). In Method 2, the borane side-products were identified spectroscopically, and the chemical shifts for $BMe(C_6F_5)_2$ were similar to literature data.[167] $BMe(C_6F_5)_2$: ^1H NMR (500 MHz, C_6D_6) δ: 1.25 (br s, 3H, B-$C\mathbf{H}_3$). $^{11}B\{^1H\}$ NMR (96.25 MHz, C_6D_6) δ: 76.8 (br). $^{19}F\{^1H\}$ NMR (282.34 MHz, C_6D_6) δ: -133.52 (d, 4F, $^3J_{F\text{-}F}$ = 20 Hz, $C_6\mathbf{F}_5$ (*o*-F)), -165.58 (br, 2F, $C_6\mathbf{F}_5$ (*p*-F)), -168.16 (br, 4F, $C_6\mathbf{F}_5$ (*m*-F)). $BMe_2(C_6F_5)$: ^1H NMR (500 MHz, C_6D_6) δ: 0.77 (br s, 6H, B-$C\mathbf{H}_3$). $^{11}B\{^1H\}$ NMR (96.25 MHz, C_6D_6) δ: 81.8 (br). $^{19}F\{^1H\}$ NMR (282.34 MHz, C_6D_6) δ: -

131.54 (m, 2F, $C_6\mathbf{F}_5$ (*o*-F)), -152.59 (t, 1F, $^3J_{F\text{-}F}$ = 8 Hz, $C_6\mathbf{F}_5$ (*p*-F)), -163.60 (m, 2F, $C_6\mathbf{F}_5$ (*m*-F)).

5.2.5 Reactions with Borane Reagents

[$ZrCp(NP^tBu_3)_2$][$BnB(C_6F_5)_3$] (**5.19**): Solid $ZrCp(NP^tBu_3)_2Bn$ (51 mg, 0.075 mmol) and $B(C_6F_5)_3$ (38 mg, 0.075 mmol) were dissolved separately in PhH (2 mL each) to give clear solutions. They were combined at RT, and a red insoluble oil separated immediately. The PhH layer was decanted off, and the oil was washed with PhH (3 x 1 mL) before drying *in vacuo*. Yield: 83 mg (93%). ^{1}H NMR (500 MHz, CD_2Cl_2) δ: 7.64 (br, 2H, $C_6\mathbf{H}_5$ (*m*-H)), 7.45 (s, 1H, $C_6\mathbf{H}_5$ (*p*-H)), 7.17 (br, 2H, $C_6\mathbf{H}_5$ (*o*-H)), 6.81 (s, 5H, $C_5\mathbf{H}_5$), 3.42 (br, 2H, $C\mathbf{H}_2C_6H_5$), 1.69 (d, 54H, $^3J_{P\text{-}H}$ = 13 Hz, $C(C\mathbf{H}_3)_3$). $^{13}C\{^1H\}$ NMR (75.5 MHz, CD_2Cl_2) δ: 149.9 (s, $\mathbf{C}_6F_5$, (*ipso*-C)), 149.3 (d(br), $^1J_{C\text{-}F}$ = 240 Hz, $\mathbf{C}_6F_5$ (*o*-C)), 138.5 (d(br), $^1J_{C\text{-}F}$ = 240 Hz, $\mathbf{C}_6F_5$ (*p*-C)), 137.5 (d(br), $^1J_{C\text{-}F}$ = 240 Hz, $\mathbf{C}_6F_5$ (*m*-C)), 129.7 (s, $\mathbf{C}_6H_5$ (*ipso*-C)), 129.8 (s, $\mathbf{C}_6H_5$ (*o*-C)), 127.7 (s, $\mathbf{C}_6H_5$ (*m*-C)), 123.3 (s, $\mathbf{C}_6H_5$ (*p*-C)), 112.4 (s, $\mathbf{C}_5H_5$), 71.2 (s, $\mathbf{C}H_2C_6H_5$), 40.9 (d, $^1J_{P\text{-}C}$ = 36 Hz, $\mathbf{C}(CH_3)_3$), 30.6 (s, $C(\mathbf{C}H_3)_3$). $^{11}B\{^1H\}$ NMR (96.25 MHz, CD_2Cl_2) δ: -16.6 (s). $^{19}F\{^1H\}$ NMR (282.34 MHz, CD_2Cl_2) δ: -131.14 (d, 6F, $^3J_{F\text{-}F}$ = 20 Hz, $C_6\mathbf{F}_5$ (*o*-F)), -165.02 (t, 3F, $^3J_{F\text{-}F}$ = 20 Hz, $C_6\mathbf{F}_5$ (*p*-F)), -167.71 (t, 6F, $^3J_{F\text{-}F}$ = 20 Hz, $C_6\mathbf{F}_5$ (*m*-F)). $^{31}P\{^1H\}$ NMR (121.5 MHz, CD_2Cl_2) δ: 37.9 (s).

[$ZrCp(NP^tBu_3)(N^iPrC(CH_3)N^iPr)$][$MeB(C_6F_5)_3$] (**5.20**): $ZrCp(NP^tBu_3)Me_2$ (99 mg, 0.24 mmol) and ^{i}PrNCN^{i}Pr (40 μL, 0.24 mmol) were combined in PhH (5 mL) to give a colourless solution. A clear solution of $B(C_6F_5)_3$ (126 mg, 0.24 mmol) in the same solvent (5 mL) was added at RT, and a bright yellow oil emerged immediately. After stirring for 5 min, the solution was pipetted off, and the oil was washed with PhH (3 x 3 mL) and pentanes (3 x 3 mL). Drying *in vacuo* resulted in a bright yellow solid (132 mg, 53%). ^{1}H NMR (500 MHz, CD_2Cl_2) δ: 6.71 (s, 5H, $C_5\mathbf{H}_5$), 3.79 (sept, 2H, $^3J_{H\text{-}H}$ = 6 Hz, $C(CH_3)_2\mathbf{H}$), 2.19 (s, 3H, $NC(C\mathbf{H}_3)N$), 1.39 (d, 27H, $^3J_{P\text{-}H}$ = 7 Hz, $C(C\mathbf{H}_3)_3$), 1.19 (d, 6H, $^3J_{H\text{-}H}$ = 6 Hz, $C(C\mathbf{H}_3)_2H$), 1.11 (d, 6H, $^3J_{H\text{-}H}$ = 6 Hz, $C(C\mathbf{H}_3)_2H$), 0.52 (br s, 3H,

$\mathbf{H}_3CB(C_6F_5)_3$). $^{13}C\{^1H\}$ NMR (75.5 MHz, CD_2Cl_2) δ: 170.7 (s, N**C**(CH_3)N), 148.9 (dd, $^1J_{C\text{-}F}$ = 235 Hz, $^2J_{C\text{-}F}$ = 10 Hz, $\mathbf{C}_6F_5$ (*o*-C)), 138.1 (d(m), $^1J_{C\text{-}F}$ = 240 Hz, $\mathbf{C}_6F_5$ (*p*-C)), 136.9 (ddd, $^1J_{C\text{-}F}$ = 250 Hz, $^2J_{C\text{-}F}$ = 20 Hz, $^3J_{C\text{-}F}$ = 11 Hz, $\mathbf{C}_6F_5$ (*m*-C)), 129.6 (br s, $\mathbf{C}_6F_5$ (*ipso*)), 115.6 (s, $\mathbf{C}_5H_5$), 49.5 (s, **C**$H(CH_3)_2$), 40.8 (d, $^1J_{P\text{-}C}$ = 60 Hz, **C**$(CH_3)_3$), 29.7 (s, C$(\mathbf{C}H_3)_3$), 26.2 (s, C$(\mathbf{C}H_3)_2$H), 25.5 (s, C$(\mathbf{C}H_3)_2$H), 13.7 (s, NC$(\mathbf{C}H_3)$N), 10.6 (br q, $J_{B\text{-}C}$ = 52 Hz, $H_3\mathbf{C}B(C_6F_5)_3$). $^{11}B\{^1H\}$ NMR (96.25 MHz, CD_2Cl_2) δ: -19.1 (s). $^{19}F\{^1H\}$ NMR (282.34 MHz, CD_2Cl_2) δ: -133.27 (d, 6F, $^3J_{F\text{-}F}$ = 20 Hz, $C_6\mathbf{F}_5$ (*o*-F)), -163.54 (t, 3F, $^3J_{F\text{-}F}$ = 20 Hz, $C_6\mathbf{F}_5$ (*p*-F)), -168.03 (m, 6F, $C_6\mathbf{F}_5$ (*m*-F)). $^{31}P\{^1H\}$ NMR (121.5 MHz, CD_2Cl_2) δ: 46.5 (s). Anal. Calc'd for $C_{44}H_{52}BF_{15}N_3PZr$: C, 50.77; H, 5.04; N, 4.04. Found: C, 50.42; H, 5.19; N, 4.17.

$[ZrCp^*(NP^tBu_3)(N^iPrC(CH_3)N^iPr)][MeB(C_6F_5)_3]$ (**5.21**): $ZrCp^*(NP^tBu_3)Me_2$ (40 mg, 0.085 mmol) and $^iPrNCN^iPr$ (13 μL, 0.085 mmol) were combined in PhH (5 mL) to give a colourless solution. A clear solution of $B(C_6F_5)_3$ (43 mg, 0.085 mmol) in the same solvent (3 mL) was added at RT, and a bright yellow oil separated immediately. After stirring for 5 min, the solution was pipetted off, and the oil was washed with PhH (3 x 3 mL) and pentanes (3 x 3 mL). Drying *in vacuo* resulted in a bright yellow solid (72 mg, 77%). ^1H NMR (500 MHz, CD_2Cl_2) δ: 3.74 (s, 2H, $^3J_{H\text{-}H}$ = 6 Hz, C$(CH_3)_2\mathbf{H}$), 2.22 (s, 3H, NC$(\mathbf{C}H_3)$N), 2.21 (s, 15H, $C_5(\mathbf{C}H_3)_5$), 1.37 (d, 27H, $^3J_{P\text{-}H}$ = 13 Hz, C$(\mathbf{C}H_3)_3$), 1.23 (d, 6H, $^3J_{H\text{-}H}$ = 6 Hz, C$(\mathbf{C}H_3)_2$H), 1.15 (d, 6H, $^3J_{H\text{-}H}$ = 6 Hz, C$(\mathbf{C}H_3)_2$H), 0.50 (br s, 3H, $\mathbf{H}_3CB(C_6F_5)_3$). $^{13}C\{^1H\}$ NMR (75.5 MHz, CD_2Cl_2) δ: 172.7 (s, N**C**(CH_3)N), 148.9 (dd, $^1J_{C\text{-}F}$ = 235 Hz, $^2J_{C\text{-}F}$ = 11 Hz, $\mathbf{C}_6F_5$ (*o*-C)), 138.0 (d(m), $^1J_{C\text{-}F}$ = 240 Hz, $\mathbf{C}_6F_5$ (*p*-C)), 136.9 (ddd, $^1J_{C\text{-}F}$ = 245 Hz, $^2J_{C\text{-}F}$ = 22 Hz, $^3J_{C\text{-}F}$ = 12 Hz, $\mathbf{C}_6F_5$ (*m*-C)), 128.9 (br s, $\mathbf{C}_6F_5$ (*ipso*)), 125.7 (s, $\mathbf{C}_5(CH_3)_5$), 49.4 (s, **C**$H(CH_3)_2$), 40.7 (d, $^1J_{P\text{-}C}$ = 45 Hz, **C**$(CH_3)_3$), 29.7 (s, C$(\mathbf{C}H_3)_3$), 25.7 (s, C$(\mathbf{C}H_3)_2$H), 25.6 (s, C$(\mathbf{C}H_3)_2$H), 14.6 (s, NC$(\mathbf{C}H_3)$N), 12.8 (s, $C_5(\mathbf{C}H_3)_5$), 10.5 (br q, $J_{B\text{-}C}$ = 50 Hz, $H_3\mathbf{C}B(C_6F_5)_3$). $^{11}B\{^1H\}$ NMR (96.25 MHz, CD_2Cl_2) δ: -19.1 (s). $^{19}F\{^1H\}$ NMR (282.34 MHz, CD_2Cl_2) δ: -133.40 (d, 6F, $^3J_{F\text{-}F}$ = 20 Hz, $C_6\mathbf{F}_5$ (*o*-F)), -165.64 (t, 3F, $^3J_{F\text{-}F}$ = 20 Hz, $C_6\mathbf{F}_5$ (*p*-F)), -168.17 (m, 6F, $C_6\mathbf{F}_5$ (*m*-F)). $^{31}P\{^1H\}$ NMR (121.5 MHz, CD_2Cl_2) δ: 47.2 (s). Anal. Calc'd for $C_{49}H_{62}BF_{15}N_3PZr$: C, 52.97; H, 5.62; N, 3.78. Found: C, 52.69; H, 5.82; N, 3.79.

[ZrCp(NP^{t}Bu$_3$)Me(THF)][MeB(C$_6$F$_5$)$_3$] (**5.22**): ZrCp(NP^{t}Bu$_3$)Me$_2$ (24 mg, 0.060 mmol) and B(C$_6$F$_5$)$_3$ (31 mg, 0.060 mmol) were dissolved in 1 mL (each) of CH_2Cl_2 to give clear, colourless solutions. THF (50 mL, 0.60 mmol) was added at RT to the solution containing the Zr precursor, followed immediately by the solution of B(C$_6$F$_5$)$_3$. The pale yellow mixture was stirred for 30 min, then the solvents were removed *in vacuo*. The residue was washed with pentanes (2 x 2 mL), and dried *in vacuo* to afford a pale yellow solid. (46 mg, 78%) ^{1}H NMR (500 MHz, CD_2Cl_2) δ: 6.51 (s, 5H, C$_5$**H**$_5$), 4.02 (br, 4H, OC**H**$_2$CH$_2$), 2.05 (br, 4H, OCH$_2$C**H**$_2$), 1.45 (d, 27H, $^3J_{P-H}$ = 13 Hz, C(C**H**$_3$)$_3$), 0.50 (s, 3H, Zr-C**H**$_3$), 0.49 (br s, 3H, **H**$_3$CB(C$_6$F$_5$)$_3$). ^{13}C{^{1}H} NMR (75.5 MHz, CD_2Cl_2) δ: 149.7 (br s, **C**$_6$F$_5$ (*ipso*)), 148.7 (d(br), $^1J_{C-F}$ = 240 Hz, **C**$_6$F$_5$ (*o*-C)), 138.8 (d(m), $^1J_{C-F}$ = 245 Hz, **C**$_6$F$_5$ (*p*-C)), 136.9 (d(m), $^1J_{C-F}$ = 240 Hz, **C**$_6$F$_5$ (*m*-C)), 113.6 (s, **C**$_5$H$_5$), 73.9 (s, OCH$_2$CH$_2$), 41.2 (d, $^1J_{P-C}$ = 45 Hz, **C**(CH$_3$)$_3$), 30.3 (s, C(**C**H$_3$)$_3$), 29.0 (Zr-**C**H$_3$), 26.1 (s, OCH$_2$**C**H$_2$), 12.5 (br q, J_{B-C} = 20 Hz, H$_3$**C**B(C$_6$F$_5$)$_3$). ^{11}B{^{1}H} NMR (96.25 MHz, CD_2Cl_2) δ: -20.8 (s). ^{19}F{^{1}H} NMR (282.34 MHz, CD_2Cl_2) δ: -132.92 (d, 6F, $^3J_{F-F}$ = 8 Hz, C$_6$**F**$_5$ (*o*-F)), -163.98 (t, 3F, $^3J_{F-F}$ = 20 Hz, C$_6$**F**$_5$ (*p*-F)), -167.80 (m, 6F, C$_6$**F**$_5$ (*m*-F)). ^{31}P{^{1}H} NMR (121.5 MHz, CD_2Cl_2) δ: 46.6 (s).

[ZrCp(NP^{t}Bu$_3$)Me(NMe$_2$Ph)][B(C$_6$F$_5$)$_4$] (**5.23**): ZrCp(NP^{t}Bu$_3$)Me$_2$ (33 mg, 0.089 mmol) and [NMe$_2$HPh][B(C$_6$F$_5$)$_4$] (66 mg, 0.089 mmol) were dissolved in 0.5 mL (each) of CD_2Cl_2 to give clear, colourless solutions. The solution containing the Zr precursor was added to the solution of borate at -35°C, and vigorous evolution of gas was observed. The solution was transferred to an NMR tube immediately for analysis. The product formed quantitatively, as indicated by multinuclear NMR spectroscopy; due to rapid decomposition, this product was not isolated, and microanalysis could not be performed. ^{1}H NMR (500 MHz, CD_2Cl_2) δ: 7.69 (pseudo t, 2H, $^3J_{H-H}$ = 8 Hz, C$_6$**H**$_5$ (*m*-H)), 7.62 (t, 1H, $^3J_{H-H}$ = 8 Hz, C$_6$**H**$_5$ (*p*-H)), 7.48 (d, 2H, $^3J_{H-H}$ = 8 Hz, C$_6$**H**$_5$ (*o*-H)), 5.87 (s, 5H, C$_5$**H**$_5$), 3.20 (s, 3H, N-C**H**$_3$), 3.03 (s, 3H, N-C**H**$_3$), 1.50 (d, 27H, $^3J_{P-H}$ = 13 Hz, C(C**H**$_3$)$_3$), 0.62 (s, 3H, Zr-C**H**$_3$). ^{13}C{^{1}H} NMR (75.5 MHz, CD_2Cl_2) δ: 148.4 (d(br), $^1J_{C-F}$ = 240 Hz, **C**$_6$F$_5$ (*o*-C)), 141.0 (s, **C**$_6$F$_5$, (*ipso*-C)), 138.4 (d(br), $^1J_{C-F}$ = 249 Hz, **C**$_6$F$_5$ (*p*-C)), 136.5 (d(br), $^1J_{C-F}$ = 244 Hz, **C**$_6$F$_5$ (*m*-C)), 133.2 (s, **C**$_6$H$_5$ (*m*-C)), 129.7 (s, **C**$_6$H$_5$ (*p*-C)), 129.2 (s, **C**$_6$H$_5$ (*ipso*-C)), 117.6 (s, **C**$_6$H$_5$ (*o*-C)), 113.3 (s, **C**$_5$H$_5$), 51.0 (s, N-**C**H$_3$), 45.8 (s,

N-CH_3), 33.9 (s, Zr-CH_3), 41.2 (d, $^1J_{P-C}$ = 45 Hz, $C(CH_3)_3$), 29.6 (s, $C(CH_3)_3$). $^{11}B\{^1H\}$ NMR (96.25 MHz, CD_2Cl_2) δ: -16.9 (s). $^{19}F\{^1H\}$ NMR (282.34 MHz, CD_2Cl_2) δ: -133.32 (d, 8F, $^3J_{F-F}$ = 8 Hz, C_6F_5 (*o*-F)), -163.93 (t, 4F, $^3J_{F-F}$ = 20 Hz, C_6F_5 (*p*-F)), -167.76 (pseudo t, 8F, $^3J_{F-F}$ = 20 Hz, C_6F_5 (*m*-F)). $^{31}P\{^1H\}$ NMR (121.5 MHz, CD_2Cl_2) δ: 47.2 (s).

[ZrCp*(NP^tBu_3)Me][$B(C_6F_5)_4$] (**5.24**): ZrCp*(NP^tBu_3)Me_2 (40 mg, 0.085 mmol) and [Ph_3C][$B(C_6F_5)_4$] (78 mg, 0.085 mmol) were dissolved in 2 mL (each) of CH_2Cl_2 to give clear, colourless solutions. The solution containing the borate was added to the solution of zirconium precursor at -35°C, and the solution was stirred for 30 min. The solvent was removed *in vacuo*, and the oily yellow residue was washed with PhMe (3 x 3 mL) and dried exhaustively *in vacuo* to afford a sticky yellow residue. ^1H NMR (500 MHz, CD_2Cl_2) δ: 1.95 (s, 15H, $C_5(CH_3)_5$), 1.34 (d, 27H, $^3J_{P-H}$ = 13 Hz, $C(CH_3)_3$), 0.07 (br s, 3H, Zr-CH_3). $^{13}C\{^1H\}$ NMR (75.5 MHz, CD_2Cl_2) δ: 149.7 (br s, C_6F_5 (*ipso*)), 148.8 (d(br), $^1J_{C-F}$ = 240 Hz, C_6F_5 (*o*-C)), 140.4 (d(m), $^1J_{C-F}$ = 245 Hz, C_6F_5 (*p*-C)), 136.9 (d(m), $^1J_{C-F}$ = 245 Hz, C_6F_5 (*m*-C)), 120.9 (s, $C_5(CH_3)_5$), 40.9 (d, $^1J_{P-C}$ = 46 Hz, $C(CH_3)_3$), 39.9 (s, Zr-CH_3), 29.9 (s, $C(CH_3)_3$), 12.1 (s, $C_5(CH_3)_5$). $^{11}B\{^1H\}$ NMR (96.25 MHz, CD_2Cl_2) δ: -20.9 (s). $^{19}F\{^1H\}$ NMR (282.34 MHz, CD_2Cl_2) δ: -133.33 (br, 6F, C_6F_5 (*o*-F)), -164.02 (t, 3F, $^3J_{F-F}$ = 41 Hz, C_6F_5 (*p*-F)), -167.82 (m, 6F, C_6F_5 (*m*-F)). $^{31}P\{^1H\}$ NMR (121.5 MHz, CD_2Cl_2) δ: 43.8 (s).

5.2.6 Reactions with Aluminum Reagents

[$ZrCpCl_2$]$_3$CH (**5.25**): ZrCp(NP^tBu_3)Cl_2 (**5.3**) (90 mg, 0.20 mmol) was dissolved in PhH (10 mL), and Al_2Me_6 (40 μL, 2.0 mmol) was added at RT via syringe. After stirring for several hours, the solvent and excess Al_2Me_6 were removed *in vacuo*. The crude residue was dissolved in CD_2Cl_2 for analysis without isolation of the product; the product had formed quantitatively by NMR spectroscopy. The by-product $Al_2(NP^tBu_3)Me_5$ was also

observed, and spectroscopic data were consistent with previously determined values.[xiv] ^{1}H NMR (500 MHz, CD_2Cl_2) δ: 15.9 (s, 1H, $Zr_3C\mathbf{H}$), 6.31 (s, 15H, $C_5\mathbf{H}_5$). $^{13}C\{^{1}H\}$ NMR (75.5 MHz, CD_2Cl_2) δ: 336.1 (s, $Zr_3\mathbf{C}H$, DEPT 90-confirmed), 115.8 (s, $\mathbf{C}_5H_5$).

5.2.7 X-Ray Experimental

X-ray structural solutions of $Zr(NP^tBu_3)_2(NEt_2)_2$ (**5.1**), $Zr(NP^tBu_3)_3(NMe_2)$ (**5.2**), $ZrCp(NP^tBu_3)Cl_2$ (**5.3**), $ZrCp^*(NP^tBu_3)Cl_2$ (**5.4**), $ZrCp(NP^tBu_3)Bn_2$ (**5.13**) and $ZrCp(NP^tBu_3)_2Bn$ (**5.15**) were obtained using direct methods, while $ZrCp_2(NP^tBu_3)Cl$ (**5.6**) was solved using a Patterson map. In addition, a preliminary solution was obtained for $ZrCp(NP^tBu_3)_2Cl$ (**5.5**), although the data was too poor for a detailed discussion. The solution for structure **5.2** is disordered, therefore 18 of the atoms were refined isotropically (3 *t*-butyl groups), while 34 of the 46 atoms were refined anisotropically (6 extra atoms due to disorder). Cell parameters, R, R_w and GoF values are located in Table 5.1, while detailed structural parameters have been included as an appendix on CD. No residual electron density remained in any of the solutions that was of any chemical significance. ORTEP drawings of **5.2**, **5.13** and **5.15** are depicted in Figures 5.2 and 5.6, while select bond distances and angles are provided in Tables 5.2, 5.3 and in the text.

[xiv] J. E. Kickham, unpublished results.

Table 5.1: Crystallographic parameters for $Zr(NP^tBu_3)_2(NEt_2)_2$ (**5.1**), $Zr(NP^tBu_3)_3(NMe_2)$ (**5.2**), $ZrCp(NP^tBu_3)Cl_2$ (**5.3**).

	5.1	**5.2**	**5.3**
Molecular formula	$C_{32}H_{72}N_4P_2Zr$	$C_{38}H_{60}N_4P_3Zr$	$C_{17}H_{32}Cl_2NPZr$
Formula weight	666.10	757.03	443.53
a(Å)	17.79(2)	13.306(9)	10.252(2)
b(Å)	17.80(2)	13.409(9)	14.886(3)
c(Å)	25.81(3)	16.00(1)	28.717(6)
α(°)	90.00	79.10(1)	90.00
β(°)	90.00	73.21(1)	90.00
γ (°)	90.00	60.70(1)	90.00
Crystal system	Orthorhombic	Triclinic	Orthorhombic
Space group	Pbca	P-1	Pbca
Volume ($Å^3$)	8180 (1)	2379(3)	4382(2)
D_{calc} (gcm^{-3})	1.082	1.057	1.344
Z	8	2	8
Abs coeff, μ, mm^{-1}	0.370	0.357	0.816
θ range (°)	1.80-20.50	1.74-23.32	1.69-25.00
Reflections collected	23352	9774	17365
Data $F_o^2 > 3\sigma(F_o^2)$	2081	5405	3152
Parameters	352	379	199
R(%)	0.1074	0.0722	0.0657
R_w(%)	0.2386	0.1864	0.1638
Goodness of Fit	0.982	1.187	1.167

The data was collected at 20°C with Mo Kα radiation (λ = 0.71069 Å)

$R = \Sigma \, | \, |F_o| - |F_c| \, | \, / \, \Sigma \, |F_o|$, $R_w = [\Sigma(|F_o| - |F_c|)^2 / \Sigma \, |F_o|^2]^{0.5}$

Table 5.1 (continued): Crystallographic parameters for $ZrCp^*(NP^tBu_3)Cl_2$ (**5.4**), $ZrCp(NP^tBu_3)_2Cl$ (**5.5**),[xv] $ZrCp_2(NP^tBu_3)Cl$ (**5.6**).

	5.4	**5.5**	**5.6**
Molecular formula	$C_{22}H_{42}Cl_2NPZr$	$C_{29}H_{59}ClN_2P_2Zr$	$C_{22}H_{37}ClNPZr$
Formula weight	513.66	624.42	473.19
a(Å)	11.888(6)	17.492(1)	8.472(4)
b(Å)	16.743(9)	14.6264(8)	14.295(7)
c(Å)	13.508(7)	27.369(2)	19.506(9)
α(°)	90.00	90.00	90.00
β(°)	96.934(9)	90.10(1)	90.00
γ (°)	90.00	90.00	90.00
Crystal system	Monoclinic	Monoclinic	Orthorhombic
Space group	$P2_1/n$	$P2_1/c$	$P2_12_12_1$
Volume ($Å^3$)	2669(2)	7002(7)	2362(2)
D_{calc} (gcm^{-3})	1.278	1.165	1.330
Z	4	4	4
Abs coeff, μ, mm^{-1}	0.680	0.499	0.653
θ range (°)	1.95-23.24	1.16-23.26	2.09-23.20
Reflections collected	11059	29627	10186
Data $F_o^2 > 3\sigma(F_o^2)$	3400	5934	2705
Parameters	244	616	235
R(%)	0.0249	0.1088	0.0493
R_w(%)	0.0694	0.2961	0.1288
Goodness of Fit	1.025	1.104	1.018

The data was collected at 20°C with Mo Kα radiation (λ = 0.71069 Å)

$R = \Sigma \, | \, |F_o| - |F_c| \, | \, / \, \Sigma \, |F_o|$, $R_w = [\Sigma \, (|F_o| - |F_c|)^2 / \Sigma \, |F_o|^2]^{0.5}$

[xv]Only preliminary X-ray data were obtained.

Table 5.1 (continued): Crystallographic parameters for $ZrCp(NP^tBu_3)Bn_2$ (**5.13**), $ZrCp(NP^tBu_3)_2Bn$ (**5.15**).

	5.13	**5.15**
Molecular formula	$C_{31}H_{46}NPZr$	$C_{36}H_{66}N_2P_2Zr$
Formula weight	554.88	680.07
a(Å)	11.35(6)	10.759(6)
b(Å)	15.765(8)	19.55(1)
c(Å)	16.780(9)	19.43(1)
α(°)	90.00	90.00
β(°)	90.00	103.55(1)
γ (°)	90.00	90.00
Crystal system	Orthorhombic	Monoclinic
Space group	$P2_12_12_1$	$P2_1/c$
Volume ($Å^3$)	3004(3)	3974(4)
D_{calc} (gcm^{-3})	1.227	1.137
Z	4	4
Abs coeff, μ, mm^{-1}	0.437	0.381
θ range (°)	2.17-23.19	2.16-23.37
Reflections collected	12830	16934
Data $F_o^2 > 3\sigma(F_o^2)$	4067	3645
Parameters	307	370
R(%)	0.0217	0.0339
R_w(%)	0.0560	0.0850
Goodness of Fit	1.031	0.872

The data was collected at 20°C with Mo Kα radiation (λ = 0.71069 Å)

$R = \Sigma \, | \, |F_o| - |F_c| \, | \, / \, \Sigma \, |F_o|$, $R_w = [\Sigma \, (|F_o| - |F_c|)^2 / \Sigma \, |F_o|^2]^{0.5}$

5.2.8 Polymerization Protocol

Purification of reagents used in the polymerizations was similar to that described in Section 3.2.9. The Schlenk flask and Büchi autoclave polymerizations were performed according to the procedure described in Section 4.2.10, with modifications detailed in the Tables in Section 5.3. Recorded exotherms upon activation with $[Ph_3C][B(C_6F_5)_4]$ were significant enough that they could not be adequately controlled using the heating/cooling system (typical temperature spikes *ca.* 10-30°C). In the few cases where the temperature increase necessitated the polymerization experiment to be halted, the modifications are noted in Table 5.6.

The masses of reagents and polyethylene, in addition to the raw GPC data, may be viewed in Appendix D (on CD).

5.3 Results and Discussion

Previous attempts to synthesize $Zr(NP^tBu_3)_2Cl_2$ (**5.7**) from reaction of $LiNP^tBu_3$ with $ZrCl_4$ in benzene resulted in the isolation of crystals of $Zr(NP^tBu_3)_3Cl$ (**5.8**) from an otherwise intractable mixture of products.[203] It is noteworthy that the related complex $Zr(NPPh_3)_2Cl_2(HNPPh_3)_2$ was prepared directly from $ZrCl_4{\cdot}THF_2$ using $[Cs(NPPh_3)]_4$ in THF, although no yields are reported and there is no indication that it was the sole product.[327] Thus, an alternate route from the amide precursors $Zr(NR_2)_4$ (R = Me, Et) and $Zr(NEt_2)_2Cl_2{\cdot}THF_2$[328] was envisioned to prepare the desired metal complex. Transamination is frequently successful to produce the appropriate $ZrL_2(NR_2)_2$ complex,[256,280,329,330] however, inseparable products resulted upon reaction of $Zr(NR_2)_4$ (R = Me, Et) with HNP^tBu_3 at ambient temperatures in aromatic or chlorinated solvents. X-ray quality crystals of $Zr(NP^tBu_3)_3(NMe_2)$ (**5.2**) (Table 5.2, Figure 5.2) and $Zr(NP^tBu_3)_3(OMe)$ were obtained in low yield (< 5% each) from the mixture where R = Me, therefore clean isolation in sufficient quantity for spectroscopic characterization proved problematic. X-ray analysis of a single crystal of $Zr(NP^tBu_3)_3(OMe)$ only

provided sufficient information to indicate its structure, however, the data were too poor for a detailed discussion. This by-product likely resulted from trace methanol originating from the synthesis of the ligand precursor, although when the experiment was repeated with meticulously dried HNP^tBu_3, intractable mixtures still resulted. Subsequently, $Zr(NP^tBu_3)_3(NMe_2)$ (**5.2**), was prepared in the absence of side-products via salt metathesis from $Zr(NP^tBu_3)_3Cl$ (**5.8**) and $LiNMe_2$ in moderate yield (Figure 5.3). It is also worth mentioning that the synthesis of $Zr(NP^tBu_3)_3Cl$ (**5.8**) was optimized by reacting three equivalents of $LiNP^tBu_3$ with $ZrCl_4$ in THF rather than in toluene as was previously performed,[203] and subject to work-up, provided exclusively the desired product.

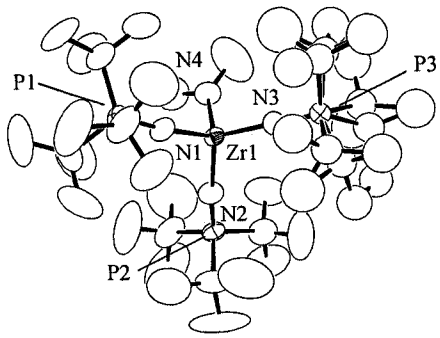

Figure 5.2: An ORTEP depiction of $Zr(NP^tBu_3)_3(NMe_2)$ (**5.2**) (50% thermal ellipsoids). One of the *t*-butyl groups is disordered, and both crystallographic positions are indicated.

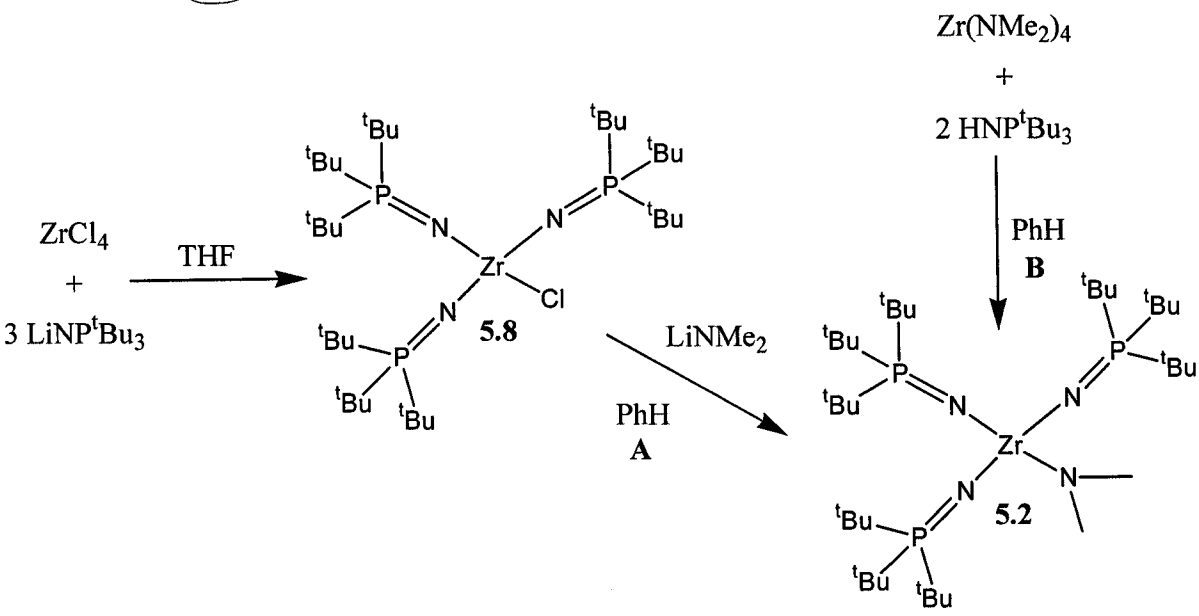

Figure 5.3: Different routes for the synthesis of $Zr(NP^tBu_3)_3(NMe_2)$ (**5.2**).

Table 5.2: Key bond distances and angles from X-ray analyses of $Zr(NP^tBu_3)_2(NEt_2)_2$ (**5.1**) and $Zr(NP^tBu_3)_3(NMe_2)$ (**5.2**).

Compound	Zr-N Å (amide)	Zr-N Å (phosphinimide)	N-P Å	Zr-N-P °
$Zr(NP^tBu_3)_2(NEt_2)_2$	2.04(2)	1.99(1)	1.54(2)	175.4(9)
(**5.1**)	2.08(2)	2.03(2)	1.60(1)	178(1)
$Zr(NP^tBu_3)_3(NMe_2)$	2.068(6)	2.005(6)	1.553(6)	171.1(4)
(**5.2**)		2.020(5)	1.552(5)	170.1(4)
		2.022(6)	1.547(6)	176.2(4)

A mixture of compounds was also obtained when $Zr(NEt_2)_2Cl_2{\cdot}THF_2$ was reacted with HNP^tBu_3 in aromatic solvents at ambient temperature. The synthesis of $Zr(NP^tBu_3)_2(NEt_2)_2$ (**5.1**) was achieved in good yield (93%), however, upon thermolysis of $Zr(NEt_2)_4$ with two equivalents of HNP^tBu_3 in toluene. X-ray quality crystals of the pentanes-soluble product (*ca.* 1 g in 2 mL) were grown from pentanes at -35°C (Table 5.2), and in combination with ^1H NMR spectroscopy, confirmed that free diethylamine was not coordinated to the monomeric zirconium centre. Coordination of volatile dialkylamines to the metal centre that have been liberated through the course of the reaction has been observed in related protonation experiments.[256,331-333] Of interest are the angles of the ligands with respect to the zirconium centre: both phosphinimide zirconium angles approach linearity (Table 5.2), and the two amide ligands are nearly planar (Zr-N-C: 120(1)°, 129(1)° and 130(2)°, 119(1)°).

The preparation of $Zr(NP^tBu_3)_2Cl_2$ (**5.7**) was subsequently achieved by reaction of the *bis*(amide) precursor $Zr(NP^tBu_3)_2(NEt_2)_2$ (**5.1**) with an excess of Me_3SiCl through exclusive cleavage of the amide ligands. Further, the synthesis of $Zr(NP^tBu_3)_2Me_2$ (**5.12**) was attempted using a number of methods. In an analogous fashion to a route that Gibson and co-workers successfully employed,[256] $Zr(NP^tBu_3)_2(NEt_2)_2$ (**5.1**) was treated with five equivalents of TMA for 30 minutes under mild conditions. Following the appropriate workup, the result was the isolation of the previously characterized complex

$Al_2(NP^tBu_3)Me_5$ (Figure 5.4).[xvi] Traditional routes involving addition of methyl lithium or methyl Grignard reagent to the dichloride metal precursor were also unsuccessful.

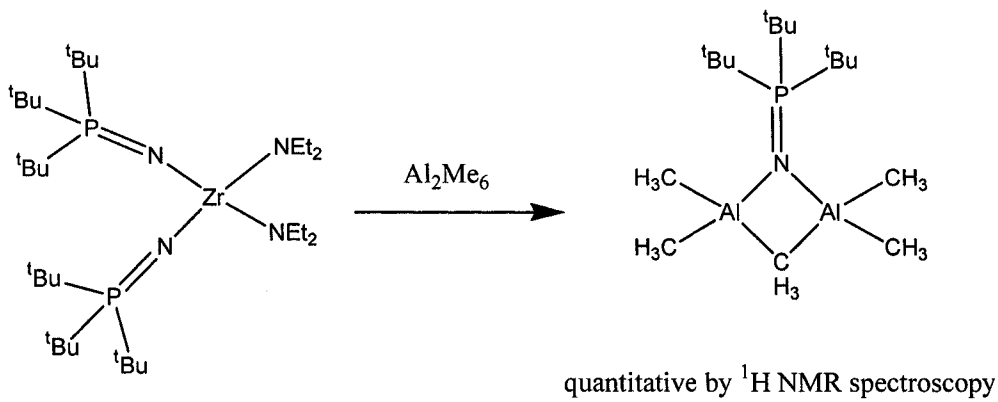

Figure 5.4: Cleavage of the phosphinimide bond from zirconium by TMA.

As a complement to $ZrCp^*(NP^tBu_3)Cl_2$ and the ensuing alkyl and aryl derivatives that were prepared by Dr. Fred Guérin and Ms. Nancy Yue, $ZrCp(NP^tBu_3)Cl_2$ (**5.3**) was analogously synthesized from reaction of one equivalent of $LiNP^tBu_3$ with $[ZrCpCl_3]_n$.[12] When two equivalents of the lithium salt were employed, isolation of $ZrCp(NP^tBu_3)_2Cl$ (**5.5**) was also feasible. In addition, $ZrCp_2(NP^tBu_3)Cl$ (**5.6**) was accessible by the reaction of Schwartz's reagent, $ZrCp_2HCl$, with HNP^tBu_3. All of the chloride Cp zirconium derivatives (Figure 5.5) were characterized by X-ray crystallography (Table 5.3). In addition, a 1:1 ratio of $ZrCp(NP^tBu_3)_2Cl$ (**5.5**) and its water adduct $ZrCp(NP^tBu_3)_2Cl{\cdot}H_2O$ (**5.5·H₂O**) co-crystallized, although no evidence of the two distinct products was observed by NMR spectroscopy. These results are somewhat dubious however, since the X-ray data is poor. Elemental (CHN) analysis successfully differentiated between **5.5**, and the sample contaminated by the water adduct. All attempts to deliberately prepare the water adduct by addition of stoichiometric amounts of water were unsuccessful. The source of water (if it was indeed present) likely originated from the solvent of crystallization, hence the reason all solvents "dried" on

[xvi] J. E. Kickham, unpublished results.

Grubbs'-type purification columns[235] were further distilled (from this point on) from the appropriate drying reagent.

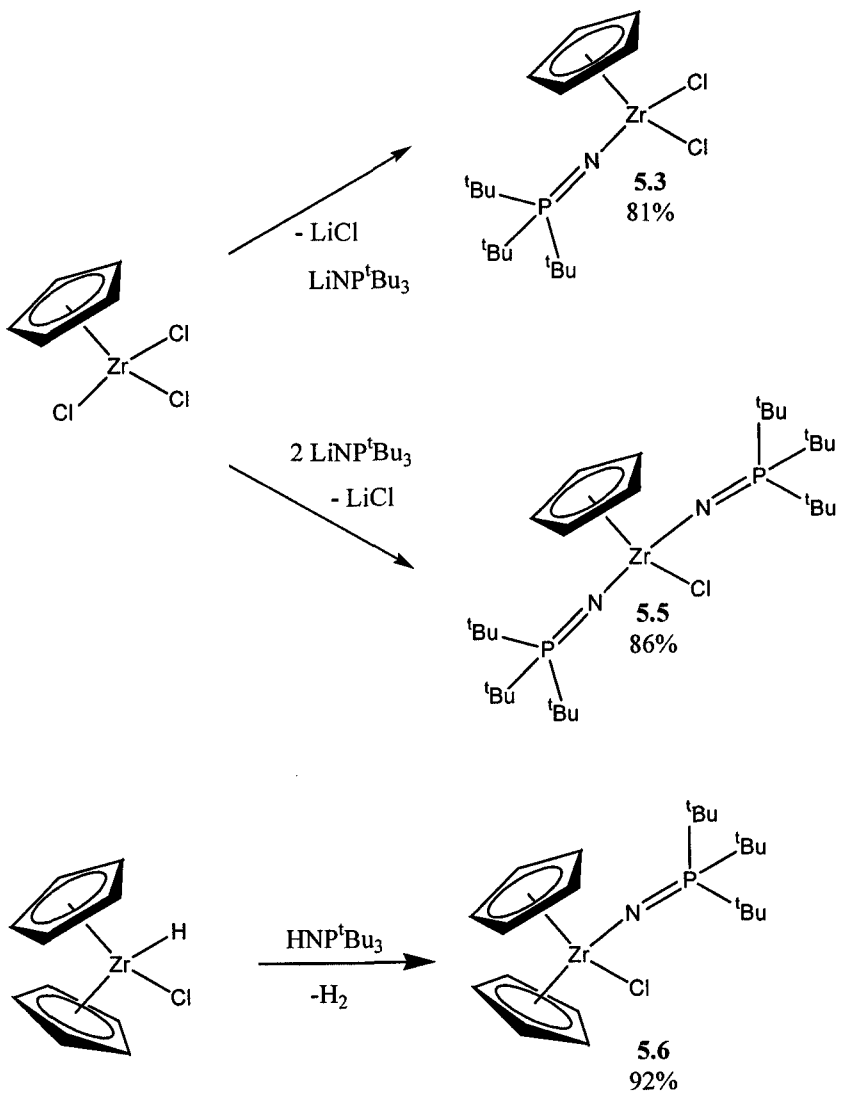

Figure 5.5: Synthesis of assorted zirconium phosphinimide chloride derivatives.

Table 5.3: Key bond distances and angles from X-ray analyses of various zirconium phosphinimide chloride complexes.

Compound	Zr-Cl Å	Zr-N Å	N-P Å	Zr-NP °
$ZrCp(NP^tBu_3)Cl_2$ (**5.3**)	2.418(2) 2.410(2)	1.902(5)	1.588(5)	174.8(4)
$ZrCp^*(NP^tBu_3)Cl_2$ (**5.4**)	2.442(1) 2.431(1)	1.923(2)	1.593(2)	163.5(1)
$ZrCp^*(NP^iPr_3)Cl_2$[a]	2.581(2) 2.559(3)	1.926(7)	1.569(7)	175.2(4)
$ZrCp^*Cp(NP^tBu_3)Cl$[a]	2.5070(8)	1.976(2)	1.565(2)	161.2(2)
$ZrCp_2(NP^tBu_3)Cl$ (**5.6**)	2.511(3)	1.978(5)	1.583(5)	171.9(3)
$Zr(NP^tBu_3)_3Cl$ (**5.8**)[b]	2.460(1)	1.989(2) 1.988(3) 1.993(2)	1.558(3) 1.560(3) 1.556(2)	167.7(2) 164.2(2) 164.8(2)

a) Yue, N. L. S.; Hollink, E.; Guérin, F.; Stephan, D. W. *Organometallics* **2001**, *20*, 4424-4433.

b) Guérin, F.; Stewart, J. C.; Beddie, C.; Stephan, D. W. *Organometallics* **2000**, *19*, 2994-3000.

Derivatization of the chloride precursors using an excess of the appropriate Grignard reagent resulted in an archive of alkyl and aryl derivatives. The methyl-containing products $ZrCp(NP^tBu_3)Me_2$ (**5.9**), $ZrCp(NP^tBu_3)_2Me$ (**5.10**) and $ZrCp_2(NP^tBu_3)Me$ (**5.11**) were prepared for the purposes of olefin polymerization and stoichiometric reactions with Lewis acids. All formulations were supported by spectroscopic data, although microanalyses of the alkyl derivatives were plagued by low carbon values from side reactions that occur during the combustion process – probably due to formation of zirconium carbides.[334,335] Additional alkyl and phenyl derivatives that were prepared in this fashion include $ZrCp(NP^tBu_3)R_2$ (R = Bn (**5.13**), CH_2SiMe_3 (**5.16**), Ph (**5.17**)), $ZrCp^*(NP^tBu_3)Bn_2$ (**5.14**) and $ZrCp(NP^tBu_3)_2Bn$ (**5.15**). Spectroscopic characterization of the aforementioned compounds was performed, and the data supports the formulations in all cases. Of interest is that the diastereotopic

methylene protons in the half-sandwich complexes $ZrCp(NP^tBu_3)Bn_2$ (**5.13**), $ZrCp^*(NP^tBu_3)Bn_2$ (**5.14**) and $ZrCp(NP^tBu_3)(CH_2SiMe_3)_2$ (**5.16**) exhibited an AB quartet in the ^1H NMR spectra, with ^2J values of 10-11 Hz. In addition, $ZrCp(NP^tBu_3)Bn_2$ (**5.13**) and $ZrCp(NP^tBu_3)_2Bn$ (**5.15**) were further characterized by X-ray methods (Figure 5.6).

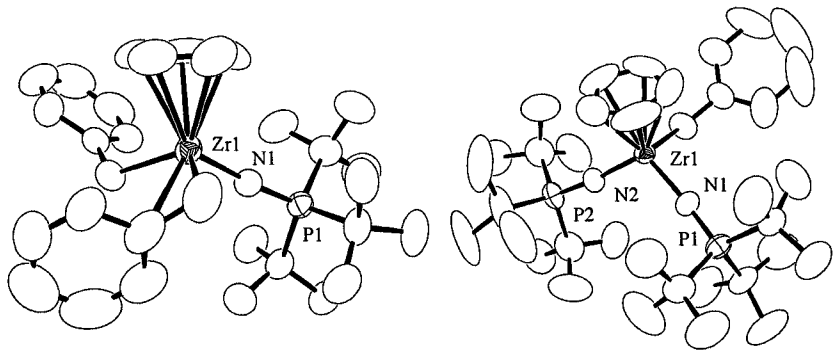

(5.13) **(5.15)**

Figure 5.6: ORTEP drawings of $ZrCp(NP^tBu_3)Bn_2$ (**5.13**) and $ZrCp(NP^tBu_3)_2Bn$ (**5.15**) (50% thermal ellipsoids).

In the X-ray structure of $ZrCp(NP^tBu_3)Bn_2$ (**5.13**), one of the benzyl ligands is coordinated in an η^2 fashion; this bonding mode has been observed in a number of related compounds such as $Zr(O\text{-}2,6\text{-}^tBu_2C_6H_3)Bn_3$,[336] $Zr[C_5H_4(RMe_2CH_2Ph)]Bn_3$, (R = C,[337] Si[338]), $Zr(p\text{-}^tBuCH_2Ph)_4$[339] and $HfCp^*Bn_3$.[340] The Zr-C_{ipso} bond distance of 2.779(3) Å, and Zr-C-C_{ipso} angle of 90.9(2)° fall within the acceptable range for η^2-bound benzyl groups (Zr-C_{ipso} <2.90 Å, Zr-C-C_{ipso} <100°).[341] In some instances, this may be duly interpreted as an electrophilic metal centre, although in other cases, factors such as solvent can play a role in this interaction in the solid state. An interesting comparison of two different X-ray analyses of $Zr\{CyNC[N(SiMe_3)_2]NCy\}Bn_3$ was performed when the complex was crystallized from pentanes and toluene, respectively resulting in the absence[341] or presence[342] of an η^2-coordinated benzyl group.

Additional evidence to support an electrophilic metal centre may be obtained from NMR spectroscopy. Rothwell and co-workers propose a significant upfield shift in the ^1H NMR spectrum for the *ortho* protons of the benzyl groups (< 6.8 ppm; "normal" region: 6.8-7.5 ppm), in addition to an increase in the $^1J_{CH}$ of the methylene fragment

(> 130 Hz).[336] Since the chemical shifts of the *ortho* protons from the benzyl groups for $ZrCp(NP^tBu_3)Bn_2$ (**5.13**), $ZrCp^*(NP^tBu_3)Bn_2$ (**5.14**) and $ZrCp(NP^tBu_3)_2Bn$ (**5.15**) are 7.22 ppm, 7.20 ppm and 7.38 ppm, respectively, and the $^1J_{CH}$ for the methylene group of $ZrCp(NP^tBu_3)Bn_2$ (**5.13**) is 120 Hz, we are not able to unequivocally state that the η^2-coordinated benzyl group is a result of an unusually electrophilic metal centre. Rather, it appears more likely this is a direct result of crystal packing forces.[341] In accordance with these observations, X-ray analysis of $ZrCp(NP^tBu_3)_2Bn$ (**5.15**) revealed an η^1-coordinated benzyl ligand (Figure 5.6).

Thermolysis of $ZrCp(NP^tBu_3)Bn_2$ (**5.13**), $ZrCp^*(NP^tBu_3)Bn_2$ (**5.14**), $ZrCp(NP^tBu_3)_2Bn$ (**5.15**) and $ZrCp(NP^tBu_3)(CH_2SiMe_3)_2$ (**5.16**) in the presence of pyridine to generate a transient alkylidene was attempted, although no reaction occurred, even upon heating to refluxing xylene temperatures for a week. This route has been used in several rare cases to produce a bridging[343] or terminal[344] zirconium carbene. In addition, thermolysis of $ZrCp(NP^tBu_3)Ph_2$ (**5.17**) in the presence of diphenylacetylene in an attempt to trap a benzyne intermediate also resulted in no reaction. Although a common pathway for the related zirconocene diphenyl derivatives,[345-348] Ms. Nancy Yue and co-workers observed the same lack of reactivity using $ZrCp^*(NP^tBu_3)Ph_2$ as a metal precursor.[349]

Stoichiometric reactions of Group IV olefin polymerization precatalysts with Lewis acids such as $B(C_6F_5)_3$ or $[Ph_3C][B(C_6F_5)_4]$ are commonly performed to generate a single active polymerization site.[92] Reaction of $ZrCp(NP^tBu_3)Me_2$ (**5.9**) with $B(C_6F_5)_3$ at room temperature resulted in the immediate formation of $ZrCp(NP^tBu_3)(C_6F_5)_2$ (**5.18**) as indicated by multinuclear NMR spectroscopy (Figure 5.7). Confirmation of this product was achieved by an independent synthesis from $ZrCp(NP^tBu_3)Cl_2$ (**5.3**) and the appropriate Grignard reagent, C_6F_5MgBr. Cleavage of the boron-C_6F_5 bond to afford polymerization-inactive Group IV compounds has been observed in a variety of cases such as $Zr(TMS_2Cp)_2(C_6F_5)Me$,[167] $Ti[CH_2(CH_2NAr)_2][CH_2B(C_6F_5)_2]C_6F_5$ (Ar = 2,6-$R_2C_6H_3$, R = Me, ^{i}Pr),[205] $[Ti(\eta^5,\eta^6\text{-}C_5H_4CMe_2Ar)(C_6F_5)Me][MeB(C_6F_5)_3]$ (Ar = 3,5-$Me_2C_6H_3$),[200] and the ketamide complex $TiCp'(NC^tBu_2)[CH_2B(C_6F_5)_2]C_6F_5$ (Cp' = Cp, Cp*).[350] Complete and instantaneous conversion to a *bis*(C_6F_5) Group IV derivative is rare, but not unprecedented. Similar reactivity has been observed from the reaction of

$Ti(NP^tBu_3)_3Me$ with one equivalent of $B(C_6F_5)_3$, which generated $Ti(NP^tBu_3)_2(C_6F_5)_2$ in good yield.[203]

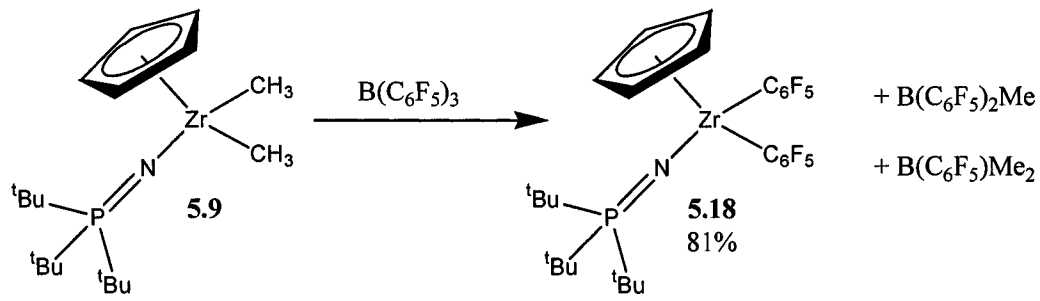

Figure 5.7: Formation of $ZrCp(NP^tBu_3)(C_6F_5)_2$ (**5.18**).

Successful isolation of cationic zirconium phosphinimide complexes was attained when the syntheses were performed in the presence of a Lewis base, or when sufficient steric bulk at the zirconium metal centre precluded ligand exchange reactions. When $ZrCp'(NP^tBu_3)Me_2$ (Cp' = Cp (**5.9**), Cp*[12]) was treated with $B(C_6F_5)_3$ in the presence of the carbodiimide $^iPrNCN^iPr$, migration of a methyl group occurred to afford the four-coordinate amidinate cations $[ZrCp'(NP^tBu_3)(N^iPrC(CH_3)N^iPr)][MeB(C_6F_5)_3]$ (Cp' = Cp (**5.20**), Cp* (**5.21**)), which appear indefinitely stable under a nitrogen atmosphere (Figure 5.8). Similarly, reaction of $ZrCp(NP^tBu_3)Me_2$ (**5.9**) with $B(C_6F_5)_3$ in the presence of ten equivalents of tetrahydrofuran permitted the isolation of $[ZrCp(NP^tBu_3)Me(THF)][MeB(C_6F_5)_3]$ (**5.22**) (Figure 5.8). In all three cases, the methyl group attached to the boron centre were clearly distinct in the ^1H and $^{13}C\{^1H\}$ NMR spectra, giving rise to broad proton signal at ~0.5 ppm, and a broad quartet in the $^{13}C\{1H\}$ NMR spectra at ~10 ppm with $^1J_{B-C}$ values of 50 Hz for **5.20** and **5.21** and 20 Hz for **5.22**. Increased steric protection at the zirconium centre, in combination with a larger alkyl substituent, also facilitated generation of the cation $[ZrCp(NP^tBu_3)_2][BnB(C_6F_5)_3]$ (**5.19**) when $ZrCp(NP^tBu_3)_2Bn$ was treated with $B(C_6F_5)_3$. The methylene protons gave rise to a broadened signal in the ^1H NMR spectrum, and the sharp ^{11}B NMR signal at -16.6 ppm confirmed a tetracoordinate boron environment.[351]

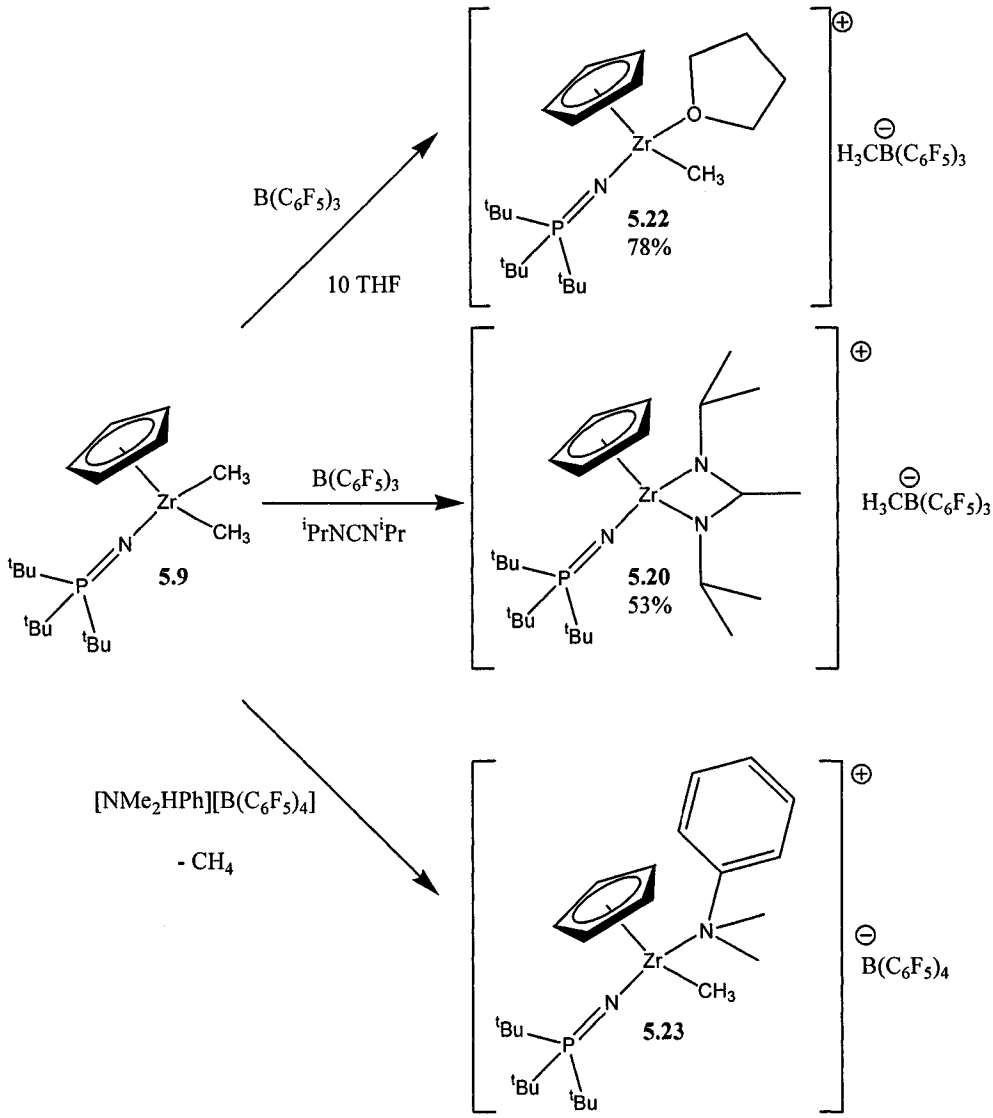

Figure 5.8: Synthesis of isolable cationic zirconium phosphinimide complexes.

Alternatively, the use of reagents that formally abstract or protonate off a methide ligand, such as $[Ph_3C][B(C_6F_5)_4]$ or $[NMe_2HPh][B(C_6F_5)_4]$, tend to generate cationic zirconium phosphinimide complexes that are unstable relative to products produced from the aforementioned routes. Only two such examples were prepared cleanly from reaction of the appropriate metal precursor $ZrCp'(NP^tBu_3)Me_2$ (Cp' = Cp (**5.9**), Cp*[12]) with the Lewis acid salt at low temperature (-35°C) to generate $[ZrCp(NP^tBu_3)Me(NMe_2Ph)][B(C_6F_5)_4]$ (**5.23**) (Figure 5.8) and

$[ZrCp^*(NP^tBu_3)Me][B(C_6F_5)_4]$ (**5.24**). Both complexes were stable long enough to characterize by NMR spectroscopy, although they decomposed rapidly in solution (within 1-2 days) to an intractable mixture of products.

In an effort to model the reactivity of the metal complex with methylaluminoxane (MAO) before using it as an activator in ethylene polymerization experiments,[9,12,13,16,18,233,234] $ZrCp(NP^tBu_3)Cl_2$ (**5.3**) was reacted with trimethylaluminum (TMA). This appears to be a reasonable model based on the work of Ziegler and co-workers, which suggests that TMA plays a role in the active/dormant olefin polymerization catalyst equilibrium process.[97] When Ms. Nancy Yue treated $ZrCp^*(NP^tBu_3)Cl_2$ (**5.4**) with TMA, numerous products were produced, two of which were identified as Zr (IV) cluster compounds.[12] Based on the similarities of features in the NMR spectra, the trimer $[ZrCpCl_2]_3CH$ (**5.25**) is proposed to be the result of the quantitative conversion of $ZrCp(NP^tBu_3)Cl_2$ (**5.3**) when reacted with TMA (Figure 5.9). The ^1H NMR spectrum possesses a signal at 15.9 ppm, which correlates (HMQC) to a carbon signal of 336.1 ppm. Performance of a DEPT 90 experiment confirmed that the shift at 336.1 ppm in the $^{13}C\{^1H\}$ NMR spectrum was due to a tertiary carbon atom. A trimer is proposed based on the integration of the methine proton with respect to the Cp protons, and is likely accommodated based on its relative size compared to Cp*, which produces zirconium clusters that possess four or five transition metal atoms.

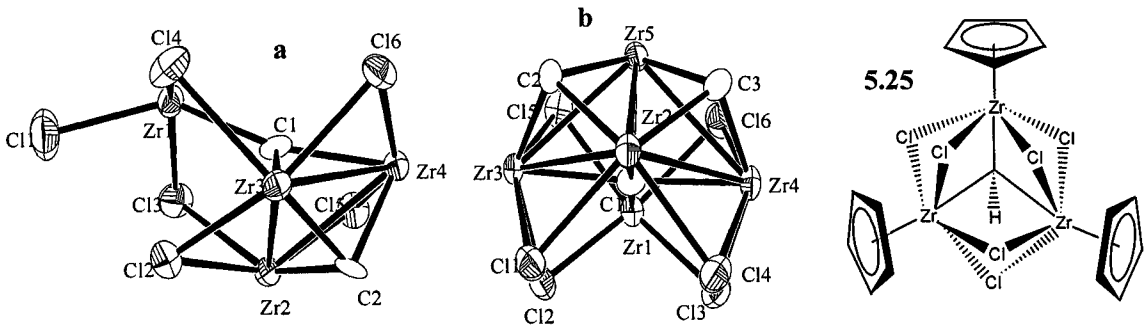

Figure 5.9: ORTEP depictions of the heavy atom cores (50% thermal ellipsoids) of Zr IV cluster derivatives derived from the reaction of $ZrCp^*(NP^tBu_3)Cl_2$ (**5.4**) with TMA (a, b)[12] compared with the proposed product $[ZrCpCl_2]_3CH$ (**5.25**).

Utility as Ethylene Polymerization Catalysts

The polymerization experiments and treatment of the polymer samples were performed in a similar manner described in Section 4.3. Only the Büchi reactor was used to determine the relative polymerization activities, however, since the data obtained from these experiments is more reliable due better control of variables such as temperature, stir rate and ethylene pressure. Preliminary screening using $ZrCp'(NP^tBu_3)X_2$ (Cp' = Cp, X = Cl (**5.3**), Me (**5.9**); Cp' = Cp*, X = Cl (**5.4**), Me[12]) and MAO as a solvent scrubber/activator resulted in moderate polymerization activities (Table 5.4) relative to the zirconocene standards. For comparative purposes, the analogous titanium precursors were also tested under identical conditions, and the polymerization results are reported with the values obtained using industrial zirconocene standards (Table 5.4). Modeling experiments with TMA demonstrate that the zirconium phosphinimide complexes react immediately at ambient temperature, but the titanium versions do not react with TMA unless heated for prolonged periods of time. Since the zirconium polymerization precursors react more rapidly with TMA, it appears likely that catalyst deactivation occurs in the presence of MAO. This would preclude high polymerization activities for the 30 minute period in which the polymerizations were conducted. In addition, this rationale could also account for why the zirconium precursors are much less active than their titanium analogues under these conditions.

Table 5.4: Comparison of the polymerization activities using $MCp'(NP^tBu_3)X_2$ (M = Ti, Zr; Cp' = Cp, Cp*; X = Cl, Me) as a precursor and activated by MAO.[a]

Precatalyst	Activity	M_n	M_w	PDI
$TiCp(NP^tBu_3)Cl_2$	890	364,200	686,700	1.89
$ZrCp(NP^tBu_3)Cl_2$ (**5.3**)	100	3,450	234,300	67.91
$TiCp^*(NP^tBu_3)Cl_2$	650	60,500	149,500	2.47
$ZrCp^*(NP^tBu_3)Cl_2$ (**5.4**)	50	3,070[b] 783,900	5,930[b] 1,261,000	1.93[b] 1.61
$TiCp(NP^tBu_3)Me_2$	735	465,900	812,000	1.74
$ZrCp(NP^tBu_3)Me_2$ (**5.9**)	90	36,500	94,300	2.58
$TiCp^*(NP^tBu_3)Me_2$	550	93,800	203,700	2.17
$ZrCp^*(NP^tBu_3)Me_2$	60	5,260	172,400	32.78[c]
$ZrCpCl_3$	10	9,480	313,600	33.08
$ZrCp_2Cl_2$	600	161,100	340,800	2.12
$ZrCp_2Me_2$	780	99,400	221,200	2.23

a) MAO activation, Ti/Zr:Al ratio 1:500, PhMe solvent, 30°C, 1.82 atm C_2, 50 μM precatalyst, 30 min, M_n and M_w in g mol^{-1}, activity in g $mmol^{-1}h^{-1}atm^{-1}$.

b) Two different polymer fractions of sufficient separation were observed from a single sample, thus the mathematical analysis was performed on each curve.

c) The majority of the polymer sample was lower molecular weight material; the PDI value is skewed due to the presence of a small fraction (< 10%) of high molecular weight polymer (M_z = 2,019,000 g mol^{-1}).

The polymer produced in the ethylene polymerization screening of $ZrCp(NP^tBu_3)Cl_2$ (**5.3**) and $ZrCp^*(NP^tBu_3)Cl_2$ (**5.4**) using MAO as activator were examined by GPC to determine the molecular weight distributions. The polymer produced by the catalyst derived from $ZrCp(NP^tBu_3)Cl_2$ (**5.3**) had an extremely high PDI of 67.91 which is indicative of multiple active sites, and is consistent with the proposed catalyst decomposition by MAO. The polymer produced using $ZrCp^*(NP^tBu_3)Cl_2$ (**5.4**) as precatalyst had a similar molecular weight distribution to the polymer produced from a blank experiment using $ZrCpCl_3$ as the catalyst precursor under identical conditions.

This suggests that a possible decomposition route may be abstraction of the phosphinimide ligand from the zirconium centre. The polymer produced by $ZrCp^*(NP^tBu_3)Cl_2$ (**5.4**) under these conditions had a distinct bimodal distribution; the lower molecular weight fraction has an M_n value of 3,070 g mol^{-1} which is reminiscent of the M_n value of 3,450 g mol^{-1} obtained from the polymerization catalyst derived from **5.3**. However, it was accompanied by a higher molecular weight fraction with M_n = 783,900 g mol^{-1}; this is likely indicative of two distinct ethylene polymerization catalysts derived from a single zirconium precursor. It should also be noted that the polymerization activity resulting from the use of $ZrCpCl_3$ as the catalyst precursor is significantly lower (*ca.* 10 times less active) then that obtained using $ZrCp'(NP^tBu_3)Cl_2$ (Cp' = Cp, Cp*), which indicates that the phosphinimide ligand does serve to increase the polymerization activity.

Conversely, when polymerizations were attempted using $Zr(NP^tBu_3)_2X_2$ (X = NEt_2 (**5.1**), Cl (**5.6**)) as a precatalyst and MAO as an activator, only moderate activities were attained (Table 5.5). In addition, the polymerization activities and polymer properties were the same, within experimental error, as the results obtained using the analogous titanium derivative $Ti(NP^tBu_3)_2Cl_2$. Given these findings, in combination with those observed in Section 3.3, it appears as though Group IV half-sandwich phosphinimide complexes are more valuable as olefin polymerization catalysts then those that possess two phosphinimide ancillary ligands.

Table 5.5: Comparison of the polymerization activities using $M(NP^tBu_3)_2X_2$ (M = Ti, Zr; X = Cl, Me) as a precursor when activated by MAO.[a]

Precursor	Activity	M_n	M_w	PDI
$Zr(NP^tBu_3)_2(NEt_2)_2$ (**5.1**)	Trace	b	b	b
$Ti(NP^tBu_3)_2Cl_2$	60	37,300	426,800	11.44
$Zr(NP^tBu_3)_2Cl_2$ (**5.6**)	55	18,300	197,000	10.77
$ZrCp_2Cl_2$	1830	95,100	293,300	3.08

a) PhMe solvent, 30°C, 1.82 atm C_2, 50 μM precatalyst, 10 min, MAO Ti/Zr:Al ratio 1:500, M_n and M_w in g mol^{-1}, activity in g $mmol^{-1}h^{-1}atm^{-1}$.

b) Too little polymer to analyze.

In an effort to achieve higher polymerization activities, the method of activation was modified to incorporate 20 equivalents of tri*iso*butylaluminum (T^iBAl) as a solvent purification agent, and two equivalents of $B(C_6F_5)_3$ or $[Ph_3C][B(C_6F_5)_4]$ as a co-catalyst. Often, substitution of the co-catalyst effectively tempers the polymerization activities based on counterion effects or rates of catalyst lifetimes, in addition to modulating the properties of the polymers that are produced.[92] In addition, these experiments were performed for ten minute intervals, with one notable exception; by performing the polymerizations of extremely active catalysts for shorter intervals of time or under more dilute catalyst conditions, issues that arise from insufficient saturation of the catalyst with monomer are minimized.[352] For example, the polymerization reactor may become so plugged with polymer after 5-10 minutes that the ethylene flow may decelerate or even be quenched, resulting in an activity that is underestimated. For the purpose of comparison, the titanium analogues were also subjected to the same polymerization conditions.

When the metal precursors $MCp'(NP^tBu_3)Me_2$ (M = Ti, Cp' = Cp[8], Cp*[21]; M = Zr Cp' = Cp (**5.18**), Cp*[12]) and $ZrCp(NP^tBu_3)Bn_2$ (**5.13**) were activated by $B(C_6F_5)_3$, an increase in polymerization activity relative to activation by MAO was observed. As illustrated when MAO was used as an activator, the titanium derivatives were more active than their zirconium counterparts. Interestingly however, the polymerization activity

decreased slightly upon addition of steric bulk on the Cp substituent from $ZrCp^*(NP^tBu_3)Me_2$ to $ZrCp(NP^tBu_3)Me_2$ (**5.8**), which contradicts the observations with the analogous titanium derivatives (see Table 5.6).

In addition, when $ZrCp(NP^tBu_3)Bn_2$ (**5.13**) was used as a catalyst precursor and activated by $B(C_6F_5)_3$, the polymerization activity is double that of the corresponding dimethyl complex $ZrCp(NP^tBu_3)Me_2$ (**5.8**). This may be accounted for by two different explanations. Bochmann and co-workers have observed that the zirconium cation behaves differently with the anion if a dimethyl *vs.* a dibenzyl metal precursor is employed (Figure 5.10).[187] This in turn, plays a crucial role in the subsequent polymerization activities. Another possible explanation for the lower polymerization activity that arose using $ZrCp(NP^tBu_3)Me_2$ (**5.8**) as a catalyst precursor with $B(C_6F_5)_3$ is the ease of formation of $ZrCp(NP^tBu_3)(C_6F_5)_2$ (**5.18**) (*vide supra*). Unfortunately, efforts to cleanly isolate the zwitterion derived from the reaction of $ZrCp(NP^tBu_3)Bn_2$ (**5.13**) with $B(C_6F_5)_3$ were unsuccessful, however, the absence of evidence of $ZrCp(NP^tBu_3)(C_6F_5)_2$ (**5.18**) by multinuclear NMR spectroscopy is a key observation that further suggests the reactivity of the two alkyl precursors is not the same.

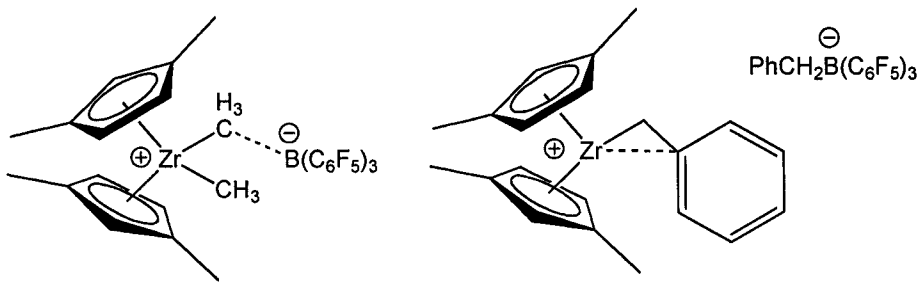

Figure 5.10: Diversity of the anion-cation interaction upon modification of alkyl groups that are σ-bound to the zirconium centre.[187]

Table 5.6: Comparison of the polymerization activities using $MCp'(NP^tBu_3)Me_2$ (M = Ti, Zr; Cp' = Cp, Cp*) as a precursor when activated with 2 equivalents of $B(C_6F_5)_3$ or $[Ph_3C][B(C_6F_5)_4]$.[a]

Precatalyst	Activator	Activity	M_n	M_w	PDI
$TiCp(NP^tBu_3)Me_2$	$B(C_6F_5)_3$	1500	130,700	547,100	4.19
$ZrCp(NP^tBu_3)Me_2$ (**5.8**)	$B(C_6F_5)_3$	400	6,640	94,900	14.29
$ZrCp(NP^tBu_3)Bn_2$ (**5.13**)	$B(C_6F_5)_3$	760	8,720	263,800	30.25
$TiCp^*(NP^tBu_3)Me_2$	$B(C_6F_5)_3$	1030	67,200	151,800	2.26
$ZrCp^*(NP^tBu_3)Me_2$	$B(C_6F_5)_3$	270	59,900	161,300	2.69
$ZrCp_2Me_2$	$B(C_6F_5)_3$	1740	69,500	192,300	2.77
$TiCp(NP^tBu_3)Me_2$	$Ph_3CB(C_6F_5)_4$	2155[b]	44,700	151,500	3.39
$ZrCp(NP^tBu_3)Me_2$ (**5.8**)	$Ph_3CB(C_6F_5)_4$	1270	7,450	24,400	3.28
$ZrCp(NP^tBu_3)Bn_2$ (**5.13**)	$Ph_3CB(C_6F_5)_4$	940	6,120	76,600	12.52
$TiCp^*(NP^tBu_3)Me_2$	$Ph_3CB(C_6F_5)_4$	7690[c]	194,000	632,700	3.26
$ZrCp^*(NP^tBu_3)Me_2$	$Ph_3CB(C_6F_5)_4$	1010	54,200	177,000	3.27
$ZrCp_2Me_2$	$Ph_3CB(C_6F_5)_4$	1010	171,000	334,800	1.96

a) Ti/Zr:Al ratio 1:20 (T^iBAl), PhMe solvent, 30°C, 1.82 atm C_2, 50 μM precatalyst, 10 min, M_n and M_w in g mol^{-1}, activity in units of g $mmol^{-1}h^{-1}atm^{-1}$.

b) Polymerization was quenched after 7 min since the temperature had spiked to 47°C and was still increasing at a relatively rapid rate.

c) Polymerization was quenched after 2.5 min since the temperature had spiked to 73°C and was still increasing at a rapid rate. Therefore, this activity is slightly inflated, although it is clear that this catalyst is extremely active under these polymerization conditions.

When $MCp'(NP^tBu_3)Me_2$ (M = Ti, Cp' = Cp[8], Cp*[21]; M = Zr, Cp' = Cp (**5.18**), Cp*[12]) were activated by $[Ph_3C][B(C_6F_5)_4]$, the polymerization activities increased significantly to become similar to, or even surpass the activity of the zirconocene standard (Table 5.6). This is a notable result, especially given the activities that result upon activation by MAO. In addition to producing catalysts that display very high polymerization activities, the catalysts derived from $MCp(NP^tBu_3)Me_2$ (M = Ti, Zr (**5.8**))

are in the same order of magnitude of the standard, which represents a breakthrough in ethylene polymerization catalysis by zirconium phosphinimide complexes. Admittedly, $ZrCp^*(NP^tBu_3)Me_2$ is also in the same range, however, the titanium analogue is extremely active under these polymerization conditions; the experiments had to be interrupted after 2.5 minutes since the temperature of the vessel had exceeded 70°C (a 40°C temperature spike in 2 minutes!), and showed no sign of stabilizing. Therefore, the activity of 7690 g polymer $mmol^{-1}$ h^{-1} atm^{-1} is likely inflated, and the (necessary) preliminary termination of the polymerization experiment attests to its unusually high activity.

5.4 Summary

A series of zirconium phosphinimide complexes of general formulae $Zr(NP^tBu_3)_2X_2$ and $ZrCp(NP^tBu_3)X_2$ have been prepared in a straightforward manner in good yields. Subsequent reaction of the half-sandwich precursors with co-catalysts and Lewis acids commonly employed in olefin polymerization has demonstrated atypical reactivity, such as the immediate, quantitative formation of $ZrCp(NP^tBu_3)(C_5F_5)_2$ (**5.18**) or $[ZrCpCl_2]_3CH$ (**5.25**). In addition, several cationic derivatives of zirconium phosphinimide complexes have been isolated and characterized by microanalysis and multinuclear NMR spectroscopy. The isolation of such compounds proved more challenging than their corresponding zirconocene derivatives due to the presence of the phosphinimide bond, and in several cases, precluded successful isolation of clean products.

Subsequent polymerization testing using $Zr(NP^tBu_3)_2X_2$ and $ZrCp(NP^tBu_3)X_2$ as catalyst precursors, upon activation with MAO, resulted only in moderate activities. However, the use of $ZrCp'(NP^tBu_3)R_2$ (Cp' = Cp, R = Me, Bn; Cp' = Cp*, R = Me) as catalyst precursors produced highly active polymerization catalysts upon activation with $B(C_6F_5)_3$ or $[Ph_3C][B(C_6F_5)_4]$ in the presence of low concentrations of T^iBAl as a solvent scrubber. This indicates that zirconium phosphinimide derivatives have potential to be

good ethylene polymerization catalysts if the appropriate polymerization conditions are developed.

6 Summary

Optimized synthetic strategies to an array of Group IV complexes that possess phosphinimide ligands have been detailed, and when applicable, their efficacy as catalysts for hydroamination or olefin insertion polymerization has been evaluated. Throughout the search for potential applications, modifications to the catalyst testing protocol were performed when required to increase the efficiency of the systems examined.

Initially, Group IV imide complexes that include a phosphinimide ancillary ligand were targeted for the purposes of performing organic transformations or inducing atypical reactivity. A Group IV phosphinimide imide complex was not isolated, however, a series of inorganic and organometallic Group IV complexes that possess amide and phosphinimide ligands was prepared by both traditional and unanticipated routes. Attempts to coerce reactivity as hydroamination catalysts were ineffective, but treatment of the half-sandwich precursor $TiCp(NP^tBu_3)(NH(2,6\text{-}^iPr_2)C_6H_3)Cl$ with TMA afforded methyl-for-amide exchange to cleanly provide $TiCp(NP^tBu_3)MeCl$, proffering evidence that the amide ligand is more labile than the phosphinimide ligand under the conditions employed.

Of consequence was the preparation of two magnesium phosphinimide complexes that were isolated in an attempt to synthesize a "softer" phosphinimide transfer reagent. Characterization of the molecular species in solution and in the solid state indicate that the structure changes from dimeric to trimeric upon reduction of the steric bulk of the ligands from *t*-butyl to *i*-propyl. Interestingly, the dimer $Mg_2(\mu\text{-}NP^tBu_3)_2(NP^tBu_3)_2$ served as an initiator for the polymerization of methyl methacrylate at ambient temperature while the trimer $Mg_3(\mu\text{-}NP^iPr_3)_4(NP^iPr_3)_2$ did not. Examination of the polymer suggested that its formation occurred by a radical process. Thus, the exploratory nature of this portion of the research resulted in a new application of phosphinimide complexes.

Next, reliable syntheses of titanium and zirconium complexes that incorporate chelating *bis*(phosphinimide) ligands were detailed. Reactivity studies with *bis*(phosphinimide) complexes of titanium, including testing as olefin polymerization

catalysts, were performed with limited success (see also Appendix B). In general, the efforts expended to obtain desirable reactivity from *bis*(phosphinimide) complexes of titanium were not in vain. Taken as a whole, the results simply imply that the analogous half-sandwich phosphinimide complexes are more practical catalytic precursors for the processes that were investigated.

The synthesis of a series of bimetallic titanium complexes of general formula *p*-$(CH_2PR_2NTiCp'X_2)_2C_6H_4$ (Cp' = Cp, Cp*; R = ^{t}Bu, Cy; X = Cl, Me), and their monometallic analogues, has been developed. Polymerization testing of these precursors proved insightful, since the polymerization activities increased in a predictable manner as the steric bulk of the ancillary ligands increased. Another important development was that the polymerization activities of the methyl precatalysts increased dramatically when the activation strategy was modified from using MAO to using $[Ph_3C][B(C_6F_5)_4]$. Of commercial significance was the discovery that the polymers produced from several of the monometallic or bimetallic catalysts activated by MAO possessed broad molecular weight distributions. Interestingly, the same bimetallic precatalysts produced polymer products that were relatively monodisperse (PDI < 3) upon activation with $[Ph_3C][B(C_6F_5)_4]$. These findings indicate that judicious choice of the alkyl group on the phosphinimide ligand, in combination with the proper catalyst activation strategy, can influence the type of polymer product that is prepared in a predictable fashion.

Finally, a synthetic route to zirconium half-sandwich phosphinimide complexes has been developed. Assessment of the ability of the zirconium analogues to function as olefin polymerization catalysts revealed that the activity depended largely on the mode of activation. However, under specific conditions, the polymerization activities rivalled that of the industrial standard $ZrCp_2Me_2$. A subsequent investigation of the reactivity of the metal precursors with stoichiometric amounts of strong Lewis acids such as TMA or $B(C_6F_5)_3$ identified possible decomposition pathways. This is of importance, since the information can be used to rationalize the activities observed using the different activators, and assist in the design of improved catalysts.

To summarize, new synthetic approaches have provided routes to a variety of Group IV phosphinimide complexes. In many cases, these new compounds demonstrated utility as precursors for olefin polymerization catalysis, and in some cases, they served to

generate commercially relevant polymers with very high activities following optimization of the experimental protocol. Exploration of the reactivity of Group IV phosphinimide complexes has also provided rationalization for the catalytic behaviour observed. In short, this thesis has identified key features that are beneficial for the design of successful titanium and zirconium phosphinimide polymerization catalyst precursors.

References

(1) Coates, G. W.; Waymouth, R. M. *Comprehensive Organometallic Chemistry II* **1995**, *12*, 1193-1208, and references therein.

(2) Bochmann, M. *Comprehensive Organometallic Chemistry II* **1995**, *4*, 273-431, and references therein.

(3) Ryan, E. J. *Comprehensive Organometallic Chemistry II* **1995**, *4*, 483-499, and references therein.

(4) Guram, A. S.; Jordan, R. F. *Comprehensive Organometallic Chemistry II* **1995**, *4*, 589-625, and references therein.

(5) Smith, S. B.; Stephan, D. W. *Comprehensive Coordination Chemistry II* **2003**, *3*, Chapter 2.

(6) Hollink, E.; Stephan, D. W. *Comprehensive Coordination Chemistry II* **2003**, *3*, Chapter 3.

(7) Stephan, D. W.; Guerin, F.; Spence, R. E. v. H.; Koch, L.; Gao, X.; Brown, S. J.; Swabey, J. W.; Wang, Q.; Xu, W.; Zoricak, P.; Harrison, D. G. *Organometallics* **1999**, *18*, 2046-2048.

(8) Stephan, D. W.; Stewart, J. C.; Guerin, F.; Spence, R. E. v. H.; Xu, W.; Harrison, D. G. *Organometallics* **1999**, *18*, 1116-1118.

(9) Carraz, C.-A.; Stephan, D. W. *Organometallics* **2000**, *19*, 3791-3796.

(10) Brown, S. J.; Gao, X.; Harrison, D. G.; McKay, I.; Koch, L.; Wang, Q.; Xu, W.; Von Haken Spence, R. E.; Stephan, D. W. In *PCT Int. Appl.*; (Nova Chemicals Corporation, Can.). Wo, **2000**, 33 pp.

(11) Von Haken Spence, R. E.; Stephan, D. W.; Brown, S. J.; Jeremic, D.; Wang, Q. In *PCT Int. Appl.*; (Nova Chemicals (International) S.A., Switz.). Wo, **2000**, 38 pp.

(12) Yue, N.; Hollink, E.; Guerin, F.; Stephan, D. W. *Organometallics* **2001**, *20*, 4424-4433.

(13) Stephan, D. W. *Macromolecular Symposia* **2001**, *173*, 105-115.

(14) Yue, N. L. S.; Stephan, D. W. *Organometallics* **2001**, *20*, 2303-2308.

(15) Spence, R. E. V. H.; Brown, S. J.; Wurz, R. P.; Jeremic, D.; Stephan, D. W. In *PCT Int. Appl.*; (Nova Chemicals (International) S.A., Switz.). Wo, **2001**, 81 pp.

(16) Kickham, J. E.; Guerin, F.; Stewart, J. C.; Urbanska, E.; Ong, C. M.; Stephan, D. W. *Organometallics* **2001**, *20*, 1175-1182.

(17) Brown, S. J.; Gao, X.; Kowalchuk, M. G.; Spence, R. E. v. H.; Stephan, D. W.; Swabey, J. *Can. J. Chem.* **2002**, *80*, 1618-1624.

(18) Kickham, J. E.; Guerin, F.; Stephan, D. W. *J. Am. Chem. Soc.* **2002**, *124*, 11486-11494.

(19) Stephan, D. W. *Can. J. Chem.* **2002**, *80*, 125-132.

(20) Stephan, D. W.; Stewart, J. C.; Brown, S. J.; Swabey, J.; William, J.; Wang, Q. In *US Patent*; Nova Chemicals (International) S.A.: US, **2002**; Vol. 6,342,463, p 17.

(21) Stephan, D. W.; Stewart, J. C.; Guerin, F.; Courtenay, S.; Kickham, J.; Hollink, E.; Beddie, C.; Hoskin, A.; Graham, T.; Wei, P.; Spence, R. E. v. H.; Xu, W.; Koch, L.; Gao, X.; Harrison, D. G. *Organometallics* **2003**, *22*, 1937-1947.

(22) Sarsfield, M. J.; Thornton-Pett, M.; Bochmann, M. *J. Chem. Soc., Dalton Trans.* **1999**, 3329-3330.

(23) Al-Benna, S.; Sarsfield, M. J.; Thornton-Pett, M.; Ormsby, D. L.; Maddox, P. J.; Bres, P.; Bochmann, M. *J. Chem. Soc., Dalton Trans.* **2000**, 4247-4257.

(24) Sarsfield, M. J.; Said, M.; Thornton-Pett, M.; Gerrard, L. A.; Bochmann, M. *J. Chem. Soc., Dalton Trans.* **2001**, 822-827.

(25) Said, M.; Thornton-Pett, M.; Bochmann, M. *J. Chem. Soc., Dalton Trans.* **2001**, 2844-2849.

(26) Said, M.; Thornton-Pett, M.; Bochmann, M. *Organometallics* **2001**, *20*, 5629-5635.

(27) Pohlki, F.; Heutling, A.; Bytschkov, I.; Hotopp, T.; Doye, S. *Synlett* **2002**, *5*, 799-801.

(28) Bochmann, M. *Nachrichten aus Chemie, Technik und Laboratorium* **1993**, *41*, 1220-1224, 1226-1228.

(29) Ashe, A. J., III; Al-Ahmad, S.; Kampf, J. W. *Phosphorus, Sulfur, Silicon Relat. Elem.* **1997**, *124 & 125*, 295-303.

(30) Bochmann, M. *J. Chem. Soc., Dalton Trans.* **1996**, 255-270.

(31) McKnight, A. L.; Waymouth, R. M. *Chem. Rev.* **1998**, *98*, 2587-2598.

(32) Britovsek, G. J. P.; Gibson, V. C.; Wass, D. F. *Angew. Chem. Int. Ed. Engl.* **1999**, *38*, 428-447, and references therein.

(33) Alt, H. G.; Koppl, A. *Chem. Rev.* **2000**, *100*, 1205-1222.

(34) Bochmann, M.; Lancaster, S. J.; Jimenez, G.; Walker, D. A.; Al-Benna, S.; Thornton-Pett, M. *Special Publication - Royal Society of Chemistry* **2000**, *253*, 10-19.

(35) Lee, D.-H.; Noh, S. K. *Korea Polymer Journal* **2001**, *9*, 71-83.

(36) Okuda, J.; Arndt, S.; Beckerle, K.; Hultzsch, K. C.; Voth, P.; Spaniol, T. P. *Organometallic Catalysts and Olefin Polymerization* **2001**, 156-165.

(37) Erker, G.; Kehr, G.; Strauch, J.; Temme, B.; Karl, J.; Dahlmann, M.; Helaja, T.; Frohlich, R.; Luftmann, H. *Polymeric Materials Science and Engineering* **2002**, *87*, 64-74.

(38) Coates, G. W.; Hustad, P. D.; Reinartz, S. *Angew. Chem. Int. Ed. Engl.* **2002**, *41*, 2236-2257.

(39) Coates, G. W. *J. Chem. Soc., Dalton Trans.* **2002**, 467-475.

(40) Gibson, V. C.; Spitzmesser, S. K. *Chem. Rev.* **2003**, *103*, 283-315, and references therein.

(41) Walsh, P. J.; Hollander, F. J.; Bergman, R. G. *J. Am. Chem. Soc.* **1988**, *110*, 8729-8731.

(42) Cummins, C. C.; Baxter, S. M.; Wolczanski, P. T. *J. Am. Chem. Soc.* **1988**, *110*, 8731-8733.

(43) Roesky, H. W.; Voelker, H.; Witt, M.; Noltemeyer, M. *Angew. Chem.* **1990**, *102*, 712-713.

(44) Mountford, P. *Chem. Commun.* **1997**, 2127-2134.

(45) Harlan, C. J.; Tunge, J. A.; Bridgewater, B. M.; Norton, J. R. *Organometallics* **2000**, *19*, 2365-2372.

(46) Asmus, S. M. F.; Regitz, M. *Tetrahedron Lett.* **2001**, *42*, 7543-7545.

(47) Ong, T.-G.; Yap, G. P. A.; Richeson, D. S. *J. Am. Chem. Soc.* **2003**, *125*, 8100-8101.

(48) Basuli, F.; Bailey, B. C.; Huffman, J. C.; Mindiola, D. J. *Chem. Commun.* **2003**, 1554-1555.

(49) Arney, D. J.; Bruck, M. A.; Huber, S. R.; Wigley, D. E. *Inorg. Chem.* **1992**, *31*, 3749-3755.

(50) Walsh, P. J.; Hollander, F. J.; Bergman, R. G. *Organometallics* **1993**, *12*, 3705-3723.

(51) Grigsby, W. J.; Olmstead, M. M.; Power, P. P. *J. Organomet. Chem.* **1996**, *513*, 173-180.

(52) Baranger, A. M.; Hollander, F. J.; Bergman, R. G. *J. Am. Chem. Soc.* **1993**, *115*, 7890-7891.

(53) Baranger, A. M.; Bergman, R. G. *J. Am. Chem. Soc.* **1994**, *116*, 3822-3835.

(54) Holland, P. L.; Andersen, R. A.; Bergman, R. G. *Organometallics* **1998**, *17*, 433-437.

(55) Bennett, J. L.; Wolczanski Peter, T. *J. Am. Chem. Soc.* **1994**, *116*, 2179-2180.

(56) Dunn, S. C.; Batsanov, A. S.; Mountford, P. *J. Chem. Soc., Chem. Commun.* **1994**, 2007-2008.

(57) Dunn, S. C.; Mountford, P.; Shishkin, O. V. *Inorg. Chem.* **1996**, *35*, 1006-1012.

(58) Collier, P. E.; Blake, A. J.; Mountford, P. *J. Chem. Soc., Dalton Trans.* **1997**, 2911-2919.

(59) Mueller, E.; Mueller, J.; Olbrich, F.; Brueser, W.; Knapp, W.; Abeln, D.; Edelmann, F. T. *Eur. J. Inorg. Chem.* **1998**, 87-91.

(60) McInnes, J. M.; Swallow, D.; Blake, A. J.; Mountford, P. *Inorg. Chem.* **1998**, *37*, 5970-5977.

(61) Male, N. A. H.; Skinner, M. E.; Bylikin, S. Y.; Wilson, P. J.; Mountford, P.; Schroder, M. *Inorg. Chem.* **2000**, *39*, 5483-5491.

(62) Blake, A. J.; Collier, P. E.; Gade, L. H.; Mountford, P.; Julian, L.; Pugh, S. M.; Schubart, M.; Skinner, M. E.; Trosch, D. J. M. *Inorg. Chem.* **2001**, *40*, 870-877.

(63) Boyd, C. L.; Guiducci, A. E.; Dubberley, S. R.; Tyrrell, B. R.; Mountford, P. *J. Chem. Soc., Dalton Trans.* **2002**, 4175-4184.

(64) Cole, S. C.; Coles, M. P.; Hitchcock, P. B. *J. Chem. Soc., Dalton Trans.* **2002**, 4168-4174.

(65) Wilson, P. J.; Blake, A. J.; Mountford, P.; Schroder, M. *Inorg. Chim. Acta* **2003**, *345*, 44-52.

(66) Dunn, S. C.; Mountford, P.; Robson, D. A. *J. Chem. Soc., Dalton Trans.* **1997**, 293-304.

(67) Blake, A. J.; Dunn, S. C.; Green, J. C.; Jones, N. M.; Moody, A. G.; Mountford, P. *Chem. Commun.* **1998**, 1235-1236.

(68) Schaller, C. P.; Cummins, C. C.; Wolczanski, P. T. *J. Am. Chem. Soc.* **1996**, *118*, 591-611.

(69) Bennett, J. L.; Wolczanski, P. T. *J. Am. Chem. Soc.* **1997**, *119*, 10696-10719.

(70) Zuckerman, R. L.; Krska, S. W.; Bergman, R. G. *J. Organomet. Chem.* **1999**, *591*, 2-7.

(71) Meyer, K. E.; Walsh, P. J.; Bergman, R. G. *J. Am. Chem. Soc.* **1994**, *116*, 2669-2670.

(72) Krska, S. W.; Zuckerman, R. L.; Bergman, R. G. *J. Am. Chem. Soc.* **1998**, *120*, 11828-11829.

(73) Zuckerman, R. L.; Krska, S. W.; Bergman, R. G. *J. Am. Chem. Soc.* **2000**, *122*, 751-761.

(74) Cao, C.; Ciszewski, J. T.; Odom, A. L. *Organometallics* **2001**, *21*, 5011-5013.

(75) Tillack, A.; Castro, I. G.; Hartung, C. G.; Beller, M. *Angew. Chem. Int. Ed. Engl.* **2002**, *41*, 2541-2543.

(76) Ong, T.-G.; Yap, G. P. A.; Richeson, D. S. *Organometallics* **2002**, *21*, 2839-2841.

(77) Bytschkov, I.; Doye, S. *Eur. J. Org. Chem.* **2003**, 935-946.

(78) Jin, J.; Chen, E. Y. X. *Organometallics* **2002**, *21*, 13-15.

(79) Jin, J.; Mariott, W. R.; Chen, E. Y.-X. *J. Polym. Sci., A: Polym. Chem.* **2003**, *41*, 3132-3142.

(80) Sweeney, Z. K.; Salsman, J. L.; Andersen, R. A.; Bergman, R. G. *Angew. Chem. Int. Ed. Engl.* **2000**, *39*, 2339-2343.

(81) Michael, F. E.; Duncan, A. P.; Sweeney, Z. K.; Bergman, R. G. *J. Am. Chem. Soc.* **2003**, *125*, 7184-7185.

(82) Bennett, J. L.; Wolczanski, P. T. *J. Am. Chem. Soc.* **1994**, *116*, 2179-2180.

(83) Cundari, T. R.; Klinckman, T. R.; Wolczanski, P. T. *J. Am. Chem. Soc.* **2002**, *124*, 1481-1487.

(84) Meyer, K. E.; Walsh, P. J.; Bergman, R. G. *J. Am. Chem. Soc.* **1995**, *117*, 974-985.

(85) Baranger, A. M.; Walsh, P. J.; Bergman, R. G. *J. Am. Chem. Soc.* **1993**, *115*, 2753-2763.

(86) Pohlki, F.; Doye, S. *Angew. Chem. Int. Ed. Engl.* **2001**, *40*, 2305-2308.

(87) Johnson, J. S.; Bergman, R. G. *J. Am. Chem. Soc.* **2001**, *123*, 2923-2924.

(88) Shi, Y.; Hall, C.; Ciszewski, J. T.; Cao, C.; Odom, A. L. *Chem. Commun.* **2003**, 586-587.

(89) Young, R. J.; Lovell, P. A. *Introduction to Polymers*; 2nd ed.; Chapman & Hall: London, 1994.

(90) Fan, L.; Harrison, D.; Woo, T. K.; Ziegler, T. *Organometallics* **1995**, *14*, 2018-2026.

(91) Kaminsky, W. *Catal. Today* **2000**, *62*, 23-34.

(92) Chen, E. Y.-X.; Marks, T. J. *Chem. Rev.* **2000**, *100*, 1391-1434, and references therein.

(93) Sinn, H.; Kaminsky, W.; Vollmer, H.-J.; Woldt, R. *Angew. Chem., Int. Ed. Engl.* **1980**, *19*, 390-392.

(94) Sinn, H.; Kaminsky, W. *Adv. Organomet. Chem.* **1980**, *18*, 99-149.

(95) Ystenes, M.; Eilertsen, J. L.; Liu, J.; Ott, M.; Rytter, E.; Stovneng, J. A. *J. Polym. Sci., A: Polym. Chem.* **2000**, *38*, 3106-3127.

(96) Babushkin, D. E.; Britzinger, H.-H. *J. Am. Chem. Soc.* **2002**, *124*, 12869-12873.

(97) Zurek, E.; Ziegler, T. *Organometallics* **2002**, *21*, 83-92.

(98) Roesky, H. W.; Walawalkar, M. G.; Murugavel, R. *Acc. Chem. Res.* **2001**, *34*, 201-211.

(99) Pedeutour, J.-N.; Radhakrishnan, K.; Cramail, H.; Deffieux, A. *Macromol. Rapid Commun.* **2001**, *22*, 1095-1123.

(100) Imhoff, D. W.; Simeral, L. S.; Sangokoya, S. A.; Peel, J. H. *Organometallics* **1998**, *17*, 1941-1945.

(101) Massey, A. G.; Park, A. J. *J. Organomet. Chem.* **1964**, *2*, 245-250.

(102) Massey, A. G.; Park, A. J. *J. Organomet. Chem.* **1966**, *5*, 218-225.

(103) Chien, J. C. W.; Tsai, W.-M.; Rausch, M. D. *J. Am. Chem. Soc.* **1991**, *113*, 8570-8571.

(104) Yang, X.; Stern, C. L.; Marks, T. J. *J. Am. Chem. Soc.* **1991**, *113*, 3623-3625.

(105) Huang, J.; Rempel, G. L. *Prog. Polym. Sci.* **1995**, *20*, 459-526.

(106) Sinn, H.; Kaminsky, W.; Vollmer, H. J.; Woldt, R. *Angew. Chem.* **1980**, *92*, 396-402.

(107) Kaminsky, W.; Kuelper, K.; Brintzinger, H. H.; Wild, F. R. W. P. *Angew. Chem.* **1985**, *97*, 507-508.

(108) Mohring, P. C.; Coville, N. J. *J. Organomet. Chem.* **1994**, *479*, 1-29.

(109) Kaminsky, W. *J. Chem. Soc., Dalton Trans.* **1998**, 1413-1418.

(110) Coates, G. W. *Chem. Rev.* **2000**, *100*, 1223-1252.

(111) Brintzinger, H. H. *Angew. Chem. Int. Ed. Engl.* **1995**, *34*, 1143-1170.

(112) Resconi, L.; Cavallo, L.; Fait, A.; Piemontesi, F. *Chem. Rev.* **2000**, *100*, 1253-1346.

(113) Halterman, R. L. In *Metallocenes*; Togni, A., Halterman, R. L., Eds.; Wiley-VCH: Toronto, 1998; Vol. 1.

(114) Hlatky, G. C. *Chem. Rev.* **2000**, *100*, 1347-1376.

(115) Fink, G.; Steinmetz, B.; Zechlin, J.; Przybyla, C.; Tesche, B. *Chem. Rev.* **2000**, *100*, 1377-1390.

(116) Jezequel, M.; Dufaud, V.; Ruiz-Garcia, M. J.; Carrillo-Hermosilla, F.; Neugebauer, U.; Niccolai, G. P.; Lefebvre, F.; Bayard, F.; Corker, J.; Fiddy, S.; Evans, J.; Broyer, J.-P.; Malinge, J.; Basset, J.-M. *J. Am. Chem. Soc.* **2001**, *123*, 3520-3540.

(117) Shapiro, P. J.; Bunel, E.; Schaefer, W. P.; Bercaw, J. E. *Organometallics* **1990**, *9*, 867-869.

(118) Stevens, J. C.; Timmers, F. J.; Wilson, D. R.; Schmidt, G. F.; Nickias, P. N.; Rosen, R. K.; Knight, G. W.; Lai, S.: Eur. Patent Appl. EP-416-815-A2, **1991**.

(119) Canich, J. M.; Exxon: Eur. Patent Appl. EP 450436-A1, **1991**.

(120) Kunz, K.; Erker, G.; Doering, S.; Froehlich, R.; Kehr, G. *J. Am. Chem. Soc.* **2001**, *123*, 6181-6182.

(121) Kunz, K.; Erker, G.; Doering, S.; Bredeau, S.; Kehr, G.; Froehlich, R. *Organometallics* **2002**, *21*, 1031-1041.

(122) Siemeling, U. *Chem. Rev.* **2000**, *100*, 1495-1526, and references therein.

(123) Kim, D.-H.; Won, J. H.; Kim, S.-J.; Ko, J.; Kim, S. H.; Cho, S.; Kang, S. O. *Organometallics* **2001**, *20*, 4298-4300.

(124) Seo, W. S.; Cho, Y. J.; Yoon, S. C.; Park, J. T.; Park, Y. *J. Organomet. Chem.* **2001**, *640*, 79-84.

(125) Woo, T. K.; Fan, L.; Ziegler, T. *Organometallics* **1994**, *13*, 2252-2261.

(126) Woo, T. K.; Margl, P. M.; Lohrenz, J. C. W.; Bloechl, P. E.; Ziegler, T. *J. Am. Chem. Soc.* **1996**, *118*, 13021-13030.

(127) Woo, T. K.; Margl, P. M.; Lohrenz, J. C. W.; Ziegler, T. *Polymeric Materials Science and Engineering* **1996**, *74*, 393-394.

(128) Woo, T. K.; Margl, P. M.; Ziegler, T.; Bloechl, P. E. *Organometallics* **1997**, *16*, 3454-3468.

(129) Beigzadeh, D.; Soares, J. B. P.; Duever, T. A.; Hamielec, A. E. *Polymer Reaction Engineering* **1999**, *7*, 195-205.

(130) Wang, W.-J.; Zhu, S.; Park, S.-J. *Macromolecules* **2000**, *33*, 5770-5776.

(131) Latham, I. A.; Leigh, G. J.; Huttner, G.; Jibril, I. *J. Chem. Soc., Dalton Trans.* **1986**, 377-383.

(132) Stephan, D. W.; Stewart, J. C.; Brown, S. J.; Swabey, J. W.; Wang, Q. In *Eur. Pat. Appl.*; (Nova Chemicals (International) S.A., Switz.). Ep, **1998**, 17 pp.

(133) Stephan, D. W.; Stewart, J. C.; Harrison, D. G. In *Eur. Pat. Appl.*; (Nova Chemicals (International) S.A., Switz.). Ep, **1999**, 21 pp.

(134) Zhang, S.; Piers, W. E.; Gao, X.; Parvez, M. *J. Am. Chem. Soc.* **2000**, *122*, 5499-5509.

(135) McMeeking, J.; Gao, X.; von Haken Spence, R. E.; Brown, S. J.; Jeremic, D.; Nova Chemicals (International) S.A.: U.S. 6,420,300, 2002.

(136) Tolman, C. B. *J. Am. Chem. Soc.* **1970**, *92*, 2956-2965.

(137) Tolman, C. B. *Chem. Rev.* **1977**, *77*, 313-348.

(138) Dehnicke, K.; Krieger, M.; Massa, W. *Coord. Chem. Rev.* **1999**, *182*, 19-65.

(139) Kretschmer, W. P.; Dijkhuis, C.; Meetsma, A.; Hessen, B.; Teuben, J. H. *Chem. Commun.* **2002**, 608-609.

(140) Matsui, S.; Mitani, M.; Saito, J.; Tohi, Y.; Haruyuki, M.; Matsukawa, N.; Takagi, Y.; Tsuru, K.; Nitabaru, M.; Nakano, T.; Tanaka, H.; Kashiwa, N.; Fujita, T. *J. Am. Chem. Soc.* **2001**, *123*, 6847-6856.

(141) Matsui, S.; Mitani, M.; Saito, J.; Tohi, Y.; Makio, H.; Tanaka, H.; Fujita, T. *Chem. Lett.* **1999**, 1263-1264.

(142) Matsui, S.; Mitani, M.; Saito, J.; Matsukawa, N.; Tanaka, H.; Nakano, T.; Fujita, T. *Chem. Lett.* **2000**, 554-555.

(143) Matsukawa, N.; Matsui, S.; Mitani, M.; Saito, J.; Tsuru, K.; Kashiwa, N.; Fujita, T. *J. Mol. Catal. A - Chem.* **2001**, *169*, 99-104.

(144) Matsui, S.; Fujita, T. *Catal. Today* **2001**, *66*, 63-73.

(145) Mitani, M.; Mohri, J.; Yoshida, Y.; Saito, J.; Ishii, S.; Tsuru, K.; Matsui, S.; Furuyama, R.; Nakano, T.; Tanaka, H.; Kojoh, S.-i.; Matsugi, T.; Kashiwa, N.; Fujita, T. *J. Am. Chem. Soc.* **2002**, *124*, 3327-3336.

(146) Mitani, M.; Furuyama, R.; Mohri, J.-I.; Saito, J.; Ishii, S.; Terao, H.; Kashiwa, N.; Fujita, T. *J. Am. Chem. Soc.* **2002**, *124*, 7888-7889.

(147) Mitani, M.; Furuyama, R.; Mohri, J.-I.; Saito, J.; Ishii, S.; Terao, H.; Nakano, T.; Tanaka, H.; Fujita, T. *J. Am. Chem. Soc.* **2003**, *125*, 4293-4305.

(148) Makio, H.; Kashiwa, N.; Fujita, T. *Adv. Synth. Catal.* **2002**, *344*, 477-493.

(149) Tian, J.; Hustad, P. D.; Coates, G. W. *J. Am. Chem. Soc.* **2001**, *123*, 5134-5135.

(150) Hustad, P. D.; Coates, G. W. *J. Am. Chem. Soc.* **2002**, *124*, 11578-11579.

(151) Hustad, P. D.; Tian, J.; Coates, G. W. *J. Am. Chem. Soc.* **2002**, *124*, 3614-3621.

(152) Lee, D.-h.; Yoon, K.-b.; Lee, E.-h.; Noh, S.-k.; Byun, G.-g.; Lee, C.-s. *Macromol. Rapid Commun.* **1995**, *16*, 265-268.

(153) Noh, S. K.; Kim, S.; Kim, J.; Lee, D.-H.; Yoon, K.-B.; Lee, H.-B.; Lee, S. W.; Huh, W. S. *J. Polym. Sci., A: Polym. Chem.* **1997**, *35*, 3717-3728.

(154) Yan, X.; Chernega, A.; Green, M. L. H.; Sanders, J.; Souter, J.; Ushioda, T. *J. Mol. Catal. A - Chem.* **1998**, *128*, 119-141.

(155) Noh, S. K.; Kim, J.; Jung, J.; Ra, C. S.; Lee, D.-H.; Lee, H. B.; Lee, S. W.; Huh, W. S. *J. Organomet. Chem.* **1999**, *580*, 90-97.

(156) Daniele, S.; Hitchcock, P. B.; Lappert, M. F. *Chem. Commun.* **1999**, 1909-1910.

(157) Novak, A.; Blake, A. J.; Wilson, C.; Love, J. B. *Chem. Commun.* **2002**, 2796-2797.

(158) Tullo, A. H. In *Chem. Eng. News*, **2001**; *79*, 35-36.

(159) Tohi, Y.; Makio, H.; Matsui, S.; Onda, M.; Fujita, T. *Macromolecules* **2003**, *36*, 523-525.

(160) Komon, Z. J. A.; Bu, X.; Bazan, G. C. *J. Am. Chem. Soc.* **2000**, *122*, 1830-1831.

(161) Li, L.; Metz, M. V.; Li, H.; Chen, M.-C.; Marks, T. J.; Liable-Sands, L.; Rheingold, A. L. *J. Am. Chem. Soc.* **2002**, *124*, 12725-12741.

(162) Juengling, S.; Muelhaupt, R.; Plenio, H. *J. Organomet. Chem.* **1993**, *460*, 191-195.

(163) Ushioda, T.; Green, M. L. H.; Haggitt, J.; Yan, X. *J. Organomet. Chem.* **1996**, *518*, 155-166.

(164) Noh, S. K.; Lee, J.; Lee, D.-h. *J. Organomet. Chem.* **2003**, *667*, 53-60.

(165) Jimenez, G.; Royo, P.; Cuenca, T.; Herdtweck, E. *Organometallics* **2002**, *21*, 2189-2195.

(166) Eisch, J. J.; Pombrik, S. I.; Zheng, G.-Z. *Organometallics* **1993**, *12*, 3856-3863.

(167) Yang, X.; Stern, C. L.; Marks, T. J. *J. Am. Chem. Soc.* **1994**, *116*, 10015-10031.

(168) Chen, Y.-X.; Metz, M. V.; Li, L.; Stern, C. L.; Marks, T. J. *J. Am. Chem. Soc.* **1998**, *120*, 6287-6305.

(169) Rappe, A. K.; Skiff, W. M.; Casewit, C. J. *Chem. Rev.* **2000**, *100*, 1435-1456.

(170) Braga, D.; Grepioni, F.; Tedesco, E.; Calhorda, M. J. *Z. Anorg. Allg. Chem.* **2000**, *626*, 462-470.

(171) Beck, S.; Lieber, S.; Schaper, F.; Geyer, A.; Brintzinger, H.-H. *J. Am. Chem. Soc.* **2001**, *123*, 1483-1489.

(172) Landis, C. R.; Rosaaen, K. A.; Sillars, D. R. *J. Am. Chem. Soc.* **2003**, *125*, 1710-1711.

(173) Mohammed, M.; Nele, M.; Al-Humydi, A.; Xin, S.; Stapleton, R. A.; Collins, S. *J. Am. Chem. Soc.* **2003**, *125*, 7930-7941.

(174) Jordan, R. F.; Bajgur, C. S.; Willett, R.; Scott, B. *J. Am. Chem. Soc.* **1986**, *108*, 7410-7411.

(175) Jordan, R. F.; Dasher, W. E.; Echols, S. F. *J. Am. Chem. Soc.* **1986**, *108*, 1718-1719.

(176) Jordan, R. F.; Echols, S. F. *Inorg. Chem.* **1987**, *26*, 383-386.

(177) Borkowsky, S. L.; Jordan, R. F.; Hinch, G. D. *Organometallics* **1991**, *10*, 1268-1274.

(178) Tjaden, E. B.; Swenson, D. C.; Jordan, R. F.; Peterson, J. L. *Organometallics* **1995**, *14*, 371-386.

(179) Casey, C. P.; Carpenetti II, D. W.; Sakurai, H. *J. Am. Chem. Soc.* **1999**, *121*, 9483-9484.

(180) Keaton, R. J.; Jayaratne, K. C.; Fettinger, J. C.; Sita, L. R. *J. Am. Chem. Soc.* **2000**, *122*, 12909-12910.

(181) Bochmann, M. *Top. Catal.* **1999**, *7*, 9-22.

(182) Piers, W. E.; Sun, Y.; Lee, L. W. M. *Top. Catal.* **1999**, *7*, 133-143.

(183) Guzei, I. A.; Stockland Jr, R. A.; Jordan, R. F. *Acta Cryst.* **2000**, *C56*, 635-636.

(184) Deck, P. A.; Beswick, C. L.; Marks, T. J. *J. Am. Chem. Soc.* **1998**, *120*, 1772-1784.

(185) Li, L.; Marks, T. J. *Organometallics* **1998**, *17*, 3996-4003.

(186) Bochmann, M.; Lancaster, S. J. *Organometallics* **1993**, *12*, 633-640.

(187) Bochmann, M.; Lancaster, S. J.; Hursthouse, M. B.; Malik, K. M. A. *Organometallics* **1994**, *13*, 2235-2243.

(188) Lancaster, S. J.; Robinson, O. B.; Bochmann, M.; Coles, S. J.; Hursthouse, M. B. *Organometallics* **1995**, *14*, 2456-2462.

(189) Gillis, D. J.; Quyoum, R.; Tudoret, M.-J.; Wang, Q.; Jeremic, D.; Roszak, A. W.; Baird, M. C. *Organometallics* **1996**, *15*, 3600-3605.

(190) Jia, L.; Yang, X.; Stern, C. L.; Marks, T. J. *Organometallics* **1997**, *16*, 842-857.

(191) Pellecchia, C.; Grassi, A.; Zambelli, A. *Organometallics* **1994**, *13*, 298-302.

(192) Doerrer, L. H.; Green, M. L. H.; Haussinger, D.; Sassmannshausen, J. *J. Chem. Soc., Dalton Trans.* **1999**, 2111-2118.

(193) Gauvin, R. M.; Osborn, J. A.; Kress, J. *Organometallics* **2000**, *19*, 2944-2946.

(194) Sassmannshausen, J. *Organometallics* **2000**, *19*, 482-489.

(195) Pellecchia, C.; Grassi, A.; Immirzi, A. *J. Am. Chem. Soc.* **1993**, *115*, 1160-1162.

(196) Siedle, A. R.; Newmark, R. A. *J. Organomet. Chem.* **1995**, *497*, 119-125.

(197) Thorn, M. G.; Etheridge, Z. C.; Fanwick, P. E.; Rothwell, I. P. *Organometallics* **1998**, *17*, 3636-3638.

(198) Thorn, M. G.; Etheridge, Z. C.; Fanwick, P. E.; Rothwell, I. P. *J. Organomet. Chem.* **1999**, *591*, 148-162.

(199) Pindado, G. J.; Thornton-Pett, M.; Hursthouse, M. B.; Coles, S. J.; Bochmann, M. *J. Chem. Soc., Dalton Trans.* **1999**, 1663-1668.

(200) Deckers, P. J. W.; van der Linden, A. J.; Meetsma, A.; Hessen, B. *Eur. J. Inorg. Chem.* **2000**, 929-932.

(201) Williams, V. C.; Dai, C.; Li, Z.; Collins, S.; Piers, W. E.; Clegg, W.; Elsegood, M. R. J.; Marder, T. B. *Angew. Chem. Int. Ed. Engl.* **1999**, *38*, 3695-3698.

(202) Dioumaev, V. K.; Harrod, J. F. *Organometallics* **1997**, *16*, 2798-2807.

(203) Guerin, F.; Stewart, J. C.; Beddie, C.; Stephan, D. W. *Organometallics* **2000**, *19*, 2994-3000.

(204) Gauvin, R. M.; Mazet, C.; Kress, J. *J. Organomet. Chem.* **2002**, *658*, 1-8.

(205) Scollard, J. D.; McConville, D. H.; Rettig, S. J. *Organometallics* **1997**, *16*, 1810-1812.

(206) Scollard, J. D.; McConville, D. H.; Vittal, J. J.; Payne, N. C. *J. Mol. Catal. A - Chem.* **1998**, *128*, 201-214.

(207) Choukroun, R.; Wolff, F.; Lorber, C.; Donnadieu, B. *Organometallics* **2003**, *22*, 2245-2248.

(208) Chen, Y.-X.; Marks, T. J. *Organometallics* **1997**, *16*, 3649-3657.

(209) Schrock, R. R.; Bonitatebus, P. J., Jr.; Schrodi, Y. *Organometallics* **2001**, *20*, 1056-1058.

(210) Bochmann, M.; Lancaster, S. J. *Angew. Chem. Int. Ed. Engl.* **1994**, *33*, 1634-1637.

(211) Bochmann, M.; Lancaster, S. J. *J. Organomet. Chem.* **1995**, *497*, 55-59.

(212) Zhang, S.; Piers, W. E. *Organometallics* **2001**, *20*, 2088-2092.

(213) Williams, V. C.; Irvine, G. J.; Piers, W. E.; Li, Z.; Collins, S.; Clegg, W.; Elsegood, M. R. J.; Marder, T. B. *Organometallics* **2000**, *19*, 1619-1621.

(214) Guerin, F.; Stephan, D. W. *Angew. Chem. Int. Ed. Engl.* **2000**, *39*, 1298-1300.

(215) Chen, E. Y.-X.; Kruper, W. J.; Roof, G.; Wilson, D. R. *J. Am. Chem. Soc.* **2001**, *123*, 745-746.

(216) Scollard, J. D.; McConville, D. H.; Payne, N. C.; Vittal, J. J. *Macromolecules* **1996**, *29*, 5241-5243.

(217) Liang, L.-C.; Schrock, R. R.; Davis, W. M.; McConville, D. H. *J. Am. Chem. Soc.* **1999**, *121*, 5797-5798.

(218) Rhodes, B.; Rausch, M. D.; Chien, J. C. W. *J. Polym. Sci., A: Polym. Chem.* **2000**, *39*, 313-319.

(219) Mehrkhodavandi, P.; Bonitatebus, P. J., Jr.; Schrock, R. R. *J. Am. Chem. Soc.* **2000**, *122*, 7841-7842.

(220) Mehrkhodavandi, P.; Schrock, R. R.; Bonitatebus, P. J., Jr. *Organometallics* **2002**, *21*, 5785-5798.

(221) Fix, R. M.; Gordon, R. G.; Hoffman, D. M. *Chem. Mater.* **1990**, *2*, 235-241.

(222) Stock, H. R.; Berndt, H.; Mayr, P. *Surface and Coatings Technology* **1991**, *46*, 15-23.

(223) Janovska, M.; Bastl, Z. *Infrared Physics & Technology* **1996**, *37*, 727-731.

(224) Galakhov, M.; Gomez-Sal, P.; Martin, A.; Mena, M.; Yelamos, C. *Eur. J. Inorg. Chem.* **1998**, 1319-1325.

(225) Cheon, J.; Guile, M.; Muraoka, P.; Zink, J. I. *Inorg. Chem.* **1999**, *38*, 2238-2239.

(226) Cross, J. B.; Schlegel, H. B. *Chem. Mater.* **2000**, *12*, 2466-2474.

(227) Akram, S. In *U.S.*; (Micron Technology, Inc., USA). Us, 2002, p 7 pp.

(228) Walsh, P. J.; Baranger, A. M.; Bergman, R. G. *J. Am. Chem. Soc.* **1992**, *114*, 1708-1719.

(229) Ackermann, L.; Bergman, R. G. *Org. Lett.* **2002**, *4*, 1475-1478.

(230) Bennett, J. L.; Wolczanski, P. T. *J. Am. Chem. Soc.* **1997**, *119*, 10696-10719.

(231) Bashall, A.; Collier, P. E.; Gade, L. H.; McPartlin, M.; Mountford, P.; Trosch, D. J. M. *Chem. Commun.* **1998**, 2555-2556.

(232) Lee, S. Y.; Bergman, R. G. *J. Am. Chem. Soc.* **1995**, *117*, 5877-5878.

(233) Guerin, F.; Stephan, D. W. *Angew. Chem. Int. Ed. Engl.* **1999**, *38*, 3698-3701.

(234) Kickham, J. E.; Guerin, F.; Stewart, J. C.; Stephan, D. W. *Angew. Chem. Int. Ed. Engl.* **2000**, *39*, 3263-3266.

(235) Pangborn, A. B.; Giardello, M. A.; Grubbs, R. H.; Rosen, R. K.; Timmers, F. J. *Organometallics* **1996**, *15*, 1518-1520.

(236) Daniele, S.; Drost, C.; Gehrhus, B.; Hawkins, S. M.; Hitchcock, P. B.; Lappert, M. F.; Merle, P. G.; Bott, S. G. *J. Chem. Soc., Dalton Trans.* **2001**, 3179-3188.

(237) Chandra, G.; Lappert, M. F. *J. Chem. Soc. A* **1968**, 1940-1945.

(238) Waggoner, K. M.; Hope, H.; Power, P. P. *Angew. Chem.* **1988**, *100*, 1765-1766.

(239) Waggoner, K. M.; Power, P. P. *J. Am. Chem. Soc.* **1991**, *113*, 3385-3393.

(240) Cromer, D. T.; Mann, J. B. *Acta Crystallogr., Sect. A.* **1968**, *A24*, 321-324.

(241) Sarter, C.; Dehnicke, S.; Aul, R.; Erker, G. "Synthese von Metallorganika zur Abscheidung von titanhaltigen Hartstoffschichten durch MOCVD," Institut fur Organische Chemie der Universtat Wurzburg, 1989.

(242) McCleverty, J. A.; James, T. A. *J. Chem. Soc. [Section] A: Inorg., Phys., Theoret.* **1970**, 3318-3321.

(243) Erker, G.; Sarter, C.; Albrecht, M.; Dehnicke, S.; Krueger, C.; Raabe, E.; Schlund, R.; Benn, R.; Rufinska, A.; Mynott, R. *J. Organomet. Chem.* **1990**, *382*, 89-102.

(244) Gorsich, R. D. *J. Am. Chem. Soc.* **1960**, *82*, 4211-4214.

(245) Brantley, J. S.; Morehouse, E. L.; Parts, L.; Union Carbide Corp.: US, 1967, p 4.

(246) Martin, A.; Mena, M.; Yelamos, C.; Serrano, R.; Raithby, P. R. *J. Organomet. Chem.* **1994**, *467*, 79-84.

(247) Eller, P. G.; Bradley, D. C.; Hursthouse, M. B.; Meek, D. W. *Coord. Chem. Rev.* **1977**, *24*, 1-95.

(248) Scollard, J. D.; McConville, D. H.; Vittal, J. J. *Organometallics* **1997**, *16*, 4415-4420.

(249) Andersen, R. A. *Inorg. Chem.* **1979**, *18*, 1724-1725.

(250) Dick, D. G.; Rousseau, R.; Stephan, D. W. *Can. J. Chem.* **1991**, *69*, 357-362.

(251) Jagirdar, B. R.; Murugavel, R.; Schmidt, H. G. *Inorg. Chim. Acta* **1999**, *292*, 105-107.

(252) Yelamos, C.; Heeg, M. J.; Winter, C. H. *Organometallics* **1999**, *18*, 1168-1176.

(253) Hascall, T.; Ruhlandt-Senge, K.; Power, P. P. *Angew. Chem., Int. Ed. Engl.* **1994**, *33*, 356-357.

(254) Gordon, J. C.; Giesbrecht, G. R.; Clark, D. L.; Hay, P. J.; Keogh, D. W.; Poli, R.; Scott, B. L.; Watkin, J. G. *Organometallics* **2002**, *21*, 4726-4734.

(255) Kaschube, W.; Porschke, K. R.; Wilke, G. *J. Organomet. Chem.* **1988**, *355*, 525-532.

(256) Gibson, V. C.; Kimberley, B. S.; White, A. J. P.; Williams, D. J.; Howard, P. *Chem. Commun.* **1998**, 313-314.

(257) Stuart, B. H. *Polymer Analysis*; John Wiley & Sons, Ltd: West Sussex, 2002.

(258) Varshney, S. K.; Hautekeer, J. P.; Fayt, R.; Jerome, R.; Teyssie, P. *Macromolecules* **1990**, *23*, 2618-2622.

(259) Adachi, T.; Sugimoto, H.; Aida, T.; Inoue, S. *Macromolecules* **1992**, *25*, 2280-2281.

(260) Adachi, T.; Sugimoto, H.; Aida, T.; Inoue, S. *Macromolecules* **1993**, *26*, 1238-1243.

(261) Soga, K.; Deng, H.; Yano, T.; Shiono, T. *Macromolecules* **1994**, *27*, 7938-7940.

(262) Deng, H.; Shiono, T.; Soga, K. *Macromolecules* **1995**, *28*, 3067-3073.

(263) Gibson, V. C.; Cameron, P. A.; Dove, A. P.; Graham, A. J.; Marshall, E. L. *Polymeric Materials Science and Engineering* **2002**, *87*, 91-92.

(264) Dove, A. P.; Gibson, V. C.; Marshall, E. L.; White, A. J. P.; Williams, D. J. *Chem. Commun.* **2002**, 1208-1209.

(265) Schwarz, A. M. *Chem. Eng. News*, 1978; Vol. 56, p 88.

(266) Stewart, J. C. *Ph.D. Dissertaion*; University of Windsor: Windsor, **2000**.

(267) Cavell, R. G. *Curr. Sci.* **2000**, *78*, 440-451, and references therein.

(268) Cavell, R. G.; Kamalesh Babu, R. P.; Aparna, K. *J. Organomet. Chem.* **2001**, *617-618*, 158-169.

(269) Kamalesh Babu, R. P.; McDonald, R.; Cavell, R. G. *J. Chem. Soc., Dalton Trans.* **2001**, 2210-2214.

(270) Siemeling, U.; Kolling, L.; Kuhnert, O.; Neumann, B.; Stammler, A.; Stammler, H.-G.; Fink, G.; Kaminski, E.; Kiefer, A.; Schrock, R. R. *Z. Anorg. Allg. Chem.* **2003**, *629*, 781-792.

(271) Gusev, D. G.; Madott, M.; Dolgushin, F. M.; Lyssenko, K. A.; Antipin, M. Y. *Organometallics* **2000**, *19*, 1734-1739.

(272) Woo, H.-G.; Freeman, W. P.; Tilley, T. D. *Organometallics* **1992**, *11*, 2198-2205.

(273) Beckhaus, R.; Duemichen, U.; Thiele, K. H. *Z. Chem.* **1986**, *26*, 261-262.

(274) Staudinger, H.; Meyer, J. *Helv. Chim. Acta* **1919**, *2*, 635-646.

(275) Wolfsberger, W. *Z. Naturforsch.* **1978**, *33b*, 1452-1456.

(276) Cross, R. J.; Kennedy Alan, R.; Muir, K. W. *J. Organomet. Chem.* **1995**, *487*, 227-233.

(277) Cross, R. J.; Kennedy Alan, R.; Manojlovic-Muir, L.; Muir, K. W. *J. Organomet. Chem.* **1995**, *493*, 243-249.

(278) Amoroso, D.; Snelgrove, J. L.; Conrad, J. C.; Drouin, S. D.; Yap, G. A. P.; Fogg, D. E. *Adv. Synth. Catal.* **2002**, *344*, 757-763.

(279) Crutchfield, M. M.; Dungan, C. H.; Letcher, J. H.; Mark, V.; Van Wazer, J. R. *31P Nuclear Magnetic Resonance*; John Wiley & Sons, Inc.: New York, 1967; Vol. Topics in Phosphorus Chemistry, Volume 5.

(280) Gibson, V. C.; Long, N. J.; Marshall, E. L.; Oxford, P. J.; White, A. J. P.; Williams, D. J. *J. Chem. Soc., Dalton Trans.* **2001**, 1162-1164.

(281) Scollard, J. D.; McConville, D. H. *J. Am. Chem. Soc.* **1996**, *118*, 10008-10009.

(282) Baumann, R.; Davis, W. M.; Schrock, R. R. *J. Am. Chem. Soc.* **1997**, *119*, 3830-3831.

(283) Hagihara, H.; Shiono, T.; Ikeda, T. *Macromolecules* **1998**, *31*, 3184-3188.

(284) Hasan, T.; Ioku, A.; Nishii, K.; Shiono, T.; Ikeda, T. *Macromolecules* **2001**, *34*, 3142-3145.

(285) Mehrkhodavandi, P.; Schrock, R. R. *J. Am. Chem. Soc.* **2001**, *123*, 10746-10747.

(286) Hagimoto, H.; Shiono, T.; Ikeda, T. *Macromol. Rapid Commun.* **2002**, *23*, 73-76.

(287) Soares, J. B. P.; Kim, J. D. *J. Polym. Sci., A: Polym. Chem.* **2000**, *38*, 1408-1416.

(288) Lo, F. Y.; Nowlin, T. E.; Shirodkar, P. P.; Mobil Oil Corporation (Fairfax, VA): United States, **1991**, No. 5,032,562, p 15.

(289) Soares, J. B. P.; Hamielec, A. E. *Polymer* **1996**, *37*, 4607-4614.

(290) Dall'Occo, T.; Baruzzi, G.; Schaverien, C. J. Basell Technology Company BV (Hoofddorp, NL). United States, **1999**, No. 6,479,609, 23 pp.

(291) Chu, K.-J.; Soares, J. B. P.; Penlidis, A. *Macromolecular Chemistry and Physics* **2000**, *201*, 552-557.

(292) Blom, R.; Dahl, I. M. *Macromolecular Chemistry and Physics* **2001**, *202*, 719-725.

(293) Tannous, K.; Soares, J. B. P. *Macromolecular Chemistry and Physics* **2002**, *203*, 1895-1905.

(294) Mink, R. I.; Nowlin, T. E.; Shirodkar, P. P.; Schregenberger, S. D.; Tsien, G. O.; Mobil Oil Corporation (Fairfax, VA): United States, **1996**, No. 5,525,678, 23 pp.

(295) Ahlers, A.; Kaminsky, W. *Makromol. Chem., Rapid Commun.* **1988**, *9*, 457-461.

(296) Nowlin, T. E.; Schregenberger, S. D.; Shirodkar, P. P.; Tsien, G. O.; Mobil Oil Corporation (Fairfax, VA): United States, **1996**, No. 5,525,678, p 19.

(297) Mink, R. I.; Nowlin, T. E.; Schregenberger, S. D.; Shirodkar, P. P.; Tsien, G. O.; Mobil Oil Corporation (Fairfax, VA): United States, **1997**, 5,614,456, p 15.

(298) Kissin, Y. V.; Mink, R. I.; Nowlin, T. E.; Mobil Oil Corporation (Fairfax, VA): United States, **1999**, No. 6,001,766, p 15.

(299) Eilerts, N. W.; Phillips Petroleum Company (Bartlesville, OK): United States, **2002**, No. 6,479,422, p 24.

(300) Tilston, M. W.; Maheshwari, V.; Davis, M. B.; Union Carbide Chemicals & Plastics Technology Corporation (Danbury, CT): United States, **2002**, No. 6,462,149, p 13.

(301) Musikabhumma, K.; Spaniol, T. P.; Okuda, J. *J. Polym. Sci., A: Polym. Chem.* **2003**, *41*, 528-544.

(302) Hagerty, R. O.; Husby, P. K.; Kissin, Y. V.; Mink, R. I.; Nowlin, T. E.; Mobil Oil Corporation (Fairfax, VA): United States, **1997**, No. 5,693,583, p 18.

(303) Brown, S. J.; NOVA Chemicals (International) S.A. (Villars-sur-Glane, CH): United States, **2002**, No. 6,372,864, p 16.

(304) Debras, G.; Razavi, A.; Michel, J.; Fina Research, S.A. (Feluy, BE): United States, **2002**, No. 6,380,311, p 15.

(305) Komon, Z. J. A.; Bazan, G. C. *Macromol. Rapid Commun.* **2001**, *22*, 467-478.

(306) Komon, Z. J. A.; Diamond, G. M.; Leclerc, M. K.; Murphy, V.; Okazaki, M.; Bazan, G. C. *J. Am. Chem. Soc.* **2002**, *124*, 15280-15285.

(307) Robert B. Wilson, J.; SRI International (Menlo Park, CA): United States, **1999**, p 22.

(308) Li, L.; Metz, M. V.; Marks, T. J.; Liable-Sands, L.; Rheingold, A. L. *Polymer Preprints* **2000**, *41*, 1912-1913.

(309) Abramo, G. P.; Li, L.; Marks, T. J. *J. Am. Chem. Soc.* **2002**, *124*, 13966-13967.

(310) Metz, M. V.; Schwartz, D. J.; Stern, C. L.; Marks, T. J.; Nickias, P. N. *Organometallics* **2002**, *21*, 4159-4168.

(311) Stewart, A. P.; Trippett, S. *J. Chem. Soc. C.* **1970**, 1263-1266.

(312) Rithner, C. D.; Bushweller, C. H. *J. Am. Chem. Soc.* **1985**, *107*, 7823-7836.

(313) Hietkamp, S.; Stufkens, D. J.; Vrieze, K. *J. Organomet. Chem.* **1979**, *168*, 351-361.

(314) Dilworth, J. R.; de Liefde Meijer, H. J.; Teuben, J. H. *J. Organomet. Chem.* **1978**, *159*, 47-52.

(315) Dehnicke, K.; Weller, F. *Coord. Chem. Rev.* **1997**, *158*, 103-169.

(316) Courtenay, S.; Ong, C. M.; Stephan, D. W. *Organometallics* **2003**, *22*, 818-825.

(317) Belov, G. P.; Gyulumyan, H. R.; Khrapova, I. M.; Maryin, V. P.; Korneev, N. N. *J. Mol. Catal. A - Chem.* **1997**, *115*, 115-161.

(318) Sangokoya, S.; Howie, M.; Owens, D.; Wiegand, K. In *54th Southwest Meeting of the American Chemical Society*: Baton Rouge, LA, **1998**.

(319) Chemicals, A. N. "Aluminoxanes from Akzo Nobel," Akzo Nobel Chemicals, 1999.

(320) Froese, R. D. J.; Musaev, D. G.; Matsubara, T.; Morokuma, K. *J. Am. Chem. Soc.* **1997**, *119*, 7190-7196.

(321) Gassman, P. G.; Winter, C. H. *J. Am. Chem. Soc.* **1988**, *110*, 6130-6135.

(322) Alameddin, N. G.; Ryan, M. F.; Eyler, J. R.; Siedle, A. R.; Richardson, D. E. *Organometallics* **1995**, *14*, 5005-5007.

(323) Richardson, D. E.; Alameddin, N. G.; Ryan, M. F.; Hayes, T.; Eyler, J. R.; Siedle, A. R. *J. Am. Chem. Soc.* **1996**, *118*, 11244-11253.

(324) McConville, D. H.; Loveday, D. R. In *PCT Int. Appl.*; (Univation Technologies, Llc, USA). Wo, **2001**, p 55 pp.

(325) Boussie, T. R.; Diamond, G. M.; Goh, C.; Hall, K. A.; LaPointe, A. M.; Leclerc, M. K.; Lund, C.; Murphy, V.; Shoemaker, J. A. W.; Tracht, U.; Turner, H. W.; Zhang, J.; Uno, T.; Rosen, R. K.; Stevens, J. C. *J. Am. Chem. Soc.* **2003**, *125*, 4306-4317.

(326) Schrock, R. R.; Baumann, R.; Reid, S. M.; Goodman, J. T.; Stumpf, R.; Davis, W. M. *Organometallics* **1999**, *18*, 3649-3670.

(327) Grob, T.; Geiseler, G.; Harms, K.; Greiner, A.; Dehnicke, K. *Z. Anorg. Allg. Chem.* **2002**, *628*, 217-221.

(328) Brenner, S.; Kempe, R.; Arndt, P. *Z. Anorg. Allg. Chem.* **1995**, *621*, 2021-2024.

(329) Daniele, S.; Hitchcock, P. B.; Lappert, M. F.; Merle, P. G. *J. Chem. Soc., Dalton Trans.* **2001**, 13-19.

(330) Daniele, S.; Hitchcock, P. B.; Lappert, M. F.; Nile, T. A.; Zdanski, C. M. *J. Chem. Soci., Dalton Trans.* **2002**, 3980-3984.

(331) Sartain, W. J.; Selegue, J. P. *Organometallics* **1984**, *3*, 1922-1924.

(332) Black, D. G.; Swenson, D. C.; Jordan, R. F.; Rogers, R. D. *Organometallics* **1995**, *14*, 3539-3550.

(333) Bowen, D. E.; Jordan, R. F.; Rogers, R. D. *Organometallics* **1995**, *14*, 3630-3635.

(334) Gelman, N. E. *Pure Appl. Chem.* **1975**, *44*, 493-507.

(335) Borda, P. P.; Legzdins, P. *Anal. Chem.* **1980**, *52*, 1777-1778.

(336) Latesky, S. L.; McMullen, A. K.; Niccolai, G. P.; Rothwell, I. P. *Organometallics* **1985**, *4*, 902-908.

(337) Rogers, J. S.; Lachicotte, R. J.; Bazan, G. C. *Organometallics* **1999**, *18*, 3976-3980.

(338) Ciruelo, G.; Cuenca, T.; Gomez, R.; Gomez-Sal, P.; Martin, A.; Rodriguez, G.; Royo, P. *J. Organomet. Chem.* **1997**, *547*, 287-296.

(339) Tedesco, C.; Immirzi, A.; Proto, A. *Acta Crystallogr., Sect. B: Struct. Sci.* **1998**, *B54*, 431-437.

(340) Swenson, D. C.; Guo, Z.; Crowther, D. J.; Baenziger, N. C.; Jordan, R. F. *Acta Crystallogr., Sect. C: Cryst. Struct. Commun.* **2000**, *C56*, e313-e314.

(341) Giesbrecht, G. R.; Whitener, G. D.; Arnold, J. *Organometallics* **2000**, *19*, 2809-2812.

(342) Wood, D.; Yap, G. A. P.; Richeson, D. S. *Inorg. Chem.* **1999**, *38*, 5788-5794.

(343) Planalp, R. P.; Andersen, R. A.; Zalkin, A. *Organometallics* **1983**, *2*, 16-20.

(344) Fryzuk, M. D.; Mao, S. S. H.; Zaworotko, M. J.; MacGillivray, L. R. *J. Am. Chem. Soc.* **1993**, *115*, 5336-5337.

(345) Erker, G. *J. Organomet. Chem.* **1977**, *134*, 189-202.

(346) Kropp, K.; Erker, G. *Organometallics* **1982**, *1*, 1246-1247.

(347) Buchwald, S. L.; Nielsen, R. B. *Chem. Rev.* **1988**, *88*, 1047-1058.

(348) Dupuis, L.; Pirio, N.; Meunier, P.; Gautheron, B.; Mahieu, A.; Igau, A.; Majoral, J.-P. *Bull. Soc. Chim. France* **1996**, *133*, 611-615.

(349) Yue, N. *M.Sc. Thesis*; University of Windsor: Windsor, **2002**.

(350) Zhang, S.; Piers, W. E.; Gao, X.; Parvez, M. *J. Am. Chem. Soc.* **2000**.

(351) Nelson, J. H. *Nuclear Magnetic Resonance Spectroscopy*; Pearson Education, Inc.: Upper Saddle River, 2003.

(352) Zhou, J.; Lancaster, S. J.; Walker, D. A.; Beck, S.; Thornton-Pett, M.; Bochmann, M. *J. Am. Chem. Soc.* **2001**, *123*, 223-237.

Appendices

Appendix A – Supplementary Data for Chapter 2

Method for Obtaining Thermodynamic Data[xvii]

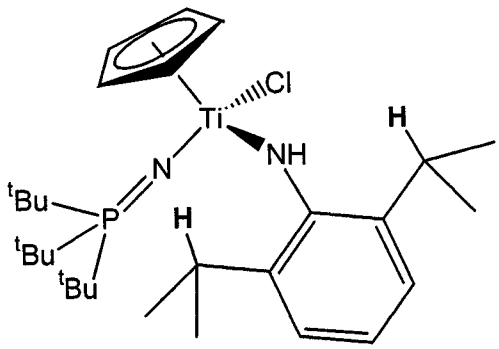

A line shape analysis was performed on the NMR peaks that originated from the two *i*-propyl methine protons. The ^{1}H NMR data was acquired on a 500 MHz NMR spectrometer in toluene-d_8 (degassed and dried with Na/K) over a temperature range of 193 K – 353 K. A coalescence temperature of 308 K was determined. Gaussian fits were performed on the peaks using XWIN-NMR 2.5. The raw data is summarized in Table A.1.

Table A.1: Raw data obtained from the VT NMR experiment.

T (K) ±0.5K	h_e (Hz)	k	1/T (K^{-1})	ln(k)	ln(k/T)
308	n/a	1070.31	0.003247	6.9757	1.2546
313	201.285(635)	2068.15	0.003195	7.6344	1.8882
323	101.570(520)	4760.39	0.003096	8.4681	2.6904
333	60.245(348)	10337.24	0.003003	9.2435	3.4354
343	40.253(270)	23859.58	0.002915	10.0799	4.2422
353	30.779(165)	62772.60	0.002833	11.0473	5.1808

[xvii] Sandstrom, J. *Dynamic NMR Spectroscopy*; Academic Press: London, 1982.

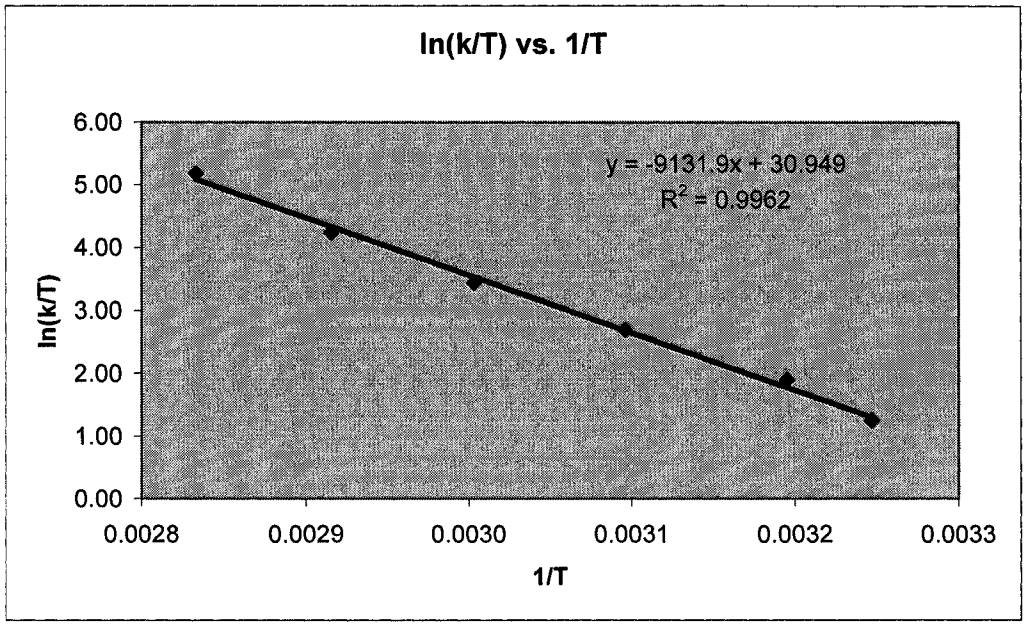

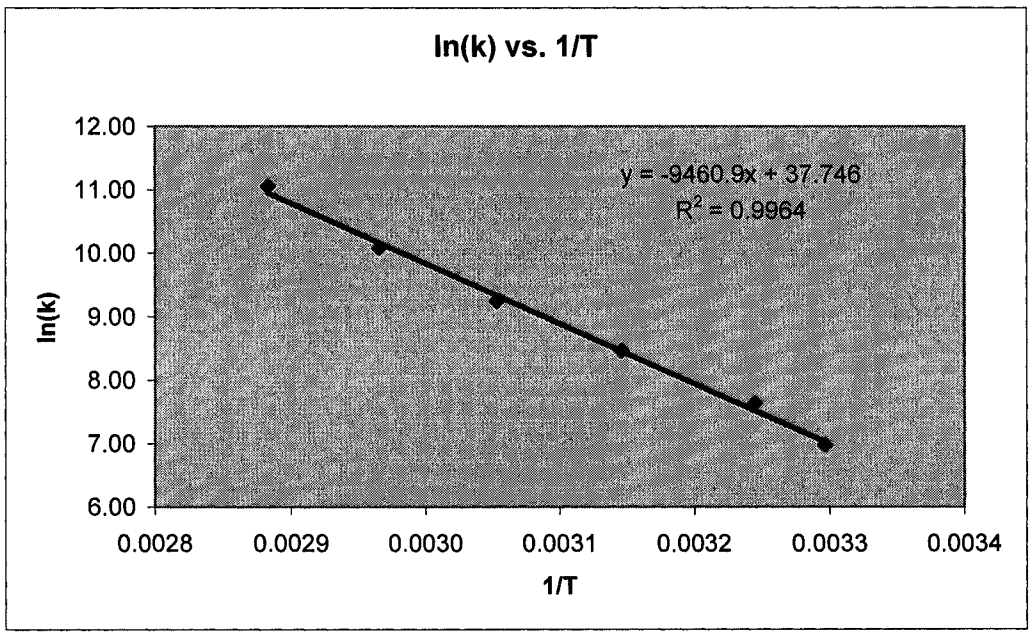

**1/T in units of degrees K^{-1}

Coalescence temperature $k = \Delta\nu_o * [\pi / 2^{1/2}]$

Rapid exchange $k = \frac{1}{2} * \pi * \Delta\nu_o^2 * (h_e - h_o)^{-1}$

From the graph of ln(k/T) *vs.* (1/T), the entropy ($\Delta S^{\ddagger}$) and enthalpy ($\Delta H^{\ddagger}$) may be calculated using values obtained from the linear regression.

$\ln(k/T) = -\Delta H^{\ddagger}/R * (1/T) + \{\ln(\kappa * k_B/h) + \Delta S^{\ddagger}/R\}$ $\Delta G^{\ddagger} = \Delta H^{\ddagger} - T\Delta S^{\ddagger}$

$-\Delta H^{\ddagger}/R = -9131.9$ $\therefore \Delta H^{\ddagger} = 75.9$ kJ mol^{-1} $\pm$ 0.3

$\ln(\kappa * k_B/h) + \Delta S^{\ddagger}/R = 30.949$ $\therefore \Delta S^{\ddagger} = 59.8$ J mol^{-1} $\pm$ 0.2 or 14.3 cal mol^{-1}

At 298 K, $\Delta G^{\ddagger} = 58.1$ kJ mol^{-1} $\pm$ 0.5

Errors calculated using R^2 from linear regression

From the graph of ln(k) *vs.* (1/T), the E_a may be calculated using values obtained from the linear regression.

$\ln(k) = (-E_a/R)(1/T) + \ln(A)$

$-E_a/R = -9460.9$ $\therefore E_a = 78.7$ kJ mol^{-1}

κ = transmission coefficient (normally assumed to be one)

k = rotational rate constant

$\Delta\nu_o$ = peak separation for spectra without exchange (Hz)

h_e = full width at half-height for peaks widened by exchange (Hz)

h_o = full width at half-height for peaks showing no exchange (Hz)

$k_B = 1.380622 \times 10^{-23}$ J K^{-1} (Boltzmann's constant)[xviii]

$h = 6.626193 \times 10^{-34}$ J s (Planck's constant)[xviii]

$R = 8.31434$ J K^{-1} mol^{-1} (Gas constant)[xviii]

T = temperature (K) E_a = activation energy

$\Delta G^{\ddagger}$ = free energy of activation A = pre-exponential factor

$\Delta H^{\ddagger}$ = enthalpy of activation

$\Delta S^{\ddagger}$ = entropy of activation

[xviii] Taylor, B. N.; Parker, W. H.; Langenberg, D. N. *Handbook of Chemistry and Physics*; 54th Ed.; Weast, R. C., Ed.; CRC Press: Cleveland, 1974, p F214-215.

Appendix B – Supplementary Data for Chapter 3

Aluminum *Bis*(Phosphinimide) Complex

In an effort to extend the application of the *bis*(phosphinimine) ligand *m*-$(CH_2P^tBu_2NH)_2C_6H_4$ (**3.6**) to other metals, a preliminary reaction with TMA was performed. NMR spectroscopy indicated the formation of a single product, even upon use of excess aluminum precursor. The ratio of *t*-butyl to methyl groups in the ^1H NMR spectrum was 2:1, which led to the formulation of the product as Al[*m*-$(CH_2P^tBu_2N)(CH_2P^tBu_2NH)C_6H_4]Me_2$ (**3.21**) (Figure B.1). In the absence of X-ray crystallographic or other evidence, it is not possible to differentiate between a monomer, dimer or oligomer where the phosphinimide ligand links the aluminum centres. It is noteworthy, however, that the majority of isolated aluminum compounds containing chelating ligands are monomeric only upon trapping with a Lewis base such as tetrahydrofuran or diethylether.[xix]

[xix] a) Beachley, O. T., Jr.; Racette, K. C. *Inorg. Chem.* **1975**, *14*, 2534-2537. b) Beachley, O. T., Jr.; Racette, K. C. *Inorg. Chem.* **1976**, *15*, 2110-2115. c) Lewinski, J.; Zachara, J.; Justyniak, I. *Organometallics* **1997**, *16*, 4597-4605. d) Lewinski, J.; Zachara, J.; Starowieyski, K. B. *J. Chem. Soc. Dalton Trans.* **1997**, 4217-4222. e) Lewinski, J.; Justyniak, I.; Ochal, Z.; Zachara, J. *J. Chem. Soc. Dalton Trans.* **1999**, 2909-2911. f) Ko, B.-T.; Wu, C.-C.; Lin, C.-C. *Organometallics* **2000**, *19*, 1864-1869. g) Ko, B.-T.; Chao, Y.-C.; Lin, C.-C. *Inorg. Chem.* **2000**, *39*, 1463-1469. g) Robson, D. A.; Bylikin, S. Y.; Cantuel, M.; Male, N. A. H.; Rees, L. h.; Mountford, P.; Schroder, M. *J. Chem. Soc. Dalton Trans.* **2001**, 157-169. h) Huang, Y.-L.; Huang, B.-H.; Do, B.-T.; Lin, C.-C. *J. Chem. Soc. Dalton Trans.* **2001**, 1359-1365. i) Hsueh, M.-L.; Huang, B.-H.; Lin, C.-C. *Macromolecules* **2002**, *35*, 5763-5768. j) Huang, B.-H.; Yu, T.-L.; Huang, Y.-L.; Ko, B.-T.; Lin, C.-C. *Inorg. Chem.* **2002**, *41*, 2987-2994. k) Liao, T.-C.; Huang, Y.-L.; Huang, B.-H.; Lin, C.-C. *Macromolecular Chemistry and Physics* **2003**, *204*, 885-892.

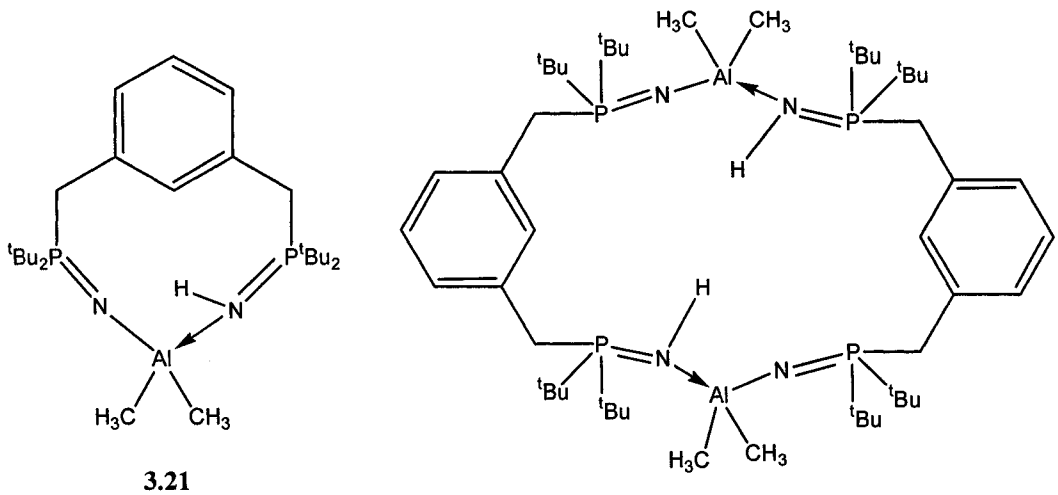

3.21

Figure B.1: Two possible structures of the product of the reaction of *m*-$(CH_2P^tBu_2NH)_2C_6H_4$ (**3.6**) with TMA.

Reactivity of Titanium *Bis*(Phosphinimide) Complexes

Prior to the reproducible, high-yield synthesis of Ti[*m*-$(CH_2P^tBu_2N)_2C_6H_4$]Br_2 (**3.13**), the *bis*(phosphinimide) complexes $Ti(NP^tBu_3)_2X_2$ (X = Cl, Me, Ph, Bn, CH_2SiMe_3) were used as model compounds to explore general reactivity since their syntheses are more straightforward.[xx] The synthesis of the new alkyl derivative $Ti(NP^tBu_3)_2(CH_2SiMe_3)_2$ (**3.18**) was readily achieved by treatment of the dichloride metal precursor with the appropriate Grignard reagent. When $Ti(NP^tBu_3)_2X_2$ (X = Me, Bn, CH_2SiMe_3) was heated in an attempt to produce an alkylidene product,[xxi] no reaction occurred. Upon prolonged thermolysis in deuterated solvent, the only soluble product was identified as HNP^tBu_3, a sign that extrusion of the phosphinimine was probably a facile process. This outcome was also observed in the presence of donors such as trimethylphosphine or pyridine.

[xx] Guerin, F.; Stewart, J. C.; Beddie, C.; Stephan, D. W. *Organometallics* **2000**, *19*, 2944-3000.

[xxi] a) Planalp, R. P.; Andersen, R. A.; Zalkin, A. *Organometallics* **1983**, *2*, 16-20. b) Fryzuk, M. D.; Mao, S. S. H.; Zworotko, M. J.; MacGillivray, L. R. *J. Am. Chem. Soc.* **1993**, *115*, 5336-5337.

Metal precursors that possess an alkyl group and a halide ligand are often targeted for a variety of further reactivity studies.[xxii] Previous efforts in our research group had exhausted the conventional mono-alkylation routes in an effort to obtain $Ti(NP^tBu_3)_2MeCl$, only to provide intractable mixtures of products.[xxiii] Recently, Piers and co-workers have reported that use of catalytic (5 mol%) amounts of $B(C_6F_5)_3$ in the presence of an equimolar distribution of dichloride and dimethyl metal precursor at -78°C afforded the related ketamide complex $TiCp^*(NC^tBu_2)MeCl$ in 90% isolated yield.[xxiv] This route was not as convenient to provide $Ti(NP^tBu_3)_2MeCl$, since only *ca.* 50% conversion was achieved (by $^{31}P\{^1H\}$ NMR spectroscopy), and the product could not be adequately separated from the starting materials due to similarities in solubility. Attempts to scramble ligands via thermolysis of $Ti(NP^tBu_3)_2Me_2$ with $Ti(NP^tBu_3)_2Cl_2$ were also unsuccessful.

Experiments to combine *bis*(phosphinimide) titanium precursors with hydridic reagents such as boranes or silanes provided variable results. For example, $Ti(NP^tBu_3)_2R_2$ (R = Me, Bn, Ph) reacted with HBPin (Pin = pinacol or $OCMe_2CMe_2O$), to afford mixtures of products, and the only identifiable species was $^tBu_3PNBPin$.[xxv] When $Ti(NP^tBu_3)_2Me_2$ was treated with silyl reagents such as Et_3SiH or $PhSiH_3$, no reaction ensued, even upon prolonged thermolysis. However, in an emulation of the work performed by Tilley and co-workers,[xxvi] addition of two equivalents of $LiSiPh_3$ to $Ti(NP^tBu_3)_2Cl_2$ provided $Ti(NP^tBu_3)_2(SiPh_3)_2$ (**3.19**) in good isolated yield (71%). The product was identified by NMR spectroscopy in spite of its instability in solution; attempts to grow X-ray quality crystals at room temperature afforded a crop of colourless crystals, which were identified crystallographically to be $SiPh_4$.

Thermolysis of $Ti(NP^tBu_3)_2Ph_2$ in the presence of *bis*(trimethylsilyl)acetylene (BTMSA) in toluene-d_8 was performed to trap a benzyne intermediate. Following

---

[xxii] a) Cam, D.; Giannini, U. *Makromol. Chem.* **1992**, *193*, 1049-1055. b) Fernandez, F. J.; Gomez-Sal, P.; Manzanero, A.; Royo, P.; Jacobsen, H.; Berke, H. *Organometallics* **1997**, *16*, 1553-1561. c) Amor, F.; du Plooy, K. W.; Spaniol, T. P.; Okuda, J. *J. Organomet. Chem.* **1998**, *558*, 139-146.

[xxiii] F. Guérin, unpublished results. Low temperature monoalkylation attempts were unsuccessful.

[xxiv] Zhang, S.; Piers, W. E.; Gao, X.; Parvez, M. *J. Am. Chem. Soc.* **2000**, *122*, 5499-5509.

[xxv] S. B. Hawkeswood, unpublished results.

[xxvi] Woo, H.-G.; Freeman, W. P.; Tilley, T. D. *Organometallics* **1992**, *11*, 2198-2205.

heating at 90°C for 48 hours, only 50% conversion to the desired insertion product was achieved (Figure B.2). In addition to producing the transformed product (**3.22**), an equimolar amount of benzene was produced (by ^{1}H NMR spectroscopy), inferring the benzyne intermediate was produced via loss of one of the phenyl ligands, followed by oxidative coupling to BTMSA. The quaternary carbon atoms were evident in the $^{13}C\{^{1}H\}$ NMR spectrum, giving rise to resonances located at 192.7, 188.8, 167.9, and 146.7 ppm. The furthest downfield signal is characteristic of the constrained *ipso* carbon atom of the phenyl ring.[xxvii] This transformation did not occur as readily as when the zirconocene diphenyl analogue ($ZrCp_2Ph_2$) is employed as precursor.

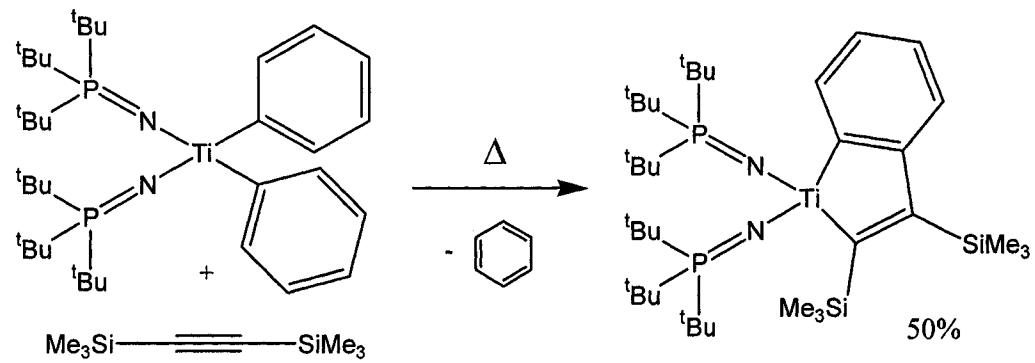

3.22

Figure B.2: Thermolytically induced loss of benzene, followed by trapping with BTMSA to provide an insertion product, **3.22**.

[xxvii] a) Erker, G. *J. Organomet. Chem.* **1977**, *134*, 189-202. b) Kropp, K.; Erker, G. *Organometallics* **1982**, *1*, 1246-1247. c) Buchwald, S. L.; Nielsen, R. B. *Chem. Rev.* **1988**, *88*, 1047-1058. d) Dupuis, L.; Pirio, N.; Meunier, P.; Gautheron, B.; Mahieu, A.; Igau, A.; Majoral, J.-P. *Bull. Soc. Chim. France* **1996**, *133*, 611-615.

Appendix C – Supplementary X-ray Data for Chapters 2-5

Appendix D – Supplementary GPC and Polymer Yield Data for Chapters 3-5

See enclosed CD on back cover.

Vita Auctoris

Emily Hollink

Date and Place of Birth: Sept. 8, 1976, North York, ON, Canada.

Present Address:

104-3015 Sandwich St.
Windsor, ON N9C 1A5
Telephone: (519) 252-6691
E-mail: emhollink@hotmail.com

Permanent Address:

4592 Sugar Maple Dr.
Ottawa, ON K1V 1Y4
Telephone: (613) 822-4554

Education

Ph.D. Candidate, Organometallic Chemistry, September 1999-Present
University of Windsor, Windsor, Ontario
Thesis supervisor: Dr. Douglas W. Stephan
Thesis title: Group IV Phosphinimide Complexes in Catalysis

B. Sc. Hon. Chemistry (cum laude), September 1995 – April 1999
University of Ottawa, Ottawa, Ontario
Honours thesis supervisor: Dr. Deryn E. Fogg
Honours thesis title: "A Novel Tandem Synthesis of Saturated Ring Systems"

Honours and Awards

- University of Windsor Summer Research Scholarship, $3000. University of Windsor, May 2003 – August 2003.
- American Chemical Society Division of Inorganic Chemistry Travel Award, $200 USD. American Chemical Society, August 2002.
- University of Windsor Conference Travel Award, $300. University of Windsor, June 11, 2002.
- Ontario Graduate Scholarship, $15,000. Government of Ontario, May 2002 – April 2003.
- University of Windsor Tuition Scholarship, $4500. University of Windsor, May 2002 – April 2003. (declined)
- University of Windsor Tuition Scholarship, $4500. University of Windsor, May 2001 – April 2002.

- University of Windsor Conference Travel Award, $350. University of Windsor, October 31, 2001.
- William Redmond Memorial Bursary, $1000. University of Windsor, Winter 2000.
- Hollink, E.; Fogg, D. E. A Novel Tandem Synthesis of Saturated Ring Systems. 27th Southwestern Ontario Undergraduate Student Chemistry Conference, March, 1999. 2nd Place finish in Inorganic Session.

Related Work Experience

August 2002 – April 2003. *University of Windsor*
Analytical Technician: I installed our departmental elemental analysis instrument, and performed CHN analyses and general maintenance of the instrument.

September 1999 – April 2002. *University of Windsor*
Teaching Assistant: I have taught first year introductory chemistry laboratories, in addition to third year analytical instrumentation laboratories. This required routine maintenance of equipment, general instruction of laboratory techniques and grading of exams and papers.

May 1999 – August 1999. *Genzyme Inc.*
Office Manager: I was responsible for managing their Ottawa Government Relations office, and participated in the process for filing a New Drug submission to Health Canada.

May 1998 – August 1998. *University of Ottawa*
Research Assistant: I worked in the laboratories of Dr. Deryn E. Fogg, synthesizing asymmetric organic ligands, and preparing novel ruthenium catalysts for ring opening metathesis polymerization (ROMP).

May 1997 – August 1997. *University of Ottawa*
Research Assistant: I worked in the laboratories of Dr. Susannah L. Scott, preparing silica-supported vanadium catalysts for the purposes of ethylene polymerization.

Publications, Accepted at Refereed Journals

Hollink, E.; Stewart, J. C.; Wei, P.; Stephan, D. W. Ti and Zr Bidentate *Bis*-Phosphinimide Complexes. *J. Chem. Soc., Dalton Trans.* (**2003**), in press.

Hollink, E.; Stephan, D. W. Zirconium and Hafnium, Comprehensive Coordination Chemistry II (**2003**), *3*, Chapter 3.

Stephan, D. W.; Stewart, J. C.; Guérin, F.; Courtenay, S.; Kickham, J. E.; Hollink, E.; Beddie, C.; Hoskin, A.; Graham, T.; Wei, P.; Spence, R. E. v. H.; Xu, W.; Koch, L.; Gao, X.; Harrison, D. G. An Approach to Catalyst Design: Cyclopentadienyl-Titanium Phosphinimide Complexes in Olefin Polymerization. *Organometallics* (**2003**), *22*, 1937-1947.

Courtenay, S.; Smith, S.; Hollink, E.; Blaschke, U.; Kehr, G.; Froehlich, R.; Erker, G.; Stephan, D. W. Synthesis of a Dinuclear μ-(η^2-Thioaldehyde)Zirconocene Cation Complex. *Zeitschrift fuer Naturforschung, B: Chemical Sciences* (**2002**), *57(10)*, 1184-1188.

Yue, N.; Hollink, E.; Guérin, F.; Stephan, D. W. Zirconium Phosphinimide Complexes: Synthesis, Structure and Deactivation Pathways in Ethylene Polymerization Catalysis. *Organometallics* (**2001**), *20*, 4424-4433.

Conferences

Cabrera, L.; Hollink, E.; Stephan, D. W. Cationic Titanium Phosphinimide Complexes. 36th Inorganic Discussion Weekend, October, 2003.

Hollink, E.; Stephan, D. W. Developments in Group IV Phosphinimide Chemistry and the Implications Toward Ethylene Polymerization Catalysis. 86th Canadian Society for Chemistry National Conference/ 39th IUPAC International Conference, August, 2003.

Hollink, E.; Stephan, D. W. Strategies in Polymer Design: The Role of Bimetallic Olefin Polymerization Catalysts. 224th American Chemical Society National Meeting, August, 2002.

Hollink, E.; Stephan, D. W. Group IV Amido- Phosphinimido Complexes. 85th Canadian Society for Chemistry National Conference, June, 2002.

Hollink, E.; Stephan, D. W. Monometallic Vs. Bimetallic Systems: Toward Control of Molecular Weight Distribution. 85th Canadian Society for Chemistry National Conference, June, 2002.

Yue, N.; Hollink, E.; Guérin, F.; Stephan, D. W. Synthesis and Structure of Zr-Phosphinimide Complexes: Implications for Ethylene Polymerization Catalysis. 34th Inorganic Discussion Weekend, October, 2001.

Yue, N.; Hollink, E.; Guérin, F.; Stephan, D. W. Zr-Phosphinimide Complexes: Activation and Deactivation Pathways in Ethylene Polymerization Catalysis. 222nd American Chemical Society National Meeting, August, 2001.

Hollink, E.; Fogg, D. E. A Novel Tandem Synthesis of Saturated Ring Systems. 27th Southwestern Ontario Undergraduate Student Chemistry Conference, March, 1999. 2nd Place finish in the Inorganic Session